UNCLASSIFIED

AD NUMBER

AD801885

NEW LIMITATION CHANGE

TO

Approved for public release, distribution unlimited

FROM

Distribution authorized to U.S. Gov't. agencies and their contractors; Adminstrative and Operational Use, Export Control; Nov 1966. Other requests shall be referred to the Air Force Flight Dynamics Laboratory, Attn: FDCL, Wright-Patterson AFB, OH 45433.

AUTHORITY

AFFDL, per ltr dtd 8 Jun 1972

THIS PAGE IS UNCLASSIFIED

AFFDL-TR-66-158

801885

CONTROL MOMENT GYROSCOPE GIMBAL ACTUATOR STUDY

The Bendix Corporation
Eclipse-Pioneer Division
Teterboro, New Jersey

TECHNICAL REPORT AFFDL-TR-66-158

NOVEMBER 1966

This document is subject to special export controls and each transmittal to foreign governments or foreign nationals may be made only with prior approval of AFFDL (FDCL), Wright-Patterson AFB, Ohio.

Air Force Flight Dynamics Laboratory
Research and Technology Division
Air Force Systems Command
Wright-Patterson Air Force Base, Ohio

NOTICES

When Government drawings, specifications, or other data are used for any purpose other than in connection with a definitely related Government procurement operation, the United States Government thereby incurs no responsibility nor any obligation whatsoever; and the fact that the Government may have formulated, furnished, or in any way supplied the said drawings, specifications, or other data, is not to be regarded by implication or otherwise as in any manner licensing the holder or any other person or corporation, or conveying any rights or permission to manufacture, use, or sell any patented invention that may in any way be related thereto.

Copies of this report should not be returned to the Research and Technology Division unless return is required by security considerations, contractual obligations, or notice on a specific document.

CONTROL MOMENT GYROSCOPE GIMBAL ACTUATOR STUDY FINAL REPORT

The Bendix Corporation
Eclipse-Pioneer Division
Teterboro, New Jersey

Best Available Copy

FOREWORD

This final report was prepared by The Bendix Corporation, Teterboro, New Jersey under USAF Contract No. AF33(615)-3465 and was submitted on 8 August 1966. The report covers work from January 1966 to September 1966.

This program sponsored by the Air Force Flight Dynamics Laboratory, Research and Technology Division, has been directed by Air Force project engineer, FDCL/Lt. D. W. Anderton. It was conducted by The Bendix Corporation through its Eclipse-Pioneer Division in association with the Research Laboratories Division.

Key Bendix personnel who have managed the program and significantly contributed to its technical accomplishments are the following:

L. Morine	T. O'Connor	J. Carnazza
D. Pool	R. DeLucia	M. Ritter
R. Kaczynski	D. Vassallo	J. Madurski
		H. Varner

This technical report has been reviewed and is approved.

H. W. BASHAM
Chief, Control Elements Branch
Flight Control Division
AF Flight Dynamics Laboratory

ABSTRACT

The purpose of this study is the determination of an optimal gimbal actuator for large double gimbal control moment gyros. The optimization study is divided into three distinct phases: torquers and transmissions, which together form the actuators, and controllers. The DC torquer and an epicyclic transmission are selected as optimal, on the basis of power, weight, size, reliability and performance. Pulse width modulation of a type designated as single channel is established as the optimal controller.

To demonstrate the application of the optimal actuator configuration, a preliminary design layout was completed for mounting at one pivot of a CMG having an angular momentum of 1000 foot-pound-seconds. The design includes all necessary structure and a tachometer generator, weighs 23 pounds, consumes less than 45 watts at full torque and also fulfills all performance requirements. It has a threshold of 3% and a reliability of 0.9741 for one year and 0.9953 for two months while in operation.

It is recommended that a brushless DC torquer be considered in the future for control moment gyro gimbal actuation, when it is better established as state-of-the-art. It has the advantage of very low threshold and potentially high reliability.

TABLE OF CONTENTS

TABLE OF CONTENTS (continued)

TABLE OF CONTENTS (continued)

TABLE OF CONTENTS (continued)

LIST OF ILLUSTRATIONS

LIST OF ILLUSTRATIONS (continued)

LIST OF ILLUSTRATIONS (continued)

LIST OF ILLUSTRATIONS (continued)

LIST OF ILLUSTRATIONS (continued)

LIST OF TABLES

LIST OF TABLES (continued)

LIST OF ABBREVIATIONS AND SYMBOLS

Symbol		Definition	Dimension
A	=	Distance from centerline of planet carrier to centerline of sun on simple planetary transmission	inches
A_L	=	Equivalent leakage area	in^2
B	=	Linear backlash between mating teeth	inches
C	=	Correction factor dependent upon machining errors	
C_o	=	Flow coefficient	$\sqrt{°R}/sec$
C_p	=	Specific heat at constant pressure	BTU/lb-°R
CPA	=	Current power amplifier	
CT	=	Center tap	
D_{co}	=	Output shaft diameter	inches
D_G	=	Pitch diameter of gear	inches
D_i	=	Pitch diameter of external (ring) gear in second-stage mesh	inches
D_m	=	Motor displacement	in^3/rev
D_o	=	Pitch diameter of internal reaction (output) gear in second-stage mesh	inches
D_p	=	Pitch diameter of pinion	inches
D_{pa}	=	Planet gear axle diameter	inches
D_r	=	Planetary ring gear pitch diameter	inches
D_s	=	Planetary sun gear pitch diameter	inches
d	=	Radius of gyration	inches
E	=	Maximum pulse voltage amplitude	volts
EHD	=	Integrated motor and harmonic drive transmission	
EHD/T_x	=	Harmonic drive with external transmission	

LIST OF ABBREVIATIONS AND SYMBOLS (continued)

Symbol		Definition	Dimension
f_c	=	Motor cutoff frequency	cps
f_M	=	Motor viscous torque coefficient at motor shaft	ft-lb-sec
f_T	=	Total viscous torque coefficient at motor shaft	ft-lb-sec
g	=	Gravitational acceleration	ft/sec^2
H	=	C.M.G. size	ft-lb-sec
h	=	Ratio of gear diameter to gear width	
I	=	Gimbal moment of inertia	$ft-lb-sec^2$
I_{av}	=	Average motor current under duty cycle	amperes
I_{max}	=	Average motor current required for maximum desired torque	amperes
I_{MP}	=	Peak motor current	amperes
I_P	=	Maximum motor current available	amperes
I_L	=	Load current	amperes
I_M	=	Motor current	amperes
::IPFM	=	Integral pulse frequency modulation	
J_e	=	Equivalent transmission inertia at motor shaft	$ft-lb-sec^2$
J_G	=	Inertia of a mass about an axis	$ft-lb-sec^2$
J_L	=	Load inertia	$ft-lb-sec^2$
J_o	=	Inertia of output ring gear	$ft-lb-sec^2$
J_M	=	Motor inertia	$ft-lb-sec^2$
J_R	=	Tachometer moment of inertia	$ft-lb-sec^2$
J_T	=	Total inertia at motor shaft	$ft-lb-sec^2$

LIST OF ABBREVIATIONS AND SYMBOLS (continued)

Symbol		Definition	Dimension
f_c	=	Motor cutoff frequency	cps
f_M	=	Motor viscous torque coefficient at motor shaft	ft-lb-sec
f_T	=	Total viscous torque coefficient at motor shaft	ft-lb-sec
g	=	Gravitational acceleration	ft/sec^2
H	=	C.M.G. size	ft-lb-sec
h	=	Ratio of gear diameter to gear width	
I	=	Gimbal moment of inertia	ft-lb-sec^2
I_{av}	=	Average motor current under duty cycle	amperes
I_{max}	=	Average motor current required for maximum desired torque	amperes
I_{MP}	=	Peak motor current	amperes
I_P	=	Maximum motor current available	amperes
I_L	=	Load current	amperes
I_M	=	Motor current	amperes
IPFM	=	Integral pulse frequency modulation	
J_e	=	Equivalent transmission inertia at motor shaft	ft-lb-sec^2
J_G	=	Inertia of a mass about an axis	ft-lb-sec^2
J_L	=	Load inertia	ft-lb-sec^2
J_o	=	Inertia of output ring gear	ft-lb-sec^2
J_M	=	Motor inertia	ft-lb-sec^2
J_R	=	Tachometer moment of inertia	ft-lb-sec^2
J_T	=	Total inertia at motor shaft	ft-lb-sec^2

Symbol		Definition	Dimension
K	=	Hydraulic system dimensional constant	watt-sec/in-lb
K_A	=	Error amplifier gain	volt/volt
K_B	=	Motor back - emf constant	volt-sec/rad
K_G	=	Feedback tachometer gain	volt-sec/rad
K_g	=	Density ratio of a mesh	
K_j	=	Dimensional constant	$lb\text{-}sec^2/ft^4$
K_m	=	Motor constant	$\sqrt{ft\text{-}lb\text{-}sec} \times 10^{-2}$
K_T	=	Motor torque constant	ft-lb/amp
K_{TY}	=	Motor gain constant of inner gimbal torque	ft-lbs/amperes
K_{VY1}	=	Inner gimbal effective back emf constant	volts/rad/sec
K_{VY2}	=	Inner gimbal tachometer constant	volts/rad/sec
K_1	=	Simple planetary transmission face-width scaling factor	
K_2	=	Simple planetary transmission weight scaling factor	
K_3	=	Simple planetary transmission weight scaling factor	
K_4	=	Simple planetary transmission volume scaling factor	
k	=	Stall torque input constant	ft-lb/volt
L	=	Length	inches
L_a, L_y	=	Motor winding inductance	henries
L_m	=	Motor inductance	henry
l	=	Length of line-of-action	inches
ℓ_c	=	Carrier flange thickness	inches
ℓ_i	=	Input shaft length	inches

Symbol		Definition	Dimension
ℓ_o	=	Output shaft length	inches
ℓ_p	=	Planet gear axle length	inches
m	=	Mass	$\frac{\text{lb-sec}^2}{\text{ft}}$
m_1	=	Ratio of one mesh	
M	=	Maximum output of ON-OFF controller	volts
m	=	Instantaneous torque motor input voltage	volts
mv	=	Millivolts	
M_L	=	Load torque-speed curve slope	ft-lb-sec
M_M	=	Motor torque-speed curve slope	ft-lb-sec
m	=	Ratio of one mesh	
N	=	Number of teeth in contact	
N_G	=	Number of teeth in gear	
N_L	=	Load speed	RPM
N_M	=	Motor speed	RPS
N_p	=	Number of teeth in pinion	
n	=	Number of planet gears	
P_A	=	Average actuator output power	watts
PAM	=	Pulse amplitude modulation	
PFM	=	Pulse frequency modulation	
PWM	=	Pulse width modulation	
PWM_1	=	Pulse width modulation, single channel	
PWM_2	=	Pulse width modulation, dual channel	

Symbol		Definition	Dimension
P_{av}	=	Motor input power under duty cycle	watts
P_{avg}	=	Average power required	watts
P_B	=	Switching bridge power consumption	watts
P_M	=	Motor input power	watts
P_d	=	Diametral pitch	
P_L	=	Hydraulic leakage power loss	watts
P_m	=	Mechanical losses	watts
P_{MM}	=	Motor input power to deliver maximum desired torque	watts
P_P	=	Motor input power to deliver peak torque	watts
PPMH	=	Parts per million hours	
P_S	=	Hydraulic power required at servovalves	watts
P_{S1}	=	Power required at maximum speed	watts
P_{S2}	=	Power required at 0.5 maximum speed	watts
P_{S3}	=	Power required at 0.25 maximum speed	watts
P_T	=	Total C.M.G. hydraulic system actuator power	watts
P_t	=	Total power consumption in motor and controller	watts
P_{T1}	=	Power required at maximum torque	watts
P_{T2}	=	Power required at 0.5 maximum torque	watts
P_{T3}	=	Power required at 0.25 maximum torque	watts
P_1	=	Pneumatic motor inlet pressure	psi
P_2	=	Pneumatic downstream pressure	psi
Δ_p	=	Hydraulic motor differential pressure	psi

Symbol		Definition	Dimension
Q	=	Ratio factor	
Q_L	=	Total hydraulic system leakage	in^3/sec
Q_{LM}	=	Total hydraulic motor leakage	in^3/sec
Q_{LP}	=	Total pump leakage (chargeable per control moment gyroscope)	in^3/sec
Q_{LV}	=	Total servovalve leakage	in^3/sec
R	=	Resistance	ohms
R_a, R_y	=	DC motor resistance	ohms
R_m	=	Motor resistance	ohms
R_S	=	Internal resistance of voltage source	ohms
R_G	=	Transmission overall ratio	
R_G	=	Gas constant	in/° R
r_G	=	Pitch radius of gear	inches
r_p	=	Pitch radius of pinion or planet	inches
r_r	=	Ring gear pitch radius	inches
r_s	=	Sun gear pitch radius	inches
S	=	Laplace operator	sec^{-1}
$S_1S_2S_3S_4$	=	Power switches	
S_b	=	Beam (Lewis) stress	psi
S_c	=	Hertz stress	psi
T	=	Gas temperature	°R
T_{em}	=	Steady-state motor torque	ft-lb

Symbol		Definition	Dimension
T_F	=	Total coulomb friction torque at motor shaft	ft-lbs
T_{LM}	=	Maximum transmission output torque (stall torque)	ft-lb
T_M	=	Instantaneous motor output torque	ft-lb
T_m	=	Maximum required output torque	ft-lbs
T_{MP}	=	Torquer rated peak torque output	ft-lbs
T_{MS}	=	Maximum motor stall torque	ft-lb
T_o	=	Transmission stall torque	ft-lb
t	=	Time	sec
T	=	Pulse period	sec
t_s	=	Period of clock pulse	sec
V	=	Transmission volume	in^3
V/F	=	Voltage-to-frequency	
V_1	=	Tooth pitch line velocity	ft/min.
VPA	=	Voltage power amplifier	
W	=	Transmission weight	pounds
W_a	=	Weight of actuator	lb
w	=	Specific weight of material	lb/in^3
$\dot{w}$	=	Gas weight flow	lb/sec
Y	=	Form factor	
α, β	=	Gimbal position angle	radians
$\dot{\alpha}, \dot{\beta}$	=	Gimbal rates	rad/sec
ζ	=	Damping factor	

Symbol		Definition	Dimension
η	=	Transmission efficiency	percent
η'	=	Ratio of inertias seen by outer gimbal and inner gimbal torquers	
η_c	=	Compressor efficiency	percent
η_m	=	Motor efficiency	percent
τ	=	Time constant	sec
μ	=	Dynamic coefficient of friction	
ω_c	=	Carrier velocity	rad/sec
ω_c	=	Motor cutoff frequency	rad/sec
ω_i	=	Input angular velocity	rad/sec
ω_m	=	Velocity of a mass about an axis	rad/sec
ω_n	=	Natural frequency	rad/sec
ω_o	=	Maximum gimbal rate	rad/sec
ω_p	=	Planet gear velocity	rad/sec
ω_s	=	Sun gear velocity	rad/sec
ω_o	=	Output angular velocity	rad/sec
ω_g	=	Ring gear angular velocity (about its center)	rad/sec
ϕ	=	Gear tooth pressure angle	degrees

SECTION I

INTRODUCTION

1.1 GENERAL

The use of large control moment gyroscopes (CMG's) for the stabilization of manned spacecraft on long duration missions has been the subject of considerable theoretical study. It is expected that the use of large CMG systems will lead to a notable improvement in attitude control accuracies and weight savings when compared to the conventional reaction jet control systems for long term missions.

There is presently a great deal of interest in the double gimbal type of CMG. NASA Langley has a program to fabricate and test a large double gimbal CMG to provide verification of previous theoretical studies. One of these studies recommended that a study of gimbal torquers be carried out to select an optimal CMG gimbal torquer design. The Flight Control Division of the Air Force Flight Dynamics Laboratory at Wright-Patterson Air Force Base decided to undertake such a torquer study to complement the NASA Langley CMG program.

To illustrate the problem, the NASA Langley CMG gyro wheel has an angular momentum of 1000 ft-lb-sec and requires gimbal torques up to 175 ft-lb. A direct-drive DC torquer with a 175 ft-lb rating could weigh over 300 pounds and also consume a maximum of over 600 watts of continuous power. Other types of torquers and speed reduction transmissions were therefore investigated for this application. The combined CMG torquer transmission assembly shall be designated as a CMG actuator in this report.

1.2 OBJECTIVES

The objective of this study is to determine optimal actuators for control moment gyroscopes having angular momentums ranging from 200 to 2000 ft-lb-sec. This study must also determine optimal controllers (control electronics) for the corresponding range of actuators, including any interface relationships between the controller and actuator. A diagram representing relationships between the controller and actuator is shown in figure 1.

The optimization study shall be made on the basis of the following characteristics:

(a) Power consumption

(b) Reliability

(c) Weight

(d) Volume

(e) Performance

More detail on required performance is given in paragraph 1.3.

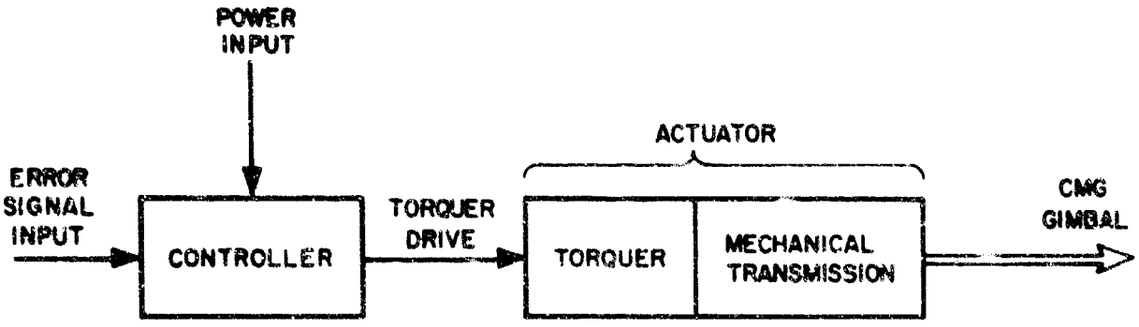

Figure 1. Basic Relationship Between Controller and Actuator

In addition to the optimization study, a preliminary design study for an angular momentum of 1000 ft-lb-sec is needed to examine its applicability to the NASA Langley CMG.

1.3 REQUIREMENTS

The study can be divided into three parts:

(a) A gimbal actuator optimization study

(b) A controller study

(c) A design study for the NASA Langley 1000 ft-lb-sec CMG.

1.3.1 A Gimbal Actuator Optimization Study

The CMG gimbal actuator torquer and transmission study is required for the angular momentum range from 200 to 2000 ft-lb-sec. The following specific requirements are to be considered:

(a) Maximum gimbal rate less than ±0.175 rad/sec (approx. ±10 deg/sec).

(b) Minimum gimbal rate greater than 0.000175 rad/sec (approx. 0.01 deg/sec).

(c) Threshold torque less than 0.5% of maximum torquer output.

(d) Torque output linearity shall be within ±5% of the maximum output torque.

(e) The dynamic response of the actuator shall be such that for a full torque output command, the gyro gimbal must respond to and remain within ±3% of the commanded value in less than 0.05 seconds.

(f) Reliability must be such that the gimbal torquer can be expected to operate for more than one year without maintenance or replacement. It should be capable of operating up to five years with limited maintenance or replacement.

(g) Power consumption must be kept at a minimum.

(h) Weight and volume must be compatible with feasible CMG designs. Design objectives shall include keeping these values at a minimum.

(i) The torquer design shall place a minimum friction and viscous restraint upon the output shaft.

With the maximum gimbal rates and gyro angular momentums required, the range of maximum actuator torques are 35 to 350 ft-lb. All possible electrical, hydraulic and pneumatic actuators are investigated for applicability to the CMG actuator. Mechanical transmissions of all applicable types are also to be studied.

1.3.2 Controller Optimization Study

Controller designs will be evolved and computer studies will be made to compare the relative results of each type of controller. The following types of controllers shall be considered for all torquers:

(a) DC proportional

(b) Pulse width modulation (single channel)

(c) Pulse width modulation (dual channel)

(d) ON-OFF

(e) ON-OFF with two gain levels

(f) Pulse amplitude modulation

(g) Pulse frequency modulation

(h) Delta modulation

These controllers will be compared on the basis of power consumption, reliability, weight, volume and performance. Performance shall consist of threshold, linearity and dynamic characteristics.

1.3.3 Actuator Design Study

As a result of the gimbal actuator optimization study and the controller study, a detailed set of requirements for a control actuator for use on the NASA Langley 1000 ft-lb-sec CMG will be examined. As a result of this, a preliminary design will be prepared which will optimize the performance of the gimbal actuator for this application. This preliminary design will include layout and outline drawings. The outline drawing shall include dimensioning for all interfaces with the NASA Langley CMG inner gimbal.

The gimbal actuator shall be capable of developing a maximum torque of ±175 ft-lb with either a torque or rate mode configuration. In addition to the specific requirements listed in paragraph 1.3.1 for the actuator optimization study, the design must also meet the following performance requirements:

Threshold torque	0.2 ft-lb
Output torque resolution	1.75 ft-lb

The actuator design will allow for modular-mounting or dismounting of the torquer, a tachometer generator and the complete actuator. It must also be interchangeable with the presently designed NASA CMG torquers.

1.4 GENERAL REQUIREMENTS

In addition to the above, some general requirements and other design objectives were dictated: such as, type of electrical power, reliability, environment and duty cycle operation.

1.4.1 Electrical Power

All phases of the study will be based upon the following types of electrical power:

DC — Regulated, 28 ± 0.5 volts

Unregulated, 24 to 31 volts

AC — 115/200 volts ± 2%

400 cps, three-phase wye

1.4.2 Reliability

A design objective of the CMG actuator will be a reliability of better than 0.99 for one year of continuous operation. With annual scheduled service, the minimum operational life shall be five years.

1.4.3 Environmental Requirements

The CMG actuator should be capable of continuous operation in the following environment:

Ambient temperature: 70°F to 120°F while operational

Pressure: 10^{-11} to 1.0 atmosphere (operational),

10^{-11} atmosphere (non-operational)

Radiation: negligible

Acceleration: 0 to 1g (operational)

1.4.4 Duty Cycle

The duty cycle of the CMG actuator will be assumed as follows:

1% of operation time — Full required torque

30% of operational time — One-half full required torque

69% of operational time — One-quarter full required torque

SECTION II

SUMMARY

2.1 PURPOSE OF STUDY

The purpose of this study is to determine optimal gimbal actuators for large double gimbal CMG's with angular momentums from 200 to 2000 ft-lb-sec. Electrical, hydraulic and pneumatic actuators, along with five different types of mechanical transmissions, were investigated with respect to power requirements, weight, size and complexity.

In addition to the actuator study, it is desirable to determine an optimal controller for driving the CMG actuator.

2.2 OPTIMIZATION STUDY AND PRELIMINARY DESIGN

An optimal actuator and controller was selected on the basis of minimum power consumption, minimum weight and size, maximum reliability and satisfaction of performance requirements. The actuator optimization is actually two studies: torquers and mechanical transmissions. Once the optimal torquers were selected, the transmission optimization study followed.

To demonstrate both physical and performance characteristics of a typically optimal actuator for the CMG application, a preliminary design of the actuator for the 1000 ft-lb-sec CMG size is developed. A layout drawing and tabulation of its performance characteristics are presented. A summary of the design's characteristics follows:

Design load torque	175 ft-lb
Design load velocity	0.175 rad/sec
Transmission gear ratio	60
Peak power consumption	43.1 watts
Duty cycle avg, power consumption	5.5 watts
Weight	23 lb
Envelope volume	380 cu in.
Reliability: 1 year	0.9741
2 months	0.9956
Threshold	3%
Actuator response	123 rad/sec
Damping factor	1.27

The major difference between this optional actuator design (175 ft-lb torque for the 1000 ft-lb-sec size) and that used for the NASA Langley CMG is the mechanical transmission. The actuator in this study uses an epicyclic transmission, while the one used on the NASA Langley CMG actuator is basically a simple two-stage planetary. The optimal actuator design has a number of significant advantages over the NASA Langley CMG actuator, mainly on the basis of the characteristics of the transmission used: namely,

(a) The number of teeth of each driven gear which are in engagement with its driver gear are much greater, thereby improving reliability.

(b) Lower Hertz stress in engaging teeth, thereby improving wear and life.

(c) Less overall weight.

(d) Smaller volume.

(e) Lower reflected moment-of-inertia back to the motor shaft, thereby minimizing problems in achieving response and dynamic stability.

(f) Higher gear ratios are available per gear pass (simple planetary is limited to 10 per stage).

Except for problems of switching high inductive loads and having high ripple torques, a DC brushless torque motor would be an optimal torquer. It has a lower threshold and potentially high reliability. But until this problem is solved, the DC torquer is considered optimum.

An excellent second choice for the mechanical transmission is the compound planetary transmission.

With regard to controller optimization, the single channel pulse width modulator was selected. An excellent alternate is delta modulation, particularly where a vehicle's attitude control system requires a digital computer for determining the desired torque output at each CMG's pivot.

The single channel pulse width modulation controller has the following characteristics for the 1000 ft-lb-sec CMG:

*Peak power consumption	50.9 watts
*Average power consumption	8.8 watts
Weight	2.5 ounces
Volume	2.5 cu. in.
Reliability (1 year, operational)	0.9775
(2 months, operational)	0.9962

*Including actuator power

2.3 RECOMMENDATIONS

The recommendations are that:

(a) The optimal actuator shall include a DC torquer and an epicyclic transmission.

(b) The optimal controller be a single channel pulse width modulator.

(c) Delta modulation be considered as an alternate controller when a digital computer is used for resolving torque commands at each CMG pivot.

(d) Brushless DC torquers should be considered for CMG gimbal actuation in the future when it may be closer to being established as "state-of-the-art".

SECTION III

APPROACH

The approach to the CMG actuator study is summarized in Figure 2. As previously described, the program was divided into three major categories:

(a) Actuator optimization

(b) Controller optimization

(c) Preliminary CMG actuator design

The actuator optimization is actually divided into two distinct studies: torquers and transmissions. As shown in Figure 2, all types of electrical, hydraulic and pneumatic torquers or motors were evaluated in a preliminary sense. This was to eliminate any torquers which were obviously inadequate for this CMG application before selecting an optimal torquer-type. This evaluation, which was based upon power required, weight, size, reliability, and performance, is presented in Section IV.

A number of transmission types for the CMG actuator application were also studied, namely: spur gears, simple planetary, compound planetary, epicyclic and the harmonic drive. The study was made for five different actuator torque outputs: 35, 87.5, 175, 262, and 350 ft-lb. The transmissions were evaluated on the basis of weight, volume, reflected moment of inertia to torquer, efficiency, threshold and backlash as a function of torque output and gear ratio. This study is made in Section V.

Other aspects of the actuator optimization are given in Section VI. Once the torquer and transmission types have been selected, the actual torquer type and size and the transmission sizing are determined for the five actuator sizes. Final characteristics of the five actuators are then tabulated.

Controller candidates for the optimum actuators are described in Section VII. They include the following:

(a) DC proportional

(b) Pulse width modulation, single channel (PWM_1)

(c) Pulse width modulation, double channel (PWM_2)

(d) ON-OFF

(e) ON-OFF with two gain levels

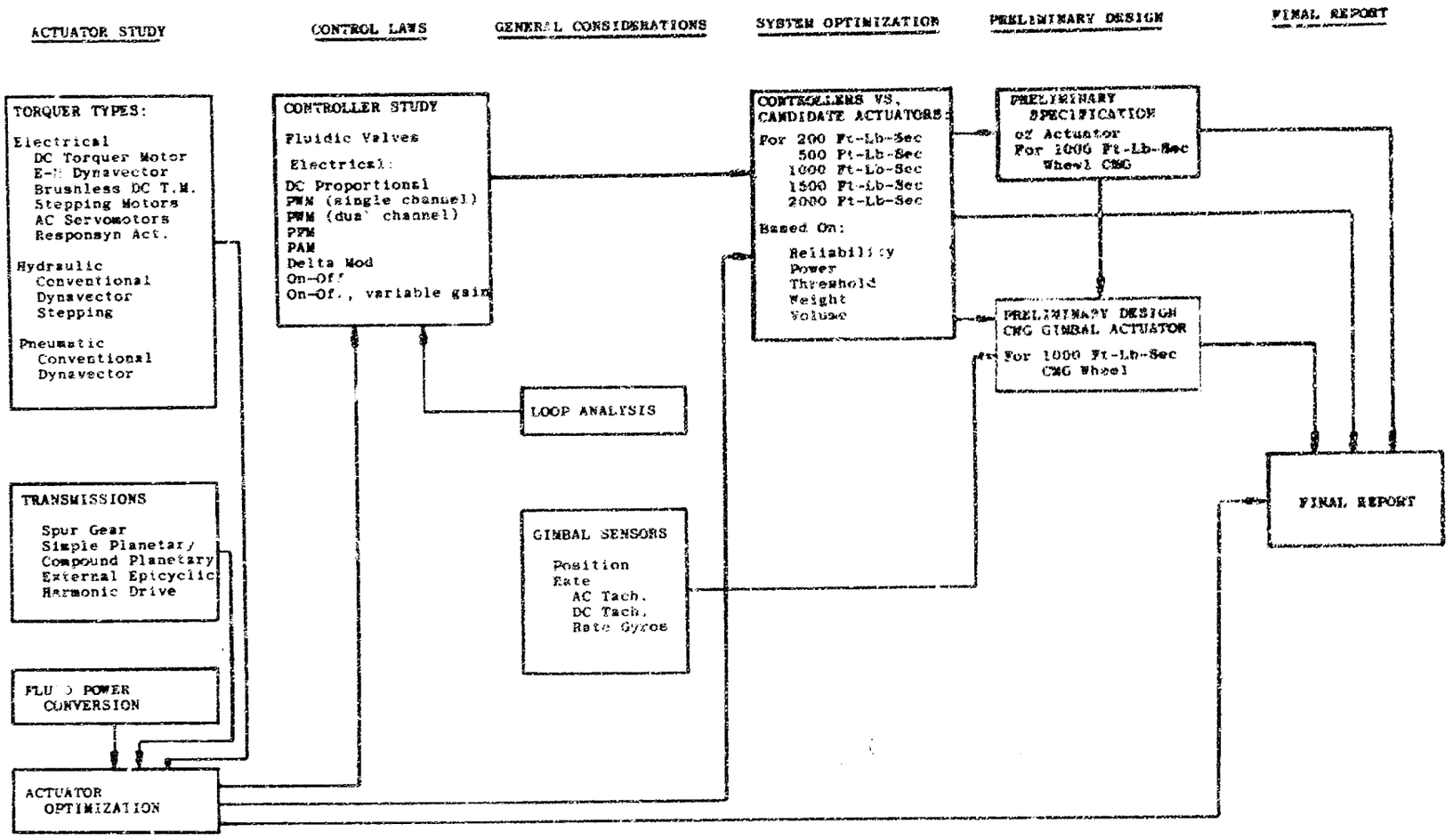

Figure 2. Approach to the CMG Actuator Study

(f) Pulse amplitude modulation

(g) Pulse frequency modulation

(h) Delta modulation

Power dissipation, reliability, threshold, weight and volume are determined for all eight controllers in Section VIII. Final selection of the optimal controller is made in Section IX, where the optimal actuator is also reviewed.

A preliminary design of a 175 ft-lb CMG actuator can then be made on the configuration determined in the optimization study.

Included in the design are the selected torquer, transmission, tachometer generator and associated hardware for mounting to the structure and gimbal. A layout drawing and an outline drawing are then prepared. This preliminary design is presented in Section X.

Three appendices are needed to support the preliminary design of the CMG actuators is in Appendix A. A study of the types of gimbal displacement and rate sensors is given in Appendix B. Appendix C contains a brief analysis for the selection of bearings for the actuator design.

SECTION IV

PRELIMINARY TORQUER EVALUATION

4.1 SUMMARY

The results of the initial phase efforts indicated that the DC torquer motors were optimal candidates for control moment gyroscope, gimbal actuator application. Brushless DC torquer motors, electromagnetic harmonic drives, and electromechanical DYNAVECTOR* are included in the broad category of DC torquer motors. However, these latter three types are generally not state-of-the-art. Currently, commutation and the required control electronics are the common problems associated with all three types.

The graphical power and weight results of this section indicate the total requirements of two actuators per CMG, one for each axis. Throughout the remainder of the report, all parameters are presented on a per actuator basis.

4.2 EVALUATION CRITERIA

4.2.1 Elementary Actuator Operation

Each double gimbal gyroscope has two actuators, one for the outer gimbal and one for the inner gimbal. The function of the actuators are twofold, but both functions are not required simultaneously on any one actuator. The first function is to exert torques at stall. The second function is to provide gimbal rates with inertia and friction loading only. The actuator that is not exerting stall torque is required to provide rates proportional to the stall torque exerted by the other actuator of a double gimbal gyroscope.

The data presented in this section illustrate the total requirements for two actuators per CMG.

4.2.2 Basic Assumptions

The control moment gyroscope size iterations used in the study are the 200, 500, 1,000, 1,500 and 2,000 ft-lb-sec sizes. The specification used as a guide was "Specifications for Control Moment Gyroscope," NASA Specification No. L-5298, dated 2 August 1965.

4.2.3 Evaluation Considerations

Primary considerations for the initial qualitative study of actuators are average power demand to meet steady-state torque-speed requirements of the load,

---

*DYNAVECTOR is a registered trade name of The Bendix Corporation

physical size and weight, efficiency and system complexity. The secondary considerations for the preliminary evaluation are gross limitations on expected response under rate mode of operation. The purpose of this phase of the study was to eliminate specific types of torquers having gross limitations in application to the control moment gyros.

For purposes of uniformity, the transmission weight estimate per actuator was equalized for all actuator types as a function of maximum transmission output torque T_{LM}. The assumed expressions for external transmission weights used were:

For ratios between 15 and 100:1

$$W = 0.029 \text{ lb/ft-lb } T_{LM} + 3.5 \text{ lb} \quad (4\text{-}1)$$

For ratios between 100 and 200:1

$$W = 0.035 \text{ lb/ft-lb } T_{LM} + 4.2 \text{ lb} \quad (4\text{-}2)$$

These two expressions are empirically formulated because of the scarcity of the required data. The formulation included application of engineering judgement since transmission weight data available included the weight of the housing, and, further, the bearings and gear face widths were not directly applicable to the life requirements of the CMGs. These equations, though not rigorously justifiable, served a useful purpose in permitting the use of a common transmission baseline for comparing the various torquer types, and permitting the completion of the preliminary qualitative evaluation.

The weights of the electromechanical and hydraulic DYNAVECTORS were estimated from data made available by the DYNAVECTOR program currently being conducted by The Bendix Corporation.

For purposes of the preliminary evaluation, the transmission efficiency was assumed to be 90 percent.

The torque-speed requirements of the gimbal actuators are defined for the five CMG sizes under consideration, with maximum speed being common for all sizes at 0.175 rad/sec and stall torque being the CMG size times the maximum speed. The minimum speed capability required is 0.000175 rad/sec. Other pertinent specifications derived during this study are illustrated in Appendix A.

The average steady-state operation power requirements per CMG derived in this study were based on the following load distribution:

$$\frac{P_{avg}}{CMG} = 0.1(P_{T1} + P_{S1}) + 0.30(P_{T2} + P_{S2}) + 0.69(P_{T3} + P_{S3}) \quad (4\text{-}3)$$

where

P_{T1} = power required at maximum torque

P_{T2} = power required at 0.5 of maximum torque

P_{T3} = power required at 0.25 of maximum torque

P_{S1} = power required at maximum speed

P_{S2} = power required at 0.5 maximum speed

P_{S3} = power required at 0.25 of maximum speed

Equation (4-3) states that the average power required for a two actuator CMG is the sum of the average power required to provide the stall torques above by one actuator and the average power required to provide proportional speed by the other. This arbitrary load distribution is slightly more stringent than that distribution used in the "Control Moment Gyroscope Design Report" prepared for NASA/Langley Research Center by Eclipse-Pioneer Division, dated 1 November 1965.

The response of the actuator can be obtained by considering that under the rate mode of operation, the actuator transfer function will have either of the following forms:

Single Order:

$$\frac{N_L(S)}{Em(S)} = \frac{1}{1+S\tau} \tag{4-4}$$

Second Order:

$$\frac{N_L(S)}{Em(S)} = \frac{\omega_n^2}{S^2 + 2\tau\omega_n S + \omega_n^2} \tag{4-5}$$

If a single order transfer function governs the actuator, then the required τ must be 0.05 seconds. However, if a second order transfer function governs the actuator, the step response must be within ±3 percent of the final value within the same time interval that a single order system with a time constant of τ = 0.05 seconds reaches 97 percent of its final value. The required settling frequency of the second order system must also be less than 100 cps. The required time to reach ±3 percent of final value for both types is 0.175 seconds. For a second order system with an assumed

$\zeta = 0.7$, this corresponds to a natural frequency ω_n of 5 cps and a settling frequency of 3.5 cps, which is considerably less than the required 100 cps.

Under torque mode of operation, ±3 percent of final value within 0.175 seconds is not stringent, and therefore is not considered to be a response problem.

4.3 PARAMETERS OF INDIVIDUAL ACTUATOR TYPES

4.3.1 Electric

4.3.1.1 DC Torquer Motor

DC torquers were sized to meet the maximum torque and maximum speed requirements and also to minimize the difference between the maximum and minimum suitable gear ratio. The suitable gear ratios were tabulated using various DC motors for each of the five separate actuator requirements. The optimum fixed gear ratio was estimated to be in the range of 100:1 to 200:1 with the higher gear ratio requirement for the smaller CMG sizes.

Table I illustrates the motors and transmission ratios considered, and the preliminary data on weight and volume.

The resulting gear ratios of several CMG sizes were higher than 200:1. Subsequent discussions with the motor manufacturer indicated that minor modification of motor internal construction details would result in a change in the slope of the motor's torque-speed curve, without materially altering the motor's external configuration or package weight. The resulting increase of the motor's stall torque capability permitted slight reductions of the overall gear ratio.

The motor sizing criteria used were:

(1) Minimum actuator weight consistent with required performance.

(2) Transmission ratio of 200:1 or less

(3) The product of maximum motor speed and motor stall torque must be greater than the maximum load stall torque squared divided by the slope of the load torque-speed curve. Expressed mathematically

$$N_{M_{max}} \times T_{MS} > \frac{T_{LM}^2}{M_L}$$

The final selected ratios for each CMG size are shown in Table II.

TABLE I

TABULATION OF DC TORQUER MOTORS AND TRANSMISSION RATIOS

Description																				
J_L (ft-lb-sec^2)	0.4				1.35				2				2.6				2.75			
T_{LM} (ft-lb)	35				87.5				175				362				390			
M_L (ft-lb-sec + Oz-in Momentum)	200				500				1900				1500				2600			
T^2_{LM}/M_L (ft-lb/sec)	6				14.8				38.6				66				61			
Motor No. (Model)	T-1342	T-2157	T-2170	T-2171	T-4412	T-7207	T-7203	T-2171	T-6036	T-7203	T-10036	T-2950	T-5134	T-7203	T-10036	T-5603	T-5730	T-7203	T-10036	T-4601	T-5139
$M_{M_{MAX}}$ (T_{MS}) (ft-lb-rad/sec)	20	16	24	28	42	130	180	28	48	180	360	35	90	180	360	45	120	180	700	70	60
Weight (lb)	0.6	0.6	0.9	1.5	1.5	11.5	22	1.5	3	22	60	2	5.7	125	60	1.31	8.2	22	110	0.75	8.5
O.D. (in)	1.9	2.8	2.8	2.8	5.12	9	9	2.8	5.1	9	13.5	2.73	6.2	9	13.7	6.12	7.2	9	13	5.12	6.25
Length (in)	0.84	0.62	1.0	1.5	0.6	1.6	2.5	1.5	1.25	2.5	5.5	1.34	1.3	2.5	5.6	0.67	1.6	2.5	5.4	0.56	1.56
J_M (ft-lb-sec^2 x 10^{-5})	0.010	0.656	0.097	0.115	0.53	8.4	17	0.115	0.76	17	60	0.32	2	17	60	0.63	5	17	170	0.08	3
$T_{MS}/M_{M_{MAX}} * M_M$ (ft-lb-sec x 10^{-5})	0.12	0.6	2.8	7.3	12	274	478	7.3	36	678	1360	158	111	430	1360	11	160	476	6500	1	165
Transmission Ratio																					
R_Q min to meet $M_{L_{MAX}}$	2280	942	428	312	345	134.3	115	318.5	210	115	85	274	128	114	85	378	154	114	44	890	125
R_Q min to meet T_{LM}	681	334	164	87.5	121.9	14	9.25	218	130	18.5	9	235	105	27.8	13	349	79	37	7	680	109
Selected R_Q	--	--	370	--	--	--	--	220	--	--	--	240	110	--	--	--	--	--	--	--	110
Transmission																					
No. of stages	3	3	3	2	2	1	1	3	2	3	1	3	2	2	2	3	2	2	1	3	2
Weight (lb)	4.5	4.5	6.0	3.5	6.5	3.0	5.0	7.5	4.5	6.5	5.0	7.5	6	6	6	9	9	9	7	13	9
Length (in)	3	3	3	2	3.5	2	2	3	3	3	2	4	3	3	3	4	3.5	3.5	3	4.5	3.5
Actuator Total																					
Weight (lb)	5.1	5.1	6.9	5	8	16.5	27.0	9	9.5	28.5	65	9.5	13.7	19.5	66	11	17.2	31	117	14	17.5
O.D. (in)	4	4	4	4	6	10	10	6	6	10	15	4.5	7.5	10	15	7.5	8.5	10	15	7	8
Length (in)	3.8	3.6	4	3.5	3.5	4	5	4.5	5	6.5	6	5.6	5	6.5	7	5	6	7	9.5	6	5.5
Volume (in^3)	--	--	48	--	--	--	--	126	--	--	--	80	220	--	--	220	280	--	--	--	--

J_L = Load Inertia
J_M = Motor Inertia
M_L = Load Torque-Speed Curve Slope
M_M = Motor Torque-Speed Curve Slope
$M_{M_{MAX}}$ = Maximum Motor Speed
R_Q = Transmission Ratio
T_{LM} = Maximum Transmission Output Torque (Stall Torque)
T_{MS} = Maximum Motor Stall Torque

TABLE II

TABULATION OF SELECTED MOTORS AND GEAR RATIOS

C M G Size	Inland Model Number	Gear Ratio
200	T-2170	160
500	T-2171	200
1000	T-2950	200
1500	T-5134	100
2000	T-5135	100

The average power (P_{avg}) required for the DC torquer was based on the load distribution given in equation (4-3). The average value is given by the following integration:

$$P_{avg} = \frac{1}{\tau} \int_0^{\tau} P(t)\, dt \qquad (4\text{-}6)$$

where t is time, τ is the period of operation, and P (t) the instantaneous power.

Since the power, P, required in a DC motor at stall is pure I^2R loss, using equation (4-6)

$$P_{avg} = \frac{R}{\tau} \int_0^{\tau} (I(t))^2\, dt \qquad (4\text{-}7)$$

For DC torquer motors,

$$I_M = \frac{T_m}{K_T}$$

Since the assumed loading is given in three discrete steps, the value of P_{avg} per actuator can be obtained from the following summation:

$$P_{avg} = \frac{R}{\tau} \sum_{n=1}^{3} \left(\frac{T_m}{K_T} \right)_n^2 \Delta t_n \qquad (4\text{-}9)$$

$$P_{avg} = R \left[0.01 \left(\frac{T_{max}}{K_T} \right)^2 + 0.3 \left(\frac{0.5\, T_{max}}{K_T} \right)^2 + 0.69 \left(\frac{0.25\, T_{max}}{K_T} \right)^2 \right] \qquad (4\text{-}9)$$

$$= R \left(\frac{T_{max}}{K_T} \right)^2 (0.1281)$$

$$P_{avg} = I_{max}^2 \; R \; (0.1281)$$

For two actuators, assuming the same duty cycle on each, the total average power required per CMG [Reference: equation (4-3)] becomes:

$$P_{avg}/CMG = 0.26 \; I_{max}^2 \; R \qquad (4\text{-}10)$$

Actuator parameters using DC torquer motors for a double gimbal CMG are illustrated in Figure 3 as a function of CMG size.

4.3.1.2 Electromechanical DYNAVECTOR Actuator

The information presented in this paragraph was extracted from scaling factor data made available by the DYNAVECTOR efforts currently being conducted by The Bendix Corporation. The volume, weights and power consumption, as a function of CMG size, are shown in Figure 4. The weight and volume requirements of the associated commutation circuitry have not been included in the data illustrated in Figure 4.

The transmission ratio used was 840:1. No external transmission was required since this ratio is integrated with the electric DYNAVECTOR. In general, the system weight tends to decrease as the transmission ratio is further increased. However, with very high transmission ratios, the transmission life is decreased by the high velocities of some of the transmission parts. If very high transmission ratios are used, the system should have a two-ratio transmission with a clutching or shifting mechanism to reduce the transmission ratio for high speed operation. Transmissions with the ratio selected should be capable of long life and would not require a clutch.

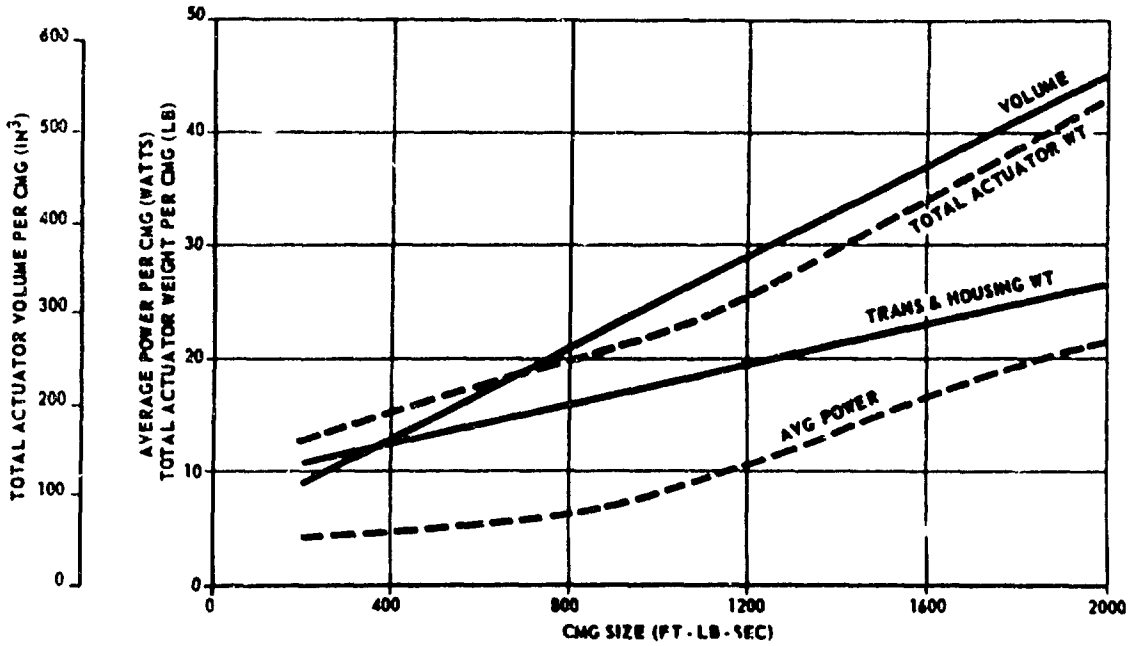

Figure 3. DC Torquer Actuator Parameters

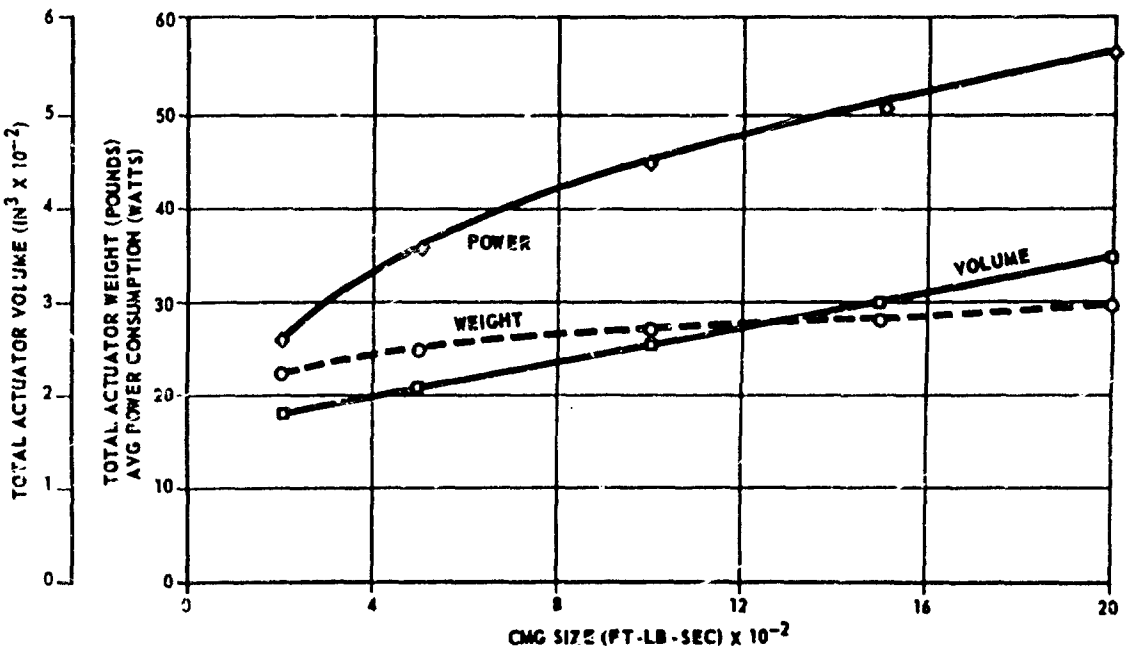

Figure 4. Electromechanical DYNAVECTOR Actuator Parameters

4.3.1.3 Brushless DC Torquer Motors

In general, brushless torquer motors are very similar to brush-type DC torquer motors when comparing motor weight, size, and efficiency alone. The primary disadvantage is a total package weight of motor and necessary commutating mechanism which, for units that have been built, cause the total motor weight to be as great as two to three times the equivalent brush-type DC torquer motor weight. A second disadvantage is the ripple torque present on the output shaft. This ripple has variations on the order of ±10 percent with present technology. Advantages of brushless units are lower friction torque and potentially higher reliability.[1]

4.3.1.4 Stepping Motors

Slo-Syn synchronous motors require 100 or 200 input power steps per shaft revolution. The stall torque values are between 0.1 ft-lb and 10 ft-lb. The maximum output speeds vary between 12 and 60 rpm. The size of the units range from 7 in^3 to 230 in^3, respectively. The larger (10 ft-lb, 12 rpm) unit would be suitable for the 400 ft-lb-sec CMG when used with a gear ratio of 7, but the volume (230 in^3) of the stepping motor alone far exceeds that of the actuator using a DC torquer motor having a volume of 80 in^3 at this particular CMG size. A second disadvantage is the variation in torque at stall, dependent upon shaft position. The major advantage is that control methods are suitable for maintaining constant speeds with variable loads; however, the size of these would be considerably larger than DC torquer motors for the given application. From the size standpoint, the Slo-Syn synchronous motors should be eliminated from further consideration for this application.

4.3.1.5 AC Servomotors

In general, to meet torque-speed requirements with AC servomotors, the required gear ratios would be between 270 and 4500:1. One Kearfott size 40 AC, 28 volt, 400 cps motor has the required torque-speed combination with 2700:1 gear ratio for the large CMG and weighs 5 pounds for the motor only. This gear ratio indicates a very good possibility of poor response capabilities and, consequently, would not be as suitable for this application as the DC torquer motors. Power servomotors from Diehl Manufacturing Company are not suitable, because frequency response characteristics, are below 2.6 cps for 400 cycle AC units. The 400 cycle AC instrument servo would require gear ratios of 4500:1, and motor frequency response would be limited to about 2 cps. This would eliminate this type of servo from further consideration.

---

[1] See Reference No. 1, Appendix D

4.3.1.6 *RESPONSYN Actuator

Servo actuators designated as RESPONSYN actuators have been built by the United Shoe Machinery Corporation, Beverly, Massachusetts. These units employ a rotating magnetic field which deflects the flex spline of a harmonic drive transmission. One of two design variations could be utilized. One approach utilizes an integrated motor and harmonic drive transmission and is designated as the EHD. The second approach uses an external transmission in addition to the integrated package and is designated as the EHD/Tx.

RESPONSYN actuators are available with stators having distributed windings for operation as synchronous motors or with stators having discrete windings for operation as stepping motors. The current state-of-the-art includes two RESPONSYN actuator sizes that are past the development stage. They are the 6 and 120 in-lb sizes. Other sizes have been built for special applications.

Table III illustrates data furnished by the manufacturer. The following requirements were used in the sizing estimate:

(1) Stall torque -	0.175 x CMG size
(2) Maximum output speed -	2 rpm
(3) Operating voltage -	30 VDC
(4) Cooling -	without external fans

The estimates presented in Table III are not fully optimized for this application, but are useful for comparative tradeoff purposes throughout the CMG size range. The weight, power and size estimates are for the RESPONSYN actuator alone, excluding electronics for controlling the field in the stator and the required external transmission for EHD/Tx approach.

The approximate dimensions of a stepping actuator that was built for a special application[2], are a cylinder having a 4-inch diameter and 4-inch length connected to another cylinder having an 8-inch diameter and 4-inch length. Its weight is only 22 pounds (as compared with 180 pounds for the size 500 CMG submitted by the manufacturer). This unit had an overall efficiency of 35 percent, a maximum output speed of 18 rpm, and a holding torque capability of 100 ft-lb. The size, weight and power consumption requirements of the motor commutation electronics packages were not supplied by the manufacturer and are not included in the above data.

---

*RESPONSYN actuator is a catalog term used by the Harmonic Drive Division, United Shoe Machinery Corporation.

[2]See Reference No. 2, Appendix

TABLE III

RESPONSYN ACTUATOR DATA

C M G Size (ft-lb-sec)	200	500	1000	1500	2000
Weight					
EHD Motor (lbs)	70	180	350	510	690
EHD/ Tx Motor only (lbs)	0.6	2.6	7	13	20
Power					
EHD @ max stall torque (watts)	520	960	1500	1940	2400
EHD/ Tx @ max. stall torque (watts)	22	56	110	160	220
Power at maximum speed is approximately 1/4 of the power at maximum stall torque					
Size					
EHD Motor					
Diameter (in)	9.5	12	14	15.5	17
Length (in)	14	18	22	23	25
EHD/Tx Motor only					
Diameter (in)	2.5	3.5	5	6.5	8
Length (in)	3.7	5	7.5	9.7	12
Additional Requirements					
External Transmission Ratio using the EHD/Tx Approach	80	35	25	20	18

4.3.2 Hydraulic Actuators

4.3.2.1 Conventional Systems

There are several basic types of hydraulic actuation systems that could be considered as possible candidates for application to the CMG. Among these are the constant flow system, the servo pump system and the servovalve system.

Constant flow systems as shown in figure 5 were discarded from further consideration as candidates for the CMG. Their operation is poorly adapted to application to two or more independent systems operating simultaneously from the same supply. This is especially true for the CMG, where one gimbal operates under low pressure, high flow conditions (rate control), and the other gimbal operates under high pressure, low flow conditions (torque control).

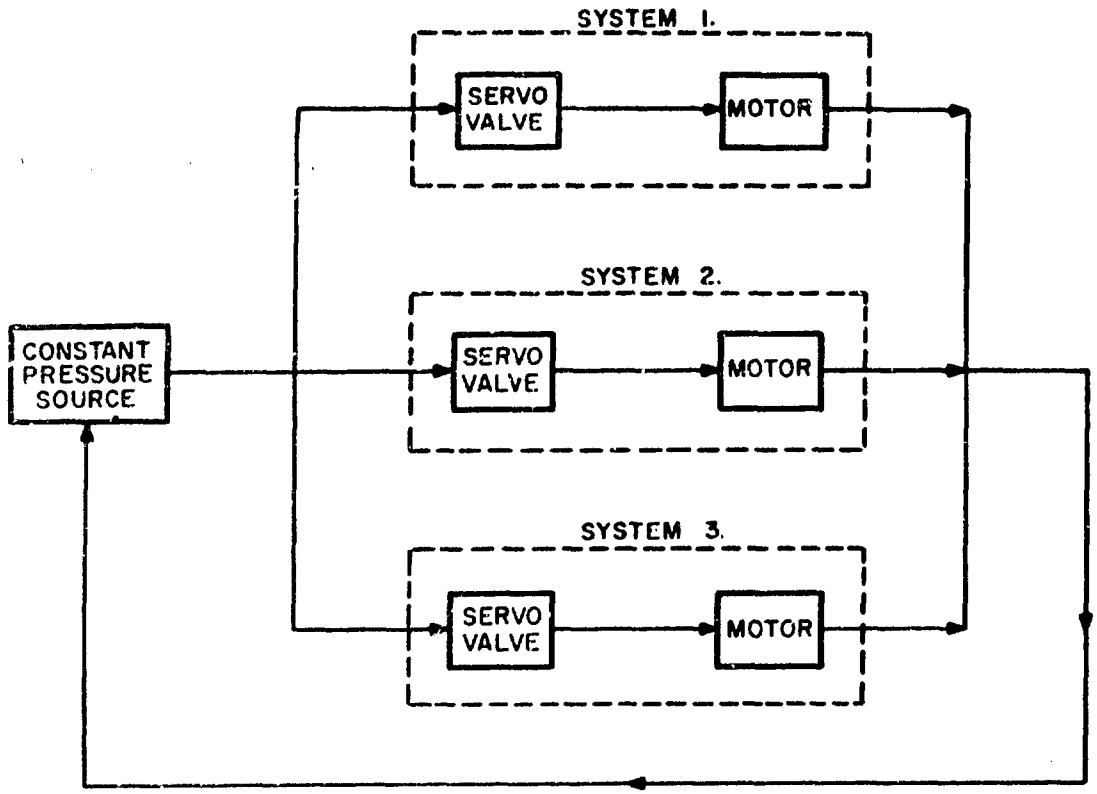

Figure 5. Hydraulic Power Supply with Constant Flow

The electrical system analogy of the constant flow hydraulic system is constant current operation. The constant flow system would be sized to provide the high flow requirement of one gimbal and the high pressure requirements of the second gimbal. The resulting extra auxiliary control equipment increases overall weight and decreases reliability. Furthermore, the operation of such a system is very inefficient in overall power consumption, and would be very nonlinear. Servo performance characteristics would at best be only fair.

Variable displacement pumps or servo pumps also were not considered for several reasons. The servo pump power efficiency is greater than servovalve efficiency on a single axis system comparison basis. However, for the CMG, two axes must be connected to a single servo pump or one servo pump must be used with each gimbal. An example is shown for a constant pressure system in figure 6.

Since use of multiple servo pumps (one per axis) is not practical from the size and weight viewpoint, a single servo pump must be used for each CMG. This servo pump would be sized to provide the peak pressure requirements. Load flow requirements, within the range of maximum demand required by the load profile, would be obtained by varying pump displacement. Auxiliary equipment in the form of

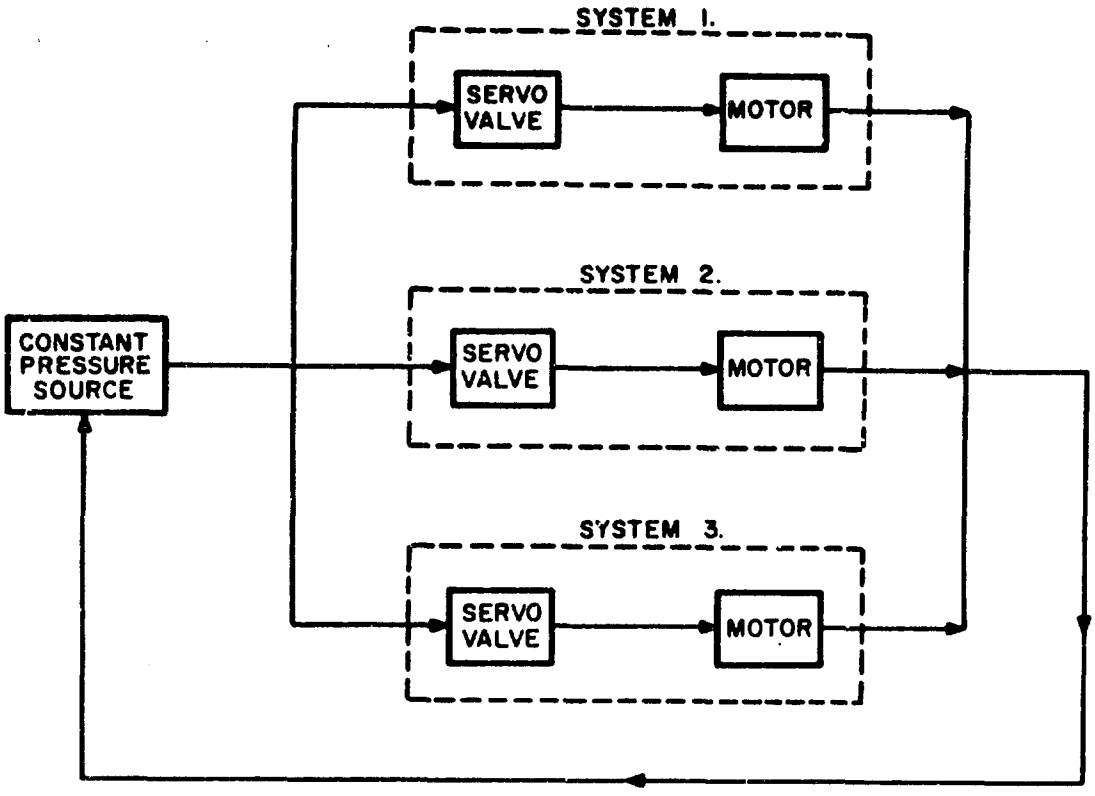

Figure 6. Hydraulic Power Supply with Constant Pressure

pressure reducing valves and switching valves would be required to implement the control circuit. Use of pressure reducing valves would lower the overall power efficiency capability of the servo pump. The extra equipment adds additional weight and physical size requirements, and reduces reliability. Finally, the larger volume of fluid under compression in the servo pump system lowers the "hydraulic spring" rate, and gives a low control response. This response generally is several times lower than an equivalent servovalve system.

A servovalve controlled hydraulic actuating system (See figure 7) for the CMG would, in general, consist of the following elements:

(1) Servovalve

(2) Rotary actuator

(3) Transmission

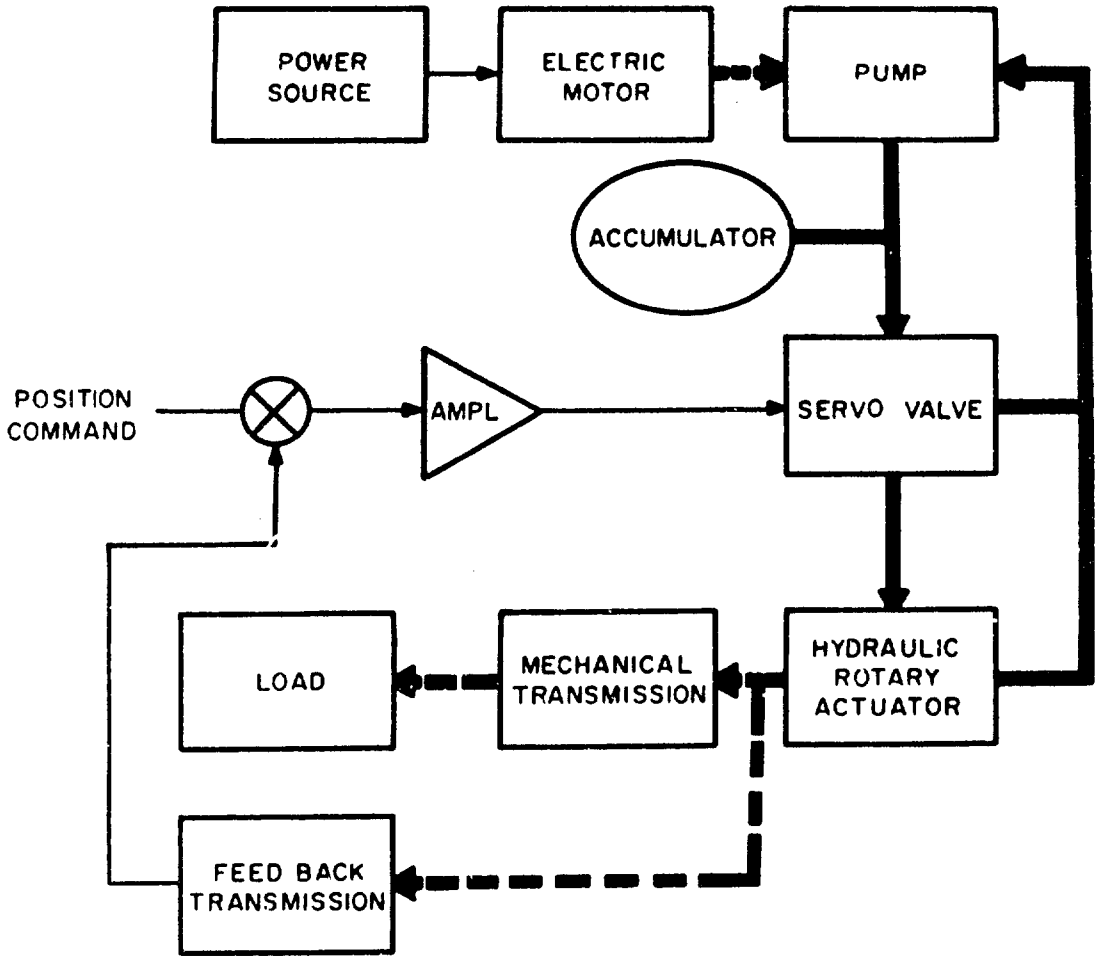

Figure 7. Servovalve Controlled Hydraulic Actuator System

(4) Auxiliary Power Unit (A. P. U.) consisting of:

(a) Electric motor

(b) Pump

(c) Accumulator

(d) Reservoir

(e) Valves, fittings, lines, etc.

Unless a suitable hydraulic power supply is available, the penalties of added weight and sacrifices in efficiency and reliability incurred in the conversion from electrical to hydraulic power must be charged to the hydraulic actuators.

The fact that the proposed units will operate over extended periods of time precludes the possibility of operating the system entirely from a charged accumulator. An optimum actuator would most likely contain an A.P.U. consisting of a motor-pump-accumulator with suitable on-off controls to meet the average and peak power demands of the system.

Preliminary considerations of system characteristics seem to indicate the need for certain redundancies if the hydraulic actuator is to meet the reliability requirements of a mission of this nature. The electric driving motor possesses sufficient reliability potential, and, because of stringent weight requirements, would not be duplicated. However, it is felt that two pumps should be provided. One pump would be held on a standby basis and would be clutched to the common electric motor in the event that the primary pump were unable to maintain system pressure. Simultaneous declutching of the primary pump would also be required. An over-running type mechanism could be designed to accomplish this task.

Standby redundancy of the hydraulic actuator would be desirable from a reliability standpoint but would be difficult to implement without introducing excessive weight and unbalance to the system at the load.

Duplication of the servovalve would most likely not be justified by the small resultant increase in reliability since a valve inactive for long periods of time would be susceptible to seizing.

The criteria of evaluation are limited to torque-speed capability, power consumption based on an average torque of 33 percent of maximum torque and an average speed of 33 percent of maximum speed [Reference: equation (4-3)], system weight and system response. Hydraulic systems are well known for their response capabilities. Consequently, response was not considered at this time.

The preliminary evaluation of an actuator for the large (2000 ft-lb-sec) CMG actuators will be carried out in some detail and will serve to illustrate the method used for evaluation of all five CMG sizes. Graphical results are presented for all sizes.

The ±360 degree and ±80 degree outer and inner gimbal rotation requirements, and the interchangeable actuator requirements for both gimbals eliminates any of the rotary types available which are not capable of meeting this requirement, and indicates the use of a vane or piston-type continuous rotation motor. Figure 8 shows a functional diagram of a reversible vane motor. One example of a piston-type motor is the cam piston motor shown in figure 9. Gear types, as shown in figure 10, were not considered because of their relatively large leakage at stall condition.

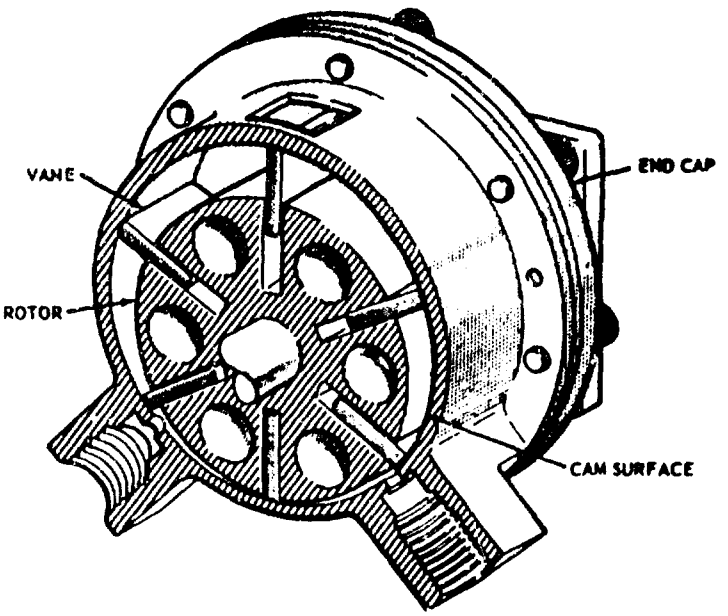

Figure 8. Schematic - Reversible Vane Motor

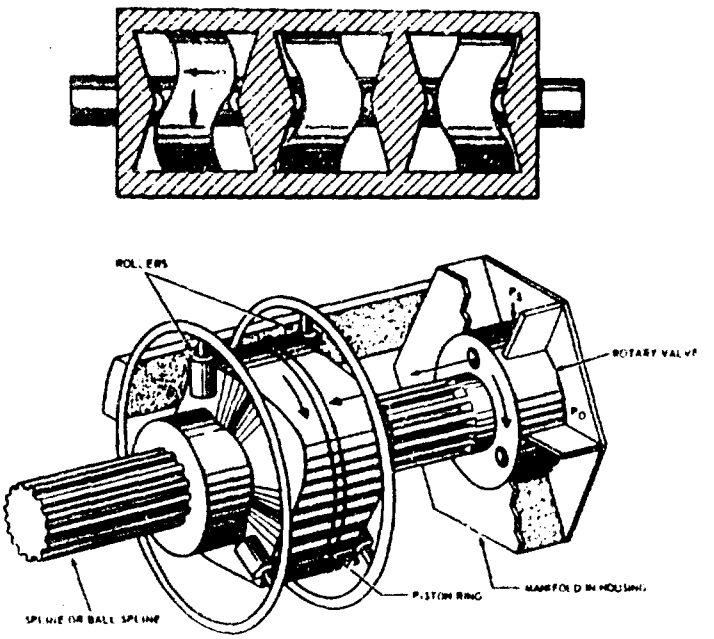

Figure 9. Cam Piston Motor

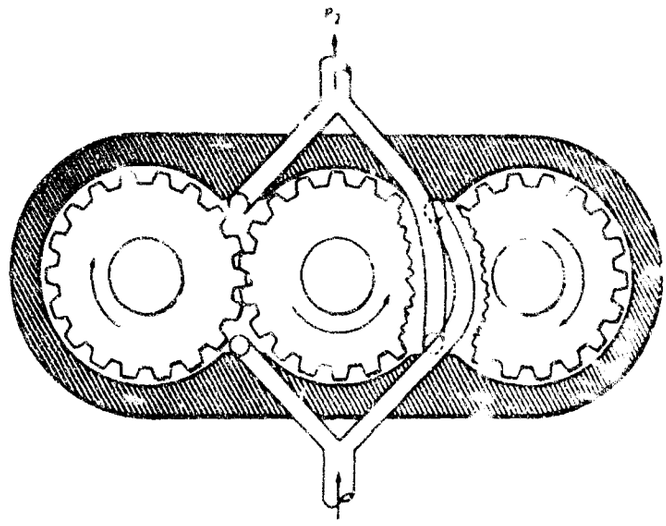

Figure 10. Gear Motor

The minimum open servo loop smooth speed of hydraulic vane and piston-type motors is estimated by motor manufacturers to be in the range of 5 to 10 rpm. This minimum range capability is primarily due to the combined effects of coulomb friction, imperfect motor displacement per revolution, and differences in motor leakage as a function of output shaft position. Use of well compensated servo control loops will permit smooth closed-loop operation as low as 0.1 rpm. Using this closed loop low speed practical limit, the minimum reduction ratio would be 60, and the minimum smooth, closed-loop output speed of the actuator would be 0.000175 rad/sec.

The displacement flow power required by a hydraulic motor is given by:

$$P_A = K\Delta p\ D_m\ R_G\ N_m \qquad (4\text{-}11)$$

where

P_A = displacement flow power (watts)

Δp = differential pressure (psi)

D_m = motor displacement (in^3/rev)

R_G = gear ratio (dimensionless)

N_m = output speed (rev/sec)

K = dimensional constant = 0.113 watt-sec/in-lb

The minimum value of R_G has been determined from the motor limitations, and N_m is fixed by the output speed specifications.

Neglecting leakage, no power would be dissipated by one actuator at stall since no flow is required. The entire power dissipation would take place in the second actuator.

If N_m in equation (4-11) is taken as $N_{avg} = 0.33\ N_{max}$, equation (4-11) becomes the expression for the average ideal power dissipation of the actuators, and

$$P_A = (0.113)\ \Delta p\ D_m\ R_G\ (0.33)\ (0.0279\ \text{rev/sec})$$

or

$$P_A = 10.4 \times 10^{-4}\ \Delta p\ D_m\ R_G \qquad (4\text{-}12)$$

The minimum differential pressure at which a hydraulic motor can produce torque T_{max} (in this case, 350 ft-lb or 4200 in-lb) is given by:

$$\Delta p_{min} = \frac{2\pi T_{max}}{D_m R_G} \qquad (4\text{-}13)$$

Combining equations (4-12) and (4-13) yields:

$$P_A = 10.4 \times 10^{-4}\ (2\pi T_{max})\ \text{watts} \qquad (4\text{-}14)$$

where

T_{max} is in in-lb

It is seen from equation (4-14) that the average power dissipated in the actuator for a hydraulic system is a function of the level of stall torque only; thus, the selection of values of Δp, D_m, and R_G must be based on considerations other than minimizing the average ideal power dissipation.

The total average power consumption of the system can be written as:

$$P_T = P_A + P_L + P_m \tag{4-15}$$

where

P_T = total average power consumption of the actuator system for a single CMG (watts)

P_A = ideal power required by the actuators (watts)

P_L = leakage flow power (watts)

P_m = mechanical losses (watts)

For the selection of any combination of values of D_m, Δp, and R_G, which satisfy the maximum torque requirement in equation (4-13), the P_A term in consumption indicates selecting Δp, D_m, and R_G to minimize the system leakage loss term P_L. Since leakage flow is proportional to the differential pressure across an element, it can be minimized by selecting a system pressure as low as possible while not compromising torque demand.

A system pressure of 500 psi was selected. While pressures lower than 500 psi would decrease leakage flow, motor physical size and weight would increase since a larger motor displacement would be required to offset the reduced pressure. The optimum system is in the 500-psi range when both the overall weight and the total power demand are considered.

With the supply pressure fixed, the selection of D_m and R_G can be made on the basis of minimum weight. The minimum gear ratio has already been determined as 60 and the stall torque as 4200 in-lb. By rearranging equation (4-13), the following relationship results:

$$D_m R_G = \frac{2\pi T_{max}}{\Delta p} \tag{4-16}$$

It is seen that increasing R_G permits the use of a smaller and lighter motor. Under the transmission assumption made in equation (4-1), the weight of the transmission, for a particular stall torque value, is constant for ratios to 100. In this case, the transmission weight would be 13.5 pounds. Thus, a ratio of 100 may be used without an additional increment of weight. Using equation (4-16) with $R_G = 100$, the necessary minimum motor displacement is 0.528 in^3/rev.

A suitable motor would be the Vickers Model 911 aircraft-type axial piston motor which has a displacement of 0.598 in^3/rev and a weight of 6.8 pounds.

Substituting the selected values of D_m, R_G and Δp into equation (4-12) yields an average ideal actuator power dissipation of 31.7 watts.

Suitable miniaturized servovalves are manufactured by Bendix Corporation, Lear-Siegler, and Moog Servo Controls, among others. Sales literature indicates the weight of such a valve to be approximately 1/3 pound. A four-way servovalve is shown in figure 11. This servovalve is usually used as a second-stage for an electrically energized low level valve, such as a flapper valve. An electrical or mechanical feedback from the four-way second stage valve to a low-level first stage valve is usually packaged as one complete servovalve.

No data is immediately available on suitable hydraulic power units since these are nonstandard items. Conversations with manufacturers of similar equipment indicate that, for the purposes of this study, 25 pounds might be a reasonable estimate of the weight of such a unit. In arriving at a system weight per CMG, it was assumed that 3 gyros will be supplied from the same A.P.U. and therefore 1/3 of the weight was charged to each.

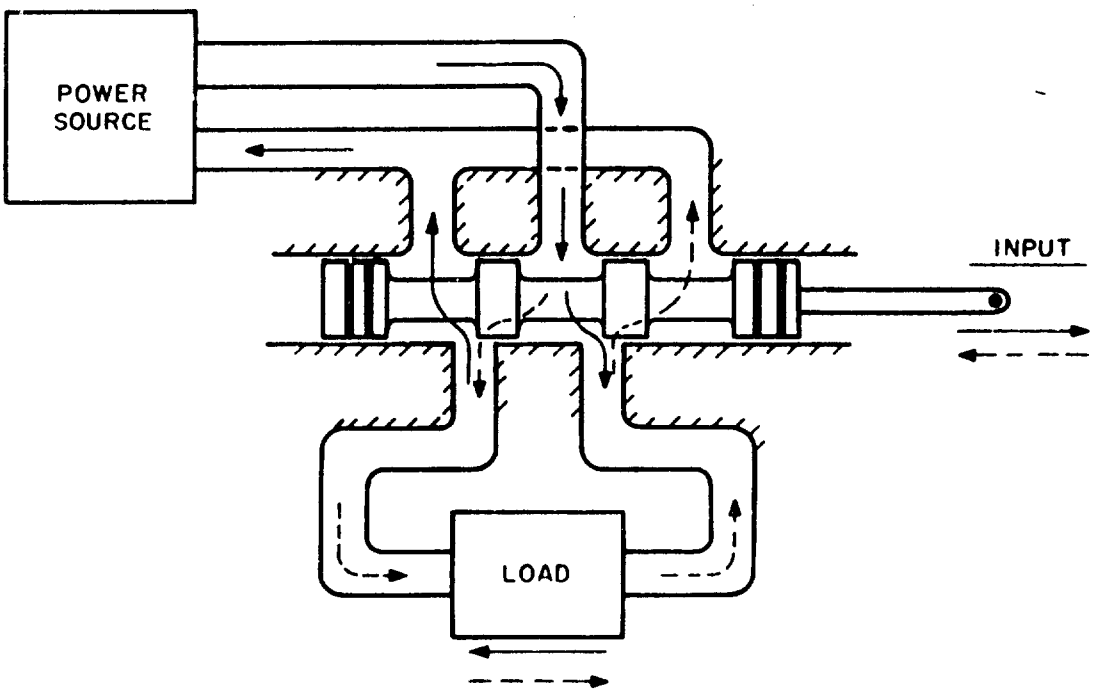

Figure 11. Four-way Valve

The estimated system weight can be found by summing the contributions of each component. From Table IV this weight is 51.3 pounds.

The power consumption of the system is evaluated on an average basis. It is assumed that an accumulator capable of providing peak demands is included in the hydraulic power unit.

The P_A portion of the total power consumption has been computed as 31.7 watts.

The leakage flow for the 911 hydraulic motor is given by the Vickers Corporation as 0.128 in^3/sec/1000 psi. Assuming the supply pump to have about the same characteristics, the leakage flow for the two motors and the pump at 500 psi is:

$$Q_{LM} + Q_{LP} = 2\left(1/2 \times \frac{0.128\ in^3}{sec}\right) + 1/3\left(1/2 \times \frac{0.128\ in^3}{sec}\right) \quad (4\text{-}17)$$

$$= 0.149\ in^3/sec$$

Leakage flow for the Lear-Siegler servovalve is given as typically 0.1 GPM/4000 psi or 1/2 (Q_{LV}) = 0.05 in^3/sec at 500 psi, or Q_{LV} = 0.10 in^3/sec.

Total system leakage is the sum of pump, motor and servovalve leakage:

$$Q_L = Q_{LV} + Q_{LM} + Q_{LP} \quad (4\text{-}18)$$

Total system leakage is then 0.249 in^3/sec at 500 psi. In terms of power, this represents about 15 watts.

TABLE IV

WEIGHT OF TWO HYDRAULIC GIMBAL TORQUERS FOR A 2000 FT-LB-SEC CMG

2 Motors	13.6 lb
2 Transmissions	27.0 lb
2 Servovalves	0.7 lb
Sub-Total	41.3 lb
1/3 (A.P.U. + Misc. Valving)	10.0 lb
TOTAL	51.3 lb

Thus far, 31.7 + 15 or 46.7 watts must be supplied to the system. This value includes volumetric, but not mechanical, inefficiencies.

The efficiency of conversion from electrical to hydraulic power was taken as 40 percent. This figure is in line with the claims of manufacturers of aircraft A.P.U.'s (e.g., Eastern Industries of Hamden, Connecticut). Reasonable efficiencies were assumed for the other components and are listed in Table V.

The total power consumption, P_T, is obtained by dividing the previously found power requirement of 46.7 watts by the overall system efficiency to yield:

$$P_T = \frac{46.7 \text{ watts}}{0.18} = 259 \text{ watts}$$

Values of actuator system weight and power consumption for CMG of other sizes were calculated in a similar manner and are illustrated in figure 12.

Should a hydraulic power supply be made available, it would be necessary to know the power required at the hydraulic servovalves. The power required at the servovalves, P_S, is the actuator power plus total leakage power less the leakage power of the pump, all divided by the mechanical efficiency of the valve and actuator. Thus

$$P_S = \frac{P_A + P_L - K \Delta p Q_{LP}}{0.8 \times 0.8 \times 0.7} \qquad (4\text{-}19)$$

Total power required, as previously defined, is the sum of actuator and leakage power divided by component and A.P.U. efficiencies. That is, from equation (4-15),

TABLE V

EFFICIENCIES OF THE HYDRAULIC COMPONENTS FOR A CMG

Hydraulic Motor (2)	70 percent
Transmission (2)	80 percent
Servovalve (2)*	80 percent
The Overall Efficiency (less A.P.U.)	45 percent
A.P.U.	40 percent
The Overall Efficiency (including A.P.U.)	18 percent

*Basic servovalve losses have been included in the determination of the average ideal power, P_A.

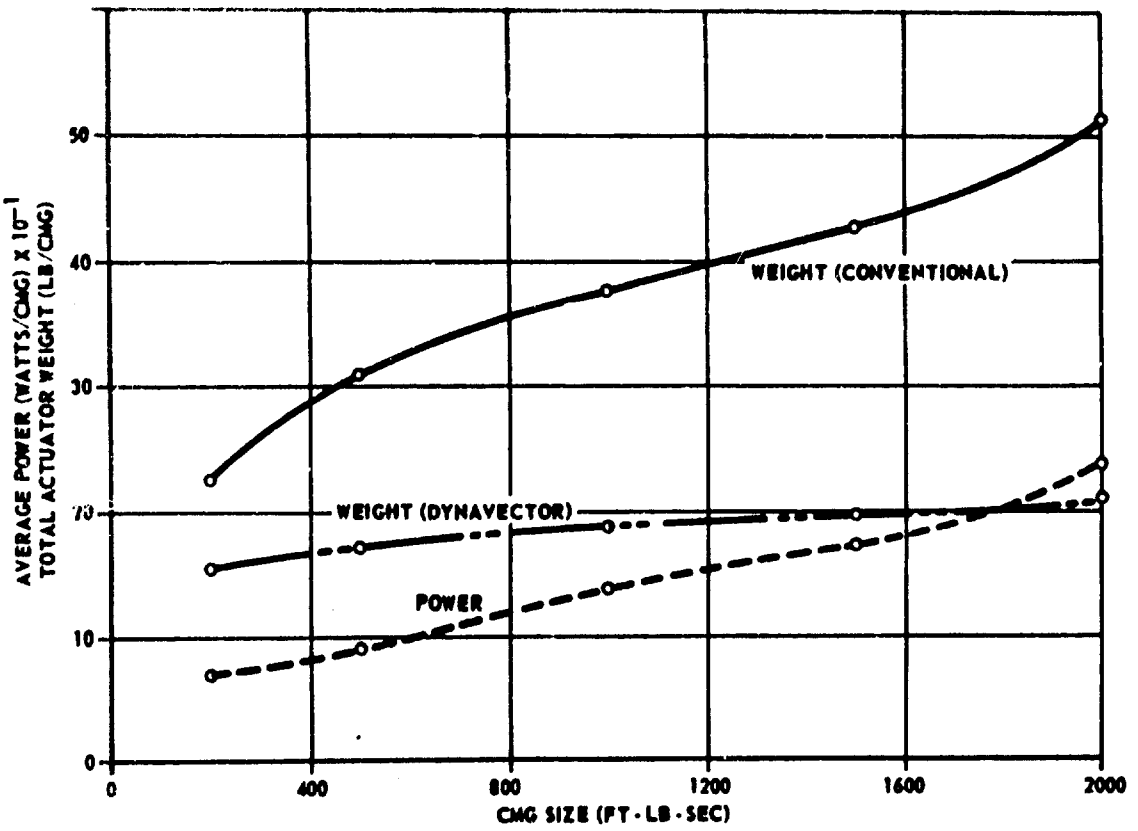

Figure 12. Hydraulic Actuation System Weight and Power Consumption

$$P_T = \frac{P_A + P_L}{0.4 \times 0.8 \times 0.8 \times 0.7} \qquad (4\text{-}15a)$$

or

$$0.4\, P_T = \frac{P_A + P_L}{0.8 \times 0.8 \times 0.7}$$

Substituting this relationship into equation (4-19), the latter becomes

$$P_S = 0.4\, P_T - \frac{K\Delta p\ Q_{LP}}{0.8 \times 0.8 \times 0.7} \qquad (4\text{-}19a)$$

The pump leakage power ($K\Delta p\ Q_{LP}$) is based on average values given by manufacturers.

What equation (4-19a) says, in effect, is this: If a hydraulic power supply is already available, then the A.P.U. efficiency does not have to be taken into account. Thus the hydraulic power required is only 40 percent of the previously calculated total input power to the A.P.U. (This accounts for the term 0.4 P_T.) Further, since a pump is not required, the leakage power of the pump (divided by efficiencies) is subtracted from the 0.4 P_T term to determine the hydraulic power that would be required at the servovalves.

A tabulation of hydraulic power requirements at the servovalves of a control moment gyroscope is shown in Table VI. This table represents power required for a 500 psi constant pressure servovalve system controlling a two actuator CMG. Note that it neglects the electric-to-hydraulic conversion losses.

TABLE VI

SERVOVALVE POWER REQUIREMENTS PER CMG

C M G Size ft-lb-sec	P_T watts	0.4 P_T watts	Q_{LP} in^3/sec	$\Delta p\, Q_{LP}\, K$ watts	P_S watts
2000	259	104	0.021	1.2	103
1500	186	74	0.015	0.9	73
1000	152	60	0.015	0.9	59
500	97	39	0.009	0.5	38
200	75	30	0.009	0.5	29

Ordinarily, one of the greatest advantages of a hydraulic system is its smaller size and weight for given power capability. This is fully exploited by designing systems to operate at high pressure levels. In this case, however, where leakage flow represents a very high proportion of system power consumption, some compromise in size and weight is indicated in order to reduce system pressure and, thus, leakage losses. The highly inefficient high pressure operation is due to the low power demand of the system, much lower than those of systems for which hydraulics are usually considered.

The following sample computation serves to demonstrate the unfeasibility of 3000 psi operation for this application. Using a small displacement motor, for example the Vickers Motor Model Number 906, the unit has a displacement of 0.095 in^3/rev and, for two units per CMG, displacement flow power of 32 watts (from equation 4-14). Each of the Model 906 motors has a leakage flow specification

of 0.04 in^3/sec/1000 psi. Thus, the leakage flow for two motors and 1/3 of the A.P.U. at 3000 psi is:

$$Q_{LM} + Q_{LP} = 2\left(3000 \text{ psi} \times \frac{0.04 \text{ in}^3/\text{sec}}{1000 \text{ psi}}\right) + \frac{1}{3}\left(3000 \text{ psi} \times \frac{0.04 \text{ in}^3/\text{sec}}{1000 \text{ psi}}\right)$$

$$Q_{LM} + Q_{LP} = 0.24 \text{ in}^3/\text{sec}$$

The leakage flow of two typical Lear-Siegler servovalves at 3000 psi is

$$Q_{LV} = 0.6 \text{ in}^3/\text{sec}$$

The total leakage flow is

$$Q_L = Q_{LV} + Q_{LM} + Q_{LP} = 0.24 + 0.6$$

$$Q_L = 0.84 \text{ in}^3/\text{sec}$$

in terms of power,

$$P_L = \Delta p \, Q_L \, K$$

$$P_L = 3000 \text{ psi} \times 0.84 \text{ in}^3/\text{sec} \times 0.113$$

$$P_L = 285 \text{ watts}$$

The total displacement and leakage flow power required is 317 watts. The inherent mechanical efficiency is 18 percent from Table V. Thus,

$$P_T = \frac{317}{0.18} = 1760 \text{ watts}$$

It can be seen that the total power requirement at 3000 psi is approximately 7 times the power at 500 psi. The ratio of leakage power to displacement flow power, P_L/P_A, is approximately 9 at 3000 psi, while it is less than 1 at 500 psi.

4.3.2.2 DYNAVECTOR Hydraulic System

The DYNAVECTOR, an integral hydraulic motor and epicyclic transmission, possesses its greatest advantage for this application in its lighter weight.

System weights are plotted in equation 4-3, showing the weight savings when a DYNAVECTOR unit replaces the hydraulic motor and planetary transmission of the conventional hydraulic system. Power consumption for the DYNAVECTOR system is assumed to remain essentially the same as that for conventional hydraulic systems.

4.3.2.3 Stepping Actuators

The smallest electrohydraulic stepping motor manufactured by Fujitsu, Limited, would be suitable for the largest CMG when coupled with a 200:1 gear ratio since it is capable of a 30 in-lb stall torque and a maximum speed of 50 rad/sec. The motor size is 3 inches in diameter and 10 inches in length. Thus, when used with a 200:1 transmission, it is considerably larger than the equivalent DC torquer motor system. Further, the unit's relatively large length-to-diameter ratio does not readily fit itself to the general "pancake" construction philosophy required by the control moment gyroscope.

4.3.3 Pneumatic Actuators

4.3.3.1 Flow Requirements

The calculations in this section are based on the test record of a pneumatic gearmotor[3] and are the basis for determining pneumatic system power requirements. The motor is approximately the size required for the 2000 ft-lb-sec CMG. Piston motors were not considered in this evaluation. Although piston motors have a slightly higher volumetric efficiency than gear motors, the overall efficiency is lower.

The weight of gas flow through the motor, using hydrogen supply, is given by:

$$\dot{w} = \frac{P_1}{R_o T} D_m N_m + C_o A_L \frac{P_1}{\sqrt{T}} \qquad \text{lb/sec} \qquad (4\text{-}20)$$

The first term on the right is the weight of gas displaced as the motor rotates. The second term is the leakage flow.

A_L = equivalent leakage area, in^2

C_o = flow coefficient, $\sqrt{°R}/sec$

D_m = motor displacement, in^3/rev

N_m = motor speec, rev/sec

---

[3] See Reference No. 3, Appendix D

P_1 = pneumatic motor inlet pressure, psi

R_o = gas constant, in/°R

T = gas temperature, °R

$\dot{w}$ = gas weight flow, lb/sec

The equivalent leakage area was calculated by substituting test data[4] into equation (4-20). For example,

$$\frac{35.4}{3600} = \frac{185}{9270 \times 500} \times 3.2 \times \frac{1000}{60} + 0.098\ A_L \frac{185}{\sqrt{500}}$$

$$A_L = 0.011\ in^2$$

The calculated values of A_L using other test points were approximately the same, even using heavier gases such as nitrogen. For constant temperature operation, the best improvement that could be expected is a 10 to 50 percent reduction in leakage.

Selecting a 200:1 transmission ratio, the required differential pressure is:

$$P = \frac{2\pi T_m}{\eta_T \eta_m D_m R_G} = \frac{2\pi \times 350 \times 12}{0.85 \times 0.86 \times 3.2 \times 200} = 56\ psi$$

where η_T and η_m are transmission and motor efficiencies.

Assuming a back pressure of 19 psia, the motor inlet pressure will be 75 psi at maximum torque. The peak flow rate, $\dot{w}_1$, at stall is then:

$$\dot{w}_1 = \frac{C A_L P_1}{\sqrt{T}} = \frac{0.367 \times 0.011 \times 75}{\sqrt{530}} = 0.0132\ lb/sec$$

The minimum leakage flow is 47 percent of the leakage at maximum stall torque due to valve leakage. Thus, the average flow at stall is:

---

[4] Ibid, See Reference No. 3, Appendix D

The second flow component is due to the average speed requirements. The peak motor speed is:

$$1.67 \text{ rpm} \times 200 = 334 \text{ rpm or } 5.56 \text{ rps}$$

The motor inlet pressure at maximum speed will be approximately 50 percent of the inlet pressure at maximum stall torque; thus

$$P_1 = 0.5 \times 60 + 15 = 45 \text{ psia}$$

The flow rate due to motor displacement is then:

$$\dot{w}_2 = \frac{P_1}{R_o T} D_m N_m = \frac{45}{662 \times 530} \times 3.2 \times 5.56 = 2.30 \times 10^{-4} \text{ lb/sec}$$

The average value is:

$$\dot{w}_{2\,avg} = 2.30 \times 10^{-4} (0.01 \times 1 + 0.3 \times 0.5 + 0.69 \times 0.25) = 7.7 \times 10^{-5} \text{ lb/sec}$$

The minimum leakage flow is 47 percent of the leakage flow at maximum stall torque. Thus, the leakage, when running at no load, is:

$$\dot{w}_3 = 0.47 \times 0.0132 = 0.0062 \text{ lb/sec}$$

The total average flow at no load is then the sum of $\dot{w}_{2\,avg}$ and $\dot{w}_3$.

$$\dot{w}_{2\,avg} + \dot{w}_3 = 0.000077 + 0.0062 = 0.0063 \text{ lb/sec}$$

which is less than stall torque flow rates.

The total flow per CMG is:

$$\dot{w} = \dot{w}_{1\,avg} + \dot{w}_{2\,avg} + \dot{w}_{3\,avg}$$

$$\dot{w} = 0.0102 + 0.0063$$

$$\dot{w} = 0.0165 \text{ lb/sec}$$

For 3 CMGs, the total flow rate is:

$$\dot{w}_T = 3\dot{w} = 3(0.0165) = 0.0495 \text{ lb/sec}$$

or

$$1.55 \times 10^{6} \text{ lb/year}$$

The above flow rate would eliminate the use of a non-circulating system with the long mission requirement since the weight of the gas alone would be excessive.

The gear actuator and DYNAVECTOR actuator have about the same efficiency; therefore, the pneumatic power supply requirement would be the same. However, the vane actuator leakage is about 46 percent of the gear actuator leakage. Since the leakage is a very significant part of the flow, the pneumatic power supply weight for the vane actuator would be 46 percent of that for the gear and DYNAVECTOR actuators. Since there is no significant difference between various types of pneumatic actuators, there is no justification for further detailed study of pneumatic actuators for this application.

Table VII illustrates the estimated weight and volume requirements for a single control moment gyroscope as a function of the CMG size.

TABLE VII

WEIGHT AND VOLUME REQUIREMENTS OF TWO PNEUMATIC ACTUATORS

C M G Size (ft-lb-sec)	200	500	1000	1500	2000
Motor Weight (lbs)	0.23	0.50	0.95	1.40	1.90
Transmission Weight (lbs)	5.90	8.00	11.10	14.20	17.40
Servovalve Weight (lbs)	0.50	0.60	0.70	0.80	0.90
Total Actuator Weight (lbs)	6.63	9.10	12.75	16.40	20.20
Total Actuator Volume (in^3)	168	212	268	322	380

4.3.3.2 Pneumatic Power Supplies

To determine the electrical power requirements, the following procedure is used:

In a recirculating system, the required compressor must be sized to supply the average flow requirement. The average flow rate is 0.0495 lb/sec, and the peak flow rate is 0.0585 lb/sec. A storage tank must be used to supply the additional flow when operating at higher than average flow rates and to provide the leakage flow that escapes into the shroud.

$$E_p = 778\ C_p\ T \left[\left(\frac{P_2}{P_1} \right)^{0.286} - 1 \right] \dot{w}$$

$$E_p = 778 \times 0.24 \times 530 \left[\left(\frac{100}{15} \right)^{0.286} - 1 \right] (0.0495) = 3,500 \text{ ft-lb/sec}$$

For estimation purposes, the compressor efficiency was determined from test data for the Gast Model 0211 compressor.[5] This compressor delivers 0.5 scfm of air at 10 psig with a 1/6 horsepower motor. The weight flow for the compressor is 6.4×10^{-4} lb/sec.

The power for compression to 10 psig (25 psia) is:

$$E = 778\ C_p\ T \left[\left(\frac{P_2}{P_1} \right)^{0.268} - 1 \right] \dot{w}$$

$$= 778 \times 0.24 \times 530 \left[\left(\frac{25}{15} \right)^{0.286} - 1 \right] (0.00064)$$

$$= 10.0 \text{ ft-lb/sec} = 0.018 \text{ HP}$$

The compressor efficiency is then:

$$\eta_c = \frac{\text{output horsepower}}{\text{input horsepower}} = \frac{0.018}{0.167} = 0.107$$

The electric motor efficiency is approximately 0.6. Thus, the input electrical pc required is:

$$\frac{3,500}{0.107 \times 0.6} \text{ ft-lb/sec} \times 1.356 \text{ watt-sec/ft-lb} = 74,000 \text{ watts}$$

Higher compression efficiency can be obtained by using a d le acting piston type compressor with cooling; however, the compressor weight wou e

---

[5] "Gast Rotary Vacuum Pumps" Catalog

considerably heavier. Assuming an 30 percent compressor efficiency, the electrical input power would be:

$$74,000 \times \frac{0.107}{0.80} = 9,900 \text{ watts}$$

Since these power requirements are unreasonable, no further efforts were applied to pneumatic actuators.

4.3.4 Qualitative Actuator Comparison

Major limitations of the many systems considered limit the number of systems that require further detailed comparison.

AC servomotors were found to have frequency response characteristics below 5 cps without transmissions, and the transmissions required for the AC servo systems have excessively high gear ratios. These two factors limit their suitability.

Stepping motors showed weight and size disadvantages when compared with DC torquer systems. A disadvantage common to both AC servomotors and stepping motors is that variable frequency inputs are required for good linearity between rate command and rate output.

The RESPONSYN actuator has some potential advantage compared with DC torquer systems for the large CMG units. The particular areas of advantage are weight and size. However, additional electronic equipment is required to produce the high-speed rotating magnetic field for its drive motor. The large number of additional electronic components required for EHD systems would tend to lower overall actuator reliability. Further, the unit is at best "near state-of-the-art" and requires further development in physical size and weight and commutation electronics development. Nevertheless, this unit should not be eliminated from possible future application.

The results shown for pneumatic systems from the standpoint of total power consumption (a minimum of 100 times greater than the equivalent electric systems) indicates that no further consideration is required.

More detailed comparisons are now limited to the following five major categories:

(1) DC torquer systems

(2) DC brushless torquer systems

(3) Electric DYNAVECTOR systems

(4) Conventional hydraulic systems

(5) Hydraulic DYNAVECTOR Systems

In figure 13 the average power required per CMG for three basic systems is given as a function of CMG size. The power for DC brushless torquer systems is assumed to be similar to DC torquer systems, and the power for hydraulic DYNA-VECTOR systems is assumed to be similar to conventional hydraulic systems.

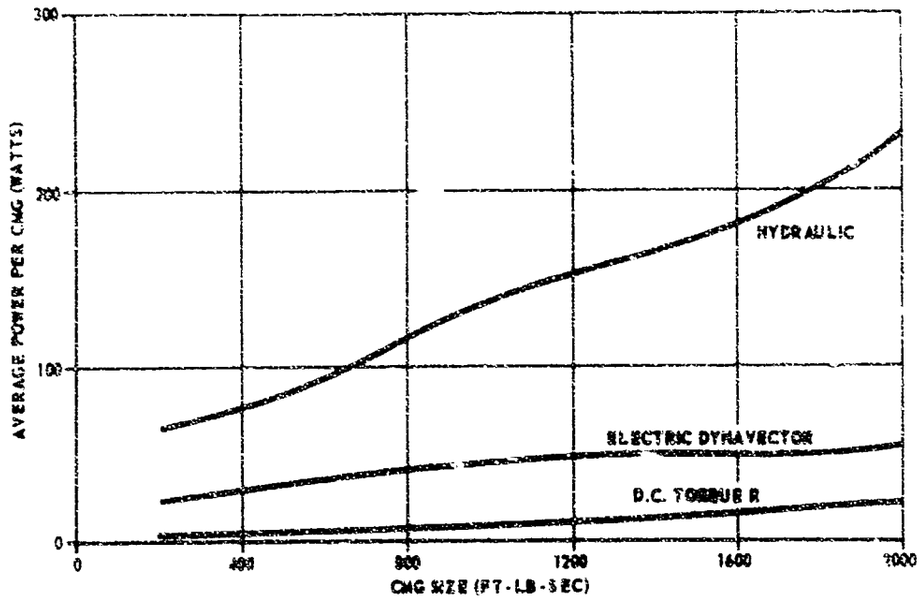

Figure 13. Optimum Actuator Systems - Power Consumption Comparison

Figure 14 shows the weight comparisons of the three basic actuators of figure 13 with the addition of the electric DYNAVECTOR.

Figure 13 shows definite power advantages for DC torquer systems, and figure 14 shows that electric and hydraulic DYNAVECTOR actuators have a weight advantage for the larger CMG sizes.

4.4 Preliminary Conclusions

The broad preliminary study indicates significant disadvantages in the use of fluid systems for long mission requirements. The disadvantages of fluid systems can be traced directly to the efficiency in converting electric power to fluid power, poor efficiency due to leakage flows, especially for pneumatic systems, and the requirement of slip rings for furnishing fluid power to the inner gimbal.

As a consequence of this broad preliminary study, further intensive study was restricted to DC electric actuators. Secondly, brushless systems (Brushless DC

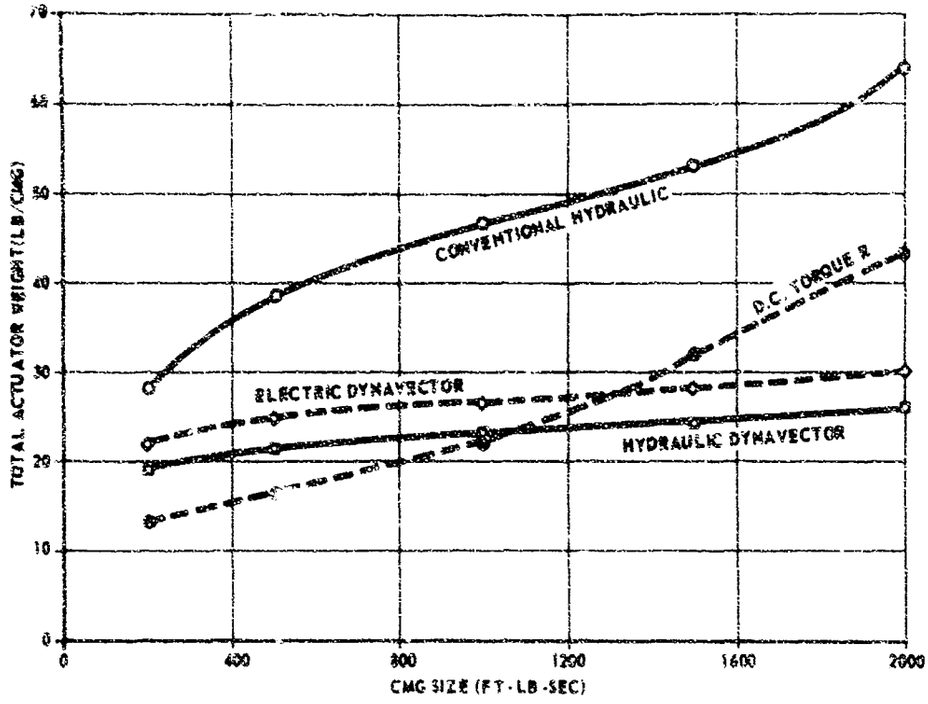

Figure 14. Actuator Weight Comparison

Torquers, Electric DYNAVECTORS and Electromechanical Harmonic Drives) currently are, at best, near the state-of-the-art because of complexities involved in high-speed electronic switching of inductive loads; therefore it is advisable to qualify any detailed study of these types to potential future applications. Also, this initial study phase indicated a scarcity of data on various transmission types for optimal use in the control moment gyroscope.

No consideration was given to the application of clutch-brake mechanisms for gimbal locking purposes, since it is anticipated that caging pins will be available for static locks and simultaneous torque and speed commands will be applied to both gimbals of a control moment gyroscope as required.

SECTION V

TRANSMISSION STUDIES

The initial phase of this study indicated the scarcity of generalized transmission data and the need for optimization of transmission types for CMG application. The parametric information required included range of ratios available, stall torque capability, size, weight, inertia, friction and nominal backlash.

To overcome this lack of data, a generalized study of transmissions, applicable to the CMG, was conducted. The transmission types considered included the following:

Spur Gears

Simple Planetary

Compound Planetary

Epicyclic

Harmonic Drive

Design calculations, schematics and outline sketches were made for transmissions where catalog data was not available. The weights and volumes calculated are for the gears, shafts, and bearings and do not include any of the supporting structure. Bearing sizes were taken from bearing catalogs.

5.1 HERTZ STRESS

The Hertz stress is generally considered to be a measure of the surface endurance of the gearing materials, and therefore is one of the factors determining the life capabilities of a set of gears. The gear and pinion sizes in the output mesh of the spur and planetary transmission types were selected to permit a maximum operating Hertz stress of 100,000 psi at maximum output torque. This criteria insures that the transmissions will meet the operational life requirements when submitted to the specified CMG load profile.

According to Buckingham[6], the standard expression for Hertz stress in external tooth gears is given by

$$S_c^2 = \frac{1.4\, F_d}{D_p\, f\, Q \sin\phi \left[\frac{1}{E_1} + \frac{1}{E_2}\right]} \qquad (5\text{-}1)$$

[6] See Reference No. 5, Appendix D

$$Q = \frac{2 N_G}{N_G + N_p} = \frac{2 D_G}{D_G + D_p} = \frac{2 r_G}{r_G + r_p} \qquad (5\text{-}2)$$

$$E = \frac{1}{\frac{1}{E_1} + \frac{1}{E_2}} = \frac{E_1 E_2}{E_1 + E_2} \qquad (5\text{-}3)$$

Assuming the use of steel material for the gears, $E_1 = E_2$; then,

$$E = \frac{E_1}{2} = 14.5 \times 10^6 \text{ psi} \qquad (5\text{-}4)$$

For 20-degree pressure angle gearing,

$$\sin \phi = 0.342 \qquad (5\text{-}5)$$

The total maximum instantaneous load on the teeth (the dynamic load) is:

$$F_d = F_t + F_i = F_t + \frac{0.05\, V_i\, (C f + F_t)}{0.05\, V_i + \sqrt{C f + F_t}} \qquad (7) \qquad (5\text{-}6)$$

Since the output velocities are very low under all modes of operation, the F_i load can be neglected and, therefore, the tangential load required for power transmission will be considered to be the dynamic load. That is,

$$F_d = F_t \qquad (5\text{-}7)$$

Substituting equations (5-2) through (5-5) and (5-7) into equation (5-1) and simplifying,

$$S_c^2 = 1.48 \times 10^7 \frac{F_t}{f} \left[\frac{1}{r_G} + \frac{1}{r_p} \right] (\text{psi})^2 \qquad (5\text{-}8)$$

The tooth contact stress (Hertz) is very low for internal gear drives such as the epicyclic transmission. The stress is especially low for teeth having nearly the same

---

(7) See Reference No. 6, Appendix D

base circle. According to Buckingham[8], the Hertz stress between internal and external 20-degree pressure angle steel gear teeth is given by

$$S_c^2 = 1.48 \times 10^7 \frac{F_t}{f}\left[\frac{r_G - r_p}{r_g \times r_p}\right] (psi)^2 \qquad (5\text{-}9)$$

It is apparent that the radii of curvature (r_G and r_p) are nearly equal in epicyclic transmissions and the Hertz stress will be low. The result is that the beam (Lewis) stress, S_b, becomes the tooth strength criteria for the epicyclic transmission.

The derivation of equation (5-9) is similar to the procedure used in deriving equation (5-8), which is applicable to external tooth gearing. The only difference occurring between the two is that the value of Q in equation (5-2) is replaced by

$$Q = \frac{2 N_G}{N_G - N_p} = \frac{2 r_G}{r_G - r_p} \qquad (5\text{-}10)$$

Detailed design data for the harmonic drive transmission is not available and, therefore, an assumption was made that an adequate safety margin (gear material yield strength versus stress level) could be provided by the manufacturer.

5.2 TYPES AND PARAMETERS

5.2.1 Spur Gear

A typical spur gear transmission schematic is shown in figure 15. The equations used for sizing these transmission are as follows:

The force acting on the gear teeth in the output mesh is given by

$$F_t = \frac{T_o}{r_p} \qquad (5\text{-}11)$$

The expression for Hertz stress is given by [Reference, equation (5-8)]

$$S_c^2 = 1.48 \times 10^7 \frac{F_t}{f}\left[\frac{1}{r_p} + \frac{1}{r_G}\right] \qquad (5\text{-}12)$$

An additional constraint was that the ratio of circular pitch to face width should not be less than 0.25. The purpose is to insure uniform contact over the total

---

[8] See Reference No. 5, Appendix D

face width. The sizes of the other gears and pinions were determined by the following equation:

$$\frac{D_{p1}}{D_{p3}} = \frac{f_1}{f_3} = (m_3\ m_2)^{1/3} = \left[\frac{D_{G2}}{D_{p2}} \times \frac{D_{G3}}{D_{p3}}\right]^{1/3} \qquad (5\text{-}13)$$

or

$$\frac{D_{p2}}{D_{p3}} = \frac{f_2}{f_3} = (m_3)^{1/3} = \left[\frac{D_{G3}}{D_{p3}}\right]^{1/3}$$

These equations are empirical relationships that tend to minimize inertia.[9]

The weight and volume calculations for the 64:1, 350 ft-lb spur gear transmission are shown as a sample of the method used. The nomenclature for this calculation is shown in figure 15.

The equation for weight calculation is:

$$W = w\,\frac{\pi}{4}\left[\sum_{1}^{n}\left(D_{Gn}^2 - D_{Gni}^2\right) f_n\right] \qquad (5\text{-}14)$$

$$W = \frac{\pi w}{4}\Big[f_1\left(D_{g1}^2 - D_{G1i}^2\right) + K_{g1}\ t_1\ D_{G1i}^2 + K_{p1}\ f_1\ D_{p1}^2 + f_2\left(D_{G2}^2 - D_{G2i}^2\right)$$

$$+ K_{g2}\ t_2\ D_{G2i}^2 + f_2\ D_{p2}^2 + f_3\left(D_{G3}^2 - D_{G3i}^2\right) + K_{g3}\ t_3\ D_{G3i}^2$$

$$+ K_{p3}\ f_3\ D_{p3}^2 + L_1\ D_{s1}^2 + L_2\ D_{s2}^2 + L_3\ D_{s3}^2 + L_4\ D_{s4}^2$$

$$+ L_a\ D_a^2 + L_b\ D_b^2\Big] + \text{bearing weights}$$

where

w = material specific weight, lb/in^3

K_{g1} = density ratio (gear) of 1st mesh

---

[9] See Reference No. 7, Appendix D

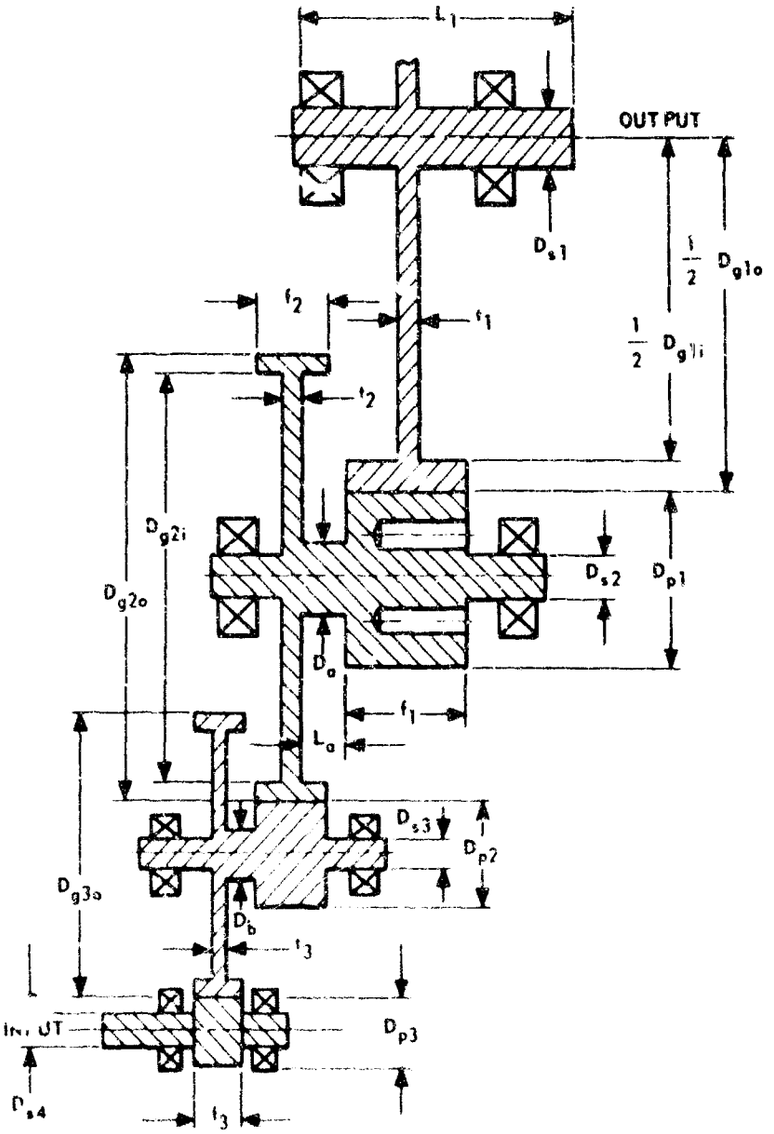

Figure 15. Spur Gear Transmission Schematic — 350 ft-lb. 64:1 Ratio

K_{p2} = density ratio (pinion) of 2nd mesh

Substituting numerical values

$$W = \frac{\pi}{4} \times 0.29 \left[1.61 (9^2 - 8.25^2) + 0.5 \times 0.25 \times 8.25^2 + 0.7 \times 1.61 \times 2.25^2 \right.$$

$$+ 1.01 (5.68^2 - 5.28^2) - 0.5 \times 0.24 \times 5.28^2 = 1.01 \times 1.42^2$$

$$+ 0.64 (3.6^2 - 3.2^2) + 0.5 \times 0.156 \times 3.2^2 + 0.64 \times 0.9^2$$

$$+ 3.75 \times 0.787^2 + 2.0 \times 0.472^2 + 1.75 \times 0.394^2 + 1.88 \times 0.394^2$$

$$\left. + 0.562 \times 0.938^2 + 0.438 \times 0.625^2 + 0.375 \times 0.625^2 \right] = 12.0 \text{ lb}$$

The total bearing weight is 0.6 pound and the total transmission weight is 12.6 pounds.

The configuration used for the sample minimum volume calculation and nomenclature is shown in figure 16. The volume is

$$V = \frac{1}{2} \times \frac{\pi}{4} \times d_a^2 \times l_a + \frac{1}{2} (d_a + d_b) \times h_a \times l_b$$

$$V = 3.75 \times \frac{1}{2} \times \frac{\pi}{4} \times 9.30^2 = 5 \times \frac{1}{2} (9.30 + 8.05) \times 8.38 = 492 \text{ in}^2$$

The results of the remaining spur gear transmission weight and volume calculations are shown in figures 17 and 18.

5.2.2 Simple Planetary

The simple planetary transmission configuration under consideration has three planet gears. The ring gear is grounded, the planet carrier is the output member, and the sun gear serves as the input member. The design equations used are from (5-15) to (5-29).

The transmission ratio is given by

$$R_G = 1 + \frac{D_r}{D_s} = 1 + \frac{r_r}{r_s} = 1 + \frac{N_r}{N_s} \qquad (5\text{-}15)$$

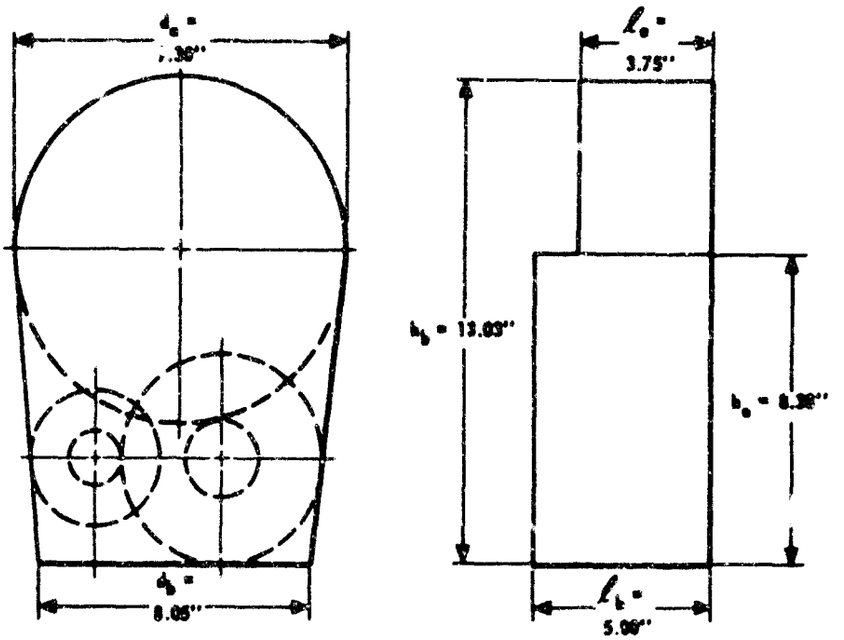

Figure 16. Configuration for Calculating Spur Gear Transmission Volume

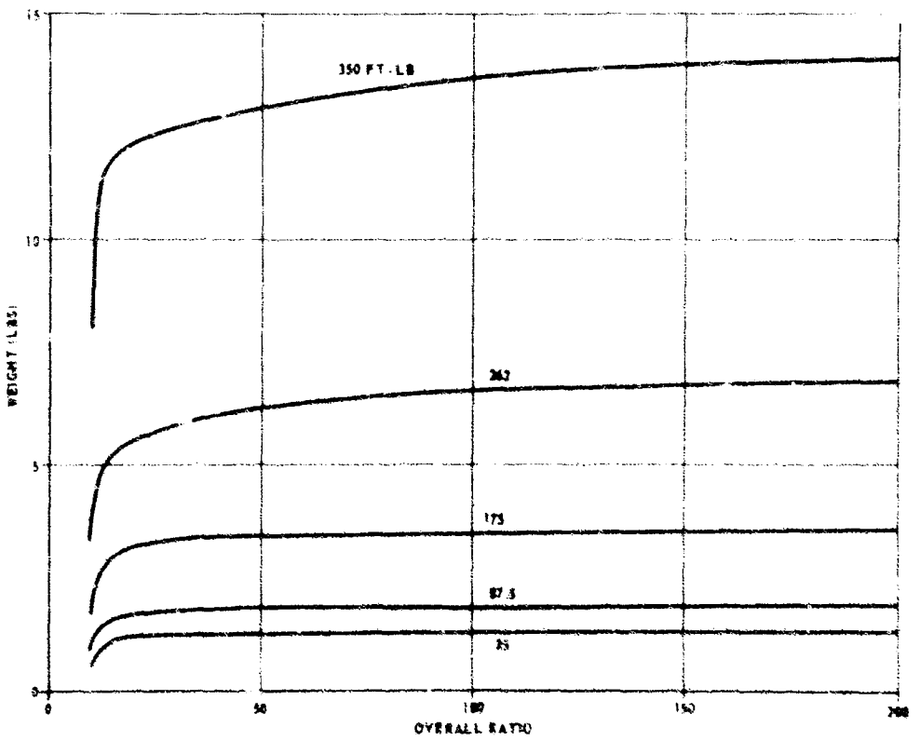

Figure 17. Spur Gear Transmission Weight Versus Overall Ratio

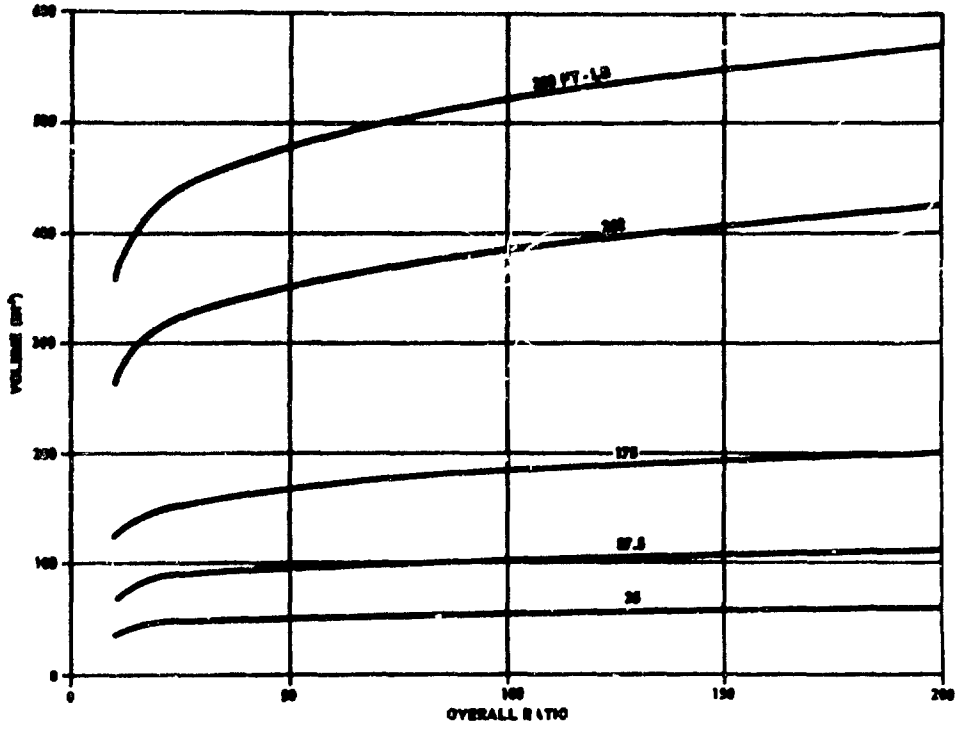

Figure 18. Spur Gear Transmission Volume Versus Overall Ratio

The force acting on the pinion (planet) center is

$$F_p = \frac{T_o}{An} \tag{5-16}$$

The force on the sun and ring gear teeth is given by

$$F_r = F_s = \frac{1}{2} F_p \tag{5-17}$$

The carrier torque arm length is

$$A = r_s + r_p = r_s \left(1 + \frac{r_p}{r_s}\right) \tag{5-18}$$

$$r_r = r_s + 2 r_p$$

$$\frac{r_r}{r_s} = 1 + 2\frac{r_p}{r_s}$$

$$\frac{r_p}{r_s} = \frac{1}{2}\left[\frac{r_r}{r_s} - 1\right] = \frac{R_G}{2} - 1 \qquad (5\text{-}19)$$

Substituting equation (5-19) into equation (5-18),

$$A = \frac{r_s R_G}{2} \qquad (5\text{-}20)$$

The expression for Hertz stress is [from equations (5-12) and (5-1

$$S_c^2 = 1.48 \times 10^7 \frac{F_s}{f}\left[\frac{1}{r_s} + \frac{1}{r_p}\right] \qquad (5\text{-}21)$$

For an allowable Hertz stress level of 100,000 psi

$$\frac{r_s f}{F_s} = 1.48 \times 10^{-3}\left[1 + \frac{r_s}{r_p}\right]$$

which [by substituting equation (5-19)] becomes:

$$\frac{r_s f}{F_s} = 1.48 \times 10^{-3}\left[1 + \frac{2}{R_G - 2}\right] = 1.48 \times 10^{-3}\left[\frac{R_G}{R_G - 2}\right] \qquad (5\text{-}22)$$

Using equations (5-16), (5-17) and (5-20)

$$F_s = \frac{T_o}{2An} = \frac{T_o}{2n}\left[\frac{2}{r_s R_G}\right]$$

$$F_s = \frac{T_o}{n r_s R_G} \qquad (5\text{-}23)$$

Substituting equation (5-23) into equation (5-22)

$$r_s f = 1.48 \times 10^{-3}\left[\frac{T_o}{n r_s (R_G - 2)}\right] \qquad (5\text{-}24)$$

Optimization of gear face width was based on the derivation of a geometric relationship utilizing a prior simple planetary design. This design was optimized on the basis of minimizing gear weight and inertia by minimizing the diameters while maximizing the face width-to-diameter ratio and maintaining uniform tooth contact. Beam strength and precision of the gears were also considered in the design. This geometric ratio is

$$f = f_1 \left[\frac{r_s}{r_{s_1}} \right]$$

$$f = K_1 r_s$$

$$f = (0.84) \frac{r_s}{0.292} = 2.89\, r_s \qquad (5\text{-}25)$$

This ratio is high for rigidly mounted gears. Therefore, the sun gear should not be tightly restrained but, rather, be permitted to bear on the three planet gears simultaneously.

The existing planetary design has a ratio of 7.5:1, a stall torque capability of 1000 inch-pounds, a weight of 4.7 pounds, a volume of 35 in^3 and a sun gear pitch radius of 0.32 inch. The remaining scaling factors were determined as exhibited below.

Substituting equation (5-25) into equation (5-24) and using three planetary gears,

$$r_s^3 = 1.71 \times 10^{-4} \frac{T_o}{R_G - 2} \qquad (5\text{-}26)$$

Rearranging equation (5-19),

$$r_r = r_s (R_G - 1) \text{ in.} \qquad (5\text{-}27)$$

The expression for transmission weight is

$$W = K_2 r_r^2 f = K_3 r_s r_r^2 \text{ lb} \qquad (5\text{-}28)$$

The expression for volume is

$$V = K_4 W \text{ in}^3 \qquad (5\text{-}29)$$

Using the model transmission,

$$r_s^3 = 1.71 \times 10^{-4} \left[\frac{1050}{5.5}\right] = 32.7 \times 10^{-3} \text{ in}^3 \left[\text{from equation (5-26)}\right]$$

$$r_s = 0.32 \text{ in.}$$

$$r_r = 0.32 \left[7.5 - 1\right] = 2.08 \text{ in.} \left[\text{from equation (5-27)}\right]$$

$$W = 4.7 \text{ lb}$$

$$4.7 = K_3 (0.32) (2.08)^2 \left[\text{from equation (5-28)}\right]$$

$$K_3 = 3.4 \text{ lb/in}^3$$

$$V = 35 \text{ in}^3$$

$$35 = K_4 (4.7) \left[\text{from equation (5-29)}\right]$$

$$K_4 = 7.45 \text{ in}^3/\text{lb}$$

SUMMARY

Given steel gears, a maximum allowable stall torque and a required ratio, the simple planetary transmission weight and volumes for the CMG can be computed using the following data:

$$K_1 = 2.89$$

$$K_3 = 3.4 \text{ lb/in}^3$$

$$K_4 = 7.45 \text{ in}^3/\text{lb}$$

$$n = 3 \text{ planet gears}$$

$$r_s^3 = 1.71 \times 10^{-4} \left[\frac{T_o}{R_G - 2}\right] \text{ in}^3$$

$$r_r = r_s (R_G - 1) \text{ in.}$$

$$W = 3.4\, r_s\, r_r^2 \text{ lb}$$

$$V = 7.45\, W \text{ in}^3$$

The results of the weight and volume computations are shown in figure 19. The outline drawing is shown in figure 20.

5.2.3 Compound Planetary

Typical compound planetary transmissions of the configuration selected for analysis are shown in figures 21, 22, and 23. The weight and volume curves are shown in figure 24. Figure 23 illustrates the nomenclature used.

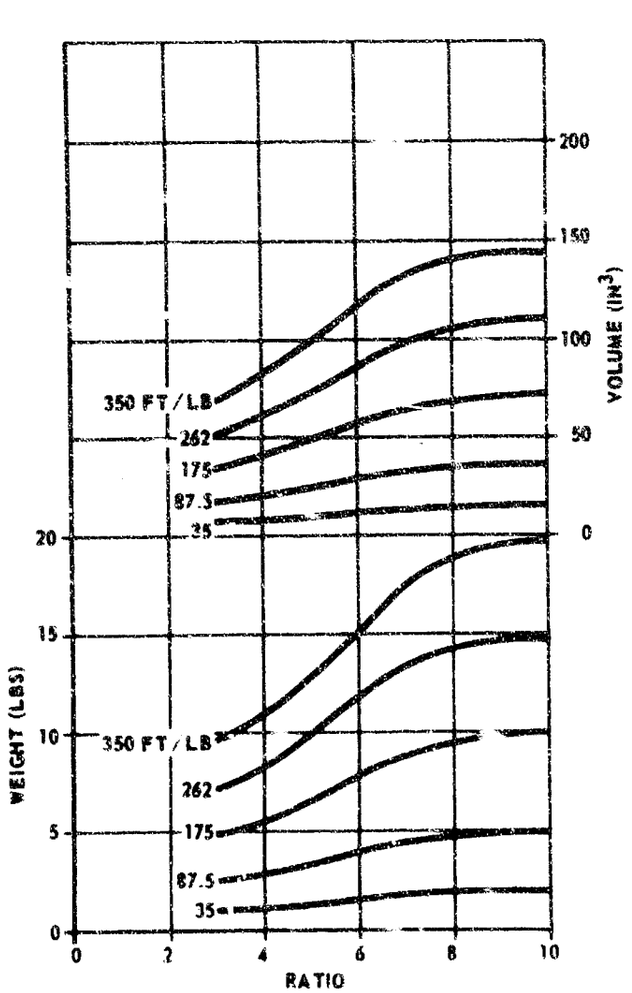

Figure 19. Simple Planetary Transmission Weight and Volume Versus Overall Ratio

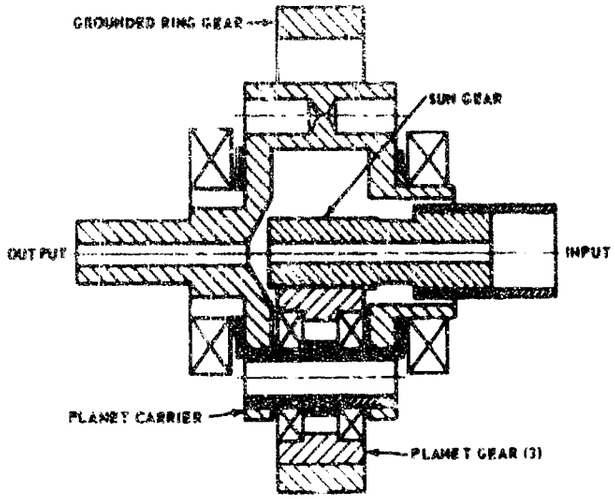

Figure 20. Schematic — Simple Planetary Transmission — 87.5 ft-lb, 7.5:1 Ratio

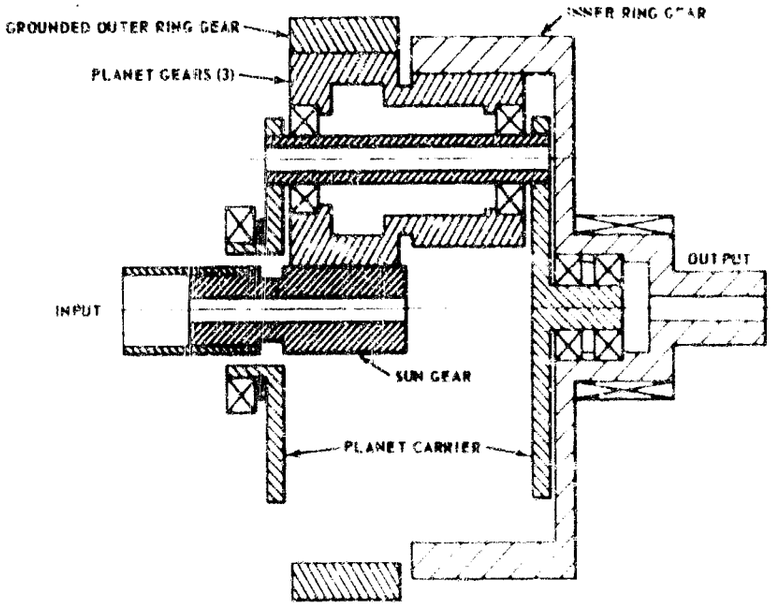

Figure 21. Schematic — Compound Planetary Transmission — 350 ft-lb, 56:1 Ratio

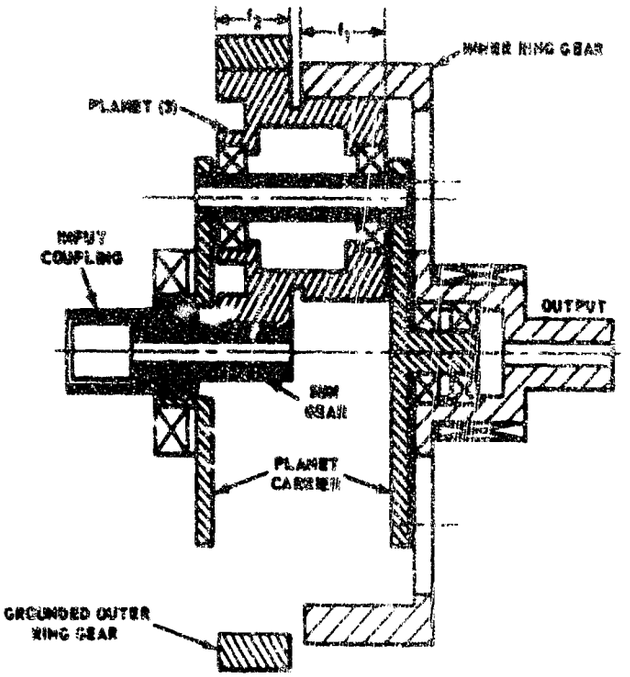

Figure 22. Schematic — Compound Planetary Transmission — 350 ft-lb, 88:1 Ratio

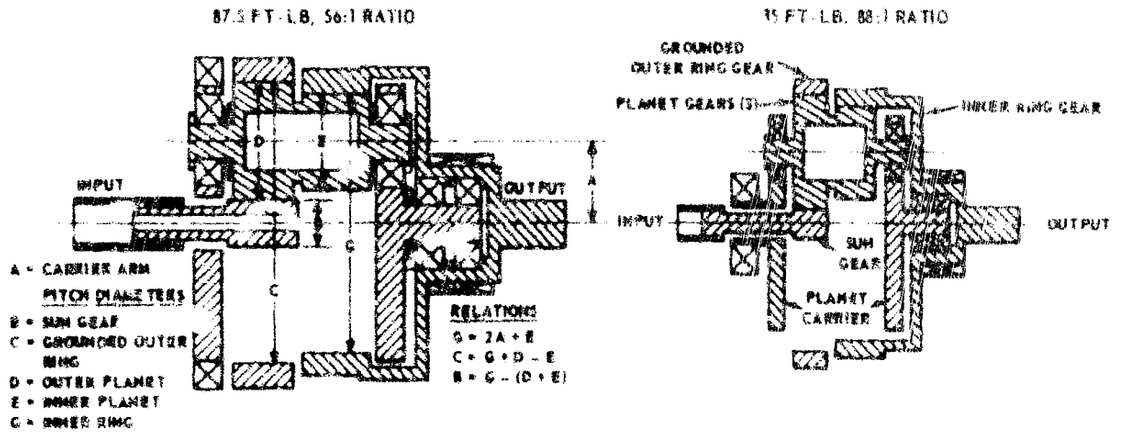

Figure 23. Schematic — Compound Planetary Transmission

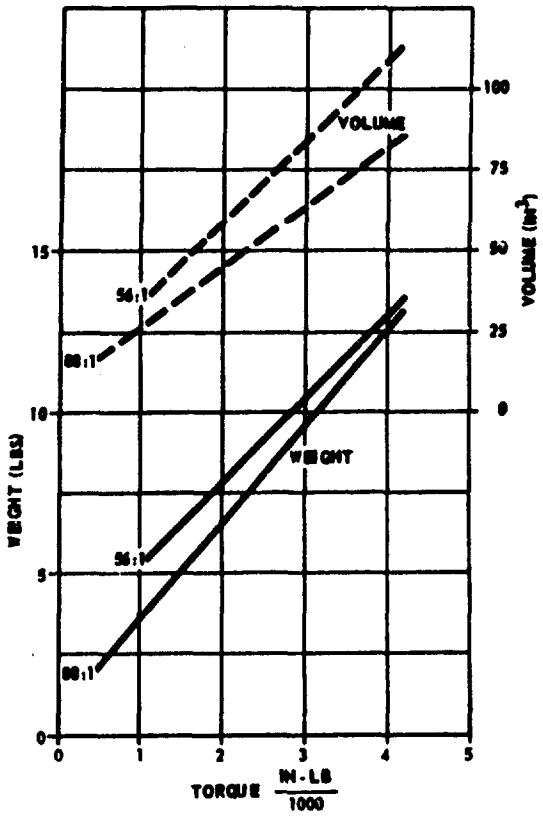

Figure 24. Compound Planetary Transmission Weight and Volume Versus Output Torque

The transmission ratio is given by

$$R_G = \frac{1 + \frac{C}{B}}{1 - \frac{CE}{DG}} \qquad (10) \qquad (5\text{-}30)$$

The force on the teeth of the output gear (E) is

$$F_E = \frac{T_o}{n\left(A + \frac{E}{2}\right)}$$

(10) See Reference No. 8, Appendix D

From figure 23,

$$G = 2A + E$$

so that

$$F_E = \frac{2T_o}{nG} \tag{5-31}$$

Three planets (n = 3) are used in this study.

Taking a free body diagram of the compound planet gear and applying moment balance, the force on the teeth of the grounded ring gear is

$$F_c = \frac{1}{2} F_E \left(1 + \frac{E}{D}\right) \tag{5-32}$$

The expression for Hertz stress [from equation (5-8)] is

$$S_c^2 = 1.48 \times 10^7 \frac{F_E}{f_1}\left[\frac{2}{E} + \frac{2}{G}\right] \tag{5-33}$$

The procedure used for sizing the compound planetary transmissions was a convergently iterative method. Given the required maximum output torque and the required transmission ratio, pitch diameters B through E were selected. The diametral pitch was held constant throughout a solution. Using equation (5-31), the load on the output teeth was determined. The required face width of the output mesh was determined using equation (5-33) and a maximum allowable Hertz stress of 100,000 psi. The load on the grounded ring gear teeth was determined using equation (5-32). The minimum face width of the gears was then calculated using the following:

$$f_2 = f_1\left[\frac{F_c}{F_E}\right] \tag{5-34}$$

Another constraint utilized was

$$1.25 \leq \frac{f_2}{B} \leq 1.50 \tag{5-35}$$

Several iterations were required for each mesh before a usable solution was obtained.

The weight and volume calculations for an 88:1, 350 ft-lb compound planetary transmission are shown as a sample of the method used. The configuration is shown in figure 22 and the nomenclature in figure 23.

The transmission weight is calculated with the equation

$$W = \sum_{1}^{n} \frac{\pi}{4} w \left(D_n^2 - D_{ni}^2 \right) L_n \qquad (5\text{-}36)$$

Substituting the numerical values:

Input coupling

$$W_1 = \frac{\pi}{4} (0.29) (0.875^2 - 0.605^2) \times 1.5 = 0.14 \text{ lb}$$

Sun Gear and Input Shaft

$$W_2 = \frac{\pi}{4} (0.29) (0.605^2 - 0.250^2) \times 1.875 = 0.13 \text{ lb}$$

Planet Carrier

$$W_3 = \frac{\pi}{4} \Big[(0.29) (1.188^2 - 1.00^2) \times 0.5 + (2.25^2 - 1.00^2) \times 0.188 + 2.25^2 \times 0.188$$
$$+ 0.472^2 \times 0.812 + 6 \times 0.875 \times 0.594 \times 0.188 + 6 \times 0.5 \times 0.875^2 \times 0.188$$
$$- 6 \times 0.5^2 \times 0.188 + 3 (0.472^2 - 0.250^2) \times 2.438 \Big]$$

$$W_3 = 0.92 \text{ lb}$$

Planets

$$W_4 = \frac{\pi}{4} \Big[(0.29) \times 3 (2.72^2 - 2.062^2) \times 0.312 + (1.406^2 - 1.125^2) \times 0.312$$
$$+ (2.72^2 - 0.938^2) \times 0.156 + (2.72^2 - 1.562^2) \times 0.405$$
$$+ (1.938^2 - 1.562^2) \times 0.125 + (2.16^2 - 1.562^2) \times 0.534$$
$$+ (2.16^2 - 0.938^2) \times 0.125 + (2.16^2 - 1.125^2) \times 0.312 \Big]$$

$$W_4 = 4.87 \text{ lb}$$

Output Ring Gear

$$W_6 = \frac{\pi}{4}(0.29)\left[(6.25^2 - 5.5^2) \times 1.281 + (6.25^2 - 1.094^2) \times 0.188 + (1.5^2 - 1.094^2) \times 0.5 + (1.5^2 - 0.938^2) \times 0.312 + (1.5^2 - 0.25^2) \times 0.25 + (0.75^2 - 0.25^2) \times 1.00 - 4 \times 1.5^2 \times 0.188\right]$$

$$W_6 = 4.37 \text{ lb}$$

Bearings Plus Spacers

$$W_7 = \frac{\pi}{4}(0.29)(0.85)\left[(2.219^2 - 1.188^2) \times 0.375 + 8(1.125^2 - 0.472^2) \times 0.312 + (1.875^2 - 1.5^2) \times 1 + (2.219^2 - 1.188^2) \times 0.094 + 6(0.75^2 - 0.472^2)(0.062) + (1.875^2 - 1.5^2)(0.078) + (1.125^2 - 0.938^2) \times 0.125)\right]$$

The weight of the bearings and spacers is

$$W_7 = 1.13 \text{ lb}$$

The total transmission weight is then

$$W_T = \sum_{1}^{7} W_n = 13.5 \text{ lb}$$

The volume is given by

$$V = \frac{\pi}{4} \sum L D^2$$

$$= \frac{\pi}{4}\left[1 \times 0.875^2 + 0.5 \times 2.19^2 + 0.25 \times 4.188^2 + 0.935 \times 6.80^2 + 1.562 \times 6.25^2 + 1.094 \times 1.875^2\right.$$

$$+ 1.00 \times 0.75^2 \Big]$$

$$V = 116 \text{ in}^3$$

A sun gear input was used in the design analysis of compound planetary transmissions. The result is that a lower level of transmission inertia is reflected back to the motor drive shaft than that obtained by using a planet carrier input. Another advantage obtained from this type of design is that a larger transmission ratio can be obtained from the same package size.

Only 56:1 and 88:1 compound transmissions have been selected for analysis. Additional ratios would require either computer solutions or laborious hand calculations for determining the required parameters because of the design analysis complexity. These extended efforts would not conform to the scope of the study requirements. However, the selected ratios yield excellent results for transmission type comparison purposes.

5.2.4 External Epicyclic

The epicyclic transmission sizing was based on data from the Bendix DYNAVECTOR Program.

The Hertz stress in the teeth of an epicyclic transmission is very low since an external tooth-internal tooth configuration is utilized and the pitch radii of the pairs of gears in mesh are very nearly equal. This is illustrated by equation (5-9).

The limiting load factor for epicyclic transmission teeth is the flexural endurance (more commonly known as the Beam or Lewis stress). For a steel gear having a Brinell hardness number of 240, the flexural endurance limit is[11];

$$S_b = 60,000 \text{ psi} \quad (11)$$

The output torque is related to tooth loads by

$$T_o = \frac{D_p F_t N}{4} \qquad (5\text{-}38)$$

An assumption made for equation (5-38) is that the load will vary linearly between maximum and minimum loaded teeth.

---

[11] Ibid, See Reference No. 6, page 327, Appendix D

The Lewis stress equation is

$$F_t = \frac{S_b Y f}{P_d} \tag{5-39}$$

From gear tooth layout studies, the number of teeth in contact is

$$N = \frac{D_p P_d}{10} \tag{5-40}$$

Substituting equations (5-39) and (5-40) into equation (5-38)

$$T_o = \frac{D_p^2 S_b Y f}{40} \tag{5-41}$$

The form factor (Y) can be assumed to be 0.5 for stubbed gears with many teeth. Using equation (5-41), the pitch diameter of the smallest gear is given by

$$D_p = \sqrt{\frac{80 T_o}{S_b f}} \tag{5-42}$$

The DYNAVECTOR program indicates that for minimum package size the maximum face width can be

$$f = \frac{1}{3} D_p$$

Substituting into equation (5-42)

$$D_p = \left(\frac{240 T_o}{S_b}\right)^{\frac{1}{3}} \tag{5-43}$$

The sizes for other gears were taken from DYNAVECTOR design tables. Typical epicyclic transmission designs are shown in figure 25. The weight and volume curves are shown in figure 26.

5.2.5 Harmonic Drive

The weight and volumes for the harmonic drive transmission were from tabulated data in the Harmonic Drive Catalog[12] for the circular spline, wave

---

[12] See Reference No. 9, Appendix D

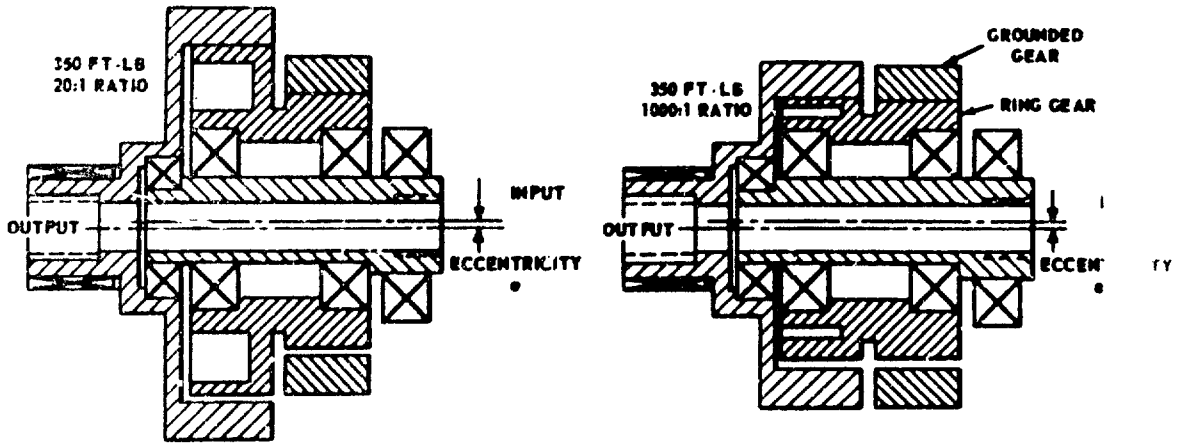

Figure 25. Schematic — External Epicyclic Transmission

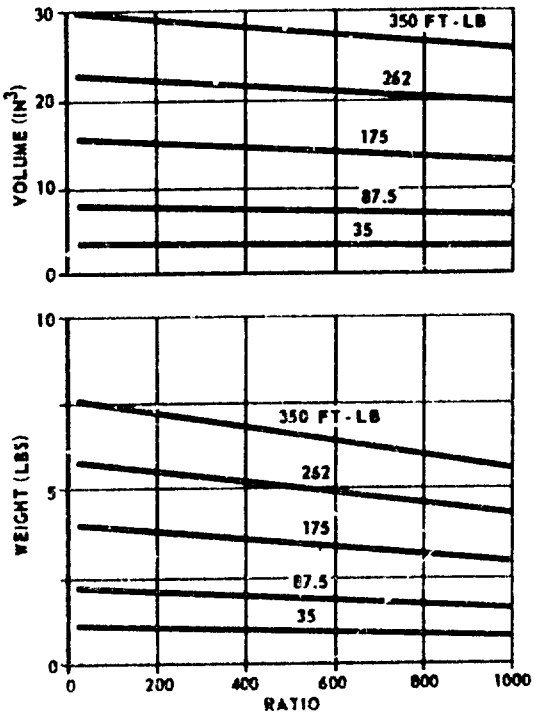

Figure 26. Epicyclic Transmission Volume and Weight Versus Overall Rat

generator and flex spline. The transmission sizes listed in the catalog are not the same as the required sizes, and the tabulated data does not include bearings and shafts. Therefore, it was necessary to extrapolate the tabulated data to obtain the required information. The following equations were used for this purpose:

$$\text{Weight} = \frac{\text{required torque}}{\text{tabulated torque}} \times 1.5 \times \text{tabulated weight}$$

$$\text{Volume} = \frac{\text{required torque}}{\text{tabulated torque}} \times 1.2 \times \text{calculated volume of listed transmissions}$$

Table VIII illustrates the harmonic drive sizes used in the computations. The weight and volume curves are shown in figure 27.

TABLE VIII

APPLICABLE HARMONIC DRIVE TRANSMISSION SIZE NUMBERS VERSUS STALL TORQUE AND GEAR RATIO

Gear Ratio	80	100	160	200	260
Stall Torque (ft-lb)	Size Number for H.D. Tx.				
350	65	50	40	---	40
262	50	50	40	---	40
175	40	40	32	---	32
87.5	40	40	32	---	32
35	25	20	20	25	32

Commonly available harmonic drive transmissions have a lower limit of about 80:1. Special transmissions have been built with ratios as low as approximately 50:1. However, parametric data for these units were not made available by the manufacturer during the course of this evaluation, and therefore are not included.

5.3 BACKLASH

Backlash is the amount by which the width of a tooth space exceeds the thickness of the engaging tooth on the pitch circles. It is usually the angular error resulting from the backlash that is of interest in servo systems. The backlash of a single mesh spur gear set is converted to angular error by the following equation:

$$E_B = \frac{B \times 360 \times 60}{\pi \times D_p} \qquad (5\text{-}44)$$

B = backlash between mating teeth, inches

D_p = pitch diameter of driven gear, inches

E_B = angular error, minutes of arc

The steps in calculating the backlash error for a complete transmission are:

(1) Calculate the individual errors for each pass in the gear train.

(2) Reflect all individual mesh errors from their source to the output shaft. For spur gears, multiply the source error by the gear ratio between the source shaft and the output shaft.

(3) Add all individual mesh errors to result in the total error.

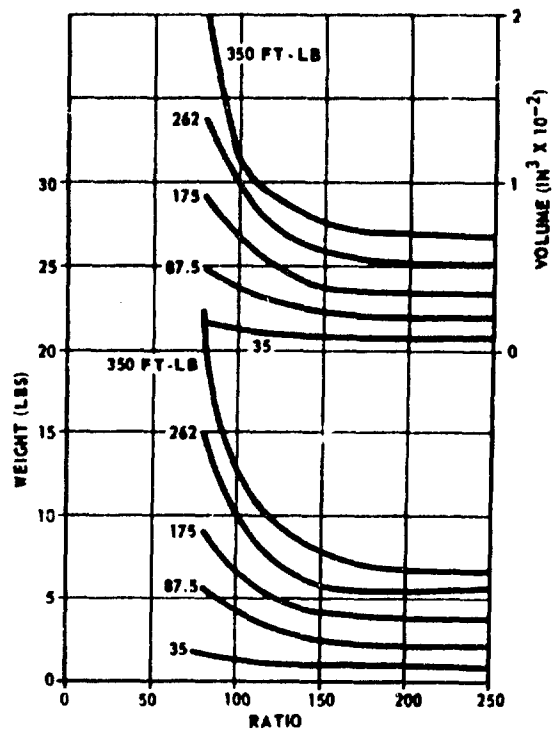

Figure 27. Harmonic Drive Weight and Volume Versus Overall Ratio

High precision gears are used in this analysis. Backlash can be further minimized by using anti-backlash methods and devices and by loading the gears to provide a tighter mesh. The high precision gears are more expensive; however, their use is justified in the CMG application. Anti-backlash gears have a high wear factor if run too fast. A tight mesh may result in increased power losses, overheating, rupture of lubricant film, overloading bearings, and premature gear failure. The final design approach can be determined only after completion of the overall servo analysis for the complete system application. The particular tradeoff desired is the maximum tolerable backlash level in the servo loop versus the complexity in design of the transmission.

Examples are presented for each type of transmission considered to illustrate the method used for backlash calculations. AGMA Quality Number 11 or 12 gears were selected for the sample calculations.

5.3.1 Spur Gears

The 125:1 transmission with 350 ft-lb output torque was selected for the example calculation. The runout tolerances were taken from pages 3 and 4 of the AGMA Gear Classification Manual.[13]

Output Mesh

Gear pitch diameter (D_{G1}) = 10 inches

Pinion pitch diameter (D_{p1}) = 2 inches

Runout of gear (e_{g1}) = 0.00073 inch

Runout of pinion (e_{p1}) = 0.00057 inch

Change in center distance (ΔC_1) = $e_{g1} + e_{p1}$ = 0.0013 inch

The backlash of mesh 1 is derived through equation (5-45)

$$E_{B1} = \frac{\Delta C}{D_{G1}} \times \frac{2}{\pi} \tan \phi \times 360 \times 60 \qquad (14)$$

---

[13] See Reference No. 10, Appendix D

[14] See Reference No. 11, Appendix D

$$= 5000 \frac{\Delta C_1}{D_{G1}} = 5000 \times \frac{0.0013}{10} \qquad (5\text{-}45)$$

$$= 0.[illegible] \text{ minute of arc}$$

Second Mesh

$D_{G2} = 5.84$ inches

$D_{p2} = 1.17$ inches

$e_{g2} = 0.0007$ inch

$e_{p2} = 0.00054$ inch

$\Delta C_2 = 0.00124$ inch

The backlash of mesh 2, reflected to the output shaft, is

$$E_{B_2} = 5000 \frac{\Delta C_2}{D_{G2}} \times \frac{1}{mi} \qquad (5\text{-}46)$$

$$= 5000 \times \frac{0.00124}{5.34 \times 5} = 0.21 \text{ minute of arc}$$

Input Mesh

$D_{G3} = 3.42$ inches

$D_{p3} = 0.68$ inch

$e_{g3} = 0.00061$ inch

$e_{p3} = 0.0005$ inch

$\Delta C_3 = 0.00111$ inch

$$E_{B_3} = 5000 \frac{\Delta C_2}{D_{G2}} \times \frac{1}{m_1 m_2} \tag{5-47}$$

$$= 5000 \times \frac{0.00111}{3.42 \times 25} = 0.07 \text{ minute of arc}$$

The total backlash is then

$$E_B = E_{B_1} + E_{B_2} + E_{B_3} = 0.93 \text{ minute of arc} \tag{5-48}$$

5.3.2 Simple Planetary Transmission

The simple planetary transmission selected for the sample calculation has a ratio of 7:5 and an output torque of 350 ft-lb. The parameters of interest are as follows:

Ring gear pitch diameter (D_r) = 6.6 inches

Planet gear pitch diameter (D_p) = 2.792 inches

Sun gear pitch diameter (D_s) = 1.016 inches

$$A = \frac{1}{2}(D_s + D_p) = 1.904 \text{ inch}$$

From the AGMA Gear Classification Manual[15] for Quality Number 12 gears:

Ring gear runout (e_g) = 0.00071 inch

Planet runout (e_p) = 0.0006 inch

Sun gear runout (e_s) = 0.00051 inch

Change in center distance between sun and planet gears

$$(\Delta C_1) = e_s + e_p = 0.00111 \text{ inch}$$

---

[15] Ibid, See Reference No. 10, Appendix D

Change in center distance between planet and ring gears

$$(\Delta C_2) = e_p + e_g = 0.00131 \text{ inch}$$

Linear backlash between sun and planet gears

$$B_1 = \Delta C_1 \times 2 \tan \phi = 0.00111 \times 0.728 - 0.000808 \text{ inch}$$

Linear backlash between planet and ring gear

$$B_2 = \Delta C_2 \times 2 \tan \phi = 0.00131 \times 0.728 = 0.000955 \text{ inch}$$

The distance the planet gear center can move with the sun gear locked is

$$z = \frac{1}{2}(B_1 + B_2) = 0.000882 \text{ inch}$$

The angular backlash at the output shaft is then

$$E_B = \frac{z \times 360 \times 60}{\pi \times 2A} = 1.59 \text{ minutes of arc} \qquad (5\text{-}49)$$

5.3.3 Compound Planetary Transmission

The compound planetary transmission selected for the sample calculation has a ratio of 88:1 and an output torque of 350 ft-lb. The significant parameters are as follows:

Sun gear pitch diameter (B) = 0.605 inch

Grounded ring gear pitch diameter (C) = 6.05 inches

Input planet pitch diameter (D) = 2.72 inches

Output planet pitch diameter (E) = 2.16 inches

Output ring gear pitch diameter (G) = 5.50 inches

From the AGMA Gear Classification Manual, for Quality Number 12 gears, the runout tolerances are

Sun gear (e_b) = 0.0005 inch

Grounded ring gear (e_c) = 0.007 inch

Input planet (e_d) = 0.00059 inch

Output planet (e_e) = 0.00057 inch

Output ring gear (e_g) = 0.00068 inch

Change in center distance between sun and input planet gears

$$\Delta C_1 = e_b + e_d = 0.00109 \text{ inch}$$

Change in center distance between input planet and grounded ring gears

$$\Delta C_2 = e_c + e_d = 0.00129 \text{ inch}$$

Change in center distance between output planet and output ring gears

$$\Delta C_3 = e_e + e_g = 0.00125 \text{ inch}$$

The linear backlash between the sun and input planet gears is

$$B_1 = \Delta C_1 \times 2 \tan \phi = 0.00109 \times 0.728 = 0.0008 \text{ inch}$$

The linear backlash between the input planet and grounded ring gears is

$$B_2 = \Delta C_2 \times 2 \tan \phi = 0.00129 \times 0.728 = 0.00094 \text{ inch}$$

The distance the planet center can move, with the sun gear locked, is

$$z_1 = \frac{1}{2}(B_1 + B_2) = 0.00087 \text{ inch}$$

This motion reflected to the output ring gear is

$$z_2 = z_1 \frac{G}{B + D} = 0.00087 \frac{5.5}{0.605 + 2.72} = 0.00144 \text{ inch}$$

The linear backlash between the output planet and the output ring gear is

$$B_3 = \Delta C_3 \times 2 \tan \phi = 0.00125 \times 0.728 = 0.00091 \text{ inch}$$

The total linear backlash at the output ring gear is

$$B_o = z_2 + B_3 = 0.00235 \text{ inch}$$

The angular backlash is then

$$E_B = \frac{B_o \times 360 \times 60}{\pi G} = \frac{0.00235 \times 360 \times 60}{\pi \times 5.5} = 2.94 \text{ minutes of arc} \qquad (5\text{-}50)$$

5.3.4 Epicyclic Transmission

The 350 ft-lb, 1000:1 epicyclic transmission has the following significant parameters.

Input external gear pitch diameter (D_1) = 2.60 inches

Grounded ring gear pitch diameter (D_2) = 2.66 inches

Output external gear pitch diameter (D_3) = 2.74 inches

Output ring gear pitch diameter (D_4) = 2.79 inches

From AGMA Gear Classification Manual[16], the runout tolerance values are

e_1 = 0.00059 inch

e_2 = 0.00059 inch

e_3 = 0.00059 inch

e_4 = 0.00059 inch

The change in center distances and linear backlash values for the two meshes are

$\Delta C_1 = e_1 + e_2 = 0.00118$ inch

---

[16] Ibid, See Reference No. 10, Appendix D

$$\Delta C_2 = e_3 + e_4 = 0.00118 \text{ inch}$$

$$B_1 = \Delta C_1 \times 2 \tan \phi = 0.00118 \times 0.728 = 0.00086 \text{ inch}$$

$$B_2 = \Delta C_2 \times 2 \tan \phi = 0.00118 \times 0.728 = 0.00086 \text{ inch}$$

The backlash values are additive for the epicyclic transmission. Thus, the total angular backlash is

$$E_B = (B_1 + B_2) \times \frac{360 \times 60}{\pi D_4} = (0.00086 + 0.00086) \times \frac{360 \times 60}{\pi \times 2.79} \quad (5\text{-}51)$$

$$= 4.3 \text{ minutes of arc}$$

5.3.5 Harmonic Drive

The following backlash data is taken from "Harmonic Drive Mechanical Power Transmission Systems,"[18] a catalog published by Harmonic Drive Division, United Shoe Machinery Corporation.

The backlash of standard harmonic drive units and component sets ranges between two and six minutes of arc. When finer backlash control is required, the components can be manufactured to closer tolerances. The standard Size 50 harmonic drive transmission has a maximum backlash of 4.7 minutes of arc. This unit, with a 100:1 ratio, is capable of driving the 350 ft-lb load. The backlash can be reduced to 0.5 minute of arc by using closer tolerances.

5.4 FRICTION AND EFFICIENCY

The efficiency of a transmission will vary with lubrication, preload, speed and torque. Very little information is available on transmission efficiencies at different operating conditions.

Single-mesh spur gears give an efficiency of 98 percent.[17] The theoretical efficiency of single-mesh spur gears is 99.6 percent.[18] Experience has indicated that an efficiency of 90 percent per mesh is typical for spur gears.

An overall efficiency of 90 percent has been obtained with a two-stage simple planetary transmission using Hi-T-Lube dry-film lubricant.[19] Thus, the efficiency per stage is 95 percent.

---

[17] See Reference No. 12, Appendix D

[18] See Reference No. 13

[19] See Reference No. 14

The overall efficiency of a compound epicyclic transmission can be calculated from the following expressions.[20]

$$\eta = \frac{1}{1 + k\left[\frac{1}{N_2} + \frac{1}{N_3} - \frac{1}{N_1} - \frac{1}{N_4}\right]\left[\frac{\omega_i}{\omega_o} - 1\right]} \qquad (5\text{-}52)$$

where

$$k = \frac{\mu \ell P_d}{2 \cos \phi}$$

and

μ = dynamic coefficient of friction

ℓ = length of line of action

ω_i = input speed

ω_o = output speed

P_d = diametral pitch

ϕ = tooth pressure angle

$$k = \frac{0.07 \times 0.175 \times 20}{2 \times 0.94} = 0.13$$

and

$$\eta = \frac{1}{1 + 0.13\left[\frac{1}{150} + \frac{1}{144} - \frac{1}{156} - \frac{1}{150}\right]\left[\frac{625}{1} - 1\right]}$$

η = 96 percent

This efficiency is theoretically correct for tooth action along the true line of action. However, as the load is increased on the transmission, the line of action will effectively be curved as additional teeth come into contact, effectively reducing the efficiency. The effect of the curved line of action would require further investigation.

---

[20] See Reference No. 15

Experience indicates that an efficiency of 92 percent could be expected under worst-case loading conditions.

The input and output torque values for Harmonic Drive industrial reducer transmissions are listed on pages 38 and 39 of Reference[21] for various torque and speed values. These transmissions are lubricated with oil and operated in the horizontal position.

The HDUC 50 unit at 3500 rpm speed and 4760 in-lb output torque was selected for the sample calculation. The input power, from the table, is 3.1 HP. The output power is

$$\frac{\text{torque (in-lb) x rpm}}{63025} = \frac{4760 \times 3500}{63025} = 2.64 \text{ HP}$$

The efficiency is then

$$\frac{2.64}{3.1} \times 100 = 85 \text{ percent}$$

.5 INERTIA

The inertia calculations presented in this paragraph are generally based on the parameters established in paragraph 5-2. The exception is the Harmonic Drive transmission. Inertia data for this transmission was supplied by the manufacturer. The inertia value of interest is that which is reflected to the input or high-speed side of the transmission.

5.5.1 Spur Gear

The inertia at the transmission input was calculated by use of the following equations:

$$J_e = J_{p3} + \frac{J_{G3}}{\left(\frac{D_{G3}}{D_{p3}}\right)^2} + \frac{J_{G2}}{\left(\frac{D_{G3}}{D_{p3}}\right)^2 \left(\frac{D_{G2}}{D_{p2}}\right)^2} + \frac{J_{G1}}{\left(\frac{D_{G3}}{D_{p3}}\right)^2 \left(\frac{D_{G2}}{D_{p2}}\right)^2 \left(\frac{D_{G1}}{D_{p1}}\right)^2} \quad (5\text{-}53)$$

---

[21] See Reference No. 16, Appendix D

where

$$J_{p3} = \frac{\pi w}{g\ 2 \times 16}\left[L_4 D_{s4}^4 + f_3 D_{p3}^4\right] \quad (1)$$

$$J_{G3} = \frac{\pi w}{g\ 2 \times 16}\left[f_3 (D_{G3}^4 - D_{G3i}^4) + K_{g3} t_3 D_{G3i}^4 + f_2 D_{p2}^4 + L_3 D_{s3}^4\right] \quad (5)$$

$$J_{G2} = \frac{\pi w}{g\ 2 \times 16}\left[f_2 (D_{G2}^4 - D_{G2i}^4) + K_{g2} t_2 D_{G2i}^4 + f_1 D_{p1}^4 + L_2 D_{s2}^4\right] \quad (6)$$

$$J_{G1} = \frac{\pi w}{g\ 2 \times 16}\left[f_1 (D_{G1}^4 - D_{G1i}^4) + K_{g1} t_1 D_{G1i}^4 + L_1 D_{S1}^4\right] \quad (7)$$

These equations neglect the inertia contribution due to bearings and fact that diameters D_{si} of the connecting shafts, L_i, between stages are not cons . The nomenclature is the same as that shown in figure 15. The dimensions used i calculating the inertia values were the same as the dimensions used in calculatin he weights in paragraph 5.2.

Figure 28 shows the sample points that were calculated and the extr la- tion used to obtain values at other stall torques and ratios.

5.5.2 Simple Planetary

The inertia as reflected to the input sun gear is a function of the ge ratio, the ratio of face width to sun gear diameter, the output stall torque, allow Hertz stress levels, gear pressure angle, material density, and suitable dimens ratios. Fixing all of these variables with the exception of the ratio and the stall torque, the inertia can be found in terms of these two variables as shown in equa (5-66). The results are shown in Table IX.

The method of calculating the inertia is based on the condition that rgy stored in a rotating part is (1/2) $J_G \omega_m^2$, where J_G is the inertia of a mass about axis, G, and ω_m is the angular velocity of that mass about the G axis. Consequ v. the total energy stored can be determined by summing the energy required by ea rotating part and equating to an equivalent inertia x ω_m^2 product as shown in eq m (5-58).

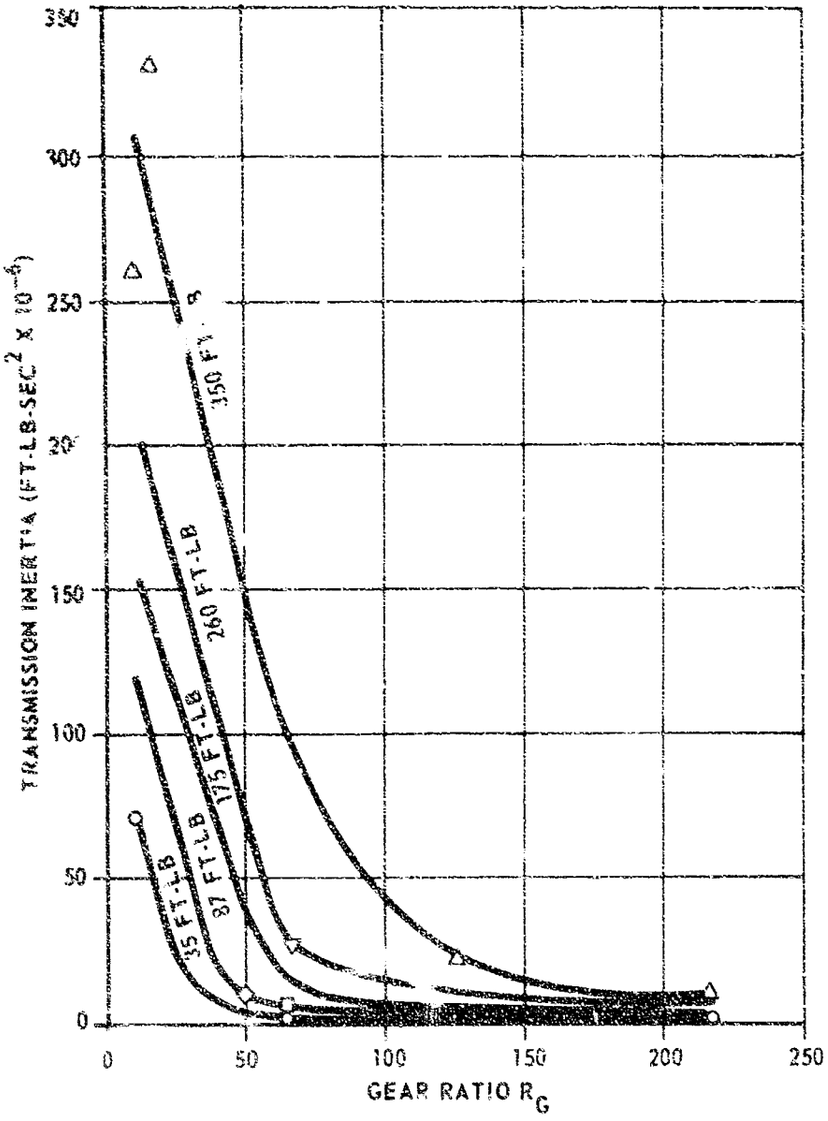

Figure 28. Inertia of Spur Gear Transmissions

TABLE IX

EQUIVALENT INERTIA OF SIMPLE PLANETARY TRANSMISSION WITH SUN GEAR INPUT AND CARRIER OUTPUT

Stall Torque T_{LM} (in-lb)	Ratio	Inertia J_e (ft-lb-sec^2 x 10^{-6})
400	3	17.8
	6	3.4
	10	8.9
	12	13.1
1000	3	86.2
	6	16
	10	41.6
	12	62.5
2000	3	272
	6	50.6
	10	130
	12	198
3000	3	538
	6	100
	10	260
	12	384
4200	3	950
	6	174
	10	453
	12	672

$$2\left(\frac{1}{2} J_e \omega_s^2\right) = \sum_i J_i \omega_i^2 \qquad (5\text{-}58)$$

i = r for the ring gear

i = p for the planet gear

i = s for the sun gear

i = c for the carrier

Some basic dimensional ratios were assumed to simplify the calculations. Also, the inertias due to bearings were neglected. The input shaft length (ℓ_1) is (a) times the face width (f) of the sun gear. The planet gear axle diameter (D_{PA}) is the diameter of the planet gear, D_p, divided by (b). The carrier flange thickness (ℓ_c) is equal to t_c x face width (f) and has a diameter equal to (D_s + 3 D_p/2). The output

shaft diameter, D_{co}, is equal to D_s and its length (ℓ_o) is t_{co} x face width (f). The planet gear axle has a length (ℓ_p) equal to (f). Also,

$$K_j = \frac{w}{32\,g}\ \frac{\text{lb-sec}^2}{\text{ft}^4}$$

The following equations define the J_i's of equation (5-58)

$$J_s = a\ K_j\ f\left[D_s^4\right] \tag{5-59}$$

$$J_p = 3\ K_j\ f\left[D_p^4 - \left(\frac{D_p}{b}\right)^4\right] \tag{5-60}$$

The factor 3 accounts for the three planets.

$$J_{pc} = 3\ md^2 = 6\ K_j\ f\left[D_p^2 - \left(\frac{D_p}{b}\right)^2\right]\left[D_p + D_s\right] \tag{5-61}$$

where

J_{pc} = the planet gear inertia for rotation about sun gear center line

$$\begin{aligned} J_c &= K_j\ f\left\{2t_c\left(D_s + \frac{3\,D_p}{2}\right)^4 + 3\left[\frac{\pi w f}{g\,2}\left(\frac{D_p}{2b}\right)^2\left(\frac{D_p}{2b}\right)^2\right.\right. \\ &\quad \left.\left. + \frac{\pi w f}{g}\left(\frac{D_p}{2b}\right)^2\left(\frac{D_s + D_p}{2}\right)^2\right] + K_j\ t_{co}\ f\ D_s^4\right\} \\ &= K_j\ f\left\{2t_c\left(D_s + \frac{3\,D_p}{2}\right)^4 + 3\left[\left(\frac{D_p}{b}\right)^4 + 2\left(\frac{D_p}{b}\right)^2\left(D_s + D_p\right)^2\right]\right. \\ &\quad \left. + t_{co}\ D_s^4\right\} \end{aligned} \tag{5-62}$$

The velocity ratios used are given below. They hold when the diametral pitch is constant for the transmission configuration used.

$$\omega_p = \omega_s \left(\frac{D_r}{D_p}\right)\left(\frac{D_s}{D_r + D_s}\right) = \omega_s \frac{D_r}{D_p}\left(\frac{1}{R_G}\right)$$

$$\omega_c = \omega_s \left(\frac{D_s}{D_r + D_s}\right) = \frac{1}{R_G}\omega_s$$

The useful dimensional ratios for this configuration are given below. They hold only when the diametral pitch is constant throughout the transmission.

$$D_s + 2D_p = D_r$$

$$R_G = 1 + \frac{D_r}{D_s}$$

$$D_p = \frac{1}{2} D_s (R_G - 2)$$

$$D_r = D_s (R_G - 1)$$

The equivalent inertia can be found by using equation (5-58) and the velocity ratios to give the relationship in equation (5-63).

$$J_e = J_s + J_p \left(\frac{D_r}{D_p R_G}\right)^2 + (J_{pc} + J_c)\left(\frac{1}{R_G}\right)^2 \qquad (5\text{-}63)$$

Substituting the values of J_i from equations (5-59) through (5-61) into equation (5-63), the following relationship can be found:

$$J_e = K_j f \left\{ a D_s^4 + 12\left[D_p^4 - \left(\frac{D_p}{b}\right)^4\right]\left[\left(\frac{R_G - 1}{R_G - 2}\right)\left(\frac{1}{R_G}\right)\right]^2 \right.$$

$$+ \left(\frac{1}{R_G}\right)^2 \left[6\left(D_p^2 - \left(\frac{D_p}{b}\right)^2\right)(D_p + D_s)^2\right] \qquad (5\text{-}64)$$

$$\left. + 2t_c\left(D_s + \frac{3D_p}{2}\right)^4 + 3\left[\left(\frac{D_p}{b}\right)^4 - 2\left(\frac{D_p}{b}\right)^2 (D_s + D_p)^2 + t_{co} D_s^4\right]\right\}$$

Equation (5-64) can be written in terms of three variables by substituting the following values:

$$\frac{D_p}{D_s} = y = \frac{R_G - 2}{2}$$

$$a = 4$$

$$\frac{f}{D_s} = y_1 = 1.5$$

$$b = 2$$

$$t_c = 1/4$$

$$T_{co} = 1.5$$

Also, using equation (5-26)

$$D_s^3 = 1.37 \times 10^{-3} \left(\frac{T_o}{R_G - 2}\right) (in^3) \qquad (5\text{-}65)$$

Using equation (5-64), the relationship $f = 1.5\ D_s$ and equation (5-65), the following expression is derived for equivalent simple planetary transmission inertia:

$$J_e = 1.5 \times 10^{-9} \left[1.37 \times T_o \times \left(\frac{1}{R_G - 2}\right)\right]^{5/3} \left\{4 + \frac{45}{4}\left[\left(\frac{R_G - 1}{R_G - 2}\right)\frac{1}{R_G}\right]^2 y^4 + \left(\frac{1}{R_G}\right)^2 \left[\frac{y^2}{16}\,(127\,y^2 + 228\,y + 114) + \frac{1}{2}\left(1 + \frac{3}{2}\,y\right)^4 + 1.5\right]\right\} \qquad (5\text{-}66)$$

The results illustrated in Table IX were obtained by substituting the various ratios and stall torques in equation (5-66).

5.5.3 Compound Planetary

The method for calculating the inertia of the compound planetary transmission is similar to the method used in paragraph 5.5.2 for simple planetary transmissions since the inertia of each rotating part about its center of rotation can be reflected to the input by the square of the proper velocity ratio.

There are four elementary rotating parts in the compound planetary transmission configuration chosen for analysis. They are (1) the input sun gear, (B), (2) the planet gears, (D) and (E), (3) the planet carrier, (A), and (4) the output ring gear, (G). The total inertia as reflected to the input sun gear is given in equation (3-67) where the subscripts refer to the various rotating parts. Refer to figure 23.

$$J_e = J_B + \left(J_D + J_E\right)\left[\left(\frac{C}{D}\right)\left(\frac{B}{C+B}\right)\right]^2 \qquad (5\text{-}67)$$

$$+ \left[J_A = \left(M_D + M_E\right)\left(\frac{D+B}{2}\right)^2\right]\left(\frac{B}{C+B}\right)^2 + J_G\left[\frac{B}{C+B}\left(1 - \frac{CE}{DG}\right)\right]^2$$

Actual calculations using equation (5-67) were made for those units shown in figures 21 through 24. The (calculated) values are shown in Table X, and plotted in figure 29.

TABLE X

EQUIVALENT INERTIA OF COMPOUND PLANETARY TRANSMISSION WITH SUN GEAR INPUT AND CARRIER OUTPUT

Stall Torque	Ratio	Inertia J_e (ft-lb-sec^2 x 10^{-6})
350 ft-lb	55:1	169
350 ft-lb	88:1	130
87.5 ft-lb	55:1	24.5
35 ft-lb	88:1	2.45

5.5.4 External Epicyclic

The input shaft was assumed symmetrical about the center of the transmission in calculating the inertia of external epicyclic transmissions. The center of the rotating gears have a circular motion about the center of the transmission at a radii equal to the eccentricity, e. The velocity ratio can be obtained from the diagram in figure 30 and the following equations:

$$\omega_g = e\,\omega_1$$

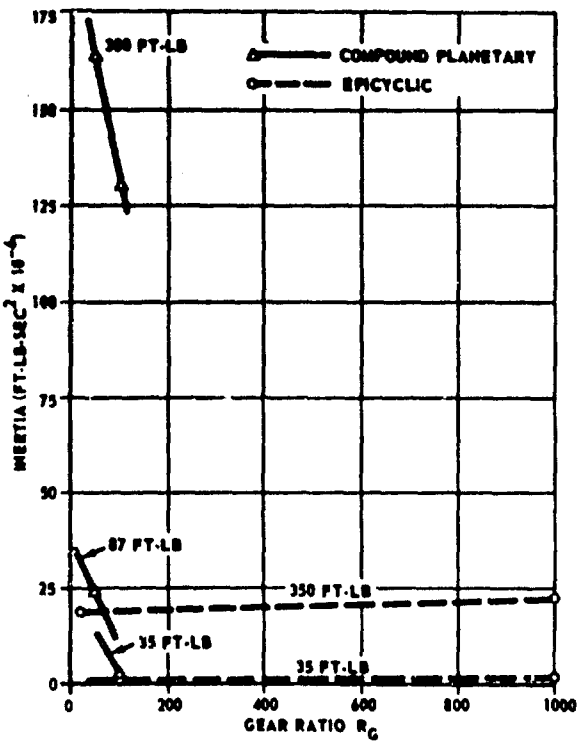

Figure 29. Inertia of Compound Planetary and External Epicyclic Transmissions

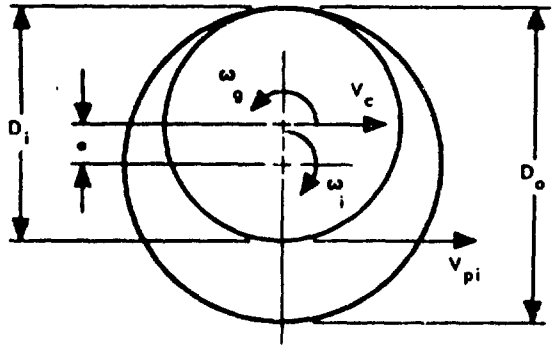

Figure 30. Diagram — Determination of ω_g/ω_i

$$v_{pi} = 2 v_c$$

$$\omega_g = \frac{1}{2} v_{pi} / D_i / 2$$

$$\omega_g = \omega_i \quad e / D_i / 2$$

$$\frac{\omega_g}{\omega_i} = \frac{D_o - D_i}{D_i}$$

$$\frac{\omega_i}{\omega_o} = R_G$$

$$J_e = J_S + m e^2 + J_G \frac{\omega_g^2}{\omega_i} + J_o \frac{\omega_o^2}{\omega_i}$$

D_i = pitch diameter of external ring gear in second stage mesh (inch)

D_o = pitch diameter of internal output reaction gear in second stage mesh (inch)

m = mass of the rotating gears (lb-sec^2/ft)

J_g = inertia about centroid of rotating gears (lb-ft-sec^2)

J_o = inertia of output ring gear (lb-ft-sec^2)

ω_i = input shaft angular velocity (rad/sec)

ω_o = output shaft angular velocity (rad-sec)

ω_g = ring gear angular velocity about its center

The values obtained are tabulated in Table XI and plotted in figure 31 for the equivalent inertia, J_e, at the high speed input shaft.

5.5.5 Harmonic Drive

The inertia values for the Harmonic Drive transmissions were supplied by the manufacturer for the various transmission sizes. The data is tabulated in Table XII. The transmission sizes available are not directly applicable; however, the sizes

TABLE XI

CALCULATED INERTIA VALUES FOR EXTERNAL EPICYCLIC TRANSMISSIONS

Stall Torque	Ratio	Inertia J_e(ft-lb-sec^2 x 10^{-6})
350 ft-lb	1000:1	22
350 ft-lb	20:1	19
35 ft-lb	1000:1	0.6

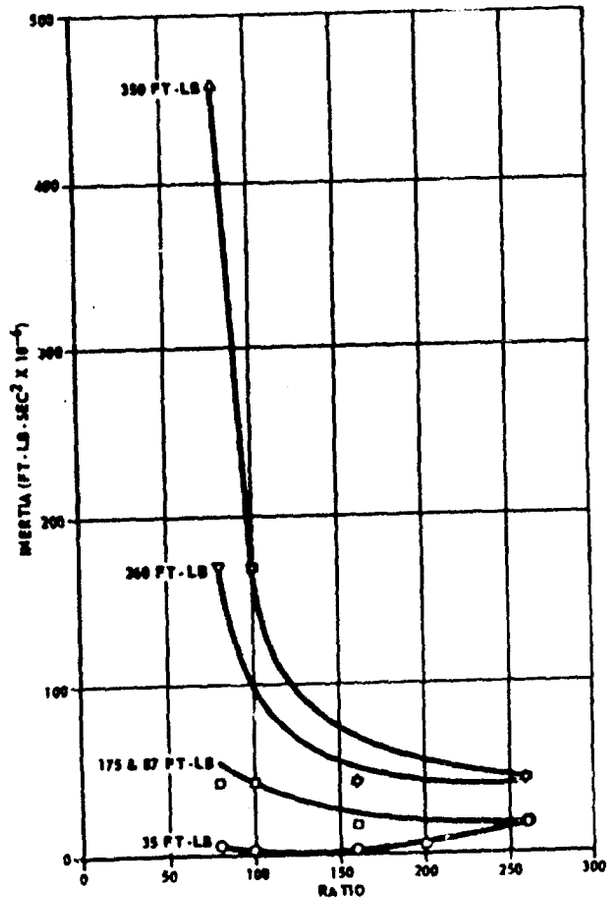

Figure 31. Inertia of Harmonic Drive Transmissions

TABLE XII

INERTIA OF HARMONIC DRIVE TRANSMISSIONS

Size Number	Inertia ($ft\text{-}lb\text{-}sec^2 \times 10^{-6}$)
20	17
25	40.6
32	170
40	444
50	1700
65	4650
80	14700
100	38400

used in the weight, volume, and inertia determinations are tabulated in Table VIII as a function of stall torque and reduction ratio. Figure 31 illustrates inertia as a function of gear ratio and stall torque.

5.6 TRANSMISSION COMPARISON

The figures illustrated in this paragraph are presented to demonstrate the weight, volume and inertia for the several transmission types. An analysis and discussion of these transmissions was presented in paragraphs 5.2 through 5.5. These figures were derived from the data presented therein. Ratios between 50:1 and 200:1, were used, since this range indicated the greatest potential for the CMG application.

Table XIII demonstrates a comparative evaluation of the transmissions. The overall ratio range was divided into two parts for comparative purposes: (1) low range, for ratios from 50:1 to approximately 125:1, and (2) high range for ratios from approximately 125:1 to 200:1.

Considering the transmission weight data presented in figure 32 the weight of the spur gear transmission is competitive at low ratios and the smaller CMG sizes. The compound planetary weight is fairly competitive for all ratios and CMG sizes to approximately 1000 ft-lb-sec. The epicyclic transmission weight is very competitive over the full range of ratios for all the CMG sizes. The harmonic drive weight is very competitive at the higher ratios for all CMG sizes.

Considering the volume requirement data shown in figure 33 the spur gear transmission volume requirement is fairly poor over the full range of ratios and CMG sizes. The compound planetary volume is very competitive, as well as the harmonic drive and epicyclic units.

TABLE XIII

TRANSMISSION EVALUATION

Transmission Type	WEIGHT		VOLUME		INERTIA		Backlash	Friction and Efficiency
	Low Range (1)	High Range (2)	Low Range	High Range	Low Range	High Range		
Spur Gear	2	1	1	1	2	3	3	2
Compound Planetary	2	0	3	0	2	0	3	2
Epicyclic	3	3	3	3	3	3	2	2
Harmonic Drive	2	3	0	3	2	1	2	1

NOTES:

(1) Low Range represents transmission ratios from 50:1 to approximately 125:1

(2) High Range represents transmission ratios from approximately 125:1 to 200:1

(3) Rating Factors: 3 = Very Good; 2 = Good; 1 = Fair; 0 = Poor.

Considering the inertia data presented in figure 34 some care must be exercised in use of the curves. The range of inertias of the DC torquer motors considered for application to the CMG is 10^{-6} to 0.178 ft-lb-sec^2. The general range of transmission inertias (except for the harmonic drive unit) is 2×10^{-6} to 165×10^{-6} ft-lb-sec^2. The relative importance of the transmission inertia is indicated only when compared with the motor inertia. If the transmission data is considered only on its own merits, the epicyclic transmission is very suitable over the full range of ratios and CMG sizes. The spur gear becomes very competitive at the higher ratios. The compound planetary generally could be acceptable. The harmonic drive units exhibit rather large inertias and, as such, their application must be qualified by further consideration of relative magnitude of the motor inertia and also the loop performance requirements.

Relative backlash and friction levels were presented in paragraphs 5.3 and 5.4. The backlash and friction ratings assigned to the transmissions were based on the discussion presented therein.

The conclusion is that the epicyclic transmission is the best selection for CMG application. Also, the compound planetary transmission is an excellent second choice.

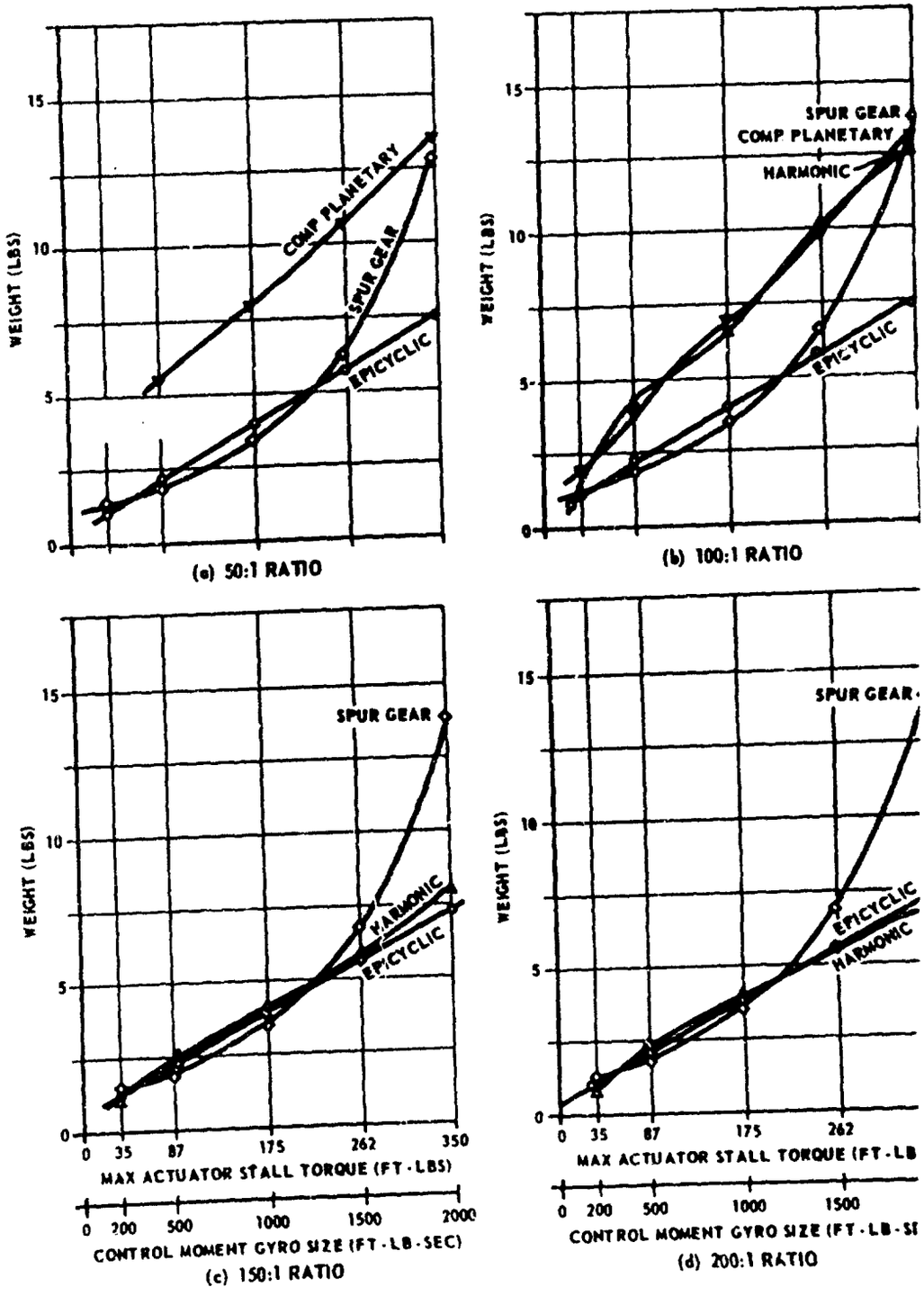

Figure 32. Transmission Weight Versus Stall Torque

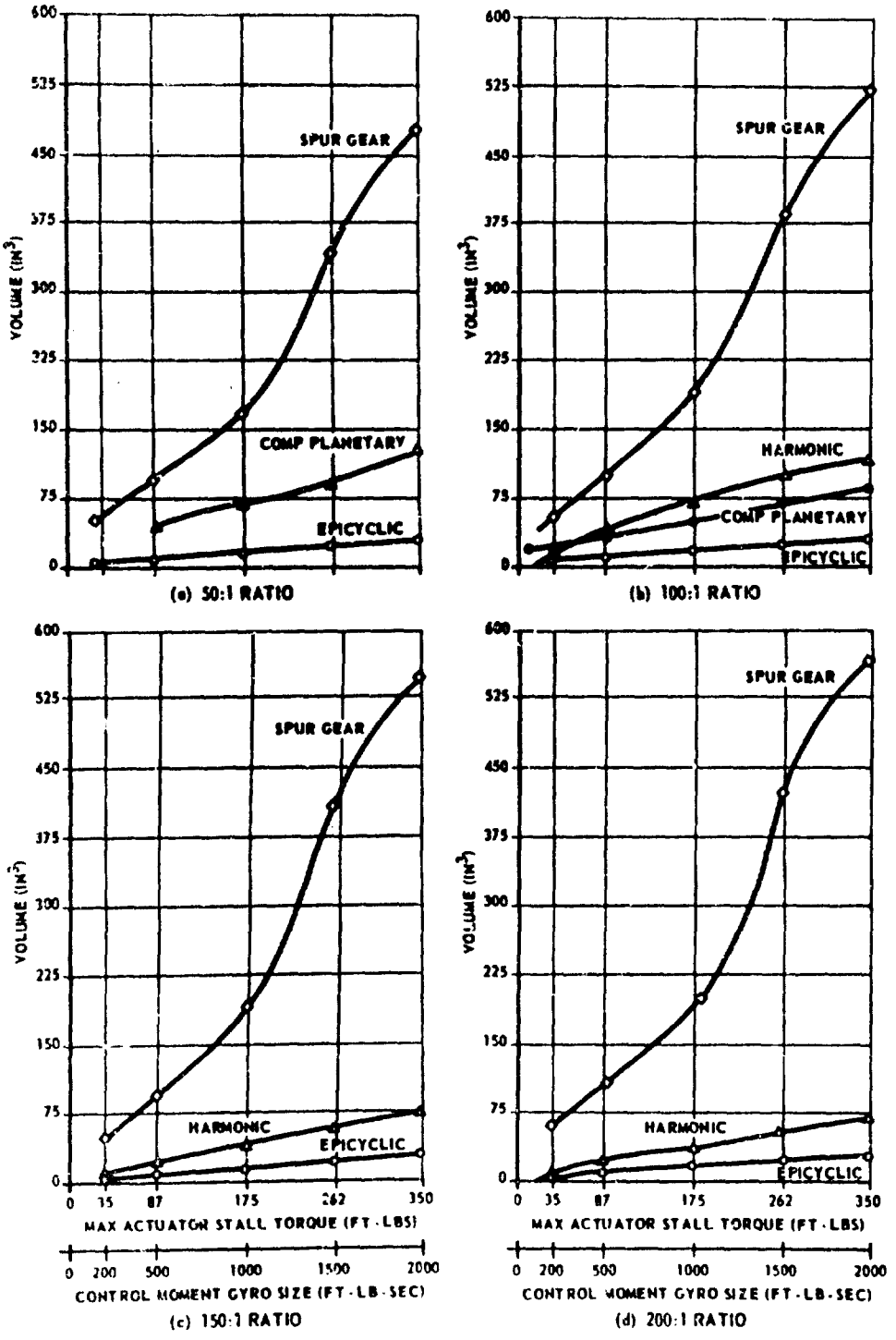

Figure 33. Transmission Volume Versus Stall Torque

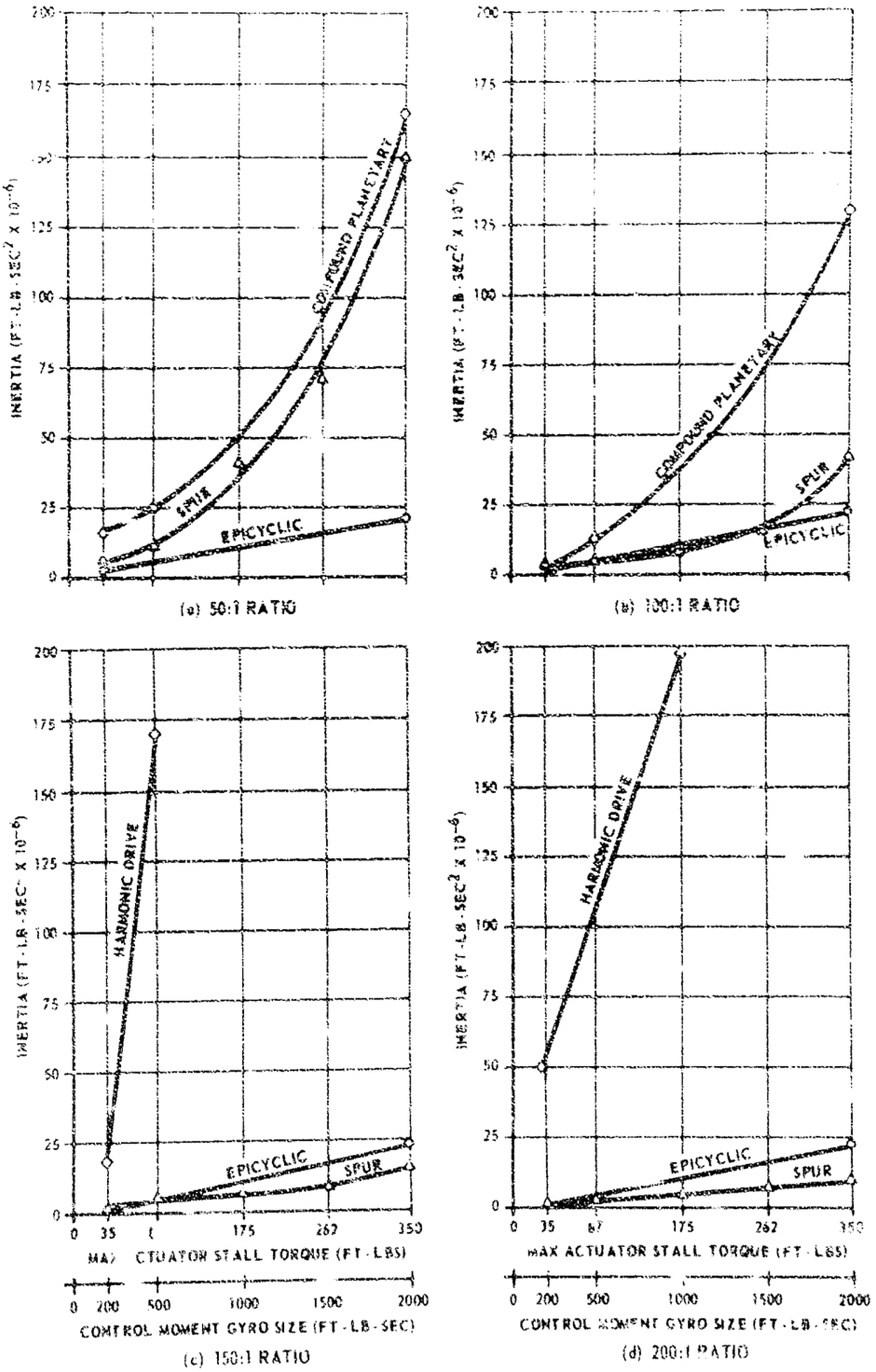

Figure 34. Transmission Inertia Versus Stall Torque

SECTION VI

ACTUATOR OPTIMIZATION

6.1 DYNAMIC CONSIDERATIONS AND ANALYTIC TRANSFORMS

The analytical transforms are the ratio of the actuator output speeds, N_L, to the input signal, E_m, in the Laplace transform or S domain. The response characteristics of the control system will generally be limited by the actuator transfer function. However, other characteristics such as resolution, threshold, stability, etc., will be a function of the total system. Figure 35 shows some of the elements that will be necessary for the total actuator system. They include an error amplifier (K_A) and tachometer feedback (K_G). The gain of these two elements will improve the response, determine the speed linearity and make the system stiffer (less susceptible to speed variation when disturbance torques are present). This block diagram illustrates one possible method for rate mode control with switching used to accomplish torque mode control. One feature of the controller shown in figure 35 merits further discussion. If the torque-commanded axis develops a rate caused by a disturbance torque acting on the rate-controlled axis, this undesired rate signal can be used to eliminate or reduce the disturbance torque.

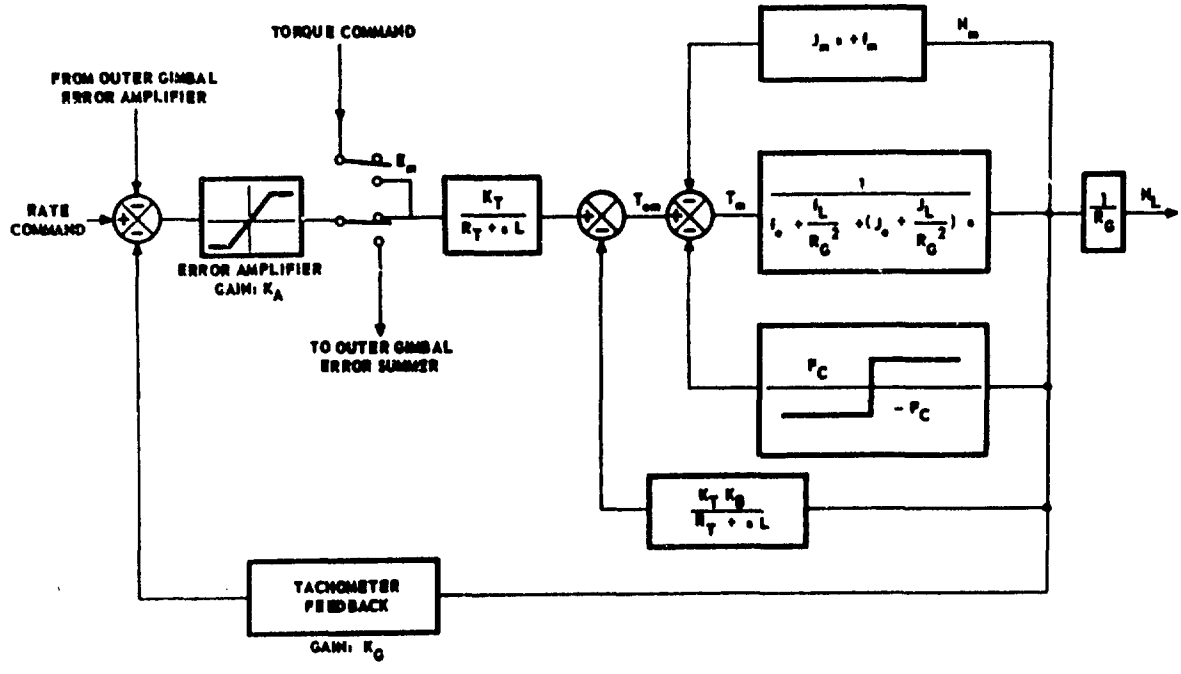

Figure 35. Block Diagram - Inner Gimbal Control System

6.1.1 Single-Order Response

The single order response is based on motors having straight line torque-versus-speed characteristics and neglects electrical time lags and external feedback elements.

The motor torque (T_{em}) under steady-state conditions has the following form:

$$T_{em} = k\,(E_m) - M_{Mmax}\,(N_M) \tag{6-1}$$

k = stall torque input constant (ft-lb/volt)

E_m = input voltage

M_{Mmax} = ratio of maximum stall torque to maximum speed (ft-lb/rad/sec)

N_M = motor speed (rad/sec)

The motor output torque (T_M) is T_{em} less motor inertia and friction torque and equal to the torque applied to the transmission.

$$T_M = T_{em} - J_M \frac{d\,N_M}{dt} - f_M\,N_M \tag{6-2}$$

The torque, T_M, applied to the transmission input is

$$T_M = \frac{1}{R_G}\left[J_L \frac{d\,N_L}{dt} + f_L\,N_L\right] \tag{6-3}$$

$N_M = R_G N_L$, thus

$$T_M = \frac{J_L}{R_G^{\,2}}\left(\frac{d\,N_M}{dt}\right) + \frac{f_L}{R_G^{\,2}}\,N_M \tag{6-4}$$

Consequently, from equations (6-2) and (6-4),

$$T_{em} = J_M \frac{d\,N_M}{dt} + f_M\,N_M + \frac{J_L}{R_G^{\,2}} \frac{d\,N_M}{dt} + \frac{f_L}{R_G^{\,2}}\,N_M \tag{6-5}$$

The total friction and inertia can be expressed as one term:

$$J_T = J_M + \frac{J_L}{R_G^2}$$

$$f_T = f_M + \frac{f_L}{R_G^2}$$

Substituting equation (6-5) into equation (6-1) as a function of speed, the following equation holds:

$$J_T S\, N_M(s) + f_T N_M(s) = k\, E_m(s) - M_{Mmax}\, N_M(s) \tag{6-6}$$

The transfer function is

$$\frac{N_m(s)}{E_m(s)} = \frac{\dfrac{k}{M_{Mmax} + f_T}}{1 + S\dfrac{J_T}{M_{Mmax} + f_T}} \tag{6-7}$$

Or, simplifying,

$$\frac{N_m(s)}{E_m(s)} = \frac{k}{\left(M_{Mmax} + f_T\right)\left(1 + S\dfrac{J_T}{M_{Mmax} + f_T}\right)} \tag{6-8}$$

For time response, when the input command $E_m(t)$ is a step function, the output $N_M(t)$ is

$$N_M(t) = (E_m)\frac{k}{M_{Mmax} + f_T}\left(1 - e^{-t/\tau}\right), \tag{6-9}$$

where t is the elapsed time after the start of the input step and $\tau = J_T/(f_T + M_{Mmax})$. The block diagram of figure 36 yields the same transfer function if L, J_e, and f_e are equal to zero and where $K_T/R_T = k$ and $K_T K_B/R_T = M_{Mmax}$.

The various values of τ can be evaluated based on the inertias (J_e) established for the transmissions in section V, the load inertia (J_L) established as $J_L = 2.35\ (\log H) - 5.06$, and the motor inertia (J_M) from the motor manufacturer's

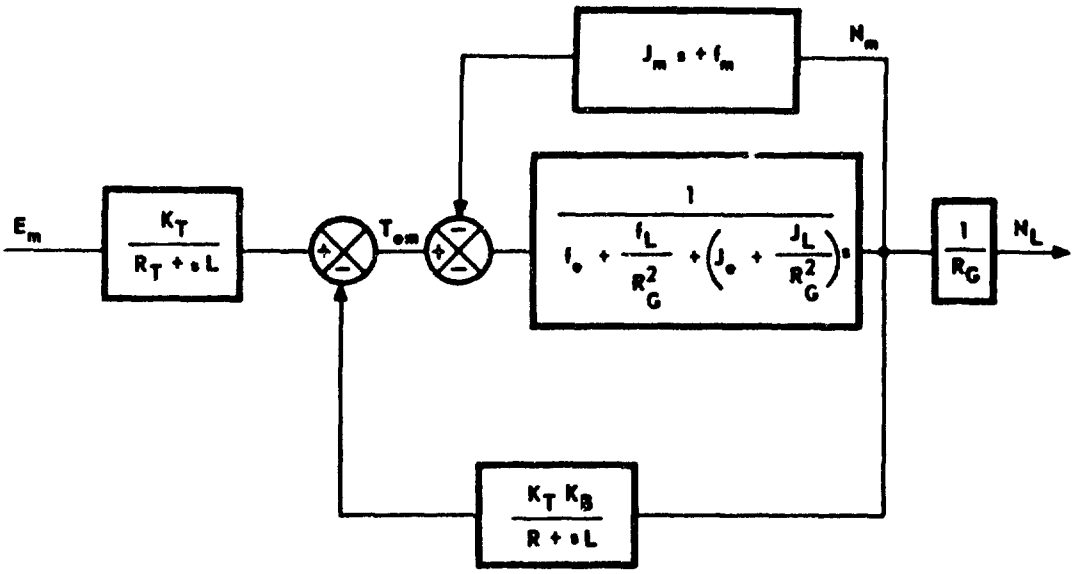

Figure 36. Block Diagram - Actuator Transfer Function

catalog. For low speed loads, the total viscous friction, (f_T), is generally much smaller than M_{Mmax} and can be neglected in the CMG response calculations.

6.1.2 Second Order Response

The second order response can be determined by including the electrical time lags of the motor. Figure 37 is a schematic diagram showing the electrical elements involved in the transfer between the output torque T_{em} (s) and the source voltage E_m (s).

Then,

$$R_T = R_S + R_M \tag{6-10}$$

$$T_{em}(s) = K_T \left[\frac{E_m(s) - K_B N_M(s)}{R_T + S L_M}\right] \tag{6-11}$$

Substituting equation (6-5) into equation (6-11), the overall transfer function is

$$\frac{N_M(s)}{E_m(s)} = \frac{K_T}{K_T K_B + R_T f_T + (R_T J_T + f_T L_m) S + L_m J_T S^2} \tag{6-12}$$

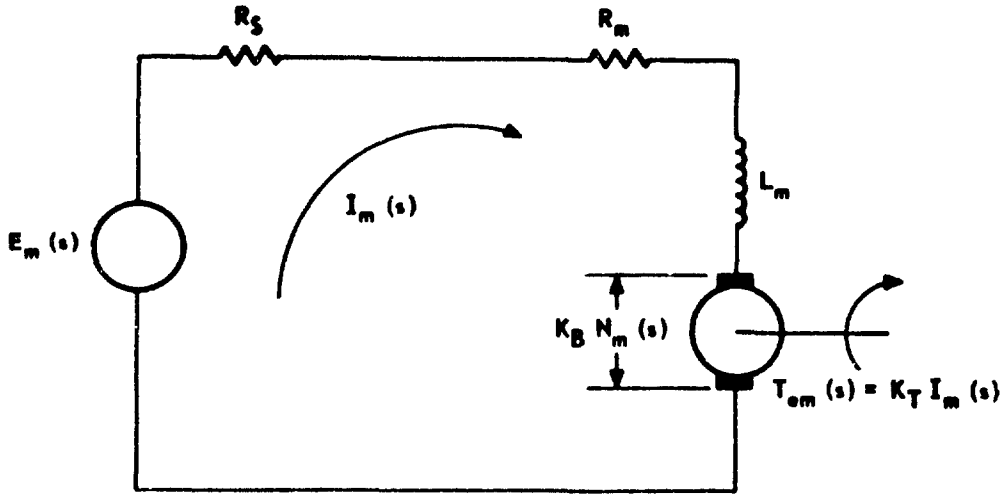

Figure 37. Schematic Diagram - DC Torquer Motor Control Circuit

Rewriting equation (6-12) in the same form as equation (2-5), the following relationship is determined:

$$\frac{N_M(s)}{E_m(s)} = \frac{\dfrac{K_T}{L_m J_T}}{\dfrac{K_T K_B + R_T f_T}{L_m J_T} + \left[\dfrac{R_T JT + f_T L_m}{L_m J_T}\right] S + S^2} \tag{6-13}$$

Thus the transfer function of the motor and transmission can be written as

$$\frac{N_M(s)}{E_m(s)} = \frac{K_T}{K_T K_B + R_T f_T}\left[\frac{\omega_n^2}{\omega_n^2 + 2\omega_n \zeta S + S^2}\right] \tag{6-14}$$

where

$$\omega_n = \sqrt{\frac{K_T K_B + R_T f_T}{L_m J_T}} \tag{6-15}$$

and

$$\zeta = 1/2 \left[\frac{R_T J_T + f_T L_m}{\sqrt{K_T K_B + R_T f_T}} \right] \frac{1}{\sqrt{L_m J_T}} \tag{6-16}$$

For f_T equal to zero, ω_n can be expressed in terms of motor constants and the total reflected inertia.

$$\omega_n = \frac{\sqrt{R_T} \sqrt{\frac{K_T K_B}{R_T}}}{\sqrt{L_m J_T}} \tag{6-17}$$

where the $\sqrt{K_T K_B / R_T} = \sqrt{F_o}$ as given in the motor catalog when $R_T = R_M$ and $\sqrt{F_o} = 1.19 K_m$. Therefore, ω_n can be evaluated for systems having zero source impedence and zero mechanical damping as follows:

$$\omega_n = 1.19 \left[\frac{\sqrt{R_m} K_m}{\sqrt{L_m J_T}} \right] \tag{6-18}$$

The damping factor can be calculated readily by using similar lumped constants and lettering f_T equal zero.

$$\zeta = 0.42 \left[\frac{\sqrt{R_m} (J_T)}{\sqrt{L_m J_T} (K_m)} \right] \tag{6-19}$$

The values of ω_n and ζ are tabulated for various motors and CMG sizes in tables XIV through XVIII.

6.1.3 Total Actuator Weight Comparison

The total actuator weight for the five CMG sizes are shown in figures 38 through 42 as a function of the minimum suitable gear ratio. The epicyclic transmission was used in determining the total actuator weight. These figures illustrate the fact that, for transmission ratios above 50:1, the major contribution to actuator weight is the transmission. The figures also illustrate that, for a given CMG size, the total actuator weight is fairly constant for ratios above 50:1. The data for these figures was obtained from tables XIV through XVIII.

TABLE XIV

DC TORQUER TRANSMISSION COMPARISON (200 FT-LB-SEC CMG SIZE)

	J_L = 0.4 ft-lb-sec^2 Stall Torque 35 ft-lb								
DC Motor Model Number	T-1342 B	T-2157 F	T-2170 D	T-2171 [illegible]	T-2967 B	T-3203 D	T-4036 C	T-5403 A	T-5134 D
Physical Size									
Weight (lb.)	0.625	0.563	0.875	1.56	1.1	1.6	3.0	1.31	5.7
O.D. (in.)	1.93	2.81	2.81	2.81	3.73	4.09	5.12	6.12	6.25
Length (in.)	0.84	0.62	1.0	1.5	0.89	1.09	1.25	0.67	1.31
Torque									
Peak (ft-lb)	0.208	0.182	0.312	0.625	0.52	1.0	1.8	1.3	2.7
Continuous (ft-lb)	0.051	0.105	0.21	0.40	0.33	0.605	1.34	0.76	2.5
Speed									
No Load (rad/sec)	400	165	75	54.5	96.2	62.5	37	65	22.5
Transmission Ratios									
Minimum Ratio	687	334	166	87.5	106	57.8	26.2	46	14
Maximum Ratio	2280	942	428	312	550	357	212	371	128
Motor Parameters									
R_m (ohms)	10	23.4	20	17	10.9	10.7	11.0	13.7	10.1
L_m (henries x 10^{-3})	2.5	15	19	26	13	24	21.0	6.6	26
J_m (ft-lb-sec^2 x 10^{-6})	10	36.4	57	115	130	270	760	630	2000
J_e (ft-lb-sec^2 x 10^{-6})	1	1	1	1	1	1.5	1.5	1.5	1.5
J_L/R_G^2 (ft-lb-sec^2 x 10^{-6})	0.845	3.59	14.5	52.3	37.7	112.5	585	189	2040
J_T (ft-lb-sec^2 x 10^{-6})	11.845	40.99	72.5	168.3	168.7	384.0	1346.5	820.5	4041.5
$K_m\left(\sqrt{\text{lb-ft-sec}} \times 10^{-2}\right)$	1.96	2.84	5.5	8.85	6.35	10.7	18.9	12	29.3
ω_n (rad/sec)	427	208.5	256	207	168	137	163	227	108
δ	4.68	8.9	2.16	1.57	2.46	1.58	2.17	4.56	1.795

TABLE XV

DC TORQUER TRANSMISSION COMPARISON (500 FT-LB-SEC CMG SIZE)

	J_L = 1.35 ft-lb-sec^2 Stall Torque 87.5 ft-lb							
DC Motor Model Number	T-4412 A	T-7202 F	T-7203 A	T-2171 E	T-3203 D	T-5134 D	T-5730 B	T-2950 E
Physical Size								
Weight (lb.)	1.5	11.5	22	1.56	1.6	5.7	8.2	2.0
O.D. (in.)	5.12	9.0	9.0	2.81	4.09	6.25	7.20	3.73
Length (in.)	0.078	1.62	2.56	1.50	1.09	1.31	1.62	1.34
Torque								
Peak (ft-lb)	1.5	11	22	0.625	1.0	2.7	7	1.2
Continuous (ft-lb)	0.72	6.3	9.45	0.40	0.605	2.5	4.45	0.76
Speed								
No Load (rad/sec)	60	23.5	20	54.5	62.5	22.5	27	48
Transmission Ratios								
Minimum Ratio	121.5	13.9	9.5	218	145	35	19.7	115
Maximum Ratio	343	134.3	114.3	310.5	357	128.5	154	275
Motor Parameters								
R_m (ohms)	8.3	1.99	1.1	17	10.7	10.1	3.5	11.6
L_m (henries x 10^{-3})	7	5.4	5	26	24	26	10	25
J_m (ft-lb-sec^2 x 10^{-6})	530	8400	17000	115	270	2000	5000	320
J_e (ft-lb-sec^2 x 10^{-6})	3.5	4.5	4.5	4.5	4.0	4.5	4.5	3.5
J_L/R_G^2 (ft-lb-sec^2 x 10^{-6})	91.5	7000	14600	28.4	64.2	1100	3480	102
J_T(ft-lb-sec^2 x 10^{-6})	625.	15404.5	31604.5	147.9	338.2	3104.5	8484.5	425.5
$K_m\left(\sqrt{\text{lb-ft-sec}} \times 10^{-2}\right)$	13.3	56.7	91.0	8.85	10.7	29.3	46.5	13.5
ω_n (rad/sec)	218	105.5	90.5	220.5	146.5	123	112	168
δ	2.717	1.785	1.24	1.475	1.52	1.58	1.56	1.37

TABLE XVI

DC TORQUER TRANSMISSION COMPARISON (1000 FT-LB-SEC CMG SIZE)

	J_L = 2 ft-lb-sec^2 Stall Torque 175 ft-lb						
DC Motor Model Number	T-4036 C	T-7203 A	T-7202 F	T-5730 D	T-2950 E	T-10036 B	T-5135 D
Physical Size							
Weight (lb.)	3	22	11.5	8.2	2	40	8.5
O.D. (in.)	5.12	9.0	9.0	7.2	3.73	13.69	6.25
Length (in.)	1.25	2.56	1.62	1.62	1.34	3.62	1.56
Torque							
Peak (ft-lb)	1.8	22	11	7.0	1.2	35	4.0
Continuous (ft-lb)	1.34	9.45	6.3	4.45	0.76	20	3.2
Speed							
No Load (rad/sec)	37	20	23.5	27	48	15	22
Transmission Ratios							
Minimum Ratio	130.5	18.5	27.8	39.3	230	8.75	54.5
Maximum Ratio	210.5	114.3	134.3	154.3	274.3	85.7	126
Motor Parameters							
R_m(ohms)	6.9	1.1	1.99	8.5	11.6	0.73	6.7
L_m(henries x 10^{-3})	13	5	5.4	2.7	25	2.3	20
J_m(ft-lb-sec^2 x 10^{-6})	760	17000	6400	5000	320	60000	3000
J_e(ft-lb-sec^2 x 10^{-6})	10	9.0	9.0	9.0	10	9.0	9.0
J_L/R_G^2(ft-lb-sec^2 x 10^{-6})	117	5850	2580	1295	37.8	26500	675
J_T(ft-lb-sec^2 x 10^{-6})	887	22859	10989	6304	367.8	86509	3684
$K_m\left(\sqrt{\text{lb-ft-sec}} \times 10^{-2}\right)$	16.9	91	56.7	46.5	13.5	126	36.7
ω_n (rad/sec)	173.5	106	123.5	130	180	90.7	131.5
δ	1.52	1.03	1.49	1.535	1.25	1.74	1.27

TABLE XVII

DC TORQUER TRANSMISSION COMPARISON (1500 FT-LB-SEC CMG SIZE)

	J_L = 2.4 ft-lb-sec^2 Stall Torque 262 ft-lb						
DC Motor Model Number	T-5403 A	T-5134 D	T-7203 A	T-5730 B	T-4036 C	T-10036 B	T-7202 F
Physical Size							
Weight (lb.)	1.31	5.7	22	8.2	3	40	11.5
O.D. (in.)	6.12	6.25	9	7.2	5.12	13.69	9.00
Length (in.)	0.67	1.31	2.56	1.62	1.25	3.62	1.62
Torque							
Peak (ft-lb)	1.3	2.7	22	7.0	1.8	35	11
Continuous (ft-lb)	0.76	2.5	9.45	4.45	1.34	20	6.3
Speed							
No Load (rad/sec)	65	22.5	20	27	37	15	23.5
Transmission Ratios							
Minimum Ratio	345	105	27.8	59	196	13.1	41.5
Maximum Ratio	371	128.5	114.3	154.3	210.5	85.7	134.3
Motor Parameters							
R_m (ohms)	13.7	10.1	1.1	3.5	6.9	0.73	7.25
L_m (henries x 10^{-3})	6.6	26	5	10	13	2.3	22
J_m (ft-lb-sec^2 x 10^{-6})	63	2000	17000	5000	760	60000	8400
J_e (ft-lb-sec^2 x 10^{-6})	16	16	15	15	16	15	15
J_L/R_G^2 (ft-lb-sec^2 x 10^{-6})	20.1	218	3100	690	62.5	14000	1390
J_T (ft-lb-sec^2 x 10^{-6})	666.1	2234	20115	5705	838.5	74015	9805
K_m $\left(\sqrt{\text{lb-ft-sec}} \times 10^{-2}\right)$	12	29.3	91	46.5	18.9	126	56.7
δ	4.0	3.78	0.973	1.305	.473	1.625	1.41

TABLE XVIII

DC TORQUER TRANSMISSION COMPARISON (2000 FT-LB-SEC CMG SIZE)

	J_L = 2.75 ft-lb-sec^2 Stall Torque 350 ft-lb						
DC Motor Model Number	T-601 A	T-5135 D	T-5730 B	T-7202 F	T-7203 A	T-10036 B	T-10035 C
Physical Size							
Weight (lb.)	0.75	8.5	8.2	11.5	22	40	110
O.D. (in.)	5.12	6.25	7.2	9	9	13.69	13.31
Length (in.)	0.58	1.56	1.62	1.62	2.56	3.62	5.31
Torque							
Peak (ft-lb)	0.8	4.0	7.0	11	22	35	100
Continuous (ft-lb)	0.54	3.2	4.45	6.3	9.45		50
Speed							
No Load (rad/sec)	157	22	27	23.5	20	15	7.7
Transmission Ratios							
Minimum Ratio	650	109.5	78.8	55.5	37.1	17.5	7.0
Maximum Ratio	897.5	125.5	154.3	134.3	114.3	85.7	44
Motor Parameters							
R_m (ohms)	18.6	6.7	3.5	7.25	1.1	0.73	0.66
L_m (henries x 10^{-3})	10	20	30	22	5	2.3	4
J_m (ft-lb-sec^2 x 10^{-6})	480	3000	5000	8400	17000	60000	178000
J_e (ft-lb-sec^2 x 10^{-6})	22	21.5	21.5	20	20	20	20
J_L/R_G^2 (ft-lb-sec^2 x 10^{-6})	6.53	251	443	890	2000	9000	56200
J_T (ft-lb-sec^2 x 10^{-6})	508.53	3272.5	5464.5	9310	19020	69020	234220
$K_m\left(\sqrt{\text{lb-ft-sec}} \times 10^{-2}\right)$	6.1	36.7	46.5	56.7	91.0	126	310
ω_n (rad/sec)	139	108	140	134.5	111.7	101	97.8
δ	6.7	1.547	1.24	1.372	0.91	1.555	0.84

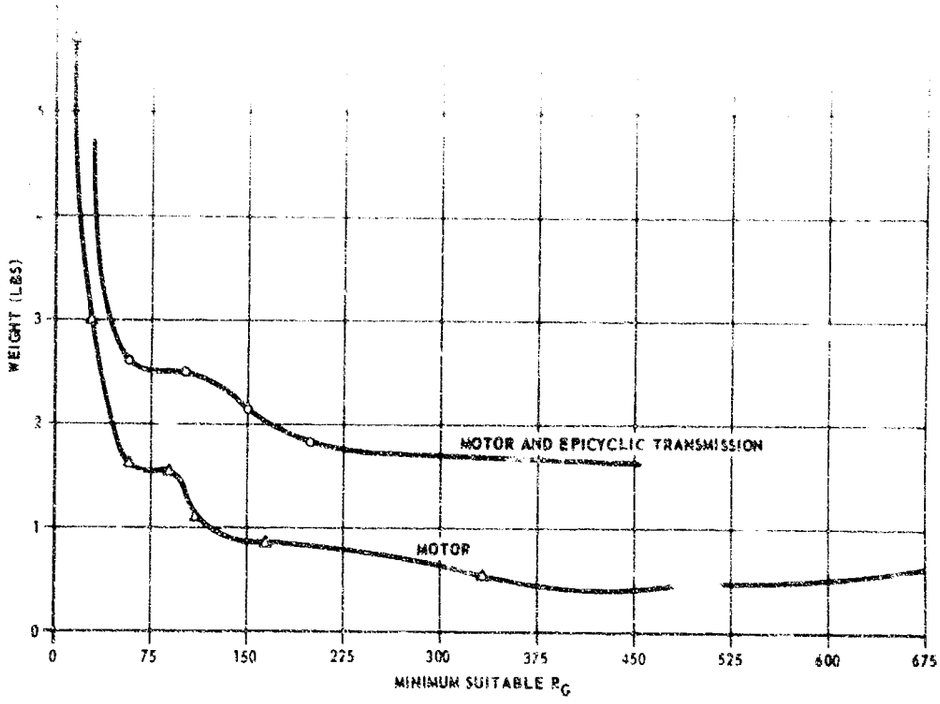

Figure 38. Actuator Weight Versus Minimum Suitable Gear Ratio - 35 ft-lb Stall Torque

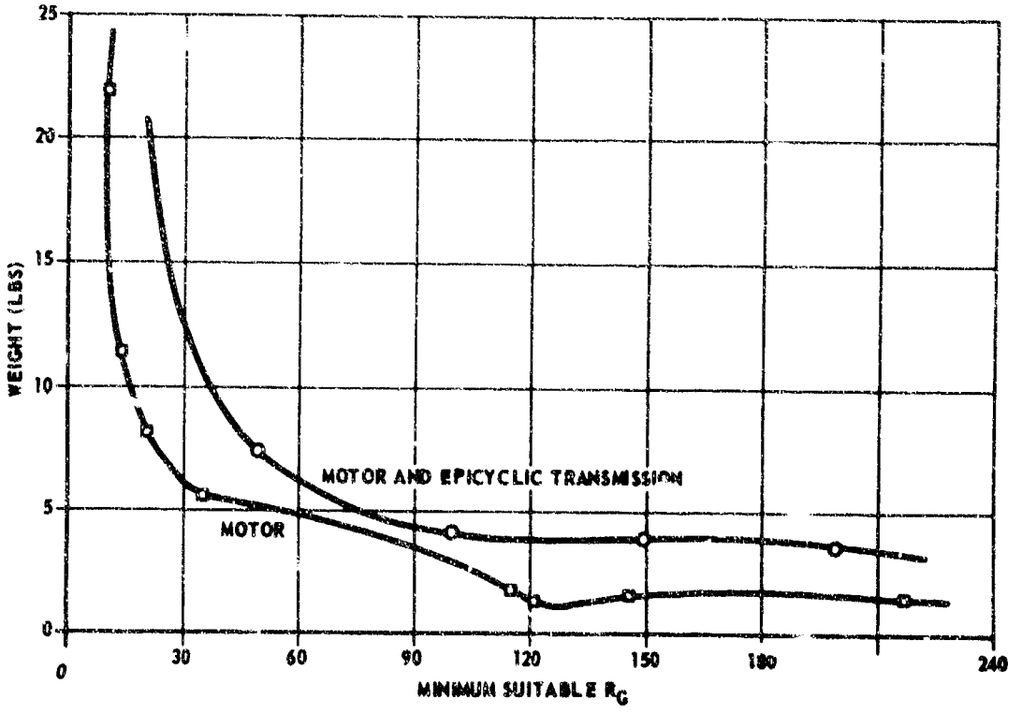

Figure 39. Actuator Weight Versus Minimum Suitable Gear Ratio - 87.5 ft-lb Stall Torque

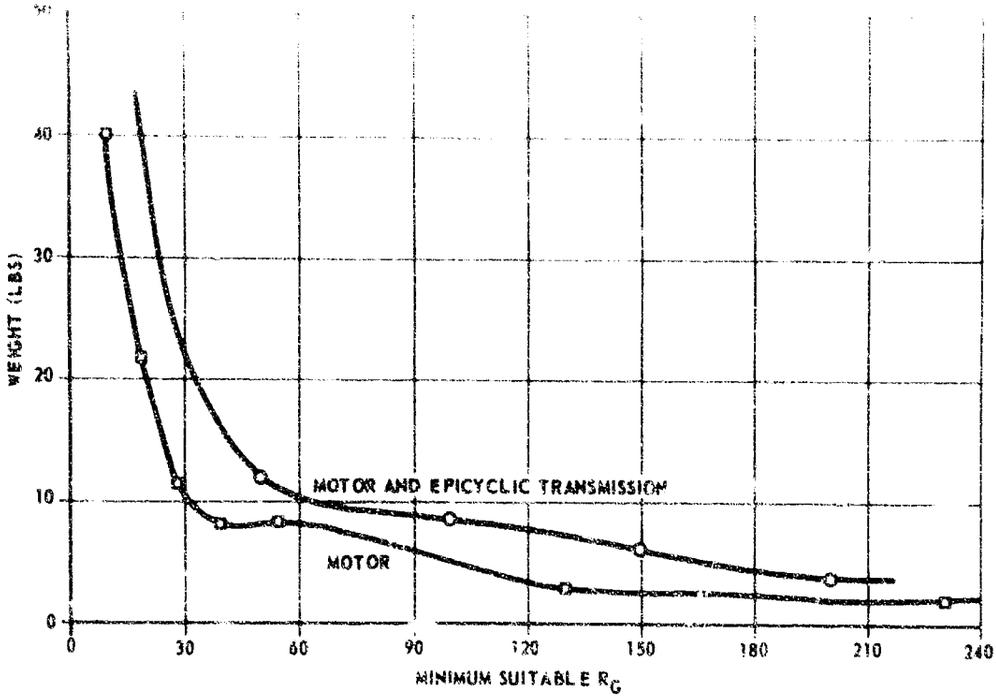

Figure 40. Actuator Weight Versus Minimum Suitable Gear Ratio - 175 ft-lb Stall Torque

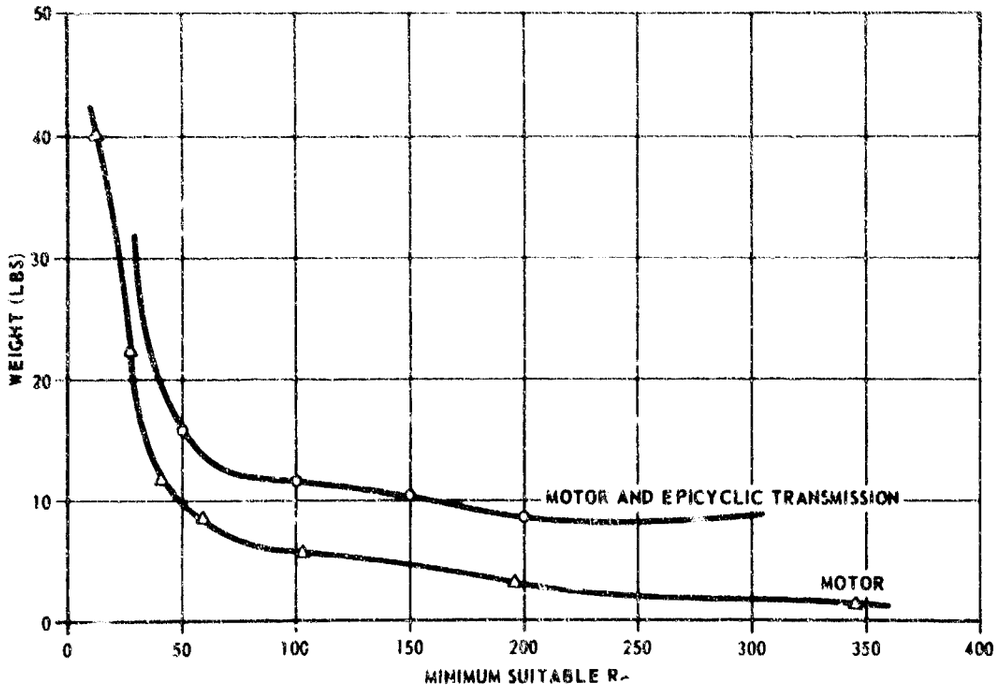

Figure 41. Actuator Weight Versus Minimum Suitable Gear Ratio - 262 ft-lb Stall Torque

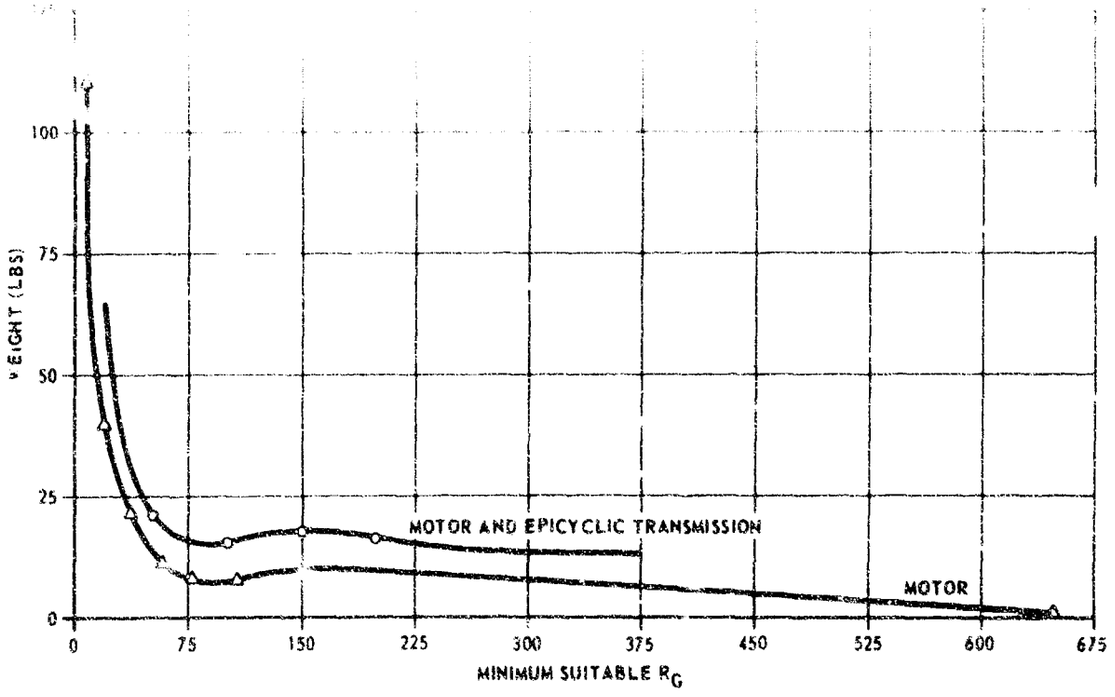

Figure 42. Actuator Weight Versus Minimum Suitable Gear Ratio - 350 ft-lb Stall Torque

6.1.4 Speed Range Considerations

The maximum speed that a load can be driven is equal to the product of the maximum motor speed and the transmission ratio. The maximum motor speed is a function of the motor torque-speed curve and the load torque. Figure 43 shows a typical motor torque-speed curve with superimposed curves of typical load torques due to coulomb and viscous friction. The torque available to accelerate the load is the motor torque T_{em} less the friction torque and is equal to T_M in figure 43. The friction torque varies with speed. Therefore, the combined friction and output torque will vary with speed, even though the motor generated torque is constant.

The motor speed, at any output torque value, is determined by the intersection of the motor and load torque-speed curves for that output torque.

The motor speed can be reduced by increasing the load or decreasing the motor torque T_{em}. The minimum speed at which the uncompensated motor will run smoothly depends on the speed history; e.g., if a lower speed is commanded, the minimum smooth speed will be at the point where $(T_{em1} - T_l)$ is slightly greater than zero. However, if an increasing speed is commanded when the motor is at zero speed, the load does not accelerate until $(T_{em2} - T_l)$ becomes greater than zero. As seen in figure 43 these two speeds do not coincide. The resulting speed oscillators will resemble those of a relaxation oscillator.

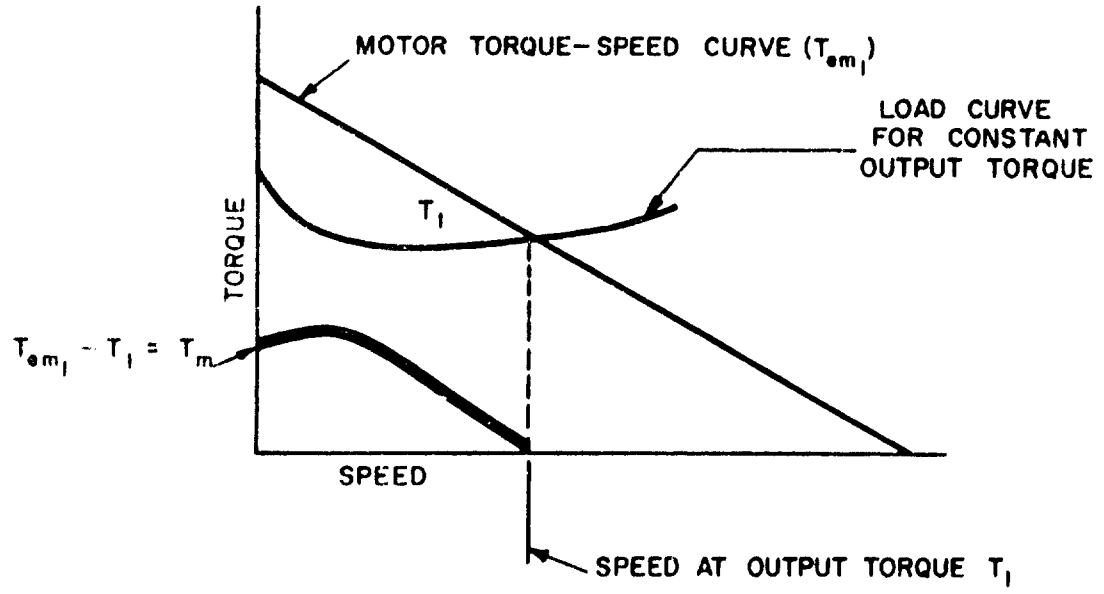

Figure 43. Motor and Load Torque-Speed Curves

The minimum motor speed can be reduced by adding rate feedback to cancel the negative damping effect of friction at low speed. The factors which limit the minimum speed that can be obtained with rate feedback are threshold of the rate feedback system, noise, and variation of friction with output shaft position. The motor speed will obviously not be smooth when the signal to noise ratio of the motor electrical input is low. The variation of friction with position is also a form of noise, and the signal level must be sufficiently high to cancel the effects of this noise.

An example of the speed range capabilities of direct drive DC torquers is a table for testing rate and integrating gyros. This table has a speed range of 0.017 RPM to 1000 RPM, or a range of 5900.[22] The range required of the CMG is 1000:1 and is not considered to be a serious problem in control circuit implementation.

6.2 TRANSMISSION OPTIMIZATION

The transmission optimization deals with the specific selection of characteristics for the epicyclic transmission chosen in the general transmission study of section V. A general technique is developed which allows the selection of an optimum transmission based on ratio, size, and efficiency. A schematic representation of the epicyclic transmission is shown in figure 44.

---

[22]See Reference No. 17, Appendix D

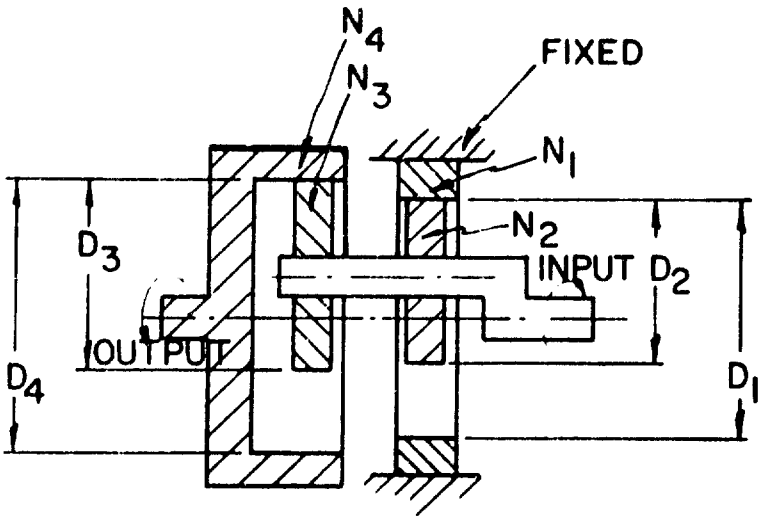

Figure 44. Epicyclic Transmission

The transmission ratio of an epicyclic transmission is given by

$$R_G = \frac{N_2 N_4}{N_2 N_4 - N_1 N_3} \tag{6-11}$$

E_Q (6-11) can be rewritten as

$$\frac{1}{R_G} = \frac{N_2 N_4 - N_1 N_3}{N_2 N_4}$$

$$= 1 - \frac{N_1 N_3}{N_2 N_4}$$

Or

$$\frac{N_1 N_3}{N_2 N_4} = 1 - \frac{1}{R_G}$$

$$= \frac{R_G - 1}{R_G}$$

For convenience take the fixed internal gear N_1 as a reference

$$\frac{N_3 - 1}{\frac{N_2}{N_1}\frac{N_4}{N_1}} = \frac{R_G - 1}{R_G} \tag{6-12}$$

From figure 44 the following relationships are evident:

$$\frac{D_1}{2} = \frac{D_2}{2} + e$$

$$\frac{D_4}{2} = \frac{D_3}{2} + e$$

Solving for the eccentricity e in both equations:

$$e = \frac{D_1}{2} - \frac{D_2}{2}$$

$$= \frac{D_4}{2} - \frac{D_3}{2}$$

Or

$$D_4 - D_3 = D_1 - D_2$$

Solving for D_3,

$$D_3 = D_4 + D_2 - D_1 \tag{6-13}$$

Assume that the diametrical pitch is the same for both gear meshes; therefore

$$N_3 = N_4 + N_2 - N_1 \tag{6-14}$$

When E_Q (6-14) is substituted into E_Q (6-12)

$$\frac{\frac{N_4}{N_1} + \frac{N_2}{N_1} - 1}{\frac{N_2}{N_1}\frac{N_4}{N_1}} = \frac{R_G - 1}{R_G} \tag{6-15}$$

Solving E_Q (6-15) for $\frac{N_4}{N_1}$ yields

$$\frac{N_4}{N_1} = \frac{1 - \frac{N_2}{N_1}}{1 - \frac{N_2}{N_1}\frac{R_G - 1}{R_G}} \qquad (6\text{-}16)$$

The form of equation (6-16) is shown in figure 45 with the transmission ratio R_G and the non-dimensional parameter $\frac{N_2}{N_1}$ as independent variables.

In paragraph 5.4, the efficiency of the epicyclic transmission was shown to be

$$\eta = \frac{1}{1 + 0.13\left(\frac{1}{N_2} + \frac{1}{N_3} - \frac{1}{N_1} - \frac{1}{N_4}\right)(R_G - 1)} \qquad (6\text{-}16)$$

The factor 0.13 contains an assumed coefficient of friction between mating gears of 0.07.

Equation (6-16) can be written in terms of the fixed gear by dividing by N_2:

$$\eta = \frac{1}{1 + \frac{0.13}{N_1} + \left(\frac{1}{N_2/N_1} + \frac{1}{N_3/N_1} - \frac{1}{N_4/N_1}\right)(R_G - 1)} \qquad (6\text{-}17)$$

N_3 can be eliminated by substituting equation (6-14) into equation (6-17), noting the assumption that the diametrical pitch is the same for both meshes:

$$\eta = \frac{1}{1 - \frac{0.13}{N_1}\left(1 + \frac{1}{N_4/N_1} + 1 - \frac{1}{(N_4/N_1 + N_2/N_1)} - \frac{1}{N_2/N_1}\right)(R_G - 1)} \qquad (6\text{-}18)$$

It can be seen from Equation (6-18) that the efficiency can not be expressed purely in terms of non-dimensional parameters, but is dependent upon the number of teeth on the reference gear, which, in this case, is N_1. On figures 46 through 48 the epicyclic transmission efficiency is plotted as a function of the non-dimensional parameters and the negative ratio for various values of N_1. Note that efficiency increases with increasing number of teeth N_1.

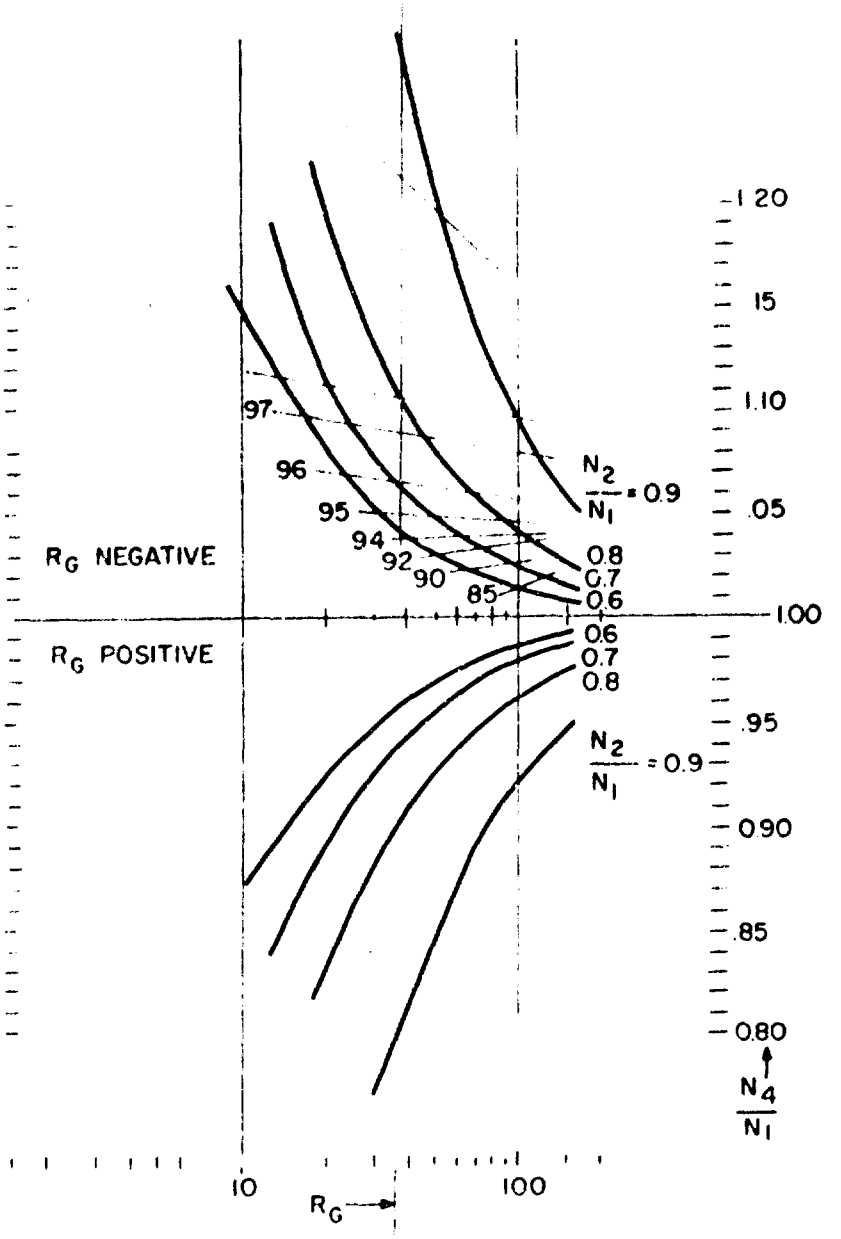

Figure 45. Non-Dimensional Parameters $\frac{N_4}{N_1}$ & $\frac{N_2}{N_1}$ Versus Transmission Ratio

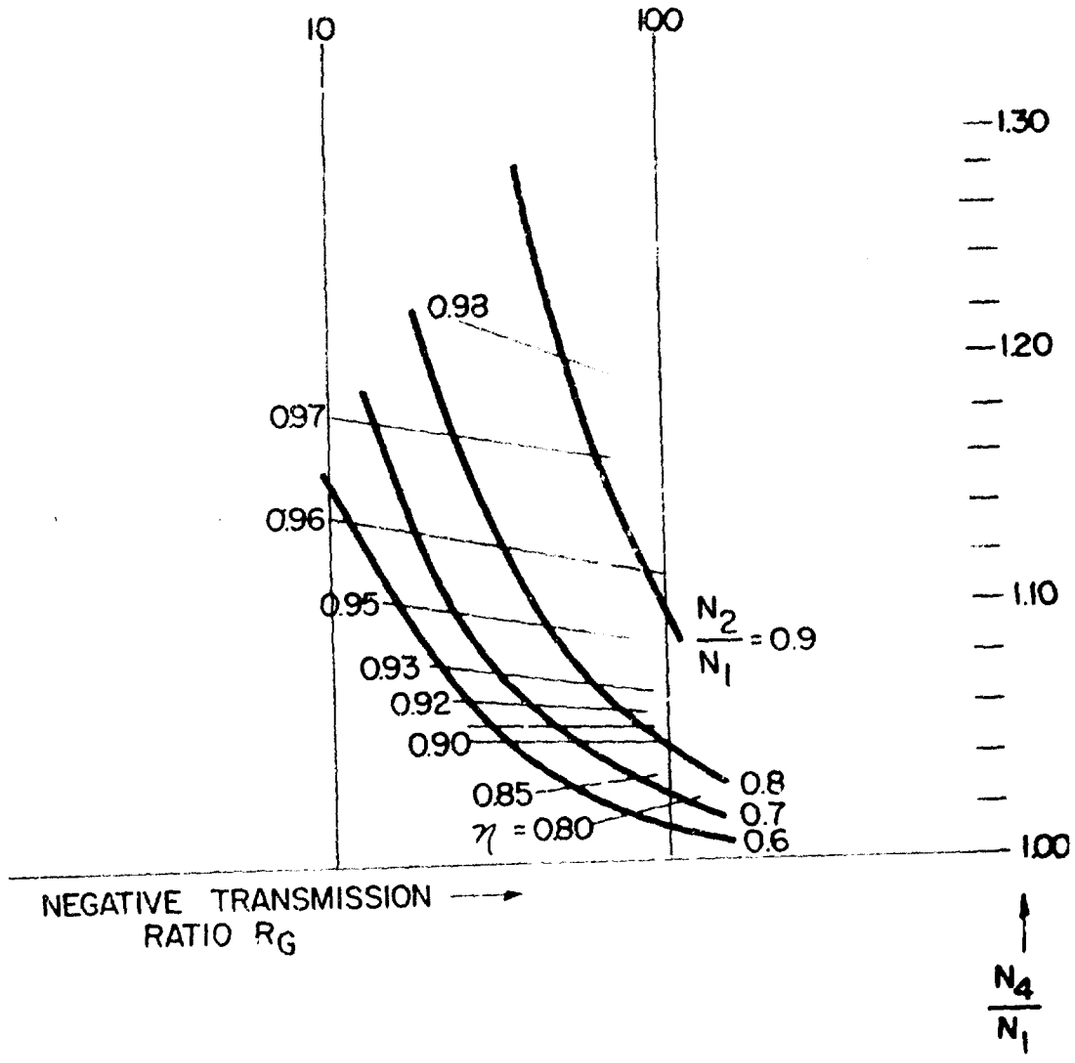

Figure 46. Epicyclic Transmission Efficiency η for $N_1 = 50$

The size of the gear train may be estimated from equation (5-42) developed in paragraph 5.2.4:

$$D_1 = \frac{80\,T_o}{S_b f} \qquad (5\text{-}42a)$$

Where T_o is the output load, lb-in; S_b is the flexural endurance stress, psi, and f is the gear face width, in.

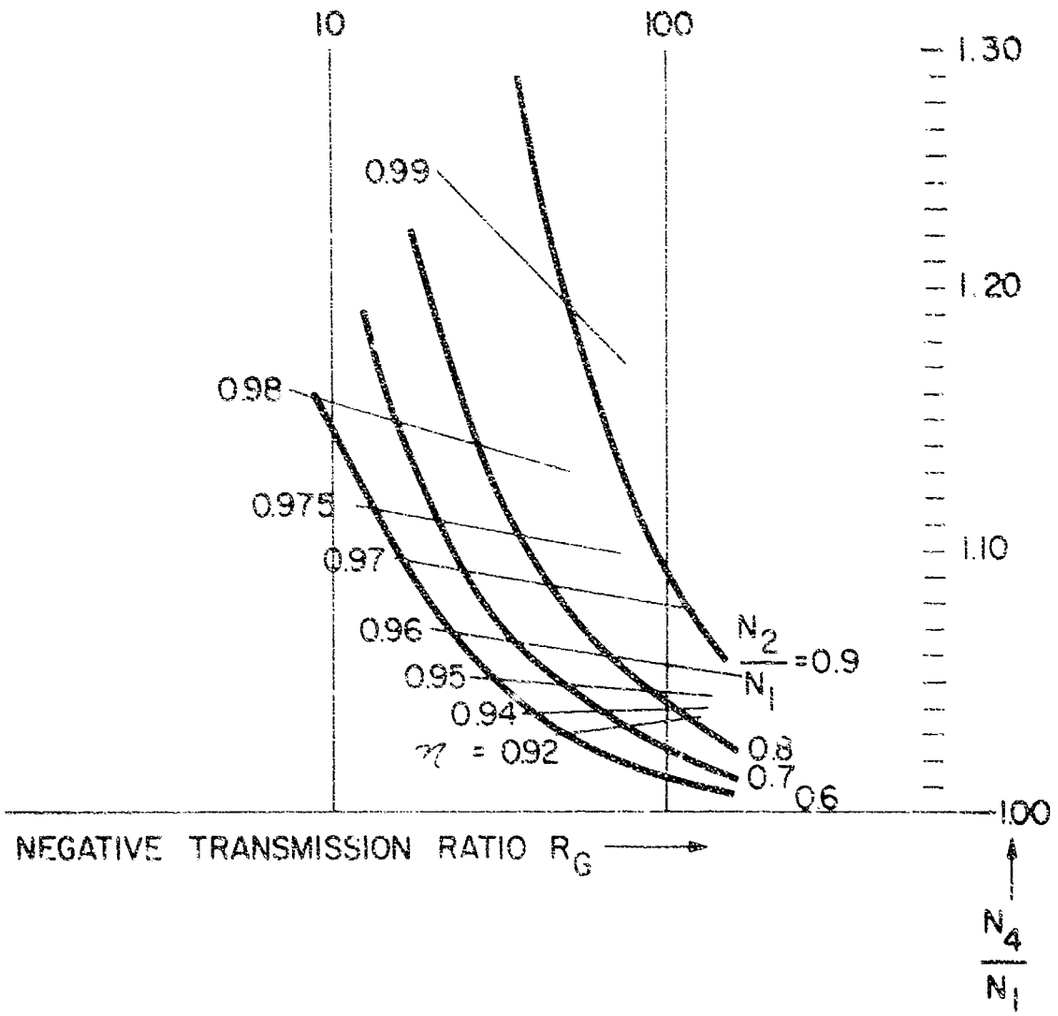

Figure 47. Epicyclic Transmission Efficiency η for $N_1 = 100$

Since

$$D_1 = N_1/P_d$$

$$N_1 = P_d \frac{80T_o}{s_b f} \qquad (6\text{-}19)$$

Now, assume $f = hD_1 = hN_1/P_d$ where h is the ratio of gear diameter to gear width selected on the basis of certain design factors to be discussed later.

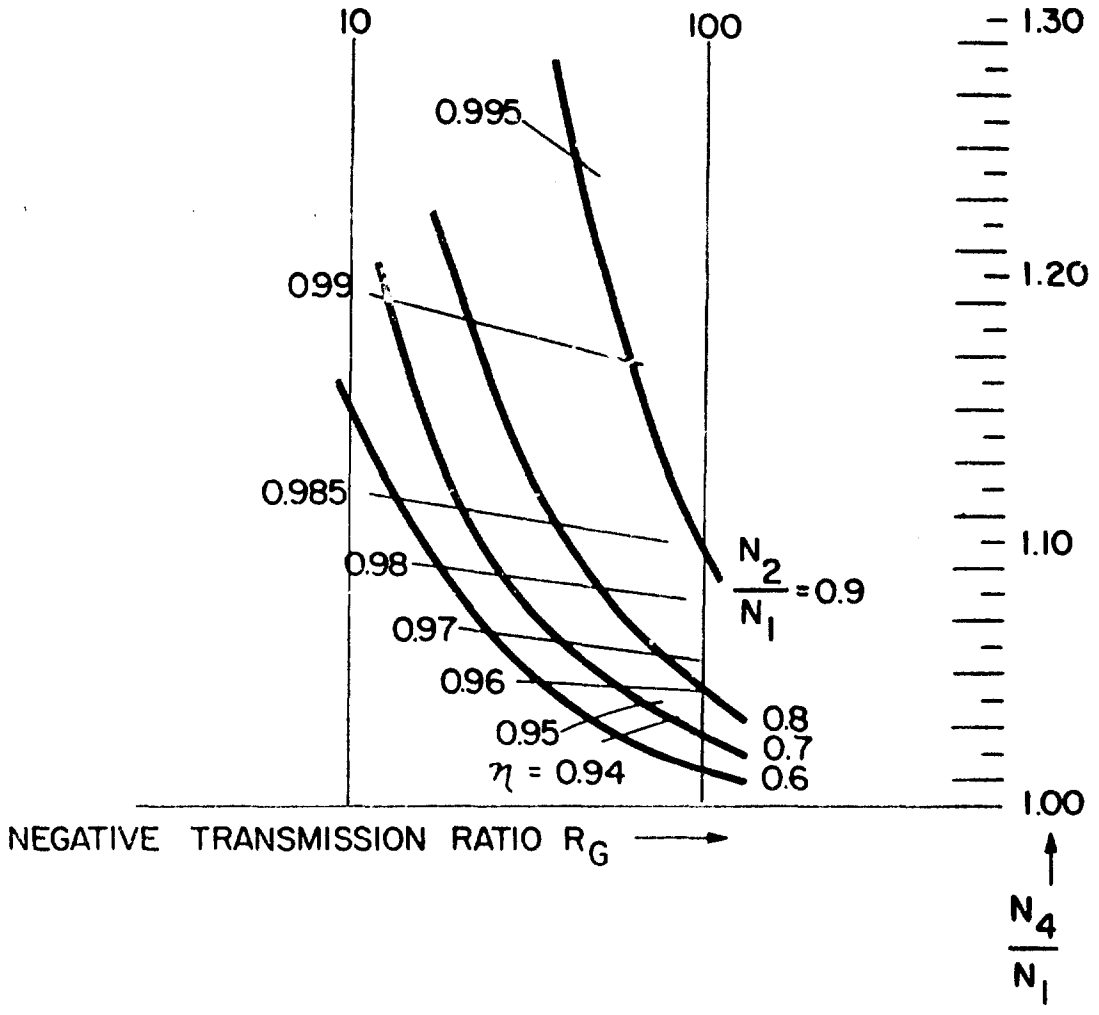

Figure 48. Epicyclic Transmission Efficiency η for $N_1 = 150$

Therefore

$$N_1 = P_d \left(\frac{80\ T_o}{S_b h} \right)^{1/3} \qquad (6\text{-}20)$$

Assume a peak torque factor of 1.5 times the maximum torque of 175 ft-lbs and a safety factor of 1.25 on the flexural endurance

$$N_1 = \frac{80 \times 1.5 \times 175 \times 12}{60,000/1.25}^{1/3} \frac{P_d}{h^{1/3}}$$

$$= 1.73 \frac{P_d}{h^{1/3}} \qquad (6\text{-}21)$$

To obtain the highest efficiency N_2 should be as large as possible. Therefore P_d should be chosen large and h small. P_d is selected as large as possible consistent with good gear cutting practice for the estimated diameter D_1. The diameter estimate can be based on such factors as minimum weight, available space, or minimum backlash.

The coefficient h should normally be chosen small to maintain accuracy of the gear teeth across the gear face. Nonuniformity of the gear tooth cross-section can lead to high local stresses which may damage the tooth face or cause lubricant breakdown.

6.3 TORQUER SELECTION

The torquers for the CMG gimbal actuator sizes (35, 87.5, 175, 262 and 350 ft-lb) are chosen on the basis of actuator requirements given in section I and the following factors:

(a) Satisfy stall torque T_{LM} and no-load speed N_L requirements of the load.

(b) Minimum size and weight of the actuator package for a particular CMG.

(c) Minimum power dissipation by the controller-actuator overall design.

(d) Minimum threshold (0.2 ft-lb for the 175 ft-lb size) and resolution (1% specified).

(e) Response: the actuator load must respond to and remain within 3% of the commanded value in less than 0.05 seconds.

(f) Minimum transmission backlash.

(g) Selection of a mechanical transmission with a gear ratio to be compatible with (a) through (f) above.

Based upon studies in sections IV and V, the actuator shall consist of two major components: DC torquer and an epicyclic mechanical transmission. A proper DC torquer size and transmission gear ratio can be selected on the basis of some of the constraints above, i.e., (a) through (f), and other considerations given in paragraph 6.1 for dynamic response and paragraph 6.2 for epicyclic transmission gear ratio, sizing and efficiency. As an example, a DC torquer and gear ratio shall be selected for the 175 ft-lb actuator size with a gyro wheel with an angular momentum of 1000 ft-lb-sec and a maximum gimbal rate of 0.175 rad/sec (approximately 10 degrees per second).

6.3.1 Selection Example

An excellent starting point for design of the 175 ft-lb actuator is table XVI which lists a number of actuator and transmission characteristics for seven different DC torquers: Inland Motor Corporation models T-4036C, T-7203A, T-7202F, T-5730D, T-2950E, T-10036B and T-5135D. Torquers T-7203A, T-7202F and T-10036B are

needlessly large and heavy, and are thereby promptly eliminated as candidates. T-4036C and T-2950E are relatively small torquers which have several inherent disadvantages: high threshold (2.24% and 2.61%) due to torquer friction alone and high gear ratios. The smaller torquers have a tendency to have a high ratio of frictional torque to maximum rated output torquer. Of the remaining candidates (T-5730D and T-5135D) the T-5730D torquer seems to have the advantage since a higher maximum torque is available even though it is slightly lighter in weight and requires less power.

A more complete tabulation of T-5730D DC torquer characteristics are listed for reference:

Weight	W = 8.2 lb.
Diameter x length	DxL = 7.2 in x 1.62 in.
Max. continuous torque	T_{MM} = 4.45 ft-lb
Peak torque	T_{MP} = 7.0 ft-lb
Friction torque	T_C = 0.07 ft-lb
Peak power (stalled)	P_P = 225 watts
Peak current	I_{MP} = 5.38 amps
DC resistance	R_M = 8.5 ohms
Inductance	L_M = 0.027 henries
Electrical time constant	τ_E = 3.2 msec
Torque sensitivity	K_T = 1.3 ft-lb/amp
Rotor moment of inertia	$J_M = 5(10)^{-3}$ lb-ft-sec^2
Motor constant	K_M = 0.465 lb-ft/amp/ohm$^{1/2}$
Back EMF	K_B = 1.77 volts/rad/sec
Max. no-load speed	N_M = 27 rad/sec

One item which is instantly observed is that the running friction is 1% of the peak torque. Additional stiction torques shall increase the actuator threshold even more, thereby exceeding the specified maximum of 0.2 ft-lb. Torquer motor friction is, in general, about 2% of maximum peak torque in sizes up to Type T-5730. Above this, the percentage tends to decrease with size, falling to about 1/2% for the largest

unit. Actuator design, therefore, must be a compromise between size and weight, power required, actuator response, threshold and resolution.

A summary of actuator requirements for a CMG with a gyro wheel angular momentum of 1000 ft-lb-sec are listed for reference:

Maximum gimbal rate (N_{LM})	$< \pm 0.175$ rad/sec
Minimum gimbal rate	$= .000175$ rad/sec
Maximum gimbal torque (T_{LM})	= 175 ft-lb
Threshold torque	< 0.2 ft-lb
Torque resolution	< 1.75 ft.-lb
Torque linearity	$< \pm 5\%$

A preliminary calculation of transmission gear ratio is found from the following expressions:

$$R_{G1} = \frac{T_L}{T_M} \tag{6-22}$$

$$T_M = K_T I_M \tag{6-23}$$

Combining Equations (6-22) and (6-23),

$$R_{G1} = \frac{T_L}{K_T I_M} \tag{6-24}$$

The magnitude of I_M to be used in the expression is that obtained when 20 volts DC is across torquer winding. This voltage was selected since the unregulated 28 volt DC power supply may drop to as low as 24 volts, and a drop of two volts DC was estimated across each power transistor in the conducting arm of the driver bridge circuit. Therefore,

$$R_{G1} = \frac{T_L R_M}{20 K_T} \tag{6-25}$$

$$R_{G1} = \frac{175 \text{ (ft-lb)}\ 8.5 \text{ (ohms)}}{20 \text{ (volts)}\ 1.3 \text{ (ft-lb/amp)}}$$

$$R_{G1} = 57.2$$

Rounding off R_G to the next highest round number to provide a margin of reserve torque, R_G was selected to be 60. The maximum motor torque T_{MM} needed for a 175 ft-lb gimbal load (assuming no losses), would be 2.92 ft-lb. A number of other conditions may now be calculated for the motor using the following duty cycle formula:

T_M (maximum) for 1% of the time

$T_M/2$ for 30% of the time

$T_M/4$ for 69% of the time

The average duty motor current I_{AV} is, therefore,

$$I_{AV} = \sum_{n=1}^{3} \frac{T_M}{K_T} \Delta t_n \qquad (6\text{-}26)$$

$$I_{AV} = I_{MAX} \left[.01 + \frac{.30}{2} + \frac{.69}{4} \right]$$

$$I_{AV} = 0.3325\ I_{MAX}$$

A summary of torquer output, current and power follows (neglecting transmission losses up to 5%):

Max. required motor torque	$T_{MM} = 2.92$ ft-lb
Max. required current	$I_{MM} = 2.25$ amps
Duty cycle avg. current	$I_{AV} = 0.75$ amps
Max. required power	$P_{MM} = 43$ watts
Duty cycle avg. power	$P_{AV} = 5.5$ watts
Voltage across coils (required)	$V_{MM} = 19.1$ volts DC

Response of the actuator can also be calculated from Equations (6-17) and (6-18):

Undamped natural frequency	$\omega_n = 123$ rad/sec
Damping ratio	$\zeta = 1.27$

Some of the physical characteristics can be estimated from a preliminary design given in Section 10 for the 175 ft-lb actuator. The following weights apply to that actuator size:

Torquer (T-5730)	8.2 lb.
Tachometer generator (TG-2801)	1 lb.
Transmission	4
Mounting plates and structure	9.8
Total actuator weight	23 lb.

The total volume of the assembly, including mounting pads and structure, is about 380 cubic inches. The volume of active components, of course, is much less, probably less than half of this volume; i.e., approximately 150 cubic inches.

6.3.2 Characteristics for Five Actuator Sizes

Torquers and gear ratios for the 35, 87.5, 262 and 350 ft-lb actuators were determined using the same method as discussed in paragraph 6.3.1. A list of all torquer characteristics, including the 175 ft-lb actuator, are tabulated in table XIX. Identical torquers were selected for both the 262 and 350 ft-lb actuators

Table XX includes the gear ratios, actual torquer power and currents, the moments of inertia reflected back to the torquer rotor and the actuator dynamic response for all five actuators. These were also determined using the method demonstrated in paragraph 6.3.1.

Actuator weights and volumes are also estimated for the five actuator sizes in table XXI The weights and volumes include the mounting pads and all of the required structure Weights and volumes of the active portion of the actuator assemblies are a fraction (about one-third) of the tabulated figures

TABLE XIX

TORQUER CHARACTERISTICS FOR VARIOUS CMG SIZES

CMG Characteristics	Symbol	Units	CMG size				
CMG Wheel Angular Momentum	H	ft-lb-sec	200	500	1000	1500	2000
Required Gimbal Torque	T_{LM}	ft-lb	35	87.5	175	262	375
INLAND MOTOR CORP. TYPE NO.			T-4036 D	T-5134 D	T-5730 D	T-7202 G	T7202 G
Torquer Characteristics	Symbol	Units					
Weight	W	LB	3.0	5.7	8.2	11.5	
Diameter x length	D x L	in x in	3.12x1.25	6.25x1.31	7.2x1.62	9.0x1.62	
Max. continuous torque	T_{KM}	ft-lb	1.34	2.5	4.45	6.3	
Peak torque	T_{MP}	ft-lb	1.8	2.7	7.0	11.0	
Friction torque	F_C	ft-lb	0.035	0.05	0.07	0.10	
Peak power - stalled	PP	watts	91.0	85.0	225	375	
Peak current	I_{MP}	amps	2.9	2.84	5.38	6.9	
DC resistance	R_M	ohms	11.0	10.1	8.5	7.25	
Inductance	L_M	henries	0.021	0.026	0.027	0.022	
Electrical time constant	τ_E	m sec	1.9	2.6	3.2	3.0	
Torque sensitivity	K_T	ft-lb/amp	0.63	0.95	1.3	1.6	
Rotor moment of inertia	J_M	ft-lb-sec^2	$0.76(10)^{-3}$	$2(10)^{-3}$	$5(10)^{-3}$	$8.4(10)^{-3}$	
Motor constant	K_M	ft-lb/amp/ohm$^{1/2}$	0.19	0.293	0.465	0.567	
Back EMF	K_B	volts/rad/sec	0.85	1.29	1.77	2.2	
Max No-load speed	N_M	rad/sec	37	22.5	27	23.5	

TABLE XX

TORQUE OPERATING CONDITIONS AND ACTUATOR RESPONSE

Characteristics	Symbol	Units					
Torquer Inland Motor Corp. Type No.	---	---	T-4036 D	T-5134 D	T-5730 D	T-7202 G	T-7202 G
CMG Sizes							
Gyro Wheel Angular Momentum	H	ft-lb-sec	200.0	500.0	1000.0	1500.0	2000.0
Required Gimbal Torque	T_{LM}	ft-lb	35.0	87.5	175.0	262.0	350.0
Actuator and Torquer							
Transmission Gear Ratio	R_G	---	35.0	50.0	60.0	60.0	75.0
Max. Required Motor Torque	T_{MM}	ft-lb	1.0	1.35	2.92	4.38	4.67
Max. Required Motor Current	I_{MM}	amps	1.59	1.84	2.25	2.73	2.93
Duty Cycle Motor Current	I_{AV}	amps	0.53	0.61	0.75	0.81	0.97
Max. Required Motor Power	P_{MM}	watts	27.8	34.1	43.1	54.1	61.7
Duty Cycle Motor Power	P_{AV}	watts	3.57	4.36	5.52	6.93	7.9
Motor Voltage for Req'd Torque	V_{MM}	volts	17.5	18.6	19.1	19.8	21.2
Moments of Inertia							
Gimbal (at load)	J_L	$ft\text{-}lb\text{-}sec^2(10)^{-3}$	400.0	1350.0	2000.0	2400.0	2750.0
Gimbal (at motor)	J_L/R_G^2	$ft\text{-}lb\text{-}sec^2(10)^{-3}$	0.328	0.54	0.556	0.667	0.49
Torquer Rotor	J_M	$ft\text{-}lb\text{-}sec^2(10)^{-3}$	0.76	2.0	5.0	8.4	8.4
Transmission	J_E	$ft\text{-}lb\text{-}sec^2(10)^{-3}$	0.003	0.005	0.1	0.015	0.02
Tachometer	J_R	$ft\text{-}lb\text{-}sec^2(10)^{-3}$	0.2	0.2	0.2	0.2	0.2
Total	J_T	$ft\text{-}lb\text{-}sec^2(10)^{-3}$	1.29	2.74	5.77	9.28	9.11
Actuator Response							
Undamped Natural Frequency	ω_n	rad/sec	144.0	131.0	123.0	128.0	130.0
Damping Factor	ζ	---	0.75	1.47	1.27	1.30	1.30

TABLE XXI

ESTIMATED PHYSICAL CHARACTERISTICS OF FIVE ACTUATOR SIZES

Actuator Size (ft-lb)	Weight (lb)	Volume (in^3)
35	10	125
87.5	16	235
175	23	380
262	32	430
350	35	465

SECTION VII

ELECTRONIC CONTROLLER DESCRIPTIONS

In this section, a brief description of each torquer will be made. This will be done for expository purposes as well as being a preliminary step in the optimization procedure. The eight controllers considered are: DC proportional, single channel pulse width modulation (PWM_1), dual channel pulse width modulation (PWM_2), basic ON-OFF, two-level ON-OFF, pulse amplitude modulation (PAM), pulse frequency modulation (PFM), and delta modulation. Each controller will be considered to be driving a DC load in accordance with an error signal.

7.1 DC VOLTAGE POWER AMPLIFIER

The voltage amplifier in figure 49 provides a floating output of either polarity from a single ended input. The circuit is entirely DC coupled and utilizes a bridge type output circuit. Output power is limited only by the current carrying capacity of the power transistors, and the saturation level is determined by the line voltage and the load. As the circuit stands as shown in figure 49, an input of approximately 0.5V or greater is necessary to produce an output. To reduce this dead zone, the preamplifier of figure 50 is added to the input of the original circuit of figure 49.

The operation of the preamp is such that for an input of 0.05 volt, the output voltage is 0.5 volt. Increasing the input further activates the diodes and the gain is then unity. Therefore, the dead zone (overall) is reduced to 0.05 volt. The transfer function, preamp included, is shown in figure 51.

The operation of the circuit in figure 49 is as follows:

At zero volts error signal to terminals 1 and 2, the bridge is inoperative and zero volts appear across the load-terminals 5 and 6. For a positive DC error signal, the left side of the bridge is operating. Q3 operates as a switch, Q1 and Q10 provide the proportional control for Q9. Negative error signals activate the right side. Resistors R3 and R4 provide voltage feedback.

The amplifier can easily be converted to a current amplifier by rearranging resistors. The voltage power amplifier (VPA) has a distinct advantage over the current power amplifier[23]. With a current power amplifier (CPA) or controller, the system is marginally stable — i.e., the system is unstable as the effective forward gain decreases as well as at higher gains, and stable at mid range. Filter requirements with CPA are also difficult to realize. With VPA the system is stable to a high gain and filter requirements are less difficult to realize.

---

[23] See Reference No. 18, Appendix D

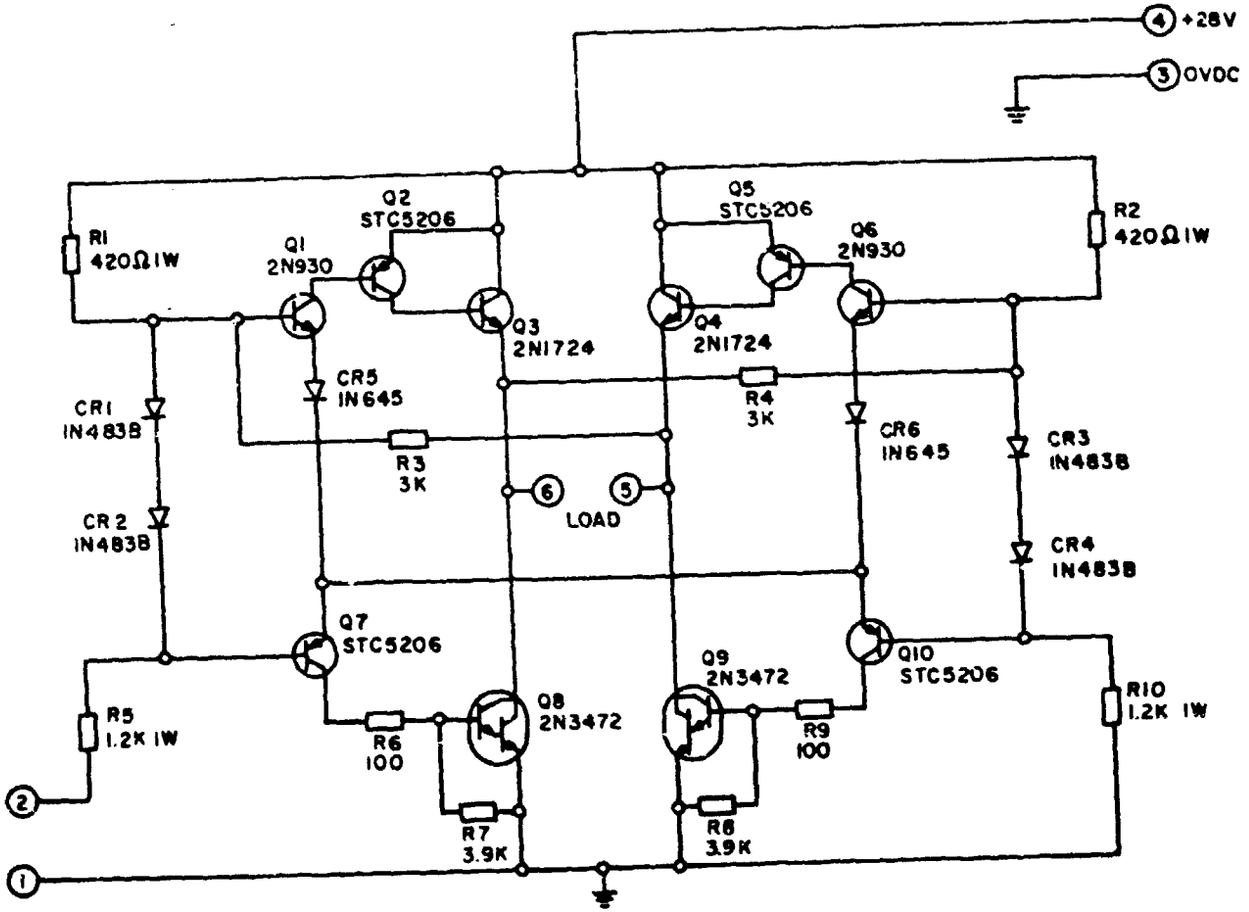

Figure 49. Schematic — DC Proportional Controller

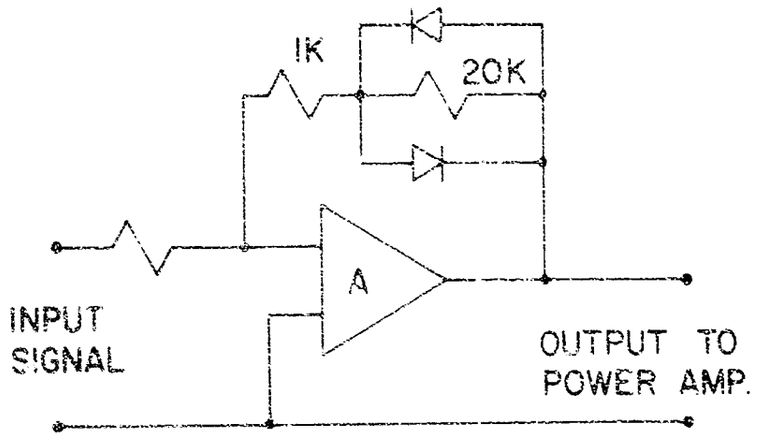

Figure 50. Preamp Required to Reduce Dead Band

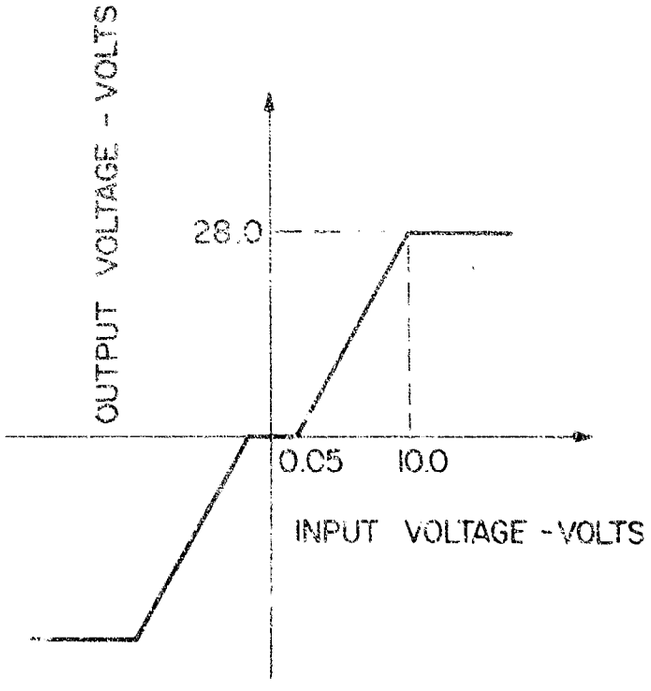

Figure 51. Voltage Amplifier Characteristics – Unloaded Gain of Approximately 2.8 v/v

7.2 SINGLE CHANNEL PWM

Pulse-width modulation (PWM) is a technique whereby large amounts of power are efficiently transferred to a load device through an amplifier. In this scheme, a pulse train of constant amplitude and period is width modulated by an error signal. There are two approaches to PWM, the single channel modulator (PWM_1) and the dual channel modulator (PWM_2). In each method, the average value of a given pulse is proportional to the value of error signal at the beginning of that pulse period. The single channel version will be discussed in the following. As in a sampled data system, the higher the pulse frequency, the better the pulse train will represent the error.

The single channel modulator emits a pulse whose value at all times is either plus or minus E. A typical pulse is shown in figure 52. The average value of the pulse is given by the following equation.

$$e_{pi}(t)_{average} = \frac{1}{T}\int_{t_1}^{t_1+T} e_{pi}(t)dt = \frac{E\tau - E(T-\tau)}{T} \qquad (7\text{-}1)$$

$$e_{pi}(t)_{average} = \frac{2E\tau}{T} - E = E\left[\frac{2\tau}{T} - 1\right]$$

The output of the PWM_1 modulator with a given input waveform is shown in figure 53.

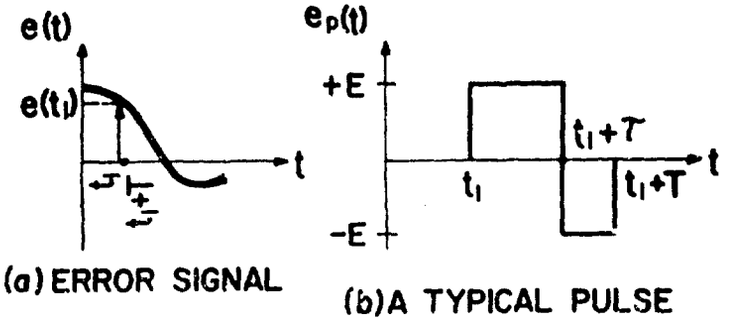

Figure 52. Single PWM Pulse Error Signal at t_1

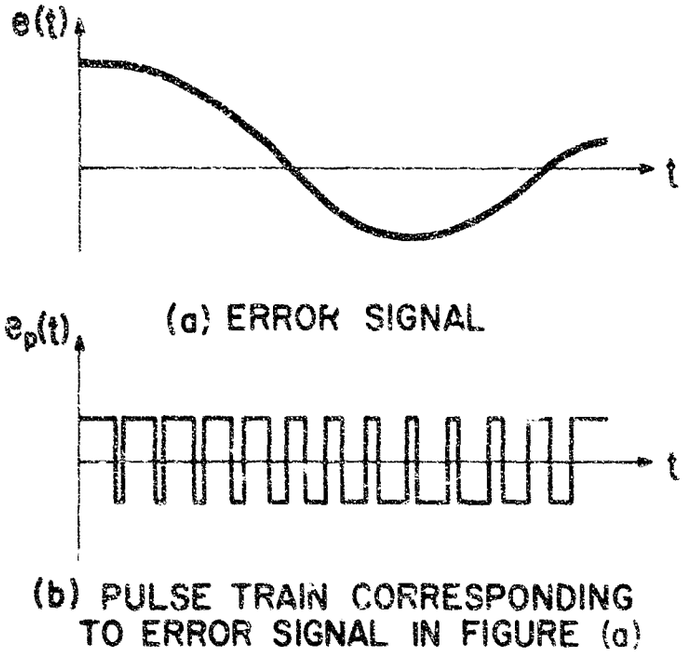

Figure 53. PWM Pulse Train for a Varying Error Signal

A simple PWM_1 scheme is shown in figure 54. The four transistors 2N3836 form a power bridge which controls the power flow in the load. Each arm of the bridge at all times is either at saturation or cut-off. The SN 355A amplifiers each provide two outputs; one identical to the input, and the other its complement. Therefore, one output is zero while the other is positive. These SN 355A units drive the power bridge which controls the flow of load current as shown in figure 55. Referring to this diagram, it can be seen that I_L is zero if S_1 and S_3 are simultaneously closed, or if S_2 and S_4 are simultaneously closed. I_L is positive as shown, if S_2 and S_3 are closed while S_1 and S_4 are open, and is negative when S_2 and S_3 are open with S_1 and S_4 closed.

Operation of the unit is described as follows. The 2N3044 generator provides a symmetric, linear, triangular waveform, e_t, to the SN 523A amplifier. This amplifier subtracts the DC error signal from the triangular waveform. Whenever this remainder is positive, the output at e_1 saturates at a positive value, while e_2 will be saturated to a negative value. When (e_t-error) is negative, e_1 becomes negative and e_2 positive.

The signals e_1 and e_2 are fed to two SN 355A amplifiers which provide the complements of e_1 and e_2. Thus, from one unit appears e_1 and e_{1C}, and from the other

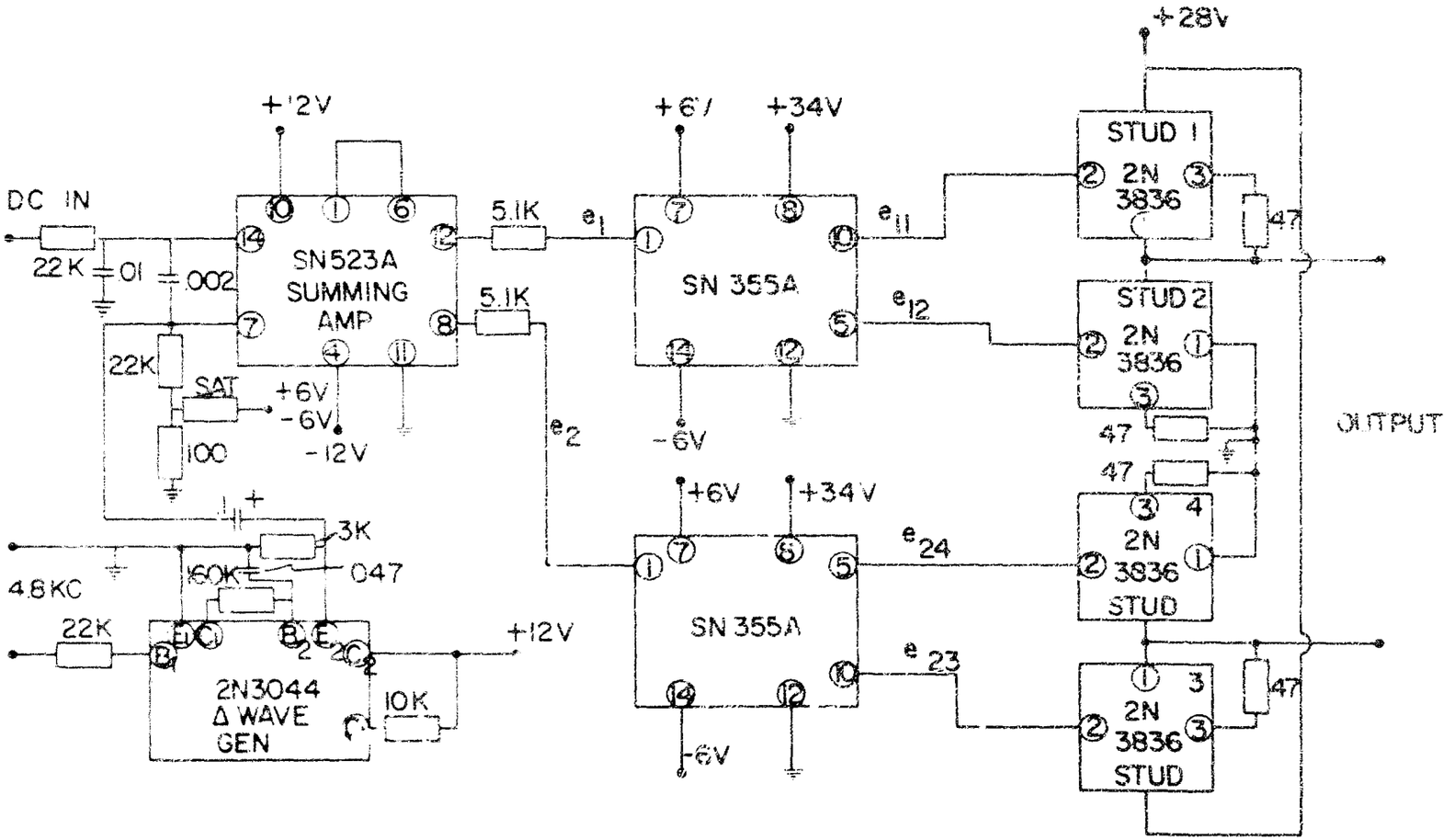

Figure 54. Single Channel Pulse Width Modulator

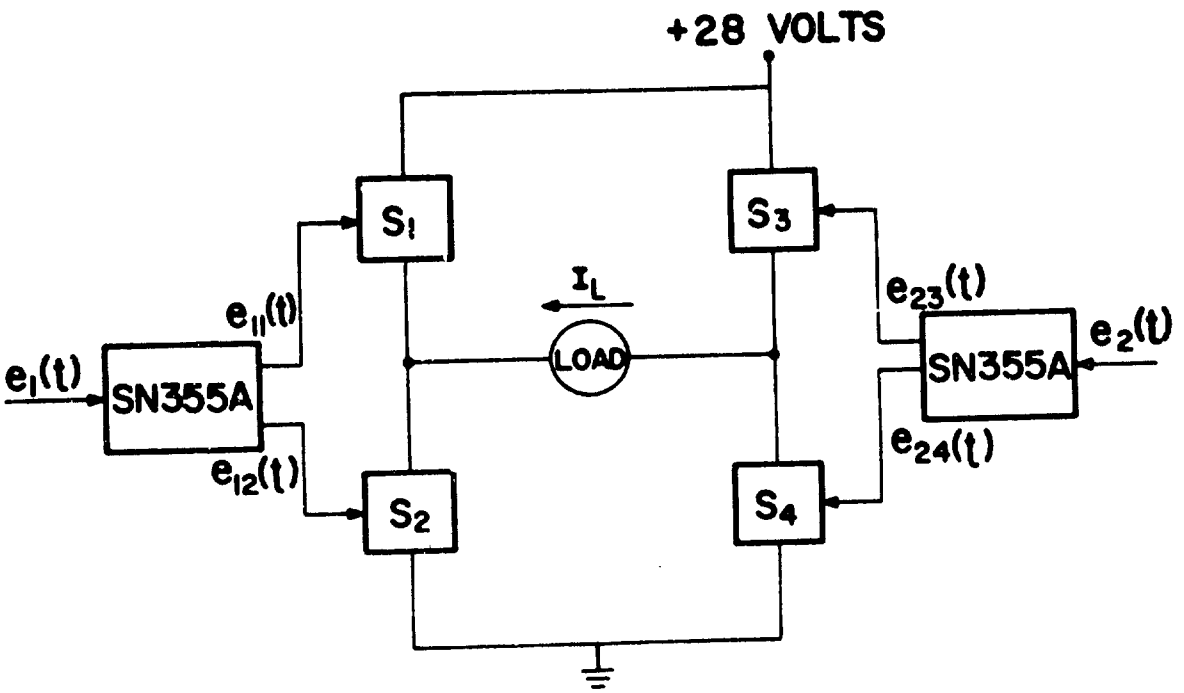

Figure 55. Power Bridge and Driving Stages

appears e_2 and e_{2C}. These signals are labelled e_{11}, e_{12}, e_{23}, e_{24} in figure 54. These four voltages drive their respective legs in the power bridge, thus determining the load current. In other words, S_1 is closed when e_{11} is positive, and open when e_{11} is positive, and open when e_{11} is negative. S_2 is closed when e_{12} is positive, etc.

Figure 56 illustrates waveforms for zero and figure 57 illustrates positive DC error signals.

7.3 DUAL CHANNEL PWM

PWM_2 and PWM_1 have identical goals, with different methods of achieving them. In each case, it is desired to produce an average value of load current proportional to the error signal.

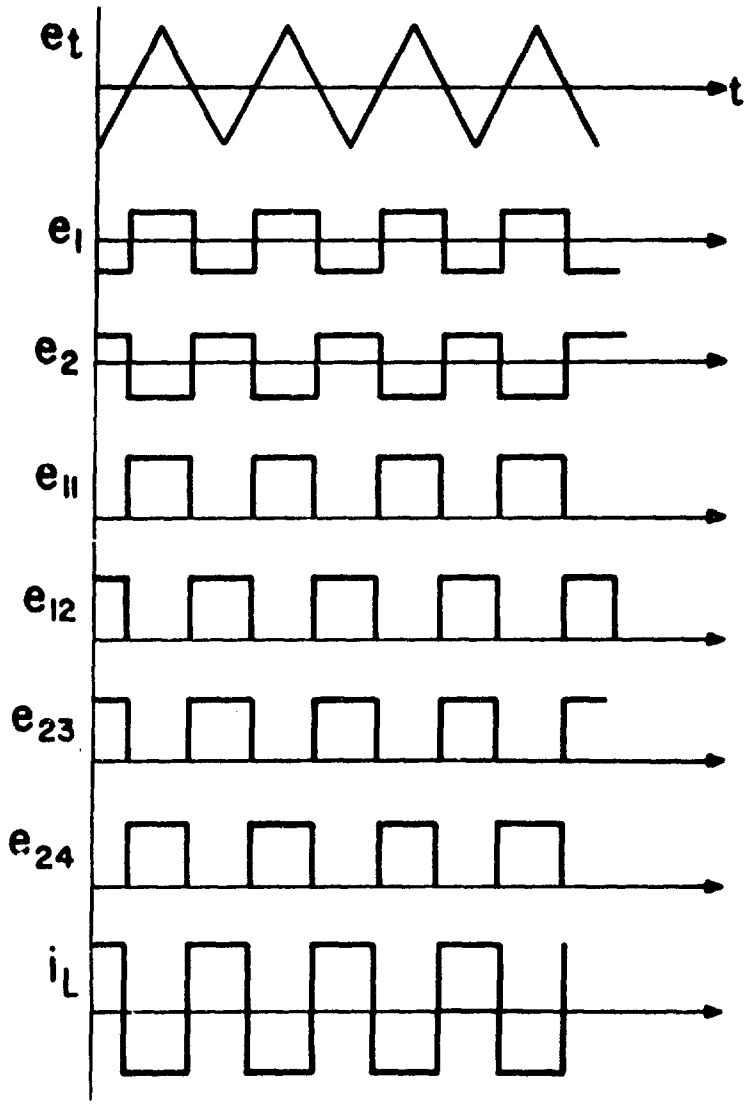

Figure 56. Zero Error Waveforms

The dual channel modulator emits a pulse of one polarity over one pulse period. A typical pulse is shown in figure 58. The average value of the pulse is given in the following equation:

$$e_{pi}(t)_{average} = \frac{1}{T} \int_{t_1}^{t_1 + T} e_{pi}(t)dt = E \frac{\tau}{T} \qquad (7\text{-}2)$$

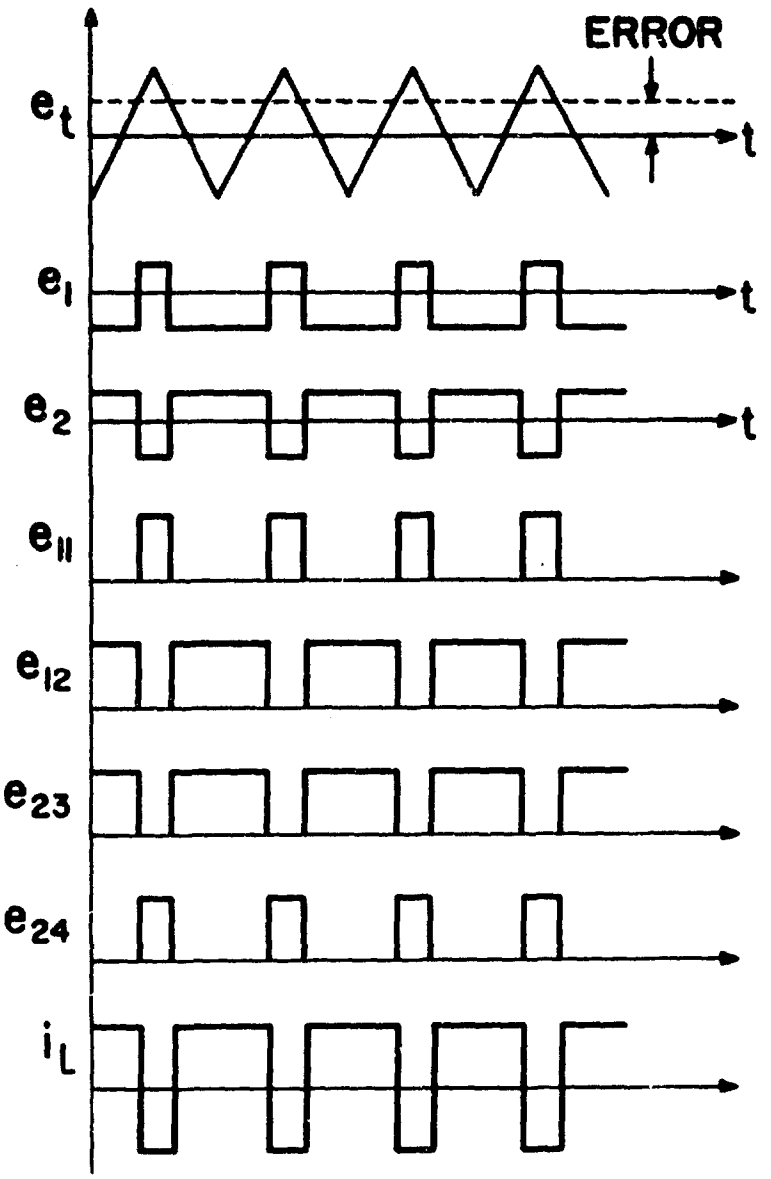

Figure 57. Positive Error Signal Waveforms

The output of the modulator under a given error signal is shown in Figure 59.

A configuration which will accomplish PWM_2 is shown in figure 60. The network composed of Q_1, Q_2, Q_3, Q_4 is the power switch section, while the four operational amplifiers and 2N3044 wave generator comprise the modulator and driver stage.

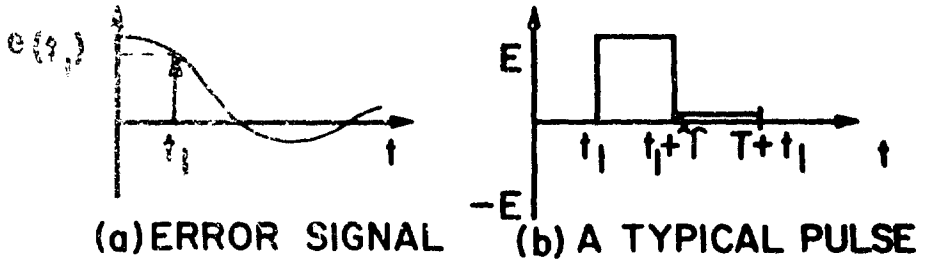

Figure 58. Single PWM Pulse — Error Signal at t_1

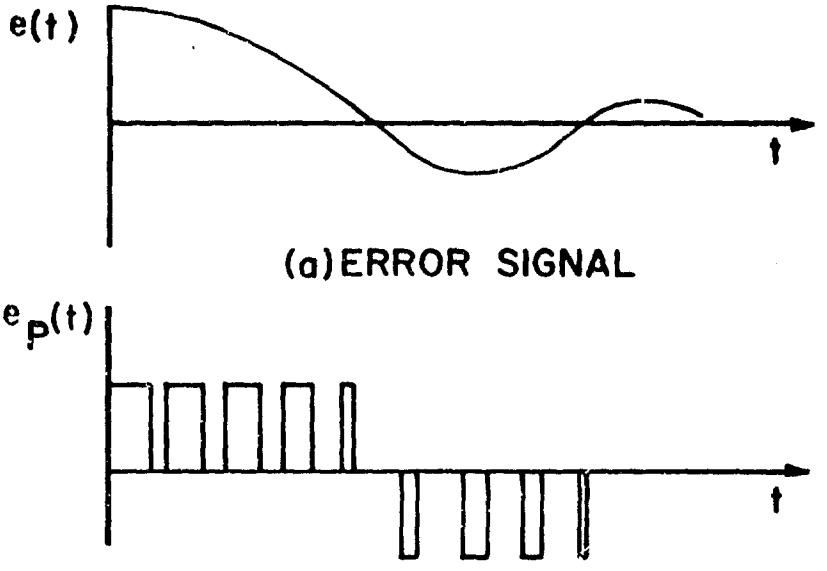

Figure 59. PWM Pulse Train for a Varying Error Signal

Operation of the unit is described below. Transformer T_1 supplies the triangular wave to the two SN 524A amplifiers, 180° out of phase. The error signal is added to these two signals by means of the CT on the transformer secondary, and the sum is applied to the two SN 524A inputs. Each SN 524A module supplies a two valued output. In amplifier No. 1, the output e_3 is saturated positive when $e_1 > 0$ and is negative when $e_1 < 0$. In the other unit, No. 2, e_4 is positive when e_2 is negative, and e_4 is saturated negative when $e_2 > 0$. These two signals, e_3 and e_4, are applied to the two SN 355A amplifiers, in which their complements are formed. Hence, from Unit No. 1

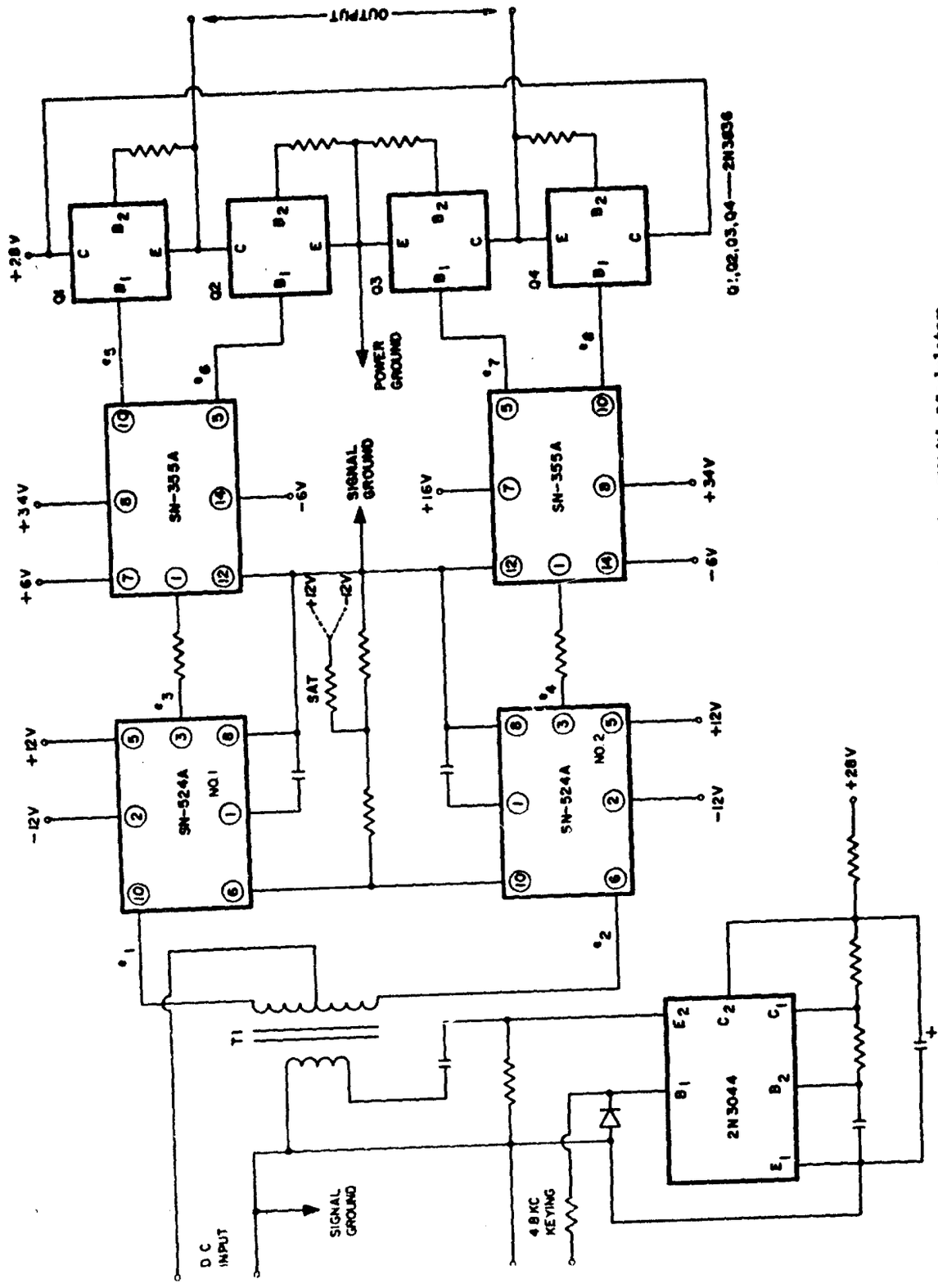

Figure 60. Schematic — Dual Channel Pulse Width Modulator

issues forth $e_5 = e_3$ and $e_6 = e_3'$, where e_3' is the complement of e_3. From Unit No. 2 comes $e_8 = e_4$, and $e_7 = e_4'$. These signals are used to drive the power bridge and thus control the load current. Operation of the bridge section is the same as the PWM bridge.

Figures 61 and 62 show waveforms with zero and positive error signals, respectively.

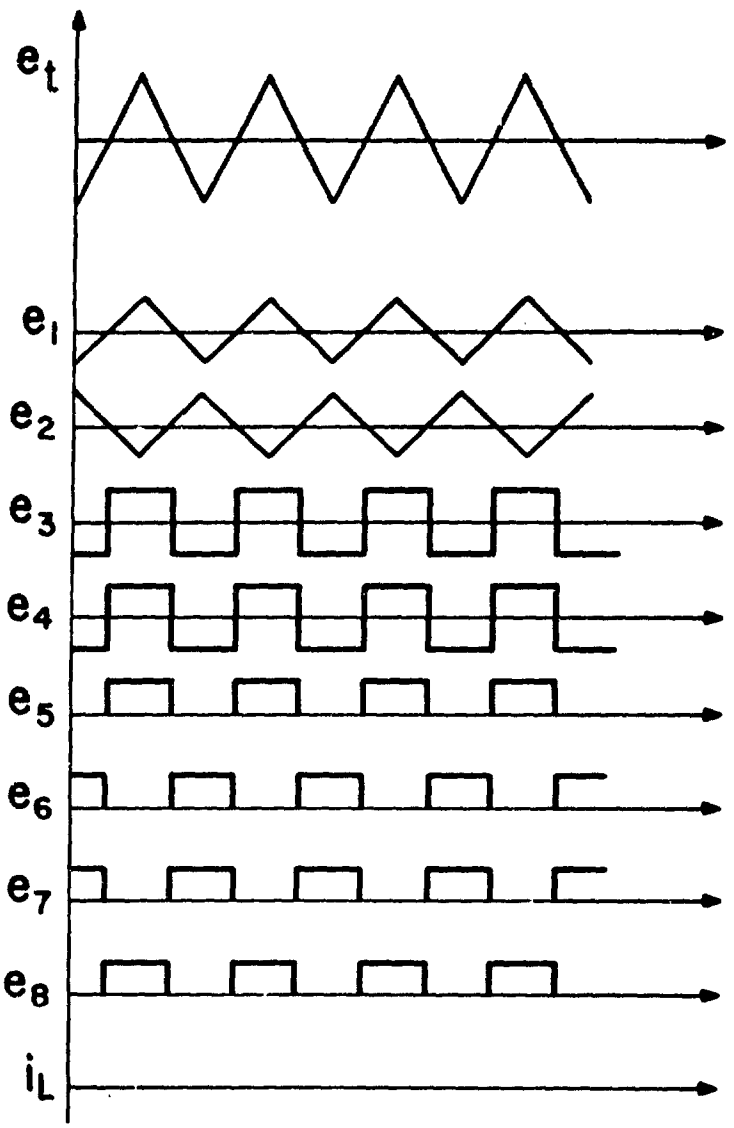

Figure 61. Zero Error Waveforms

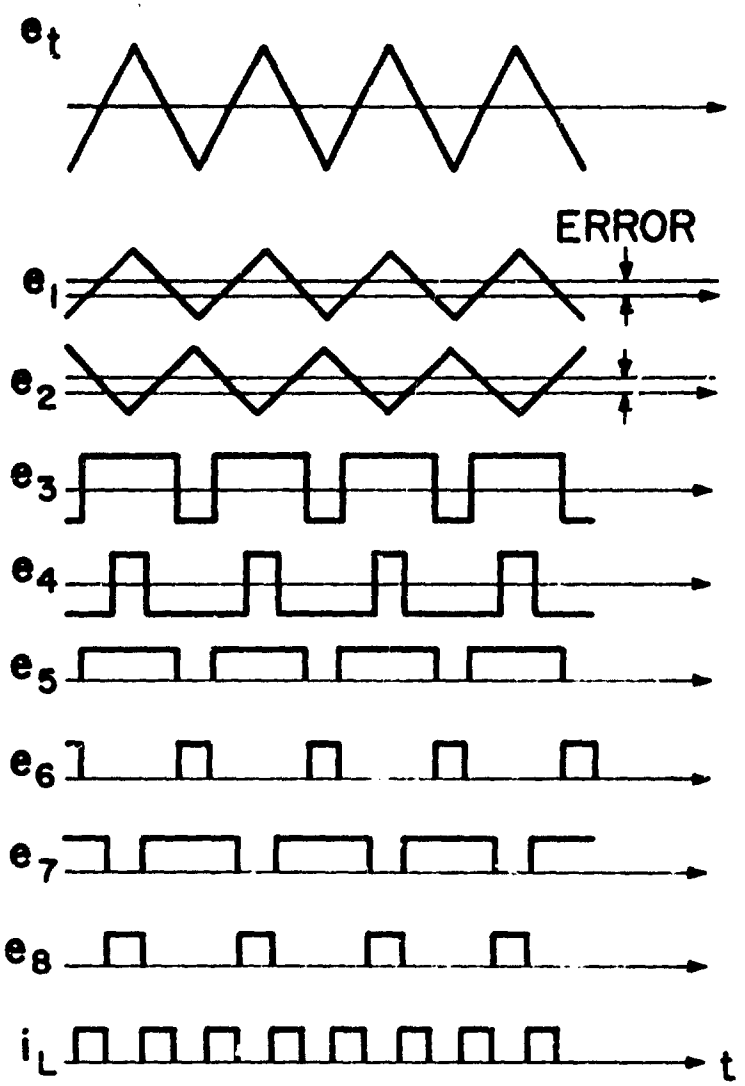

Figure 62. Positive Error Waveforms

7.4 ON-OFF CONTROLLER

On-Off or Bang-Bang control is a method whereby maximum output is demanded of an actuator at all times. The output of the controller assumes two levels only, ±M. The greatest advantage of such a system is its inherent simplicity; such systems, however, are also prone to limit cycling or even instability. A typical system is shown in figure 63. The characteristic of an ideal driver is shown in figure 64. In practice, a deadband region will exist near null, and this characteristic appears in figure 65. The size of the deadband region of the controller can be reduced by inserting a high gain device between the summing junction and polarity detector.

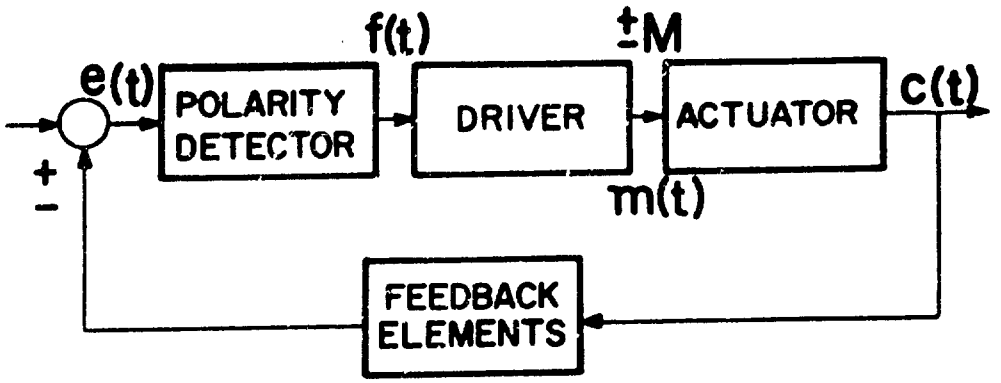

Figure 63. An ON-OFF System

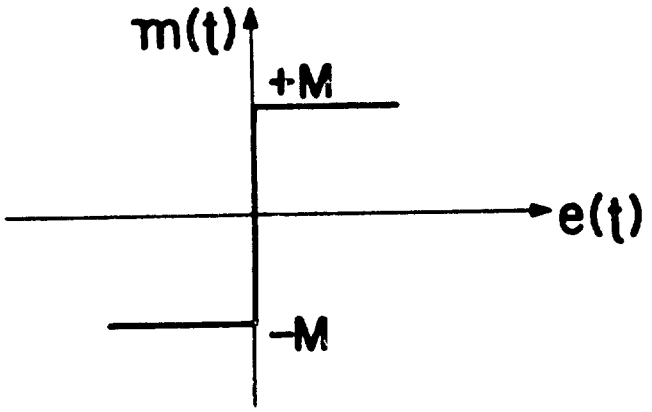

Figure 64. Ideal Controller Characteristics

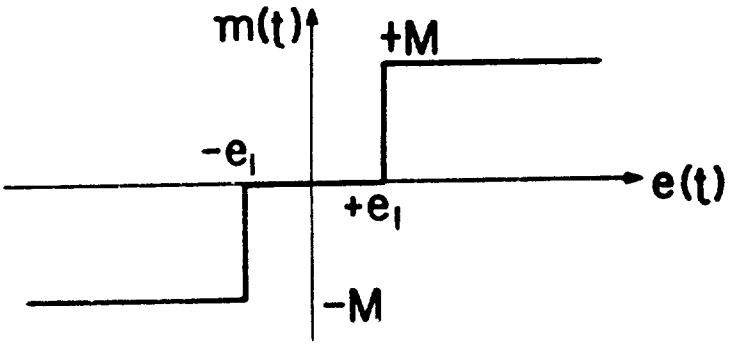

Figure 65. Controller Characteristics With Dead Band

A Bang-Bang controller will be considered in a torquer system operating under various modes; (i.e., Basic Rate, Cross Coupled Rate, Position, Torque, and Compensated Rate) as its applicability in each mode is to be determined. In the following discussion, "ideal" switching will be assumed in all cases.

7.4.1 Basic Rate

Consider a gimbal velocity servo with inertial loading and neglect cross coupling torques, (i.e., assume motor torque>>gyro torque), as shown in figure 66. This can be reduced to figure 67 where G(s) is given by equation 7-1.

$$G(s) = \frac{\dfrac{K_{TY}}{(LyS + Ry)\eta ISN}}{1 + \dfrac{K_{TY}K_{VY1}}{(LyS + Ry)\eta ISN}} = \frac{\dfrac{K_{TY}}{Ly\eta IN}}{S^2 + \dfrac{Ry}{Ly}S + \dfrac{K_{TY}K_{VY1}}{Ly\eta IN}}$$

$$G(s) = \frac{\dfrac{1}{K_{VY1}}\omega_n^2}{S^2 + 2\zeta\omega_n S + \omega_n^2} \tag{7-1}$$

where

$$\omega n = \sqrt{\frac{K_{TY}K_{VY1}}{Ly\eta IN}} \tag{7-2}$$

$$\zeta = \frac{Ry}{2}\sqrt{\frac{\eta IN}{LyK_{TY}K_{VY1}}} \tag{7-3}$$

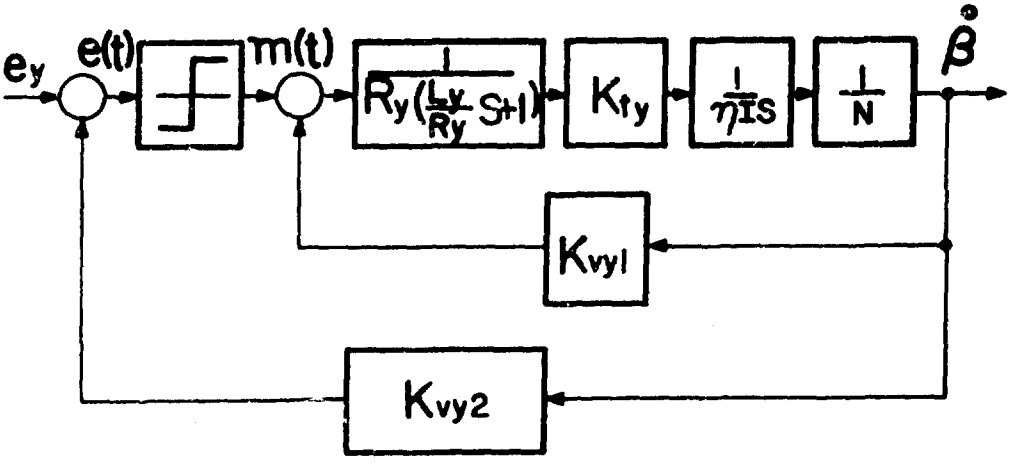

Figure 66. An ON-OFF Rate Control System

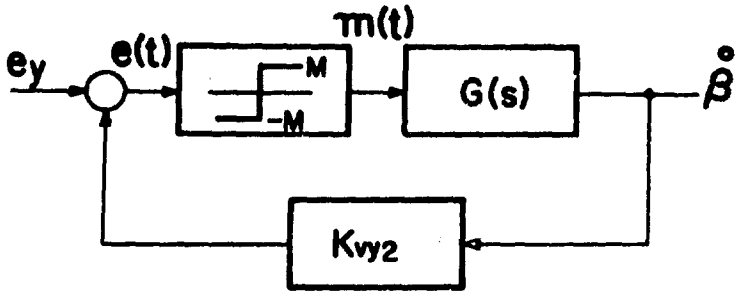

Figure 67. A Simplified ON-OFF Rate System

The response of figure 67 to a step input is given by considering the time domain equation 7-4.

$$\dddot{\beta} + 2\zeta\omega_n \ddot{\beta} + \omega_n^2 \dot{\beta} = \pm \frac{1}{K_{VY1}} \omega_n^2 M \tag{7-4}$$

The phase plane trajectories in each case, (±M), are given by spirals converging on $\pm \frac{M}{K_{VY1}}$. The transition from one set of spirals to the other occurs when e(t) = O. This implies

$$e_y - K_{VY2} \dot{\beta} = O$$

or

$$\dot{\beta} = \frac{ey}{K_{VY2}} \tag{7-5}$$

A sketch of the phase plane trajectory is shown in figure 68.

It should be noted that the output of the controller is ±M. The motor will respond to +M signal to yield a steady-state speed $+\omega_O$. In order to retain control, the commanded speed $\frac{ey}{K_{VY2}}$ must be less than ω_O.

or

$$\left| ey \right| < \left| K_{VY2} \omega_O \right| \tag{7-6}$$

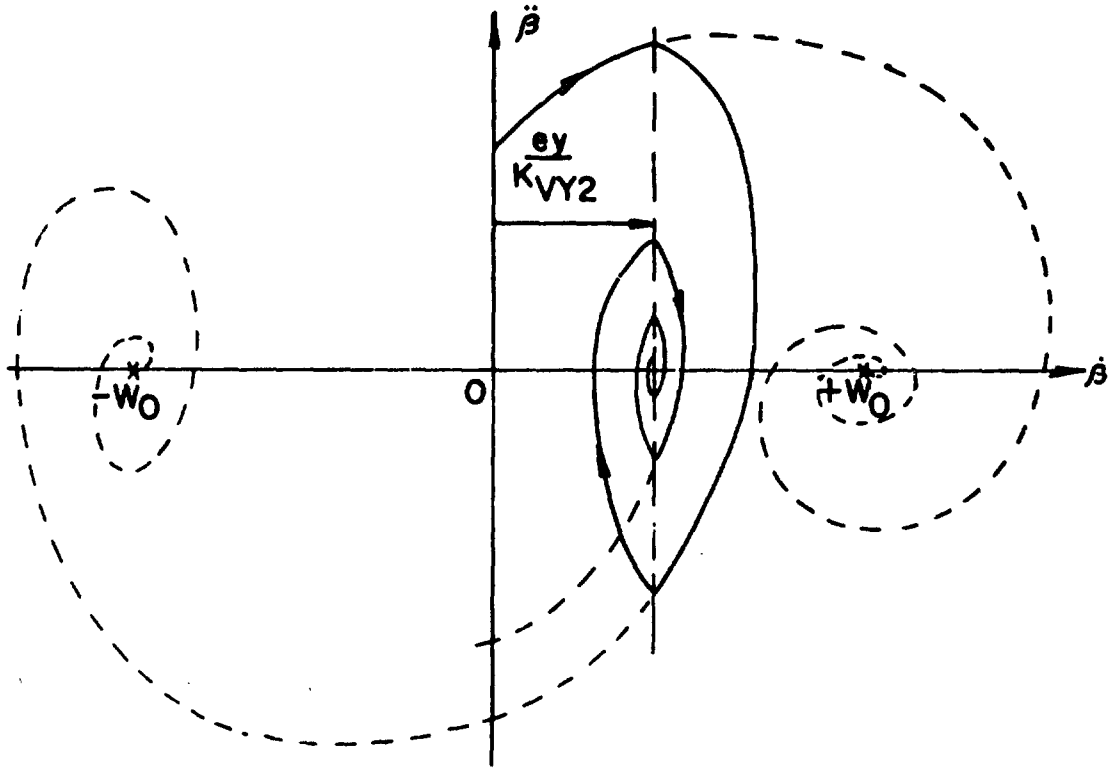

Figure 68. Phase Plane Trajectory for Standard ON-OFF System

7.4.2 Position Repeating System

A position repeating system is shown in figure 69.

$$G(s) = \frac{K\omega_\eta^2}{S(S^2 + 2\zeta\omega_\eta S + \omega_\eta^2)} \qquad (7\text{-}7)$$

ω_η and ζ are given in Equations (7-2) and (7-3) and

$$K = \frac{1}{K_{VY1}} \cdot K_p \qquad K_p = \text{gain of integrator} \qquad (7\text{-}8)$$

Here the system is low pass, and a describing function analysis will be used. The DF of the controller is given in Equation 7-9.

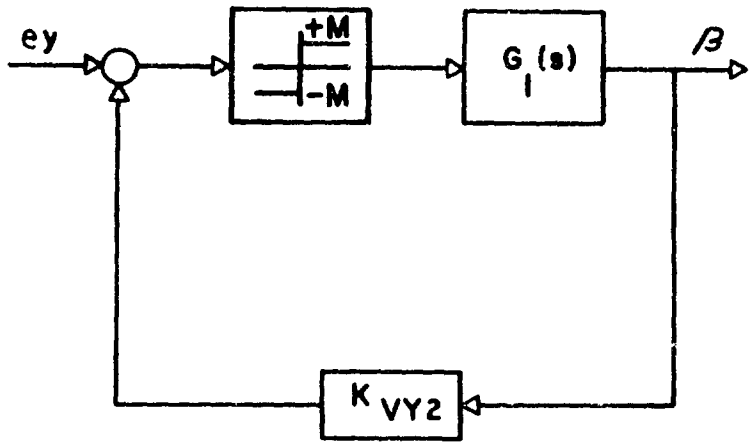

Figure 69. A Position Repeating System

$$N(E) = \frac{4M}{\pi E} \tag{7-9}$$

where M = max. output of controller

E = max. sinusoid input to controller

A polar plot of $G_1(j\omega)$ is shown in figure 70. Super-imposed on this plot is a locus of $-\frac{1}{N(E)}$ as E varies from zero to infinity. It is known that a limit cycle will exist at the intersection of these two loci.

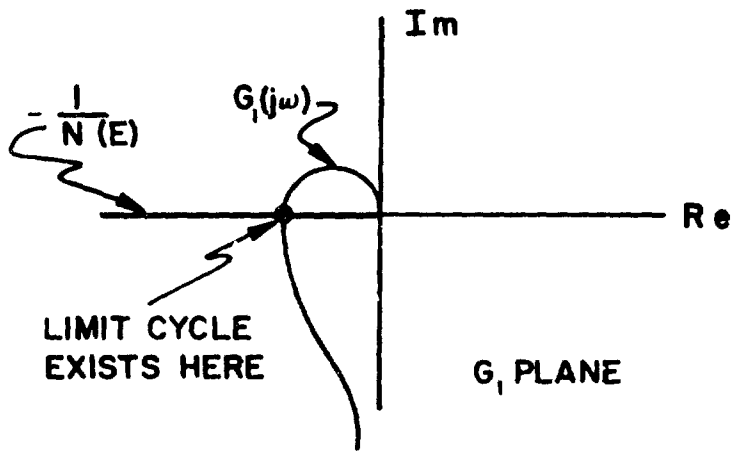

Figure 70. Polar Plot of $G_1(j\omega)$ and $\frac{-1}{N(E)}(j\omega)$

An examination of figure 70 and Equation (7-7) will yield the following results.

Frequency of limit cycle ω_1 =

where Arg $G_1(j\omega_1) = 180°$ (7-10)

$$\text{Arg } G_1(j\omega_1) = \text{Arg}\left\{ \frac{1}{(\omega_\eta^2 - \omega_1^2 + 2j\zeta\omega_\eta\omega_1)} \right\} + 90° = 180°$$

Solving for ω_1 yields

$$\omega_1 = \omega_\eta \tag{7-11}$$

The amplitude of oscillation is given by Equation (7-12).

$$A = G_1(j\omega_\eta) = \frac{K_T\ \omega_\eta^2}{\omega_\eta(2\zeta\omega_\eta^2)} = \frac{Ly}{Ry}\ K_T \tag{7-12}$$

Combining these results yields the following results.

$$\text{limit cycle amplitude} = \frac{Ly}{Ry}\ K_T$$

$$\text{limit cycle freq.} = \omega_1 = \sqrt{\frac{K_{TY}K_{VY1}}{Ly\ \eta IN}} \tag{7-13}$$

7.4.3 Torque Mode

A torque mode system, neglecting cross-coupling torque is shown in figure 71. In order to derive the torque transfer function of the motor, consider figure 72.

$$T_m = KIa \tag{7-14}$$

$$V_b = K_b S\alpha \tag{7-15}$$

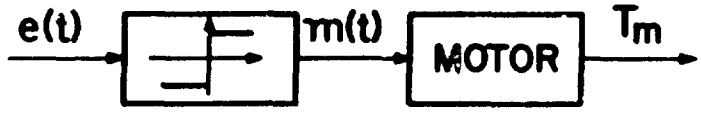

Figure 71. ON-OFF Controller in Torque Mode

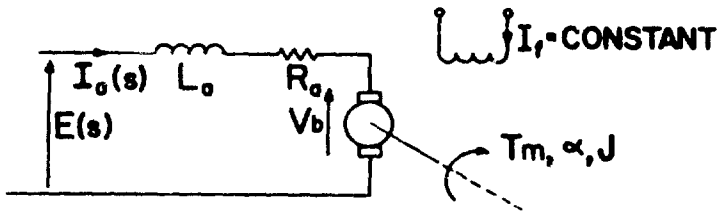

Figure 72. Equivalent Circuit of Torque Motor

$$I_a = \frac{E(s) - V_{b(s)}}{Ra + SLa} = \frac{E}{Ra + SLa} - \frac{K_b S\alpha}{Ra + SLa} \tag{7-16}$$

$$T_m(s) = \frac{KE}{Ra + SLa} - \frac{KK_b S\alpha}{Ra + SLa} \tag{7-17}$$

In the torque mode, $S\alpha \triangleq 0$ (motor does not appreciably turn)

$$\therefore \qquad T_m(s) \approx \frac{KE(s)}{Ra + SLa} \tag{7-18}$$

If $e(t) = Mu(t)$; $E(s) = \frac{M}{S}$

$$\text{then } T_m(s) = \frac{KM}{(Ra + SLa)S} \tag{7-19}$$

T_m will approach $\frac{KM}{Ra}$ exponentially.

If it is desired to develop a torque other than $\frac{KM}{Ra}$, it will be necessary to switch the input signal polarity, so that a torque of the desired value will be developed. A typical set of waveforms is shown in figure 73. If the switching is done fast enough, the system will not have time to react appreciably and an almost constant torque will be developed.

7.4.4 Compensated Rate

Operation in this mode will be essentially the same as in the basic rate mode, except that in this case the input velocity command will not be a step function. Thus ON-OFF controls seems applicable in this case.

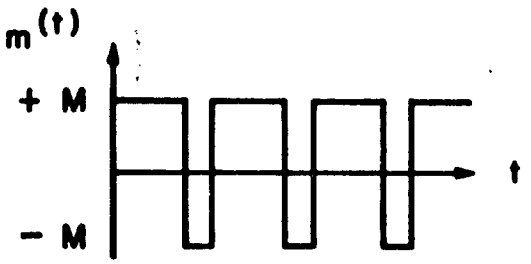

(a) POSSIBLE INPUT SIGNAL WAVEFORM

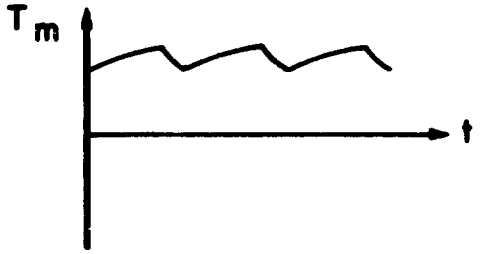

(b) RESPONSE TORQUE

Figure 73. Response Torque for Command Voltage to the Torque Winding

7.4.5 Cross Compensated Rate

By reference to figure 74, it is seen that a signal proportional to $\dot{\beta}$ is subtracted from the input. The controller senses the polarity of $(e_y - K_{VY2}\dot{\beta})$. Thus, it operates like rate mode except input is not step signal. ON-OFF control, here too, seems applicable.

The previous discussion shows the extent of applicability of ON-OFF controllers in various modes. In all instances, the controller could be of the same basic construction.

A configuration which possesses ON-OFF characteristics is shown in figure 75. The four 2N3836 transistors form a power switch which is driven by the SN 355A amplifiers. Both μA 709 amplifiers are run open loop and hence saturate. Thus e_1 will be at $\pm e_1(sat)$ depending on the polarity of the error signal e. e_2 is an inversion of e_1. (i.e., e_2 is + when e_1 is −, etc.) The SN 355A amplifiers each provide two complementary outputs. e_{11} is identical to e_1, and e_{12} is its complement (i.e., e_{12} is + when e_{11} is −, and vice versa). e_{23} is similar to e_2 and e_{24} is its

complement. These four voltages turn ON their respective legs of the bridge and determine the load current. Typical waveforms are shown in figure 76. All voltages saturate, e_1 and e_2 at the + or - saturation level of the μA 709, and $e_{11}e_{12}e_{23}e_{24}$ saturating at the max. output levels of the SN 355A amplifier.

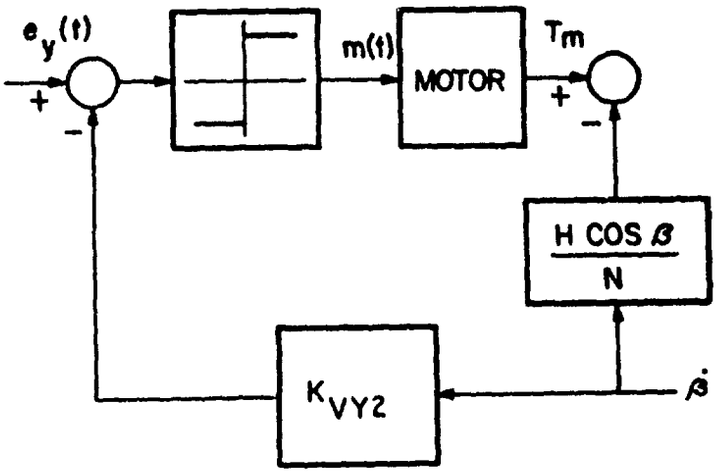

Figure 74. ON-OFF Cross Compensated Rate System

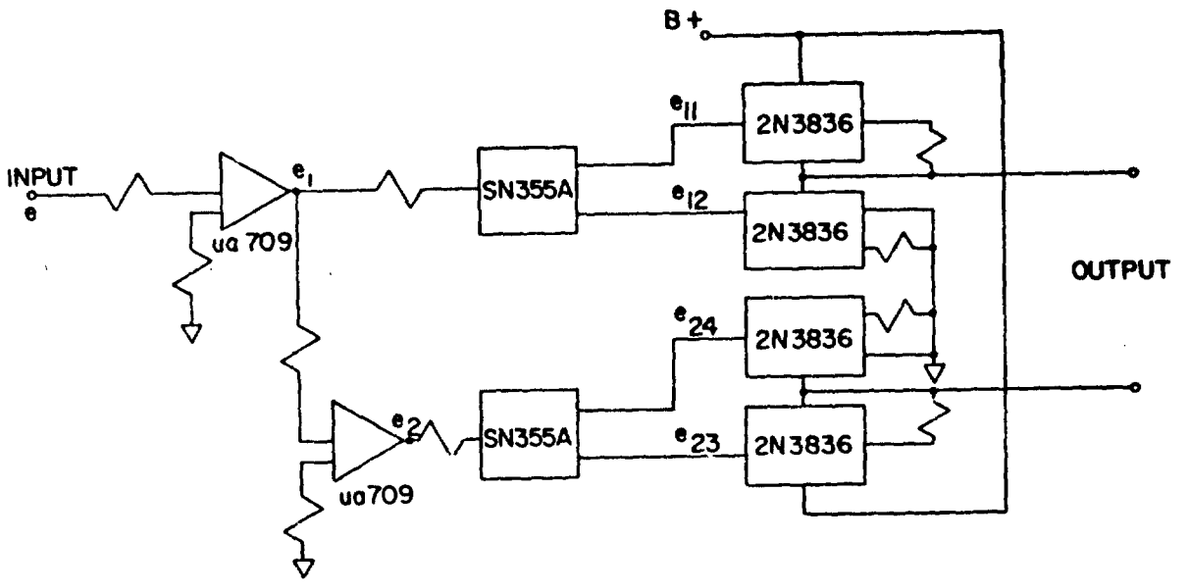

Figure 75. Solid State ON-OFF

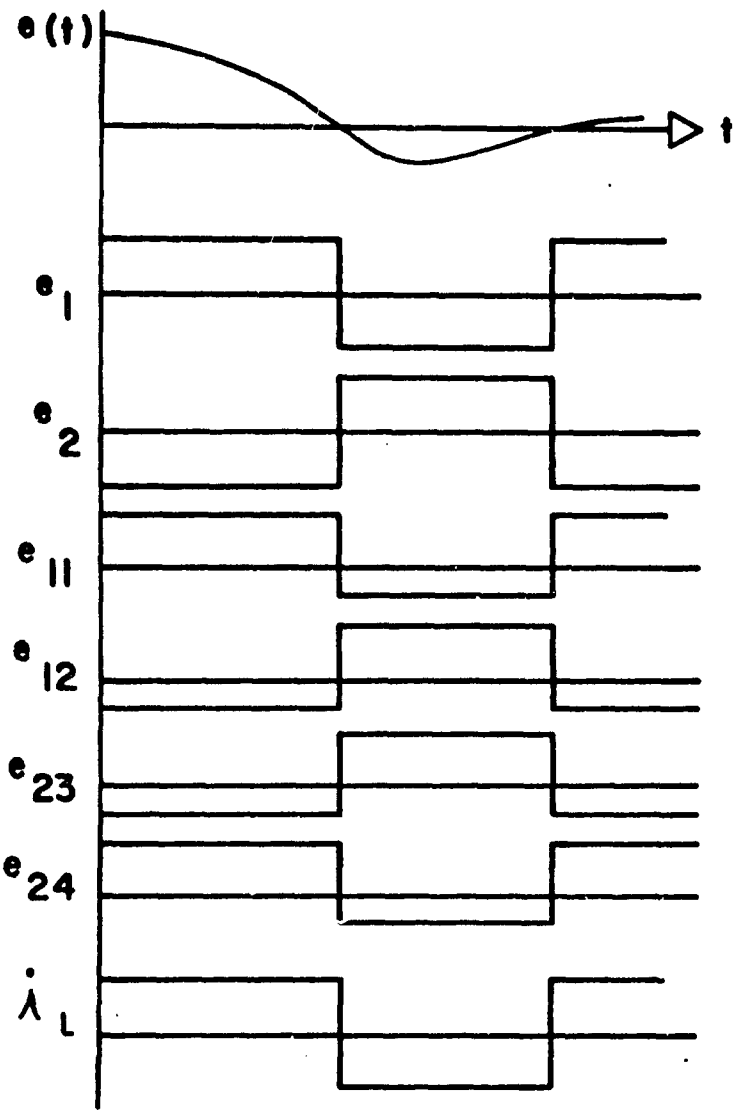

Figure 76. ON-OFF Waveforms

7.5 TWO LEVEL ON-OFF CONTROLLERS

A two valued ON-OFF controller is similar to the single valued ON-OFF controller, except that there are two levels of command signal available, $\pm M_1$ and $\pm M_2$. An ideal controller characteristic is shown in figure 77 and a characteristic with deadband is seen in figure 78. As in the single valued case, the deadband can be reduced by a high gain placed before the polarity detector. In the two level controller, the change from M_1 and M_2 occurs at some predetermined value of input signal.

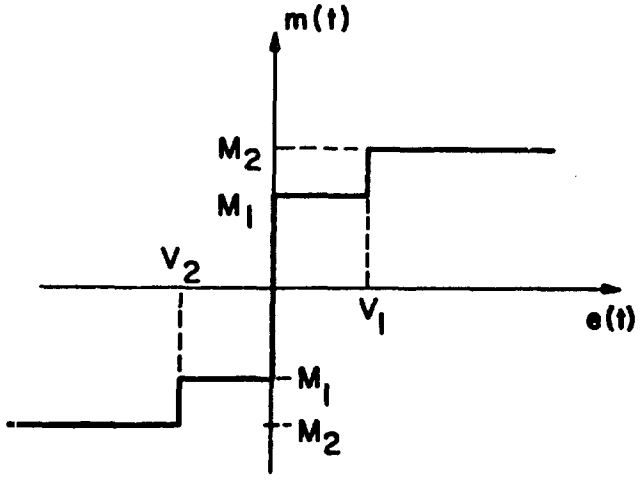

Figure 77. Ideal 2-Level ON-OFF Characteristics

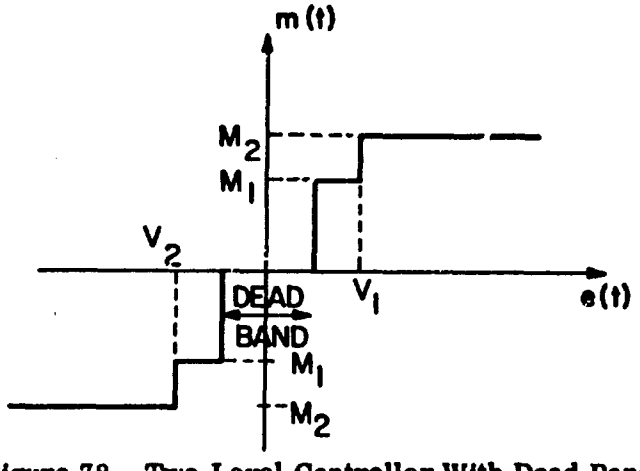

Figure 78. Two Level Controller With Dead Band

The analysis and operation of two level controllers is similar to that of single valued controllers. A two-level rate control system is shown in figure 79.

Here,

$$G(s) = \frac{\frac{1}{K_{VY1}}\omega_\eta^2}{S^2 + 2\xi\omega_\eta S + \omega_\eta^2} \qquad (7\text{-}1)$$

as in the single valued case.

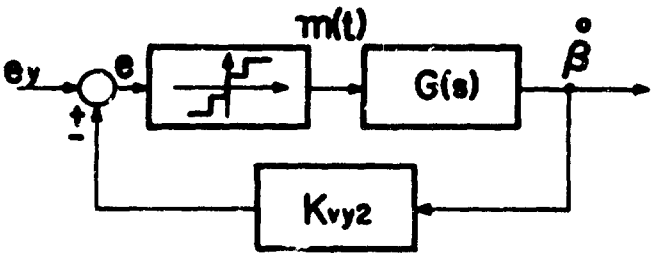

Figure 79. 2-Level ON-OFF Rate Control System

This transfer function, with a constant input, E, will correspond to a differential equation of the following form.

$$\dddot{\beta} + 2\zeta\omega_\eta \ddot{\beta} + \omega_\eta^2 \dot{\beta} = E\frac{\omega_\eta^2}{K_{VY1}} \tag{7-2}$$

The phase plane trajectory of this linear differential equation is a spiral (assuming $0<\zeta<1$) about the point $(K\frac{E}{VY1}, 0)$ in the $\ddot{\beta}$ - $\dot{\beta}$ phase plane.

In this controller, the input to the motor can assume four levels, $\pm M_1$, $\pm M_2$. Thus, there are four separate sets of spirals in the $\ddot{\beta}$ - $\dot{\beta}$ plane converging on the four points $\frac{\pm M_1}{K_{VY1}}, \frac{\pm M_2}{K_{VY2}}$. The construction of the phase plane trajectory becomes that of determining which set of spirals the system is operating on in any given region of the phase plane. When $(e_y - K_{VY2}\dot{\beta})$ is greater than V_1, the controller applies $+M_2$ to the motor. When $0<(e_y - K_{VY2}\dot{\beta})<V_1$, the motor input is $+M_1$. Similarly, $-V_2<(e_y - K_{VY2}\dot{\beta})<0$ applies $-M_1$ to the motor, and $(e_y - K_{VY2}\dot{\beta})<-V_2$ will result in $-M_2$ applied at the motor input.

The phase plane trajectory assuming $M_1 = \frac{M_2}{2}$ and $|V_1| = |V_2|$ is sketched in figure 80. The response in this case is slower than that of the single valued on-off controller, however, this system seems less subject to disturbance near null than its single valued counterpart.

In Region I,

$$(e_y - K_{VY2}\dot{\beta}) > V_1, \quad m(t) = +M_1$$

or

$$\dot{\beta} < \left(\frac{e_y - V_1}{K_{VY2}}\right) \tag{7-3}$$

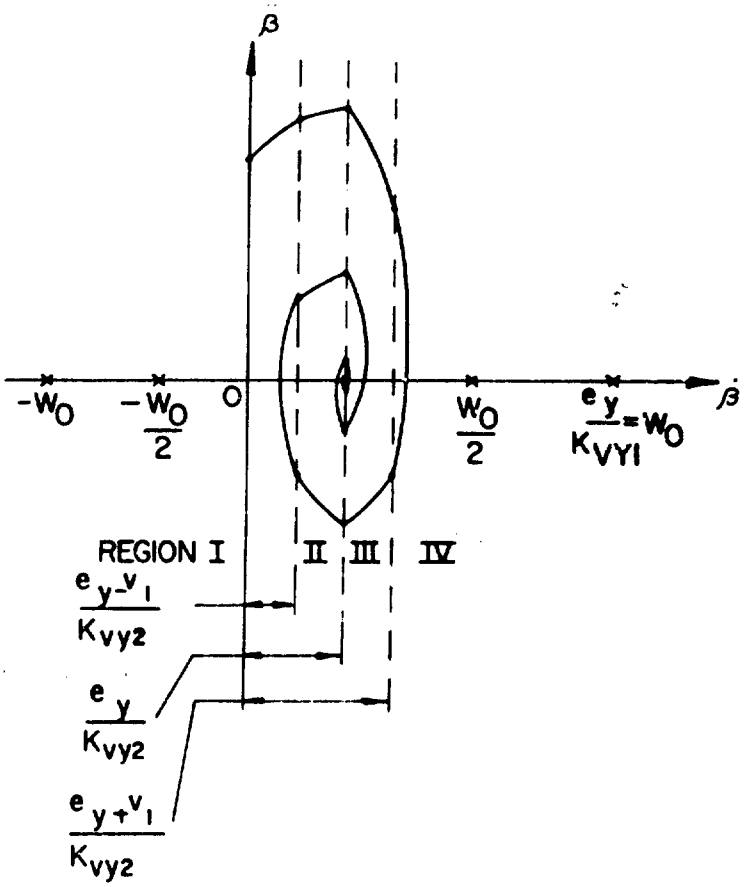

Figure 80. Phase Plane Trajectory for 2 Level ON-OFF Controller With 2nd Order System

In Region II,

$$0 < (e_y - K_{VY2}\dot{\beta}) < V_1, \; m(t) = \frac{M_1}{2}$$

or

$$\left(\frac{e_y - V_1}{K_{VY2}}\right) < \dot{\beta} < \frac{e_y}{K_{VY2}} \qquad (7\text{-}4)$$

In Region III,

$$-V_1 < (e_y - K_{VY2}\dot{\beta}) < O$$

$$\frac{e_y}{K_{VY2}} < \dot{\beta} < \left(\frac{e_y + V_1}{K_{VY2}}\right) \qquad (7\text{-}5)$$

In Region IV,

$$(e_y - K_{VY2}\dot{\beta}) < -V_1$$

$$\dot{\beta} > \left(\frac{e_y + V_1}{K_{VY2}}\right)$$

.....

A configuration which has two level ON-OFF controller characteristics as shown in figure 81. The switch section containing the four 2N3836 transistors, 2-SN355A and 2-ρA 709 amplifiers is identical with the single-valued controller. In addition, two ρA 709 units are used as level detectors. When $e > V_1$, e_3 saturates at $e_{3(+sat)}$. This turns $Q_1 - Q_2$ ON, and applies B^+ to the bridge. In addition, Q_3 is turned ON, which prevents Q_4-Q_5 from switching on. As e decreases such that $O < e < V_1$, e_3 goes negative to $e_{3(-sat)}$ turning off Q_1-Q_2. This also turns Q_3 off which then allows Q_4Q_5 to turn on, applying B+/2 to the bridge. As e goes negative, a point is reached when $e < -V_2$. At this point e_4 saturates at $e_{4(+sat)}$, turning on $Q_1Q_2Q_3$. This applies B+ to the switch section.

The zener diodes are used to prevent damage to Q_1 and Q_3, while the signal diodes in the base circuits of Q_1 and Q_3 are used for isolation.

7.6 PULSE AMPLITUDE MODULATOR

In pulse-amplitude modulation the information carrier is the amplitude of a pulse whose repetition rate and width are fixed. The PAM scheme in this report uses a pulse generator to generate a fixed frequency pulse carrier, the amplitude of which increases or decreases in accordance with input signal (signal positive or negative). The output of this scheme is referred to as double-polarity, amplitude-modulated pulses (See figure 82).

If the pulse frequency is sufficiently high, the response of a load device to the pulse train will be the same as if a continuous signal of magnitude equal to the average value of the pulse train were applied. Therefore PAM can be used to amplify slowly varying DC signals.

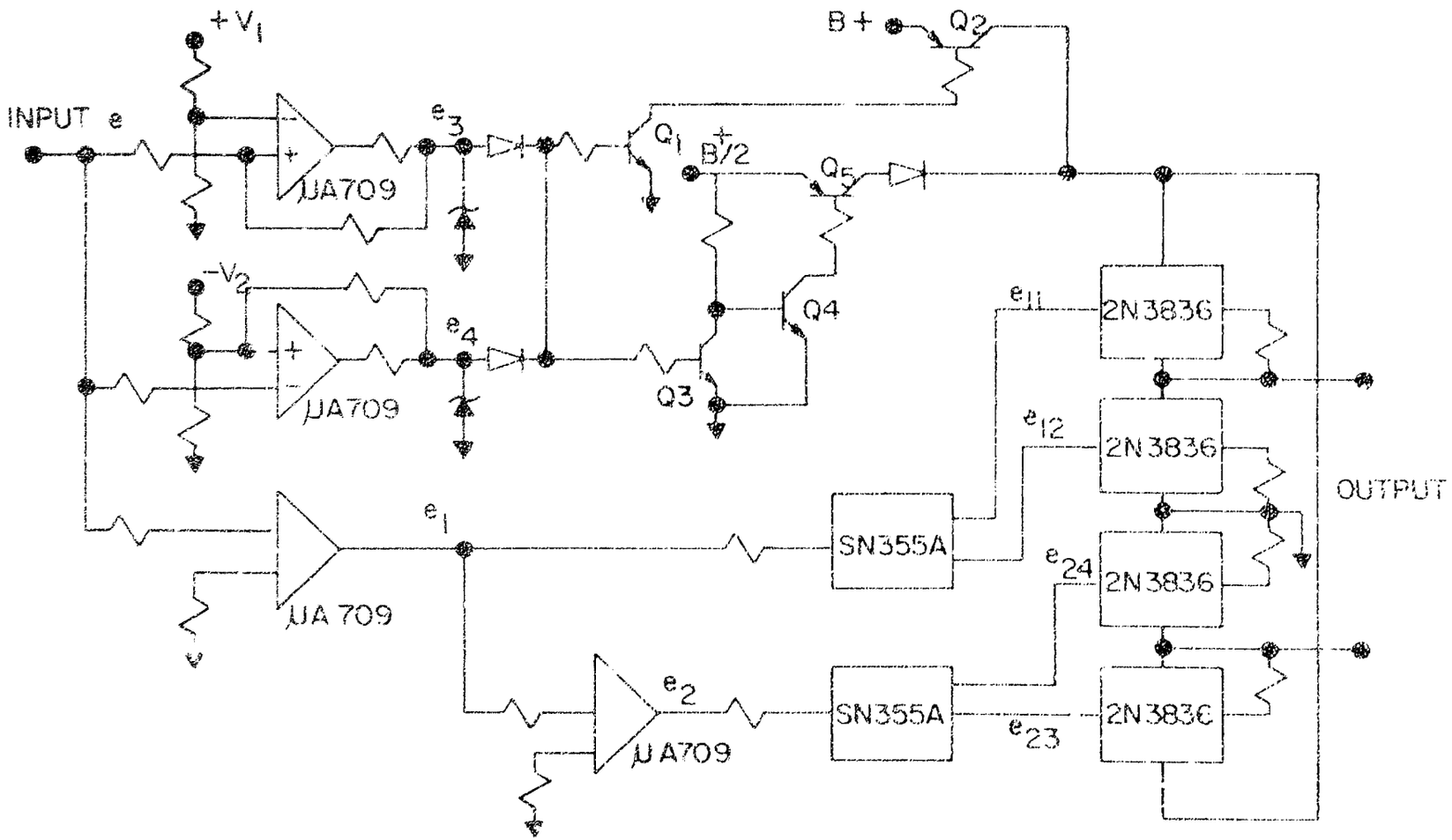

Figure 81 Schematic Solid State ON-OFF With Gain Change

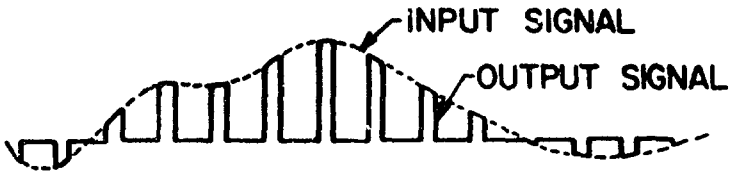

(a) DOUBLE-POLARITY PULSES

(b) SAMPLED-DATA-SYSTEM WITH FINITE DURATION SAMPLER

Figure 82. Equivalent PAM System

A block diagram of a possible double-polarity PAM is shown in figure 83. The pulse direction through the load is determined by the steering logic, and the magnitude of each pulse is the magnitude of the amplifier output signal for the pulse duration. This system is analogous to a sample-data system where the analog signal is amplified and then sampled by a finite duration sampler (See figure 82). A Schematic diagram of the system in figure 83 is shown in figure 84.

7.7 PULSE FREQUENCY MODULATOR

In pulse-frequency modulation, the information carrier is the time between the emission of two pulses of identical shape and amplitude. A common feature of all pulse-frequency modulated schemes is that their input has to be observed for a finite time before the emission of a pulse is decided. The simplest way to implement this is to integrate the input and decide on the emission of a pulse by observing the value of the integral at certain times (delta modulation) or when it reaches a specific level (integral pulse-frequency modulation or IPFM).

If the pulse frequency is sufficiently high, the response of a load device to the pulse train will be the same as if a continuous signal of magnitude equal to the average value of the pulse train were applied. Therefore a PFM can be used as a controller for a dc device. Incremental servos, or stepper motors are also natural candidates for pulse frequency control. Pulse frequency modulation can also be used in the control of three phase motors.

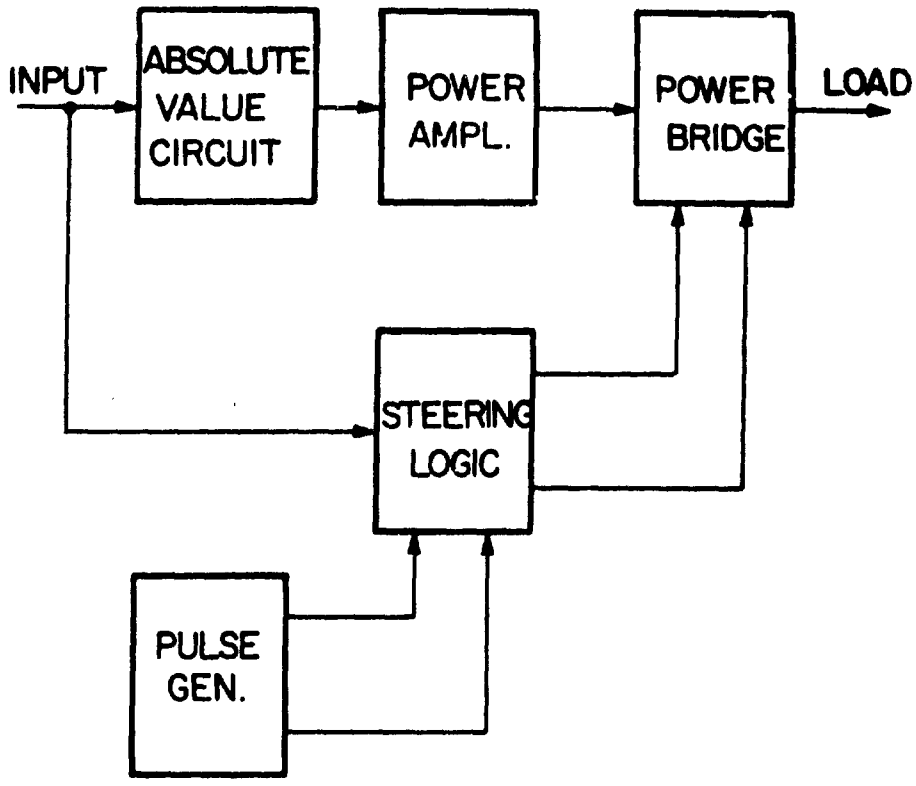

Figure 83. Pulse Amplitude Modulator - Double Polarity

An integral pulse-frequency modulator system is shown in figure 85 and figure 86. The voltage to frequency converter output is a train of spikes at a frequency determined by the integral of the input signal. This stage is followed by a monostable flip-flop (one-shot) which generates the desired pulse height and width. The converter operates on positive inputs and therefore is preceded by an absolute value circuit. The steering logic routes the one-shot output to the proper side of the power bridge.

A voltage to frequency converter is shown in figure 87. This circuit has been temperature tested from 20°C to 55°C for the NASA Langley CMG and found to be accurate to within 1.3%. The operation is as follows:

A positive step voltage applied to A1 produces a negative going ramp at the input of A2. Until the negative ramp voltage reaches a fixed threshold value, a negative voltage appears at the base of Q2 and keeps the transistor on, thereby producing zero volts at capacitor C2. When the input to A2 exceeds the threshold value, a positive voltage appears at the base of Q2 which turns the transistor off and -C volts appears at C2. This voltage is fed back to the field effect transistor Q1 (across A1) which shorts out capacitor C1. Therefore the input to A2 is switched back to a less negative

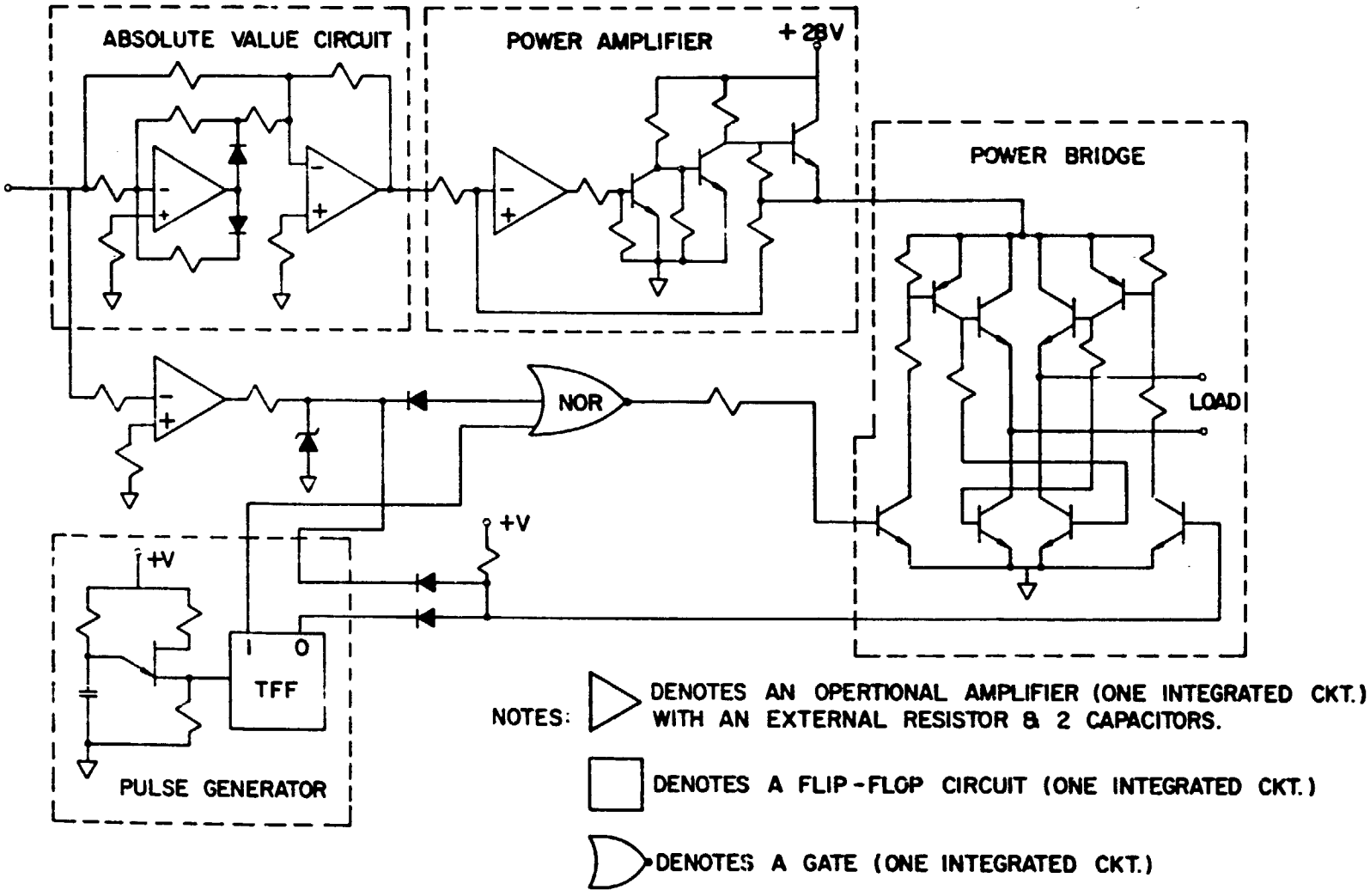

Figure 84. Schematic - Pulse Amplitude Modulator

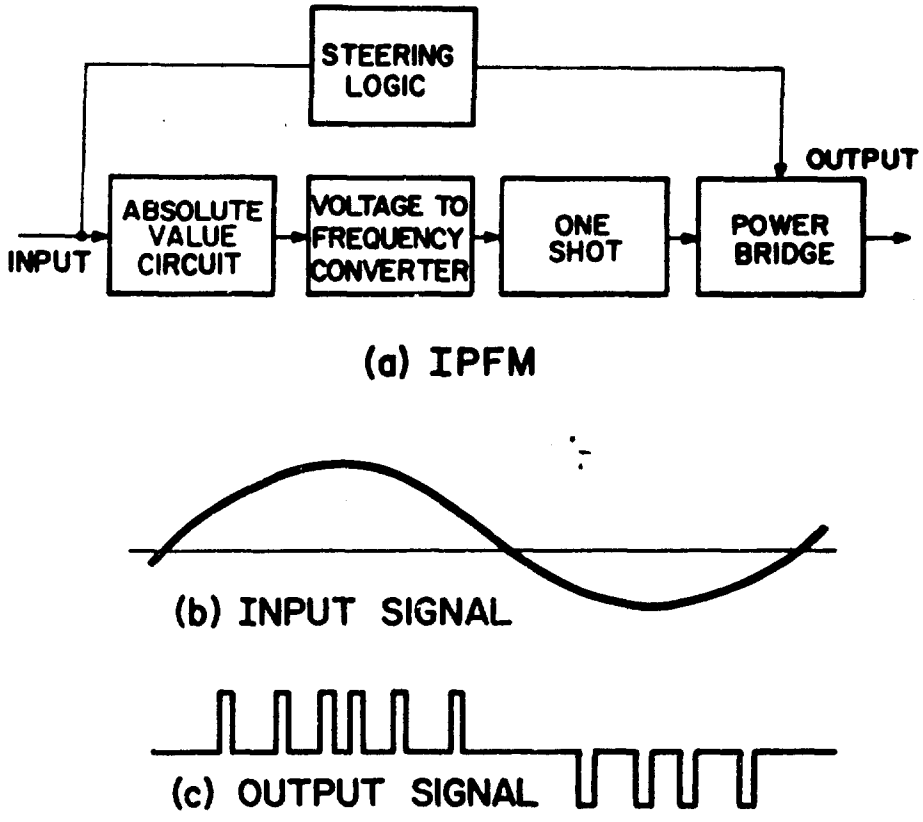

Figure 85. Block Diagram - IPFM With Input and Output Wave Shapes

voltage and transistor Q2 is turned on again, and so on. Typical wave shapes are shown in figure 88.

The product $T_w f_p$ or duty ratio versus input magnitude is shown in figure 89; T_W is pulse width and f_p is pulse frequency. Saturation occurs at $T_w f_p=1$ where the pulse period is equal to the pulse width. At zero input, $f_p=0$ and therefore $T_w f_p=0$.

An integral pulse-frequency modulator can accurately amplify DC or low frequency signals with high efficiency. High efficiency because power amplification is accomplished in the power bridge where efficiency approaches 90%. IPFM also presents a high degree of noise immunity; and can be used in control systems where certain parts are contaminated by strong noise. If the IPFM is to be used to control a DC motor, one can suspect that, at low input signals where the pulse frequency is low, the DC motor will attempt to follow at the pulse rate. Limit cycles therefore are probable.

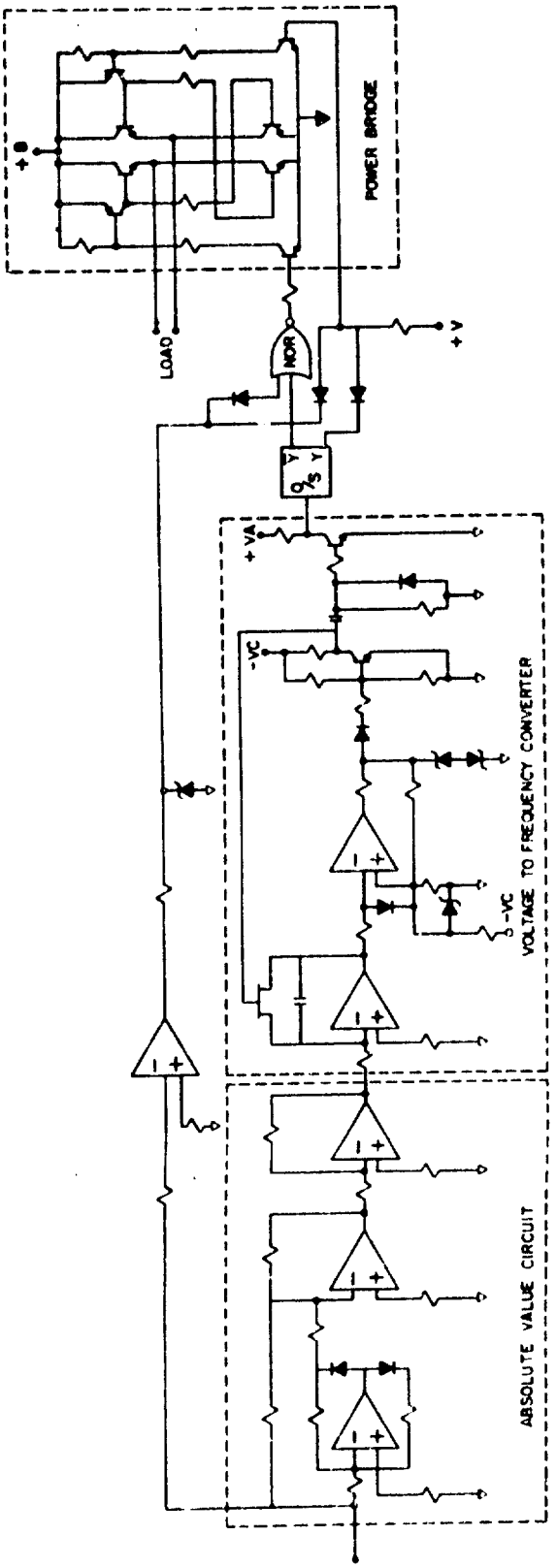

Figure 86. Schematic - Pulse-Frequency Modulation

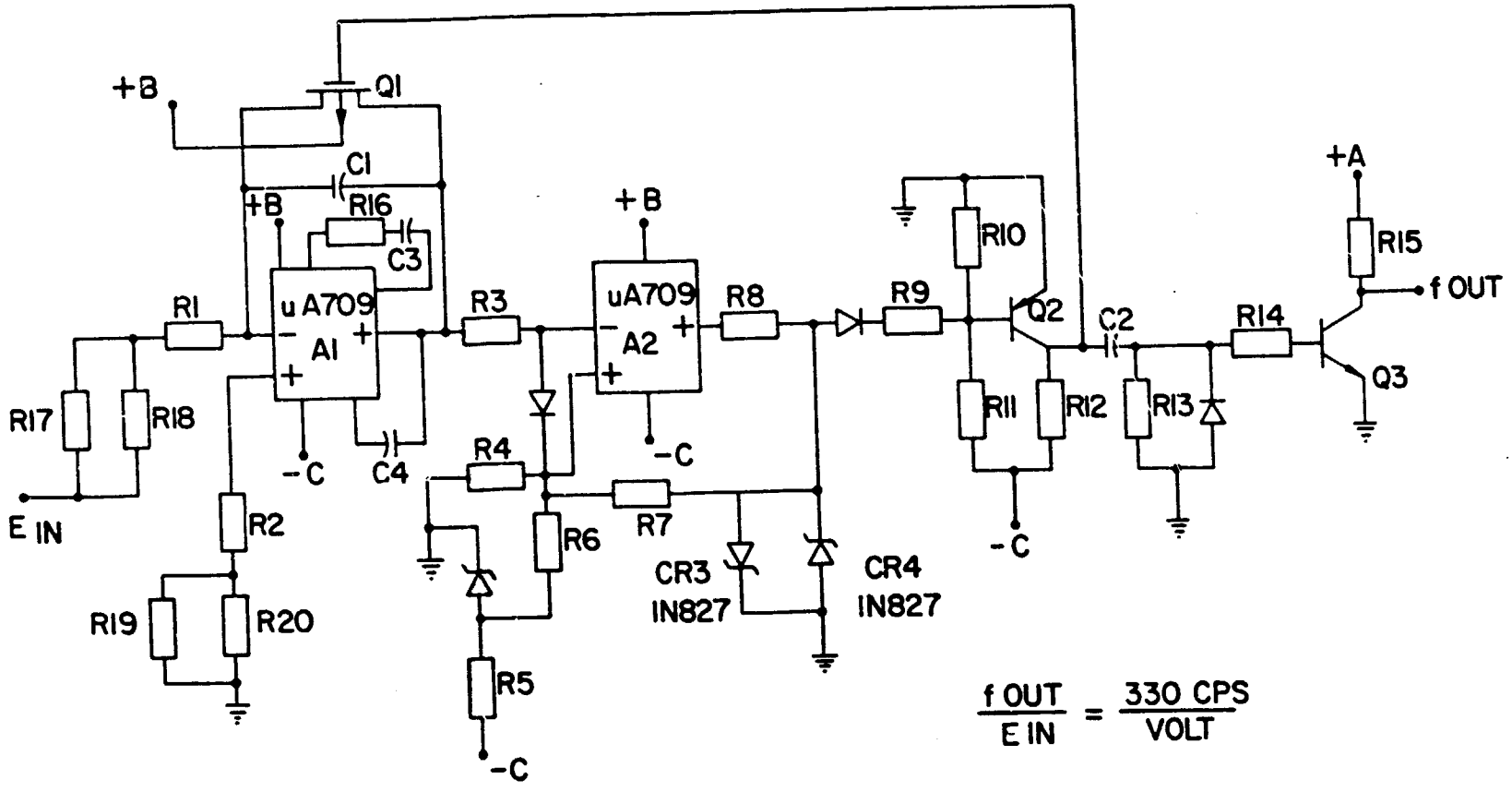

Figure 87. Voltage to Frequency Converter

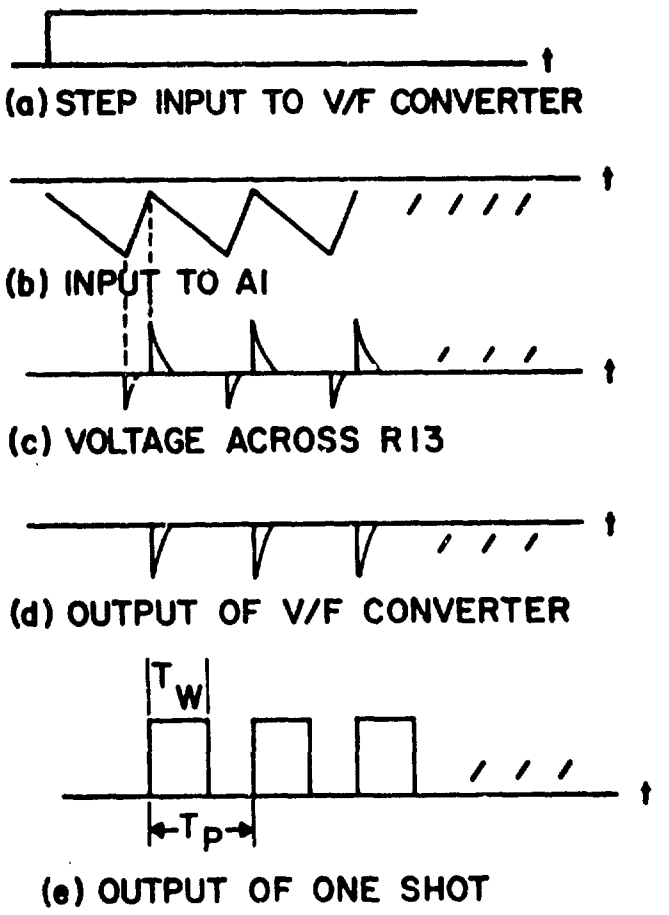

Figure 88. Wave Shapes From V/F Converter to Power Bridge

7.8 DELTA MODULATION

A delta modulator system is shown in figure 90. Block A1 itself is a delta modulator. Block A2 is the required steering logic to operate the power bridge, where the power amplification is accomplished. The operation of the modulator (A1) is as follows.

Assume a zero error signal and the instantaneous output voltage of the high gain difference amplifier to be positive. The output is fed back positively through R_d, thereby keeping the difference input negative with respect to ground as the capacitor C charges to a positive value. The amplifier is therefore driven to saturation and the output voltage is fixed by the zener diodes. At the clock pulse the output is shorted to ground and instantaneously the difference input is the voltage across the capacitor C which is positive, causing the amplifier output to invert to a negative fixed voltage. Capacitor C then charges toward a negative value until the next clock pulse occurs. The process is continued as illustrated in figure 91. At zero error signal, the output

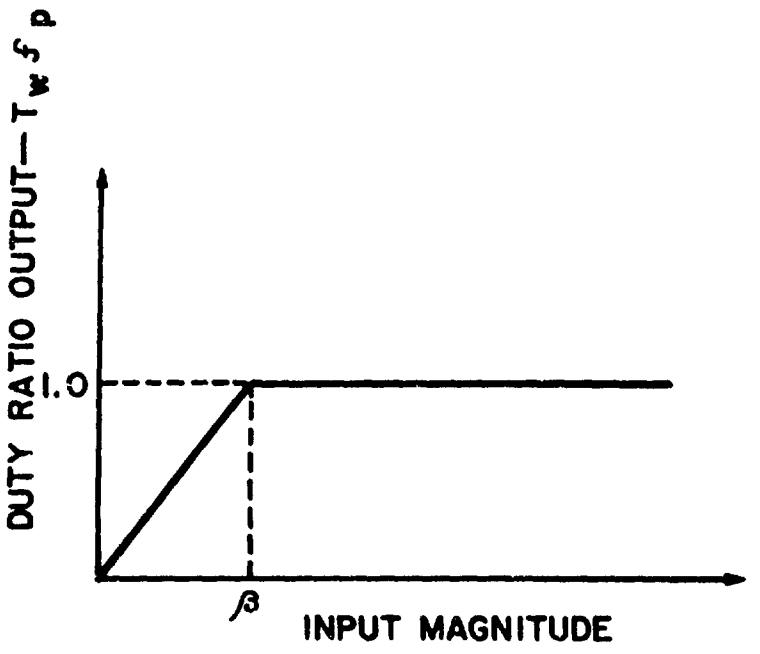

Figure 89. Duty Ratio Versus Input Magnitude

of the delta modulator (A1) is a train of square waves whose repetition rate is one half the clock rate and the pulse width is equal to the clock time t_s. The operation of blocks A2 and A3 is as follows:

The flip-flop state is identical to its input, and can change its state at clock times. Therefore the "and" gate outputs e_{o1} and e_{o2} are high for two consecutive +5 volt pulses and -5 volt pulses at the modulator output, respectively. At zero error signal neither "and" gate is high, thus the power bridge is inoperative. Note that the first pulse in a consecutive sequence is always lost in the steering logic.

In figures 92 and 93, voltage patterns resulting from positive error signals of 1.0 volt and 0.5 volts respectively are illustrated. The illustrations are based on zener breakdown voltages of 5 volts, $R = R_f$ and a clock time, t_s, of 1/100 of the time constant, $\tau = \frac{R_f RC}{R+R_f}$. To insure correct operation, the capacitor voltage should be kept very much smaller than the zener breakdown voltage. This is accomplished by setting the clock time very much smaller than the time constant, τ. The following relations were used as a guide in drawing figures 91 through 93.

$$t_s = .01\tau$$

$$t_s = \tau V_s / V_f$$

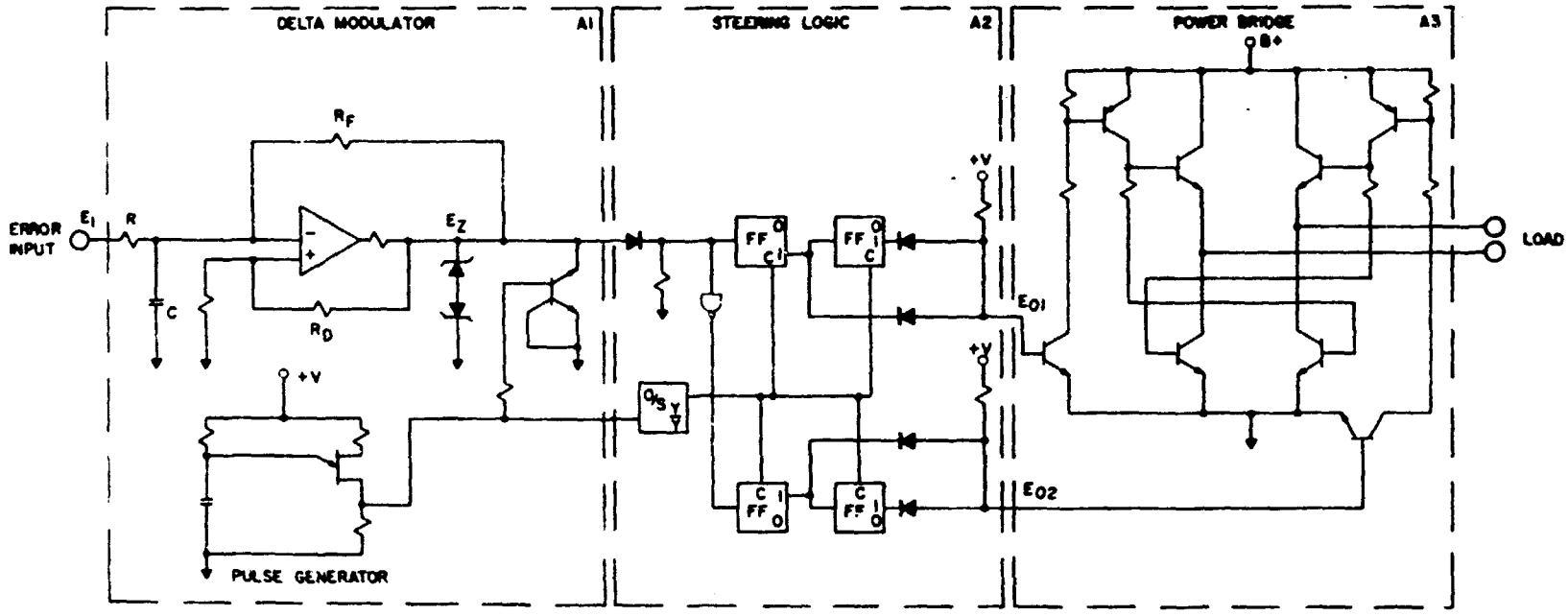

Figure 90. Schematic - Delta Modulator System

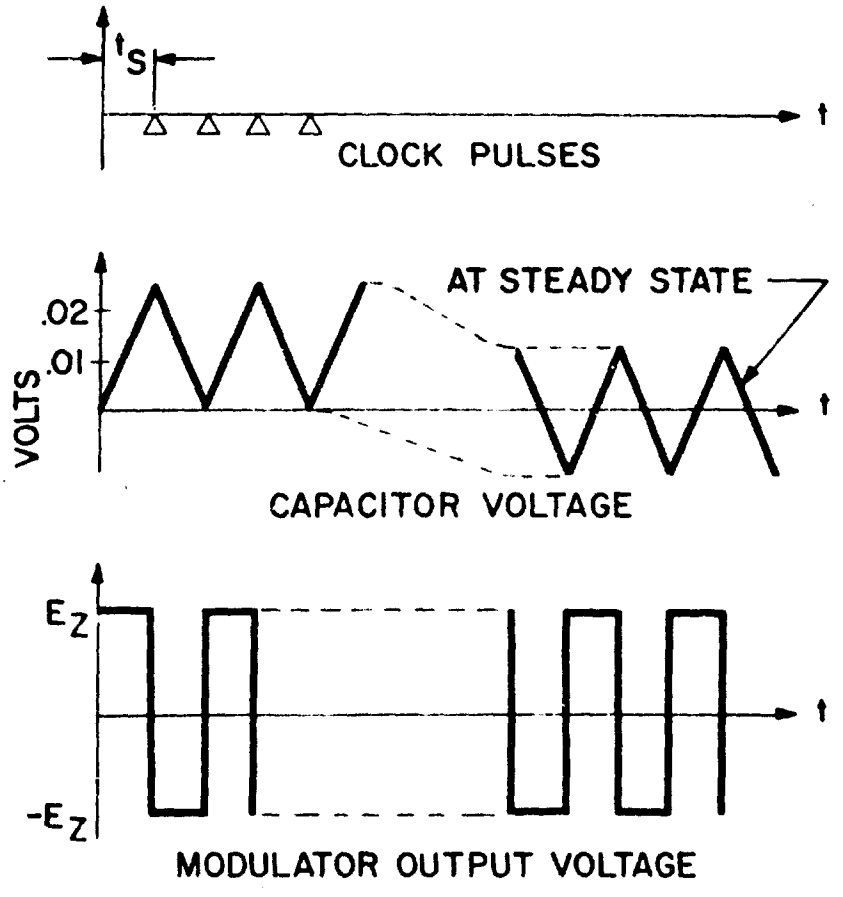

Figure 91. Voltage Wave Shapes - Zero Error Signal

where V_f is the final voltage the capacitor can charge to and V_S is the voltage at clock time. The above equations yield $V_S = .01\ V_f$. V_f is the total change in capacitor voltage -- from the voltage at clock time to the final voltage from zero it can reach if allowed to fully charge. Letting $V_S(i)$ represent the capacitor voltage at the previous clock time and E_f represent the final voltage from zero reference, the following is true:

$$V_S(i+1) = -.99 \left| V_S(i) \right| + .01 \left| E_f^+ \right| \text{ if } V_S(i) < 0$$

and

$$V_S(i+1) = .99\ V_S(i) - .01 \left| E_f^- \right| \text{ if } V_S(i) > 0$$

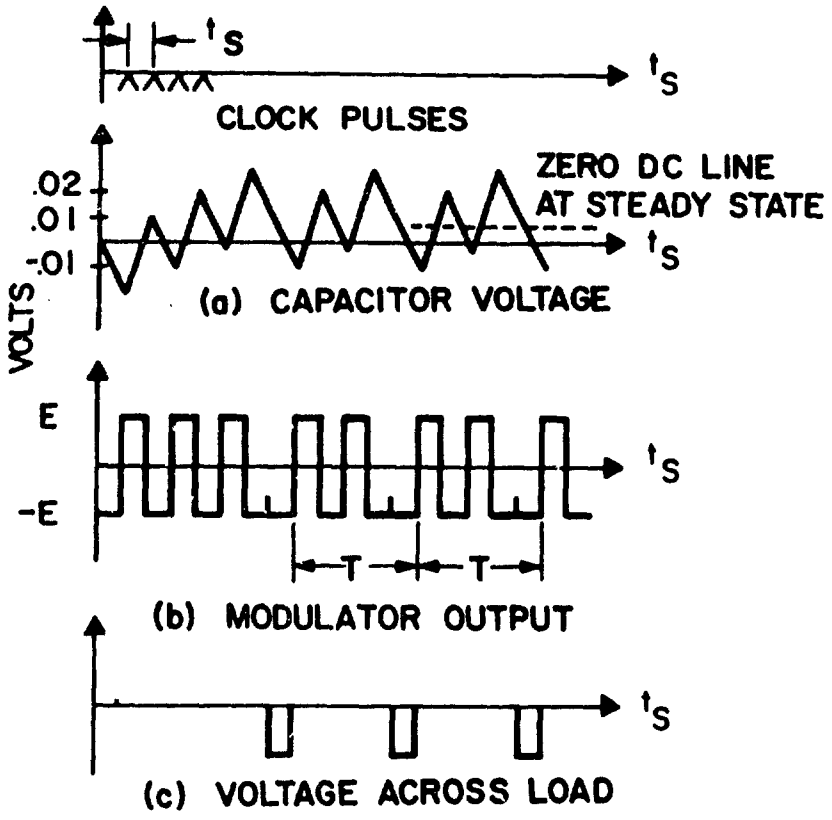

Figure 92. Voltage Patterns for Error Signal of 1 Volt

In figures 91, 92, & 93 the slopes are assumed to be constant and equal to .01 E_f/clock time. E_f from figure 90 is

$$E_z \frac{R}{R + R_f} + E_1 \frac{R_f}{R + R_f}$$

Note that the pulse width changes in multiples of clock times. The dc component of the train of pulses can be found from noting the number of positive and negative pulses in a period. The relation is as follows:

$$\text{dc (out)} = E(\text{max}) \frac{P-N}{P+N}$$

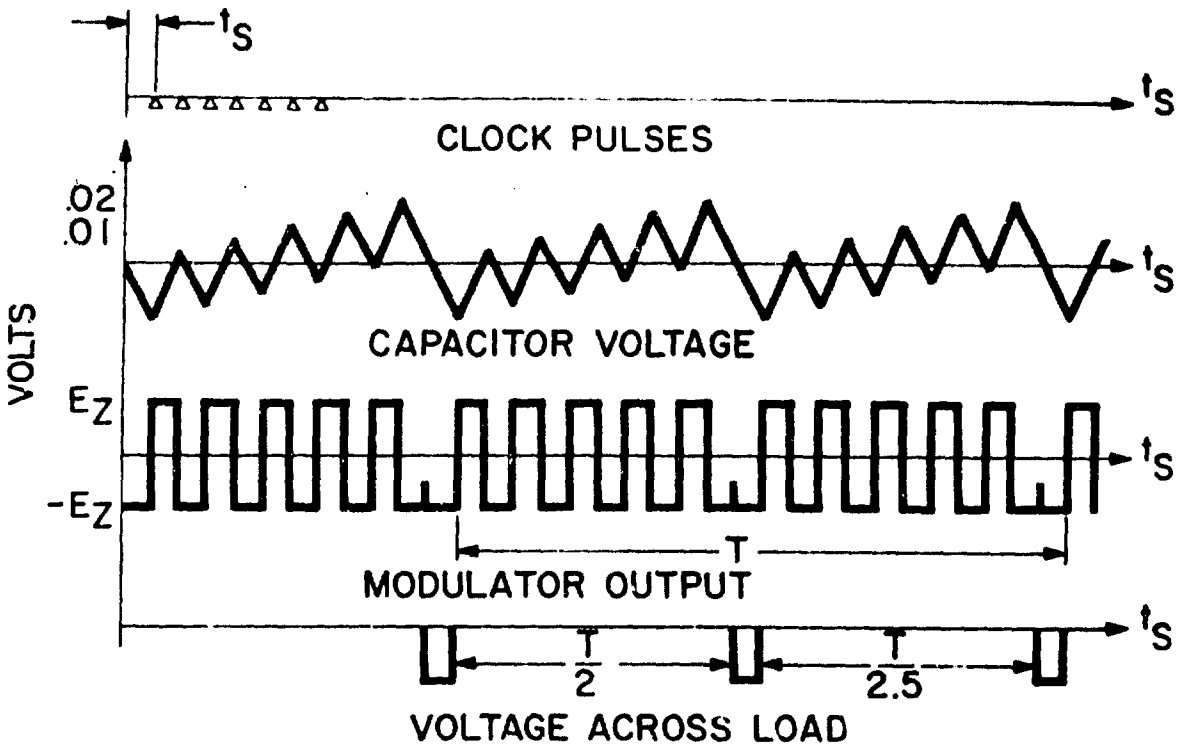

Figure 93. Voltage Pattern For An Error Signal of 0.5 Volts

In figure 93 a dc component of 0.5 volts is desired - i.e. 1/10 of 5 volts. Therefore $\frac{P-N}{P+N} = \frac{1}{10} = \frac{11-9}{11+9}$. That is to say, to obtain a dc component of 0.5 volts, a period of 20 clock times is required with 11 pulses up and 9 down. In our example we want -0.5 volts so reverse the order -9 up and 11 down. Consider now a dc component of 0.25 volts or 5/20, then $\frac{P-N}{P+N} = \frac{1}{20} = \frac{21-19}{21+19}$. Here a period of 40 clock times is needed made up of 21 positive pulses and 19 negative pulses. As the error signal decreases the pulse frequency decreases.

A necessary condition to insure the capacitor polarity follows that of the zener voltage E_z is

$$E1R_f < E_z R$$

$$E1 < \frac{R}{R_f} E_z$$

For $R_f = 2R$ and a dc input of 0.5 volts, the pulse period would be that of figure 93. Thus for the same input, the pulse frequency has increased at the expense of losing allowable input range.

SECTION VIII

CONTROLLER EVALUATION

In this section, each controller will be quantatively evaluated as to power consumption, efficiency, reliability, weight, volume, and threshold. The purpose of these calculations is to provide data with which to perform an optimization of the complete actuator. Each candidate controller will be considered separately, and appropriate calculations will be outlined. In each case, a torque motor load will be assumed with parameters as given below in Table XXII.

TABLE XXII

BRIEF SUMMARY OF ACTUATOR CHARACTERISTICS

$\frac{H}{\text{(ft-lb-sec)}}$	$\frac{N}{\text{(Gear ratio)}}$	$\frac{T_m}{\text{(ft-lbs)}}$	$\frac{\text{DC Torquer}}{\text{(Inland Corp)}}$	$\frac{R_m}{\text{(ohms)}}$
200	35	1.0	T-4036D	11.0
500	50	1.75	T-5134D	10.1
1000	60	2.92	T-5730D	8.5
1500	60	4.38	T-7202G	7.25
2000	75	4.66	T-7202G	7.25

8.1 POWER AND EFFICIENCY

In many of the discussions in Section VII, a purely resistive load was assumed in order not to obscure the basic operation of each controller. In actuality, the load is more precisely represented by an R-L network, since the load is a DC motor. The effects of the armature inductance must be considered.

In all of the pulse techniques, the motor is driven by a pulse train. Under constant error conditions, the input to the actuator is a periodic wave and can be represented by its Fourier series.

$$m(t) = \sum_{n=-\infty}^{\infty} {}_{\infty}{}_{n}{}_{\infty} e^{in\omega_o t} \qquad (8\text{-}1)$$

where

$$T = \text{pulse period}$$

$$\omega_o = \frac{2\pi}{T}$$

$$\infty_n = \frac{1}{T} \int_C^{C+T} m(t) e^{-in\omega_o t}\, dt$$

Expressing $m(t)$ in a sin-cos expansion,

$$m(t) = a_o + \sum_{n=1}^{\infty} a_n \cos n\omega_o t + \sum_{n=1}^{\infty} b_n \sin n\omega_o t \qquad (8\text{-}2)$$

The motor torque is given by

$$T_m(S) = \frac{K}{\tau_E S + 1} \cdot M(S) \qquad (8\text{-}3)$$

From equation (8-2), it can be seen that the motor input contains frequency components at $\omega = n\omega_o \quad n = 0, 1, 2, 3, \ldots$.

The characteristic of the motor (equation 8-3) is essentially that of a low pass filter. Hence, if ω_o (the lowest frequency present in the input) is much higher than the cut-off frequency of the motor ($\omega_c = \frac{1}{\tau_E}$), the motor torque will be in response to the DC term, a_o. It is desirable, when driving a DC motor, that the pulse frequency, ω_o, be much higher than the cutoff frequency of the motor. One cannot set the pulse frequency arbitrarily high, however, since transients reflecting back to the power source would necessitate heavy decoupling. For the torque motors considered,

$$\tau_E \cong 0.002 \text{ sec} \quad \text{or} \quad f_C = \frac{1}{2\pi\tau_E} = 79.6 \text{ CPS.}$$

A reasonable approximation is to set

$$T = \frac{1}{10} \frac{1}{f_c} \quad \text{or} \quad f_p = \frac{1}{T} \quad 769 \quad \text{CPS.}$$

Since the load is not purely resistive, the motor current, instead of being a series of square pulses, now becomes a series of pieces of exponentials as shown in figure 94. Provision for transistor protection in the power switch must be provided by power diodes. Consider the power switch shown in figure 95 with Q_1 and Q_4 conducting. A current i_L will flow as shown. When the inputs to Q_1 and Q_4 are removed, as at the end of a pulse, the motor inductance will prevent the current from dropping to zero. Thus, current will continue to flow in the i_L direction. The current path during this time period is, as shown in figure 95, flowing through diodes D_2 and D_3.

When Q_1 and Q_4 are ON, the motor current will exponentially approach the value,

$$I_p = \frac{\text{(Power Supply Voltage)} - \text{(Power Switch Drop)}}{\text{(Motor Resistance)}} \qquad (8\text{-}4)$$

During the period when Q_1 and Q_4 are OFF, and D_2-D_3 are ON, the load is effectively connected to -28 volts, and the load current will exponentially approach $-I_p$.

In steady state, the current will hover about the desired average value of current as shown in figure 94.

In this section, a power consumption and efficiency analysis will be presented. Power consumption calculations will be outlined for each controller.

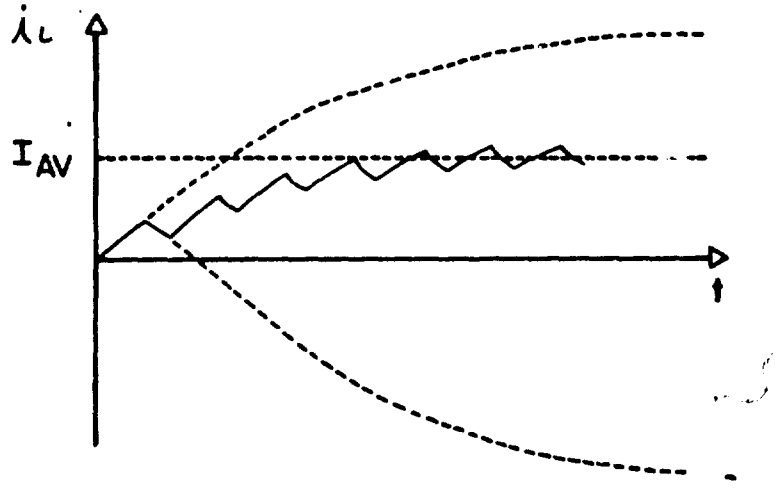

Figure 94. Load Current vs Time For Step Error Input

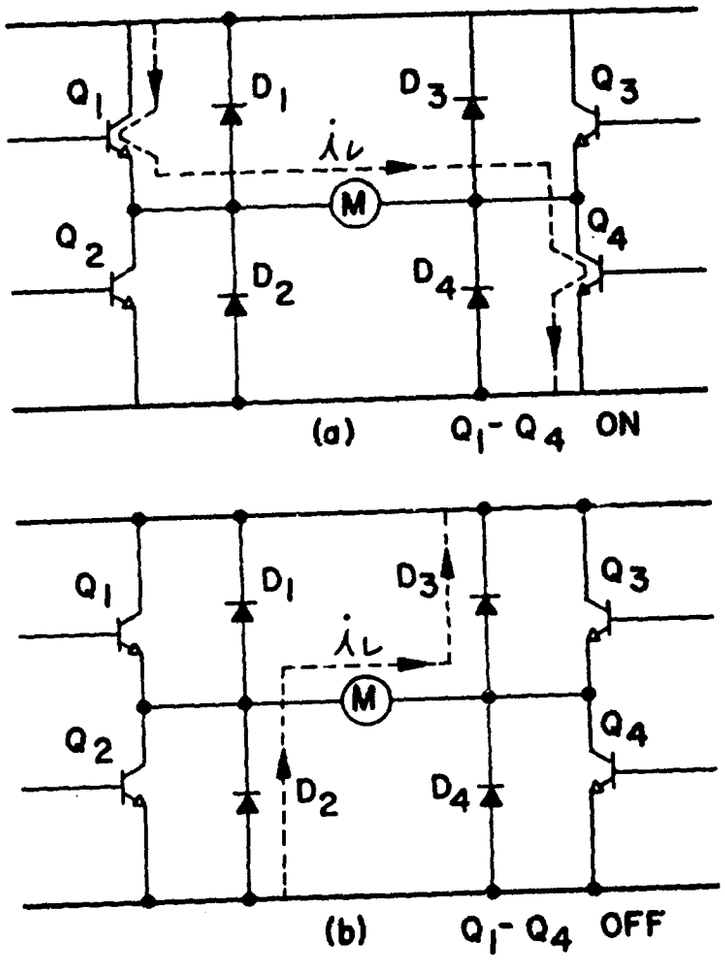

Figure 95. Current Path In Power Switch

8.1.1 Motor Power

The average value of motor power is given by:

$$P_m = I_m^2 R_m \text{ (watts)} \qquad (8\text{-}5)$$

where: I_m = average current required to develop desired torque

R_m = DC torquer resistance

Since $T_m = KI_m$ for a DC torquer,

$$I_m = \frac{T \text{ desired}}{K} \quad \text{(amp)} \tag{8-6}$$

where K = motor torque constant $\left(\frac{\text{ft-lbs}}{\text{amp}}\right)$

Define $I_{max} = \frac{T \text{ max}}{K}$ (8-7)

as the value of current required to develop maximum torque.

Under duty cycle operation,

$$I_{av} = \frac{1}{100}\left[I_{max} + \frac{30}{100}\frac{I_{max}}{2} + \frac{69}{100}\frac{I_{max}}{4}\right]$$

$$I_{av} = 0.3325\ I_{max} \tag{8-8}$$

The motor power consumption under duty cycle operation is:

$$P_m = \left[\frac{1}{100} I_{max}\ R_m + \frac{30}{100}\left(\frac{I_{max}}{2}\right)^2 R_m + \frac{69}{100}\left(\frac{I_{max}}{4}\right)^2 R_m\right]$$

$$P_m = 0.128\ I_{max}^{\ 2}\ R_m \tag{8-9}$$

For example, consider the H = 1000 ft-lb-sec unit operating at full torque.

$T = 175$ (ft-lbs.)

$I_{max} = 2.25$ (amp)

$R_m = 8.5$ (ohms)

$P_m = I_{max}^{\ 2} R_m = (2.25)^2 (8.5) = 43.1$ watts

If this unit is operated under duty cycle, the power consumption is

$$P_m = 0.128\ I_{max}^2 R_m = I_{av}^2 R_m$$

$$P_m = 0.128(43.1) = 5.52 \text{ watts}$$

8.1.2 Bridge Power

The bridge power consumption is the same in six out of eight controllers. In these controllers (PWM_1, PWM_2, ON-OFF, ON-OFF VG, PFM, DELTA MOD.), the bridge components are saturated or cut-off. In order to calculate power consumption, assume that the motor current will flow through two semi-conductors at all times. (See figure 95). Assuming a 1.5 volt drop in each semi-conductor, the power lost in the bridge will be:

$$P_B = 2(1.5)\ I_m = 3I_m$$

For example:

$$T = 175 \text{ ft-lbs}$$

$$I_{max} = 2.25 \text{ amps}$$

$$P_B = 3(2.25) = 6.75 \text{ watts}$$

The electronics power was estimated at 250 mw per integrated circuit. Individual estimates for the controllers are given below.

PWM_1:	4 modules at 250 mw	1.0 watt
PWM_2:	5 modules at 250 mw	1.3 watt
ON-OFF:	4 modules at 250 mw	1.0 watt
ON-OFF VG:	6 modules at 250 mw 1 power diode 1 power transistor 2 low power transistor	} 3.1 I_m

or $P = 1.5 + 3.1\ I_{max}$

$= 1.5 + (3.1)\ (2.25) = 8.47$ watts

PFM:	6 modules at 250 mw	1.5 watts
DELTA:		300 mw

In calculating the power consumption in the DC proportional and PAM controllers, a simplifying assumption was made. Since a portion of the bridge is operated in its active region, the power consumed in the bridge itself was assumed to be much greater than the power consumed in the remaining components. Total bridge power is given by:

$$P = EI_m \tag{8-11}$$

where

E = supply voltage

I_m = average motor current

Thus, for the H = 1000 ft-lb-sec case,

T = 175 ft-lbs

I_{max} = 2.25 amp

P = (28) (2.25) = 63.0 watts

8.1.3 Efficiency

Controller efficiency was calculated according to the following relation.

$$\eta = \text{efficiency} = \frac{P_{motor}}{P_{total}} \times 100 \tag{8-12}$$

ex. PWM_1 controller P_{motor} = 43.1 watts

T = 175 ft-lbs P_{total} = 50.9 "

H = 1000 ft-lb-sec

$$\eta = \frac{43.1}{50.9} \times 100 = 84.7\%$$

In Table XXIII is shown the power consumption of each controller operating at full torque, and under the specified duty cycle. Table XXIV gives efficiencies based upon the data in Table XXIII. Figures 96 and 97 show curves of power consumption and efficiency for each controller plotted versus torque and CMG size.

8.2 WEIGHT AND VOLUME ESTIMATION

Weights and volumes of the controller electronics are presented in this paragraph. It was found that weight and volume requirements of the associated electronics components in the controller section remained relatively constant, independent of CMG size.

Since the controller weight and size was assumed independent of CMG size, one estimate of these parameters for each controller type was made. These are presented in Table XXV.

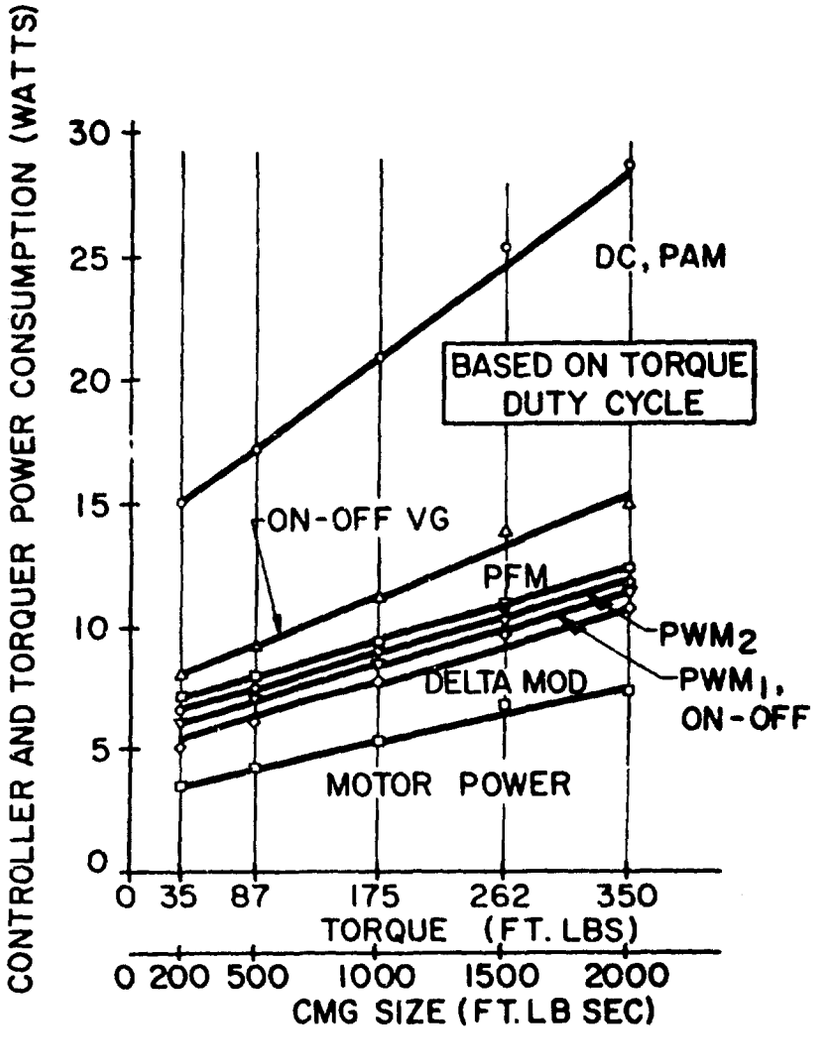

Figure 96. Controller Power Consumption vs Torque and CMG Size

TABLE XXIII

POWER CONSUMPTION OF EIGHT CONTROLLERS

Load and Torquer Characteristics				Controller Power Consumptions: Electronics + Motor + Switching (Watts)								
T_{LN} (ft-lb)	R_m (ohms)	I_m (amp)	P_m (watts)	DC	PWM_1	PWM_2	ON-OFF	ON-OFF VG	PAM	PFM	Delta Mod.	
35	11.0	1.59	27.8	44.5	33.6	33.9	33.6	39.0	44.5	34.1	32.9	Full Torque
87.5	10.1	1.84	34.1	51.5	40.6	40.9	40.6	46.8	51.5	41.1	39.9	
175	8.5	2.25	43.1	63.0	50.9	51.2	50.9	58.3	63.0	51.4	50.2	
262.5	7.25	2.73	54.1	76.4	63.3	63.6	63.3	72.3	76.4	63.8	62.6	
350	7.25	2.97	61.7	81.7	71.5	71.8	71.5	80.9	81.7	72.0	70.8	
35	11.0	0.53	3.57	14.8	6.16	6.46	6.16	8.30	14.8	6.66	5.41	Torque Duty Cycle
87.5	10.1	0.61	4.36	17.1	7.20	7.50	7.20	9.60	17.1	7.70	6.45	
175	8.5	0.75	5.52	20.9	8.77	9.07	8.77	11.6	20.9	9.27	8.02	
262.5	7.25	0.91	6.93	25.4	10.7	11.0	10.7	14.0	25.4	11.2	9.91	
350	7.25	0.97	7.90	27.2	11.8	12.1	11.8	15.3	27.2	12.3	11.1	

TABLE XXIV

EFFICIENCY OF EIGHT CONTROLLERS

Load and Torquer Characteristics				Controller Efficiency (%)								
T_{LM} (ft-lb)	R_m (ohms)	I_m (amp)	P_{motor} (watts)	DC	PWM_1	PWM_2	ON-OFF	ON-OFF VG	PAM	PFM	Delta Mod.	
35	11.0	1.59	27.8	62.5	82.7	82.0	82.7	71.2	62.5	81.5	84.5	Full Torque
87.5	10.1	1.84	34.1	66.2	84.0	83.4	84.0	72.8	66.2	82.9	85.5	
175	8.5	2.25	43.1	68.4	84.7	84.2	84.7	73.9	68.4	83.3	85.9	
262.5	7.25	2.73	54.1	70.8	85.5	85.1	85.5	74.8	70.8	84.7	86.4	
350	7.25	2.92	61.7	75.5	86.3	85.9	86.3	76.3	75.5	85.7	87.1	
35	11.0	0.53	3.57	24.1	58.0	55.3	58.0	43.0	24.1	53.5	64.9	Torque Duty Cycle
87.5	10.1	0.61	4.36	25.5	60.6	58.1	60.6	45.4	25.5	56.6	67.7	
175	8.5	0.75	5.52	26.4	62.9	60.9	62.9	47.6	26.4	59.5	69.0	
262.5	7.25	0.91	[illegible]	27.3	64.8	63.0	64.8	49.5	27.3	61.9	70.0	
350	7.25	0.97	7.90	28.9	66.7	65.0	66.7	51.9	28.9	64.0	70.9	

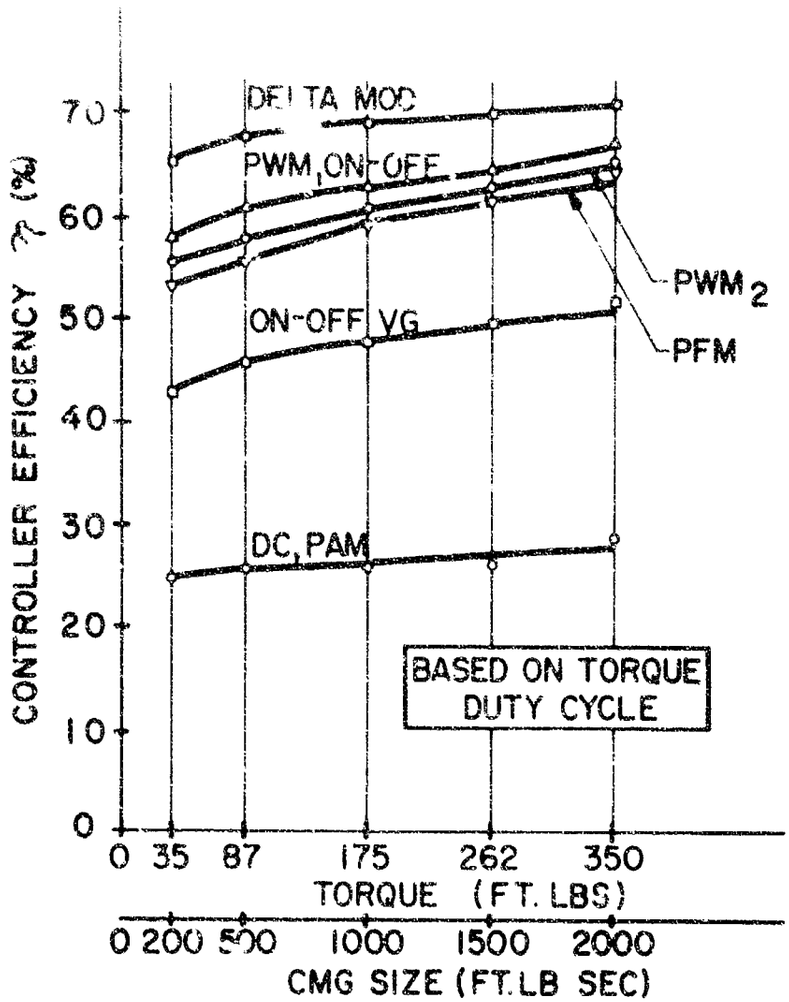

Figure 97. Controller Efficiency Vs Torque and CMG Size

TABLE XXV

CONTROLLER ELECTRONICS - WEIGHT AND VOLUME ESTIMATE

Controller Type	Volume (in^3)	Weight (oz)
DC	15	16
PWM_1	2.5	2.5
PWM_2	3	3
ON-OFF	4	4
ON-OFF VG	5	5
PAM	8	7
PFM	7	6
DELTA MOD	7	6

8.3 RELIABILITY

Each controller was subjected to a reliability evaluation using the MIL-HDBK-217A[24] reliability data table. The assumed operating conditions were:

a. Time of mission - 1 year (8760 hours)

b. Ambient temperature - 70°C (158°F)

c. Ground test conditions - 1 atmosphere

- 1 g. acceleration

It was assumed that the electronics reliability would be independent of CMG size, and so one reliability evaluation was made for each type of controller. Reliability indexes are for the electronics components only, exclusive of torque motor, gear train, or feedback transducers. These figures appear in Table XXVI.

Reliability evaluation was made at test conditions rather than actual flight conditions to facilitate comparisons between controller types rather than to obtain true operational reliability figures.

TABLE XXVI

RELATIVE RELIABILITY OF ELECTRONIC CONTROLLERS

Controller Type	Failure Rate (PPMH)*	Reliability
DC	6.81	0.942
PWM_1	2.59	0.978
PWM_2	2.95	0.974
ON-OFF	2.40	0.979
ON-OFF VG	4.81	0.958
PAM	3.73	0.968
PFM	4.87	0.958
DELTA MOD	4.39	0.962

*PPMH = Parts per million hours.

[24] See Reference No. 19, Appendix D.

8.4 THRESHOLD

Each controller is analyzed in order to determine its threshold value. The threshold is defined as the percentage of the input signal range over which the system will not respond. This is obtained by considering the value that the error signal must reach before the controller commands corrective action from the actuator, and dividing it by the error signal necessary to produce maximum torque required. Each type of controller is considered separately below.

In the DC proportional controller, the threshold value was experimentally determined to be about 50 MV. for the circuit shown in this report (see figures 49 and 50). This represents about 0.5% of the available input signal range.

The PWM_1 threshold is essentially zero. Experimental evidence shows the output current to be a linear function of error voltage throughout the entire input signal range.

Dual channel PWM showed a non-linearity about zero input signal when experimental data is used to plot output current versus error signal. A PWM_2 was constructed and its characteristics are shown in figure 98. Although a true threshold does not exist the gain with torquer loading is non-linear for small error signals. Thus, PWM_2 has no threshold, but possesses non-linear gain for input error signals less than about 7% of the maximum input signal range.

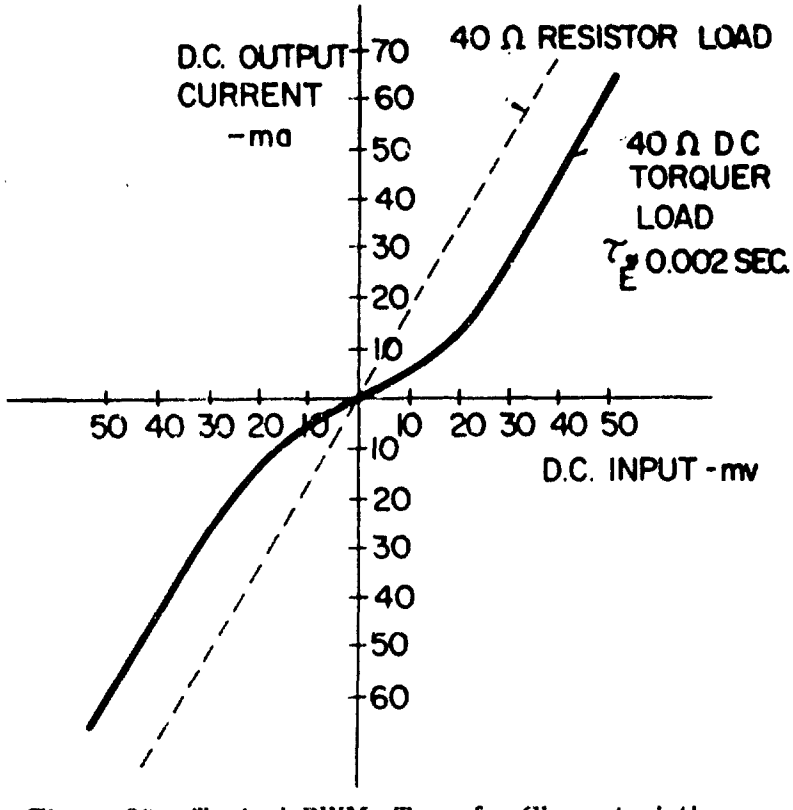

Figure 98. Typical PWM_2 Transfer Characteristics

Threshold in the ON-OFF controller is essentially at the discretion of the designer. A large gain preceding the polarity detector will effectively reduce the dead-band, and thus the threshold. This gain cannot be set arbitrarily high, because of the presence of noise in the error input signal. It can, however, be set high enough to reduce any threshold to an insignificantly small value.

The switching circuitry of ON-OFF VG is identical with that of basic ON-OFF, and so threshold in this section is identical with the single level circuit. Any threshold present in the level detector would also be insignificant. This is due to the fact that the μA-709 level detectors are operated in an open-loop saturating configuration. The open loop gain of this amplifier is about 40,000.

Threshold in the PAM controller will be comparable to that of the DC proportional case, since they operate on similar principles.

Pulse frequency modulation threshold can be made as small as desired by increasing appropriate gains to desired levels.

Delta modulation threshold is essentially zero. There is, however, an additional phenomenon which must be considered.

In both the PFM and delta modulation schemes, the controller output is a pulse train, the frequency of which is dependent upon the error signal. Thus, for small errors, it is possible that the pulse train frequency is not much greater than the cutoff frequency of the torquer, as desired. If such a condition occurs, the torquer response will not be as desired. Although this phenomenon cannot be eliminated, (i.e., there will always exist some non-zero error which will produce a pulse train frequency less than the torquer cutoff) its effect on the torquer response can be minimized by increasing the gain of the voltage to frequency converter in the PFM or by increasing the clock frequency in the delta modulator.

It should be noted that small values of threshold present (See table XVII) in the controller will not appreciably affect the overall operation of the actuator due to the levels of Coulomb friction and stiction present in the torque motor and gear train.

TABLE XVII

CONTROLLER THRESHOLD

Controller Type	Threshold
DC	0.5%
PWM_1	0
PWM_2	0*
ON-OFF	0*
ON-OFF VG	0*
PAM	0.5%
PFM	0*
DELTA MOD	0*

*Threshold is essentially zero with high amplifier gain before transistor bridge driver.

SECTION IX

SYSTEM OPTIMIZATION

9.1 REVIEW OF ACTUATOR ASSEMBLY OPTIMIZATION

In Section VI it was shown that the optimum actuator assembly comprised of a DC torque motor coupled to an epicyclic transmission. This was the motivation for the assumption of a DC motor as the load in the controller evaluation of Section VIII. The optimal actuator characteristics for each CMG size was tabulated in Paragraph 6.3.

9.2 CONTROLLER OPTIMIZATION

The optimization procedure will be carried out in the following paragraphs, and suggestions pertaining to the selection of a controller will be made. Characteristics considered will be power consumption, weight, volume, reliability, threshold, as well as any inherent properties of specific controllers which would contribute favorably or unfavorably to performance in the actuator system.

Since the best choice of torquer appears to be of the DC torquer motor variety, the controller optimization will be performed under the assumption that this type of torquer is to be controlled.

As can be seen from the preliminary evaluation in Section VIII, the weight, volume, reliability, and threshold will be essentially independent of CMG size. Thus, the only parameter remaining to be considered is the power consumption. This quantity varies in a quasi-linear manner, as can be seen in Figure 96. From this graph, one can deduce an equation for power consumption of each controller in the following form.

$$P_t = P_o + P_g H \tag{9-1}$$

where P_t = total power consumption of motor and controller

P_o = constant

P_g = rate of power consumption increase with an increase in CMG size

H = angular momentum of CMG

Based upon the linear, non-intersecting power consumption curves for the eight controller types and on previous discussions, it will be assumed that a controller type which is optimal for one CMG size will be optimal for the other sizes in the 200-2000 ft-lb-sec range as well. Hence, the optimization will be carried out for the 1000 ft-lb-sec case only.

To aid in the optimization procedure, data for the 1000 ft-lb-sec CMG has been condensed into Table XXVIII.

TABLE XXVIII

SUMMARY OF ELECTRONIC CONTROLLER CHARACTERISTICS

Electronic Controller	Average Power (watts)	Reliability Failure Rate (ppmh)	Weight (oz.)	Volume (in^3)	Threshold (%)	Remarks
DC	20.9	6.81	16	15	0.5	
PWM_1	8.77	2.59	2.5	2.5	0	
PWM_2	9.07	2.95	3	3	0	
ON-OFF	8.77	2.40	4	4	0	Undesirable for positi... and torque mode operation
ON-OFF VG	11.6	4.81	5	5	0	Inferior to basic on-off controller
PAM	20.9	3.73	7	8	0.5	
PFM	9.27	4.87	6	7	0	Low repetition rates for low error signals
DELTA MOD	8.02	4.39	6	7	0	Low repetition rates for low error signals

Threshold in all controllers was of the order of magnitude of 0.5%, or less. Based upon a previous discussion of the levels of Coulomb friction and stiction present in the torque motor and gear train, this quantity was deemed insignificant.

In considering the eight controllers, it is best to group them into four separate categories. These are: PWM_1 and PWM_2; ON-OFF and ON-OFF VG; PAM and DC; PFM and delta modulation.

Operation of the PWM_1 and PWM_2 controllers in all modes was considered identical. Reference to Table 9-1 discloses slight advantages in weight, volume, reliability, and power consumption for the PWM_1 type. There appears to be no advantage in using PWM_2 instead of PWM_1 in this system, and hence PWM_2 will be eliminated from further study.

ON-OFF VG controller performance was considered to be inferior to that of its single level counterpart. In addition, the two-level scheme requires greater volume, weight, and power consumption, while possessing a lower reliability. In the preliminary evaluation of ON-OFF control discussed in paragraph 7-3, analysis showed its applicability in rate mode while difficulties presented themselves in the torque or position modes.

When PWM_1 is compared with ON-OFF control essentially equal power consumption and reliability are observed, while PWM_1 possesses advantages in weight and volume. Considering these relations and the applicability of PWM_1 to all modes, it was decided to eliminate ON-OFF controller from further consideration.

A comparison of DC and PAM shows a significant advantage for PAM in the areas of reliability, weight, and volume, while both have identical threshold and power requirements. For use in a system which is purely DC, the DC proportional controller may offer more linearity and less decoupling problems than PAM. However, where pulsing is not undesirable, advantages of PAM become significant, making this scheme more attractive than the DC proportional controller.

Both PFM and delta modulation controllers possess the property that the repetition rate is a function of the error signal, which was deemed undesirable at very low error signal levels. An examination of Table XXVIII reveals a power consumption and reliability advantage for the delta modulation configuration. Delta modulation lends itself quite readily to systems which are basically digital in nature. In situations where a digital computer is the master controller of attitude control systems, the need for the clock pulse generator and modulator sections of the delta modulation scheme is eliminated since the signals required for the various flip-flop circuitry could be generated within the computer itself.

As a result of the preceding comparisons, one is led to the result that for systems which are digital in nature, delta modulation seems to be the optimal controller type, while PWM_1 is most desirable in continuous, or analog systems. Both of these controllers have relatively high efficiency, small size, high reliability and applicability to all modes of operation.

9.3 ACTUATOR CONTROLLER OPTIMIZATION

Based upon the conclusions of paragraph 9.2 and the actuator selection of paragraph 6.3, the complete actuator system can be obtained. This system, for the 1000 ft-lb-sec CMG, would consist of a single channel pulse width modulator, an Inland T-5730D DC torquer motor, a 60:1 epicyclic transmission, and an Inland tachometer generator, type TG-2801A.

To obtain reliability data on the complete CMG actuator assembly, an analysis was performed for the 175 ft-lb assembly while in an operational environment. Reliability was calculated for both two and twelve month mission time, and are shown in Table XXIX.

TABLE XXIX

CMG ACTUATOR RELIABILITY

CMG Actuator Configuration	Reliability	
	2 months	12 months
Complete actuator assembly	0.9956	0.9741
Single Channel Pulse Width Modulator Controller	0.9962	0.9775
Composite Actuator Controller	0.9919	0.9523

SECTION X

CONCEPTUAL DESIGN

10.1 DESCRIPTION

Figure 99 illustrates a conceptual design of the inner gimbal actuator assembly. The basic components are:

a. Inland Motor Corp. Torque Motor No. T-5730D

b. Inland Motor Corp. Tachometer Generator T.G. No. 2801A

c. A 60:1 Ratio Epicyclic Transmission

The motor and tachometer specifications are given in Tables 32 and 34, respectively. The transmission particulars are given in paragraphs 10.2 and 10.3. The basic control moment gyroscope size used for this design was the 1000 ft-lb-sec unit.

The inner gimbal was selected for this conceptual design, since it has less space availability than the outer gimbal. Therefore, an interchangeable actuator assembly that will fit the inner gimbal can also be used on the outer gimbal.

Each actuator assembly is self-contained and may be replaced as a plug-in module merely by disconnecting the bayonet-type power-cable plug and the mounting capscrews.

Provision has been made in the design to utilize the same type of porous lubricant reservoir within the transmission output shaft and within the motor shaft bore. Thus, adequate lubrication of the gear meshes is assured.

An expandable seal and seal plate are provided between the transmission housing and the gimbal drive plate to prevent loss of lubricant from the actuator and transmission housing. The remainder of the housing assembly interfaces are sealed with "O" rings.

Figure 100 is an outline drawing showing the basic envelope dimensions of the actuator and all the interface dimensions for installation in a CMG.

The total estimated weight of the Actuator Assembly is 23 pounds and the volume of its envelope is approximately 380 cubic inches.

10.2 TRANSMISSION DESIGN

The design of the epicyclic transmission was based on the considerations developed in paragraph 6.2, Transmission Optimization. The minimum allowable pitch diameter D_1 for the fixed interval gear can be obtained from equation 6.21:

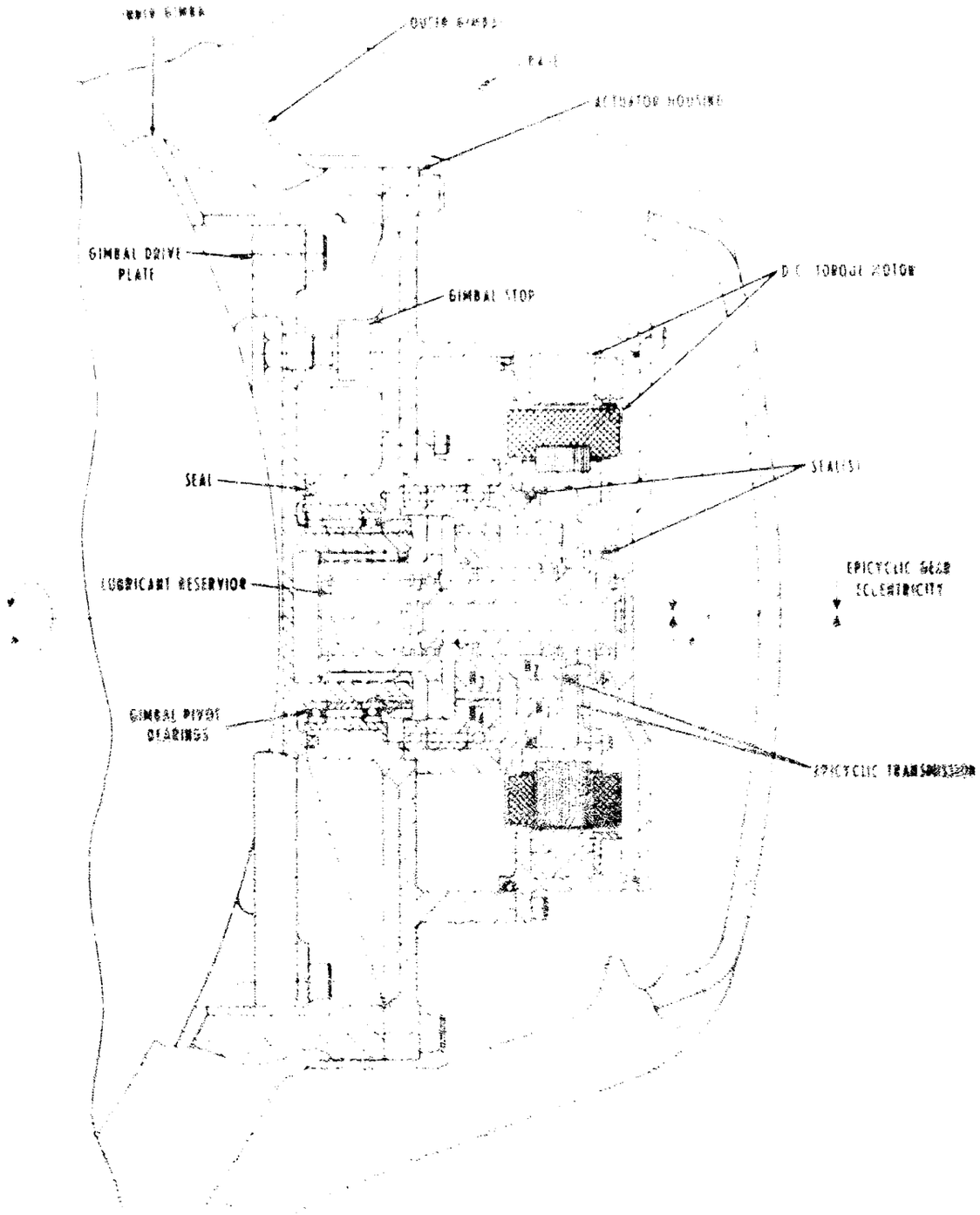

Figure 39. Layout for Gimbal Actuator Assembly

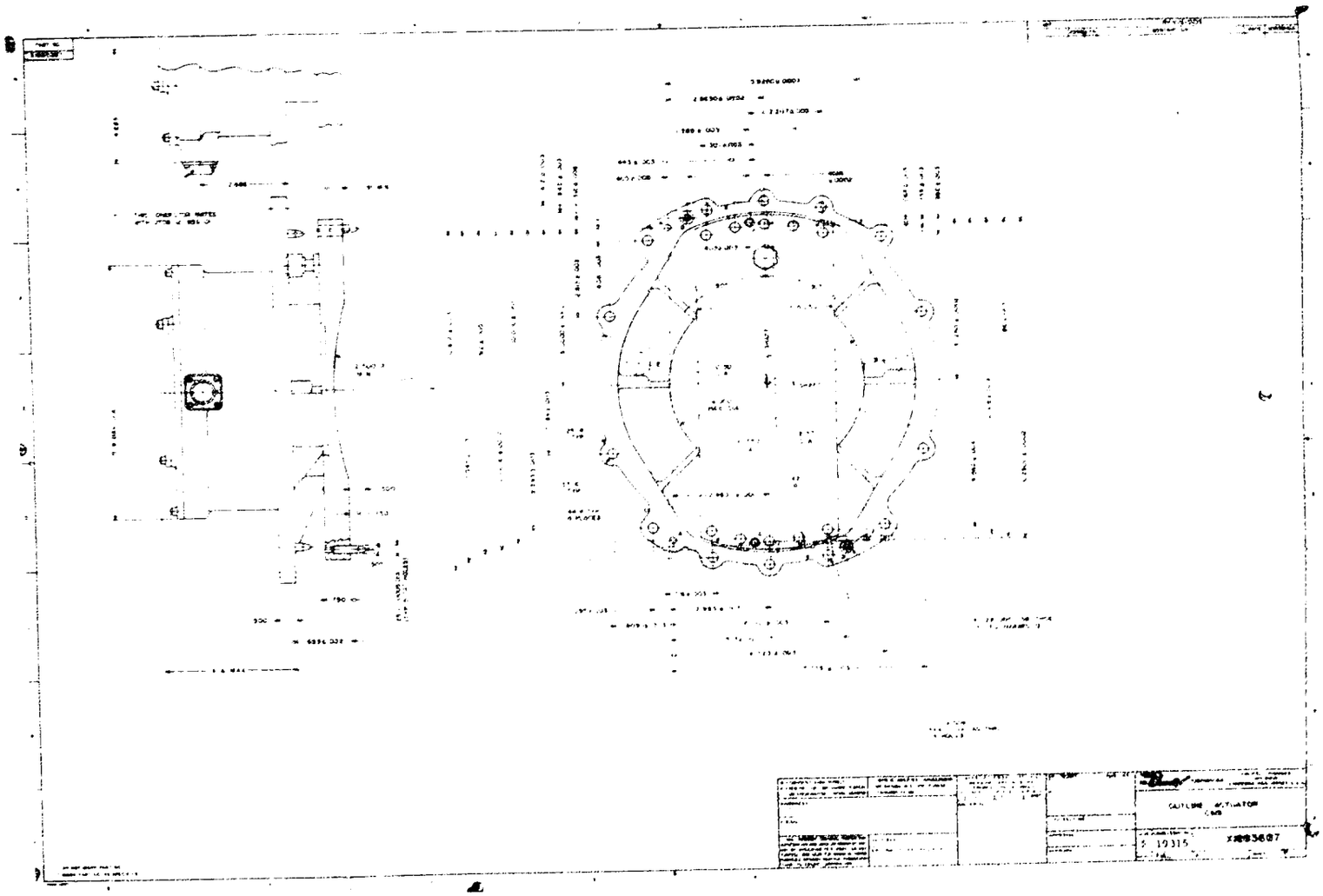

Figure 100. Actuator Outline Drawing

$$N_1 = 1.73 \frac{P_d}{h^{1/3}} \tag{6.21}$$

or

$$D_1 = \frac{N_1}{P_d} = \frac{1.73}{h^{1/3}} \tag{10.1}$$

D_1 was selected to be 2.875 inches. This dimension allows a substantial part of the transmission to be packaged within the I.D. of the selected torquer motor, as shown in figure 38, thereby decreasing the overall volume of the actuator. From equation (10.1) h was found to be 0.225. By definition the face width f = hD_1 = 0.645 inches. This was considered to be a satisfactory gear width for maintaining gear tooth face accuracy. The diametrical pitch was selected to be 32 for all gears in the transmission. Thus $N_1 = 32D_1 = 92$ teeth. To allow clearance between the epicyclic pinion gear N_2 and N_1 the ratio $\frac{N_2}{N_1}$ was selected to be 0.825. N_2 is then 0.825 N_1 or 76 teeth. Since $N_1 = 92$, the curves plotted in Figure 47 apply. For $\frac{N_2}{N_1} = 0.825$ and a ratio of 60:1, $\frac{N_4}{N_1}$ is found to be 1.09 and the theoretical efficiency 97.2%. Thus $N_4 = 1.09N_1 = 100$ teeth. N_3 is found from Equation 6-14:

$$\begin{aligned} N_3 &= N_4 + N_2 - N_1 \\ &= 100 + 76 - 92 \\ &= 84 \text{ teeth} \end{aligned} \tag{6-14}$$

The above data is summarized in Table XXX.

10.3 TRANSMISSION AND GIMBAL BEARINGS

The analysis of bearing loads and the procedure used for the selection of the transmission and gimbal bearings is described in Appendix C. Table XXXI lists all the bearings selected for the 1000 ft-lb-sec CMG actuator.

TABLE XXX

EPICYCLIC TRANSMISSION GEARS

Gear	Gear Type	Diametrical Pitch	Pitch Diameter (inches)	No. of Teeth	Gear Face Width (inches)
N_1	Internal 20° PA full involute modified tooth thickness	32	2.8750	92	0.645
N_2	External 20° PA full involute modified addendum	32	2.3750	76	0.925
N_3	External 20° PA full involute modified addendum	32	2.6250	84	0.750
N_4	Internal 20° PA full involute modified tooth thickness	32	3.1250	100	0.530

TABLE XXXI

TRANSMISSION AND GIMBAL BEARINGS

Bearing Description	Manufacturer and Catalog No.
B_1	New Departure ND 3LL04, or equivalent
B_2	New Departure ND 3LL08, or equivalent
B_3	New Departure ND 3LL08, or equivalent
B_4	New Departure ND 3LL04, or equivalent
B_5	Kaydon KA40CP, or equivalent
B_6	Kaydon KA40CP, or equivalent

SECTION XI

CONCLUSIONS AND RECOMMENDATIONS

11.1 GIMBAL

The optimal design for double-gimbal CMG actuators for the range of 35 to 350 ft-lb (200 to 2000 ft-lb-sec) is a DC torquer with an epicyclic transmission. The design was selected mainly on the basis of minimum power consumption, size and weight.

A preliminary design for the 175 ft-lb actuator weighs 23 lbs, including structure and mounting plate for attachment to the gimbals. Peak power consumption of the actuator is less than 45 watts. This design meets all performance requirements listed in Section I with the exception of threshold and reliability. The threshold of the actuator is almost completely the result of the DC torquer's brush-commutator friction. Whereas the required threshold is specified as 0.5% of maximum torque, the threshold for the actuators using DC torquers are expected to be from 2% to 4% (depending upon size) of maximum output torque. The reliability of the actuator assembly was determined as 0.9741 for one year and 0.9956 for two months of operation; this compares with the requirement of 0.99 for one year of operation.

When combined with a pulse width modulator (single channel type) controller, the one year and two month composite operational reliabilities are .9523 and .9919, respectively.

11.2 TORQUERS

A broad preliminary study indicated that hydraulic and pneumatic actuators are not adequate for the CMG actuator application because of high power consumption, thereby being penalized with a high weight penalty for long missions. This is directly linked to the losses in converting electrical power to hydraulic or pneumatic power. Other problems are the possibility of leakage flows and the requirement for development of a "fluidic slip ring" for furnishing power to the inner gimbal.

With regard to electrical actuators, AC servo motors were found to have inadequate frequency response characteristics and required transmissions with extremely high gear ratios to obtain required torques. Stepping motors were found to be deficient in both size and weight.

The other category of electrical actuators studied were of the DC type: the DC torque motor and several types of brushless DC torquers -- the basic brushless DC motor, the electromechanical DYNAVECTOR and the RESPONSYN actuator. The DC torque motor was selected for the CMG actuator since it is more efficient than all other actuators for a long term mission. It also rates well in weight and size relative to all other torquers.

The DYNAVECTOR and RESPONSYN actuators indicate some weight advantages for the larger CMG units, and the brushless DC torquer has a lower threshold and a potentially higher reliability. All of these brushless torquers, however, are not fully accepted as state-of-the-art because of complexities involved in high speed electronic switching of inductive loads. The DC brushless torquer motor is the closest to the state-of-the-art, but has the disadvantages of additional electronic complexity and high ripple torques.

11.3 TRANSMISSIONS

The epicyclic transmission was selected because of its very low weight, volume and reflected moment-of-inertia for a wide range of gear ratios. It also is fairly good relative to backlash and friction.

The compound planetary was selected as an excellent second choice to the epicyclic transmission. It was comparable in all aspects, except for its slightly higher weight.

Simple planetary transmissions are completely unacceptable because of severe dimensional limitations with gear ratios higher than 10:1.

Spur gear transmissions are comparatively large in size, and they also weigh more than epicyclic transmissions for the larger CMG's. They are competitive, however, for low ratios and small CMG's.

Disadvantages of the harmonic drive transmission are relatively low efficiency and high friction. It also has the characteristic or reflecting large moments-of-inertia back to the torquer thereby affecting the response of the actuator.

11.4 DUAL ACTUATOR CONTROL

The study indicated that the use of two actuators per gimbal, one a high level stall torque device and the other a low level rate device, does not offer any particular significant advantages. Actuators such as that recommended in Paragraph 11.1 have the capability of meeting the overall torque-speed requirement envelope. The use of a stall torque device and a rate device would only increase the overall actuator power and weight, and would then have difficulty in meeting response requirements. The only justification for using a low rate device in addition to the torquers mentioned in this report would be in meeting threshold requirements or in providing a method of coarse-fine rate control. The penalties involved in implementing this requirement are the additional hardware and the power requirement and weight penalties involved.

11.5 CONTROLLERS

Electronic controllers were the only type completely studied, since all fluid actuators were eliminated early in the torquer study. Of the eight electronic controllers studied, a single channel pulse width modulation controller was selected as optimal for

the whole range of CMG actuators (35 to 350 ft-lb). This was based on its low power consumption, light weight, small size, reliability and zero threshold.

An excellent alternate controller for certain applications is delta modulation. If a digital computer is used for resolving torque commands for one of the multi-unit double gimbal CMG configurations, the delta modulation signal is easily derived as an output of the computer. Under this condition the delta modulation controller would need no clock or delta modulation circuitry, thereby making it an excellent second choice on the basis of power consumption weight, size reliability and essentially zero threshold.

Other controllers which would show to advantage for certain CMG system configurations are dual channel pulse width modulation, DC proportional and ON-OFF. The double channel pulse width modulator is only slightly larger and heavier and less reliable than the optimal single channel type. In certain small low torque applications, the double channel pulse width modulator consumes less power; it has a finite threshold, but this is usually lower than the torque stiction level.

The DC porportional controller is larger, heavier, less reliable and consumes more power than any of the eight controllers. These disadvantages may be offset in an all DC system.

For example, in the pulse width modulation schemes a carrier frequency power supply is also needed for the complete servo amplifier and other items, such as for excitation of rotational sensors.

The ON-OFF controller offers some advantages in power consumption, reliability, threshold, weight and size. The CMG loop would go into limit cycle, however, if ON-OFF were used for either torque or position modes.

ON-OFF variable gain, pulse amplitude modulation and pulse frequency modulation have no practical application to controlling CMG actuators since they offer no improvement in performance, and yet are more complex than related controllers (i.e., ON-OFF, DC proportional and delta modulation, respectively.)

11.6 RECOMMENDATIONS

It is recommended that:

(a) Actuators for double-gimbal CMG units use DC torquers and epicyclic transmissions.

(b) Brushless DC torquers be reconsidered at a future date, since these devices indicate excellent promise but, at best, currently are "near state-of-the-art".

(c) Single channel pulse width modulation be used as an electronic controller of the CMG actuator.

(d) Delta modulation be considered as a controller in CMG system configurations where a digital computer is necessary to resolve attitude errors into individual actuator commands.

APPENDIX A

ACTUATOR SPECIFICATIONS

A.1 INTRODUCTION

At present, the guiding specifications for the gimbal torquers are determined from "Specifications for Control Moment Gyroscopes," Specification L-7298 by NASA Langley Research Center, 2 August 1965, and requirements presented in RFP Nr. (G) 20949 by Systems Engineering Group of Wright-Patterson Air Force Base, Dayton, Ohio, 24 August 1965.

A.2 GENERAL REQUIREMENTS

Inner and outer gimbal torquers should be identical. The configuration should be similar to the present CMG configuration, having a diameter to length ratio greater than one. All concepts considered must be within one year of the state-of-the-art.

A.3 TORQUER SPEED REQUIREMENTS

A.3.1 Speed

Speed range shall be from 0.175×10^{-3} to 0.175 rad/sec for all CMG sizes. The allowable variation in speed is to be ± 3 percent of the command speed, after steady-state value is reached.

A.3.2 Torque

The maximum stall torque capability must be H times 0.175 rad/sec where H is the angular momentum of the CMG. The actuator torque capability, T_{em}, at any actuator steady-state speed must be at least H times (0.175 rad/sec) minus M_m times the actuator speed.

A.4 RESPONSE

A.4.1 Rate Response Requirements

A.4.1.1 The rate transfer function (output speed response to input speed command) when characterized by a single-order lag shall have a time constant of 0.05 second or less.

A.4.1.2 For actuators with complex rate transfer functions, the response shall be within ± 3 percent of the final value within the same time interval that a single-order system with a time constant of 0.05 second reaches 97 percent of its final value. The settling frequency shall be less than 100 cps.

A.4.2 Torque Response Requirements

A.4.2.1 The torque transfer function (output torque response to the input torque command) when characterized by a single-order lag shall have a maximum time constant of 0.5 second.

A.4.2.2 For actuators with complex torque transfer functions, the response shall be within ± 3 percent of the final value within the same time interval that a single-order system with a time constant of 0.5 second reaches 97 percent of its final value. The settling frequency shall be less than 100 cps.

A.5 LOAD DEFINITION

A.5.1 Gimbal Rotation

The inner gimbal rotation capability shall be ± 80 degrees. The outer gimbal rotation capability shall be ± 360 degrees.

A.5.2 Inertia

The load is defined as inertia only and $J_L = m(\log H) + b$ where:

$m = 2.35$ ft-lb-sec^2

$b = -5.06$ ft-lb-sec^2

H = Angular momentum of the CMG

A.5.3 Friction

Levels allowable to be established.

A.5.4 CMG Cross Coupling

Cross-coupling effects are to be neglected in this phase.

A.5.5 Physical Size

A.5.5.1 Dimensions must be consistent with present diameter-to-length ratios of one or greater, with emphasis on minimizing overall size.

A.5.5.2 Guideline for Gear Train Volume Definition

$$V = m \log H + b$$

$$m = 139 \text{ in}^3$$

$$b = 649 \text{ in}^3$$

H = Numerical value of angular momentum of CMG.

The total volume could feasibly be duplicated on both ends of the axis.

A.5.6 Weight

Weight should be minimized, consistent with weight-to-power tradeoff, such that the actuator weight, W_A, times the tradeoff value of 1 watt/pound, plus the average power, P_A, is a minimum.

A.6 ENVIRONMENT

A.6.1 Ambient temperatures of 70°F to 120°F

A.6.2 Pressures of 10^{-11} to 1.0 atm.

A.6.3 Radiation - negligible

A.6.4 Acceleration of 0 to 1 g (operational)

A.6.5 Heat due to actuator losses must be dissipated by conduction and radiation.

A.7 MISSION TIME AND RELIABILITY

The gimbal torquers shall be capable of operating continuously without maintenance for at least one year under the load and environmental conditions specified. Overall operating life shall not be less than 5 years.

A.8 EXPECTED LOAD DISTRIBUTION

Steady-state torque and speed profiles are identical and are as follows: 1 percent of maximum, 30 percent at one-half of maximum, and 69 percent at one-fourth of maximum. These values are used to determine average power required of potential gimbal torquers.

APPENDIX B

B.1 INTRODUCTION

To select a feedback transducer for a position or rate reference of the CMG, the following design requirements for the Gimbal Actuator System must be met:

1) Maximum Regulated Speed - 0.175 rad/sec

2) Minimum Regulated Speed - 0.000175 rad/sec

3) Threshold - $.05^{o}$ and $.01^{o}$/sec

4) Resolution - $\pm .05^{o}$ and $.01^{o}$/sec

5) Command Range - .005V to 5V

6) Linearity - $\pm$ 5%

7) Range - $\pm 80^{o}$ (Inner Gimbal),
- Unlimited (Outer Gimbal)

Within each of the two major categories, various types of transducers will be surveyed as indicated in Table XXXII.

TABLE XXXII

ANGULAR DISPLACEMENT AND VELOCITY TRANSDUCERS

Angular Displacement	Angular Velocity
Electromagnetic 1. Synchro 2. Resolver 3. Induction Potentiometer 4. Inductosyn	Tachometric 1. DC Tachometer 2. AC Induction Generator
Resistive 1. Potentiometer	Gyroscopic 1. Rate Gyro
Shaft Encoders 1. Brush Type 2. Optical 3. Electrostatic	

The angular displacement transducers will be used in the position mode as a feedback element. They may also be used for aligning and monitoring the positions of the different CMG's used in controlling the vehicle motion. Since all the angular displacement transducers mentioned in Table XXXII will meet CMG specifications, this report will not try to select a specific angular displacement transducer. Instead, a qualitative description of operation and practical applications will be discussed.

The more stringent requirements placed on the rate transducer limit the available types of rate transducers that can meet the CMG specifications. Since the implications are that the optimum mode of operation may be the rate mode, a detail discussion and selection of the optimum rate transducer will be covered in this Appendix.

B.2 ANGULAR DISPLACEMENT TRANSDUCERS

B.2.1 ELECTROMAGNETIC ANGULAR DISPLACEMENT TRANSDUCERS

B.2.1.1 Synchro

The term synchro covers a range of AC electromechanical devices which are used in data transmission and computing systems. For use in the CMG Program a synchro control transmitter would be applicable, this device has an electrical output which represents some function of the angular displacement of its shaft. Synchro devices are basically variable transformers. As the rotor of a synchro rotates it couples and decouples one or more windings of the stator. The output of the control transmitter varies as the sine of the input angle.

B.2.1.2 Resolver

Resolvers are precision induction type devices whose outputs vary as the sine or cosine of its rotor position. (See figure 101).

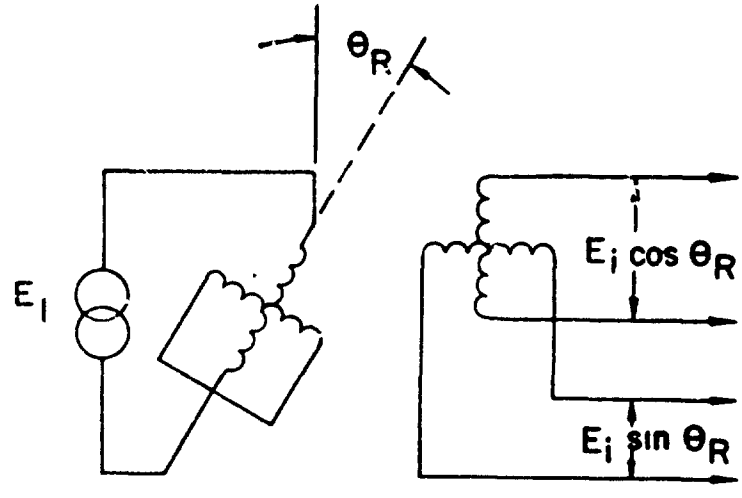

Figure 101. Schematic - Resolver with Single Phase Input

This device can be used not only for position feedback but also for coordinate transformation, resolution into components, and conversion from rectangular to polar coordinates. The output of this unit can be readily transformed into digital information and may be applied for proper alignment information to the computer when more than one CMG is used to control the vehicle. Another advantage of this type component is that one and two speed systems are readily incorporated into the CMG gimbal pivot assemblies.

B.2.1.3 Induction Potentiometer

Induction potentiometer or linear synchro transformer, provides accurate linear indication of shaft rotation about a reference position in the form of a polarized voltage whose magnitude is proportional to angular displacement and whose phase relation indicates direction of shaft rotation. (See figure 102). The principal difference between an induction potentiometer and a resolver or synchro is that its output voltage varies directly as the angle and not as the sine of that angle.

The induction potentiometers are analogous to resistance potentiometers, but since they are induction type components they have less restraining forces acting upon their rotors, and are therefore capable of providing better resolution. Since these devices do not require sliders such as those used in resistance types, circuit interruptions are eliminated, no wear occurs. As a result of no rubbing parts, accuracy is continuously maintained at the original level throughout the operational life of these type components.

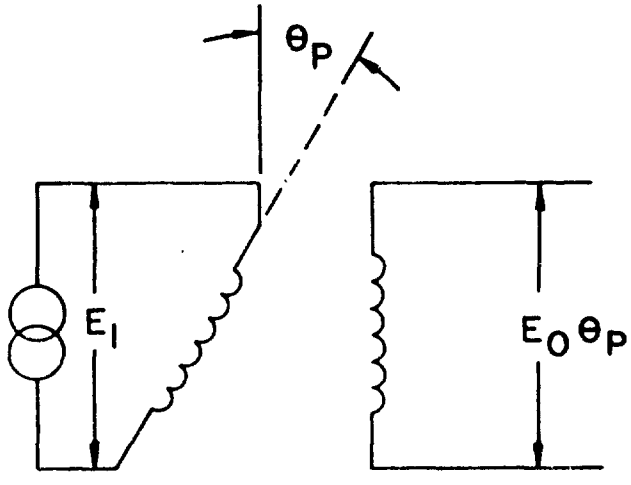

Figure 102. Schematic - Induction Potentiometer

B.2.1.4 Inductosyn

Where precise positioning accuracies greater than those obtainable with multispeed transmission systems are required, the inductosyn may be considered. With this device accuracies of 5 seconds of arc and sensitivities of 0.25 seconds of arc can be achieved. Since the CMG requirements are far less than the inductosyns characteristics and can be implemented with simpler more reliable components without the auxiliary equipment needed for the inductosyn, no further explanation of inductosyn operating principles will be given in this report.

B.2.2 RESISTANCE POTENTIOMETER

Standard type wire would linear potentiometer are devices that develop an electrical output signal proportional to the product of an input electrical signal and shaft angle. There are many available resistance potentiometers to meet CMG requirements for readout of gimbal position. The disadvantages of these units are discussed in Paragraph B.2.1.3 on induction potentiometers.

B.2.3 SHAFT ENCODERS

Shaft encoders encompass angular position transducers whose outputs are in digital form. The main types of shaft encoder are brush type, optical and electrostatic. If it is found desirable to readout CMG gimbal positions directly in digital form, these type transducers may be investigated further. The two-speed resolver previously described, when used with a small electronic digitizing module, may actually be a more economical and reliable method of obtaining a digital readout.

B.3 DISCUSSION OF DC AND AC RATE SENSORS

B.3.1 TACHOMETRIC ANGULAR VELOCITY TRANSDUCERS

B.3.1.1 DC Rate Generator

Most frequently used DC rate generator is the permanent magnet type where the permanent magnet in the stator sets up the DC field and therefore requires no excitation voltage. A wound armature with a commutator can be used to derive the voltage output in conventional manner. To minimize variations in output with position, the commutator is designed with a large number of segments. Because its output is direct voltage, it requires brushes operating on a commutator. The friction load from these brushes is a disadvantage to the system.

A summary of the advantages and disadvantages follows:

Advantages

1) Constant output unaffected by line voltages and temperature.

2) High dynamic range

3) Low residual output

Disadvantages

1) High frictional torque

2) High inertia armature

3) Life limited by brush wear

4) DC output requires modulator where a carrier type servo amplifier is employed.

5) Has ripple voltage superimposed on the output due to commutation.

B.3.1.2 AC Rate Generator

The AC rate generator resembles a two phase AC motor. An AC reference voltage is applied to one phase of the tachometer generator, and a voltage of reference frequency and amplitude proportional to shaft speed is generated on the other phase. Two typical types of AC rate generators exist: the induction generator, using a squirrel cage rotor, and the drag-cup generator, using a light conducting cup as rotor. Since the rate generator is often coupled directly to the servo motor shaft and adds directly to that inertia, the rate generator inertia should be kept minimal. For this reason the dragcup unit finds widest application.

The two phase drag cup type of tachometer consists of a stator with two windings in space quadrature. Inside the stator is a cup-shaped aluminum or copper rotor. This is attached to a shaft which extends through a bearing in the end of the housing. One stator winding is excited from an AC reference supply and the other acts as the output winding. With the cup stationary, no voltage is induced in the output winding due to their physical arrangement. When the cup is rotated, the eddy currents which are induced in it have an additional component due to rotation. This current generates an AC magnetic flux linking the secondary winding, resulting in an output voltage proportional to the rotor speed.

Advantages

1) Low driving torque required

2) Low inertia rotor

3) Long life

4) AC output convenient for all carrier type servos, no modulator required.

Disadvantages

1) Limited

2) High residual output

3) Variation in residual output with shaft position leads to position effect, which may have adverse stability effects on system.

4) Output varies with excitation voltage.

5) Output varies with cup temperature. 5% sensitivity drift in output may occur in the first hour of operation as a result of unit temperature rising to its steady state value.

6) Output is not in-phase with excitation voltage.

B.3.1.3 Selection of Optimum Type Tachometer Generator Sensor for CMG Application

Where a high performance velocity servo is required, as is the case for CMG application, the DC tachometers wide linear operating range of speeds would make it preferable to the drag cup AC tachometer since the CMG loops are to have a dynamic range of 1000 to 1 and the command voltages are to be in the order of .005V to 5 volts. The inherent residual output of the AC tachometer would adversely affect the system.

The directly driven DC tachometer may be used for the CMG feedback sensor. Since the actuator used will be a conventional DC or brushless DC torquer, these DC tachometers are particularly suited for the system, due to size, weight, mounting, packaging and very fine resolution requirements. For CMG applications a combination unit consisting of a DC torque motor and DC tachometer generator in a common housing is readily available to reduce space, servicing and assembly requirements.

The advantages of the directly driven DC tachometer generator are as follows:

1) High coupling stiffness - the tachometer generator is directly coupled to the motor thereby eliminating backlash errors and eccentricities. It offers a distinct advantage in precision rate systems.

2) High voltage gradient

3) Fast response

4) High resolution

5) High accuracy at low speed

6) Compact, adaptable design

7) High linearity

A DC tachometer for the rate reference of the CMG must meet the design requirements listed in paragraph B.1. The minimum tachometer-generator sensitivity K_G which is the voltage output per rad/sec, of the chosen generator must fall between the lower and upper limit established by the system requirements. The lower limit is governed by the relationship of error signal to required accuracy and is obtained from formula below:

$$K_G = \frac{\text{MINIMUM ERROR SIGNAL}}{\text{MINIMUM ALLOWABLE ERROR}} \qquad \text{(B-1)}$$

Each tachometer generator has a maximum voltage rating which must not be exceeded without danger of damaging the unit. A given generator must not be applied where the shaft speed exceeds that which produces the maximum rated voltage.

DC tachometer generators, because of commutation, have a voltage ripple superimposed on the output. Both magnitude and frequency of this voltage vary with shaft speed. The ripple voltage is listed, on manufacturers data sheets, in terms of percent deviation from average. The ripple frequency is listed in terms of cycles/rev. If the output-ripple approaches or exceeds the speed-regulation tolerance, the variations in the feedback voltage are interpreted by the servo as commands, and proportional speed variations may occur. One solution would be to select another generator with a substantially lower ripple voltage. However, the ripple frequency may be high enough so that the servo connot follow it.

To meet requirements of command voltages of 0.005 volts to 5 volts for 0.000175 rad/sec to 0.175 rad/sec speed regulation, the value of the feedback gain is set at that value which at maximum rate of the motor (α_M Max) the feedback rate would be equal to the maximum input (5 volts).

$$\frac{\alpha \text{ Max}}{\text{Gear Ratio}} = \text{Max. Regulated Speed} \qquad \text{(B-2)}$$

With a gear ratio of 60,

$$\dot{\theta}_M \text{ Max} = (.175 \frac{\text{rad}}{\text{sec}}) 60 = 10.5 \frac{\text{rad}}{\text{sec}} \tag{B-3}$$

$$e_X \text{ Max} - \dot{\theta}_M \text{ Max} \quad K_{FB} = 0 \tag{B-4}$$

$$K_{FB} = 0.476 \frac{\text{volts}}{\text{rad/sec}}$$

To meet the required feedback Inland DC tachometer type TG 2801 is selected. This tachometer generator has a voltage sensitivity, K_G, of 1 $\frac{\text{volt}}{\text{rad/sec}}$. Therefore, an attenuation gain of 0.476 V/V is required in the feedback loop.

Since the command voltage range was used as the criteria for selecting the sensitivity of the feedback transducer, the minimum error signal according to equation (B-1) that the system must respond to is .25 mv for 5% speed regulation.

Therefore, the noise at the input of the system must be kept under 10% of this value, or 25 uv. It should be noted that if higher command voltages are used, noise restrictions would not be as stringent.

Tachometer Generator Inland Model TG 2801 has the following characteristics tabulated in Table XXXIII.

TABLE XXXIII

TACHOMETER GENERATOR CHARACTERISTICS

Max. Voltage Sensitivity, K_G	1.0 $\frac{\text{volts}}{\text{rad/sec}}$
Linearity	1% of Local Value
Friction Torque	2.0 oz-in.
Ripple Voltage	4% Avg. to peak
Ripple Frequency	71 $\frac{\text{cycles}}{\text{rev}}$
Rotor Inertia	.028 oz-in-sec^2
Outside Diameter	3.38 in.

TABLE XXXIII (Continued)

TACHOMETER GENERATOR CHARACTERISTICS

Max. Voltage Sensitivity, K_G	1.0 $\frac{\text{volts}}{\text{rad/sec}}$
Inside Diameter	2.25 in.
Thickness	.72 in.
Weight	13.5 oz
Max. Operating Speed	59 rad/sec
Life*	3×10^6 rev.

*The life of this tachometer would be 2 years, if the system was required to run at maximum speed continuously.

B.4 GYROSCOPIC ANGULAR VELOCITY TRANSDUCER

B.4.1 DESCRIPTION OF A RATE GYRO

The rate gyro is a one-degree-of-freedom system with an elastic restraint and viscous damper about the free, or output, axis. If the gyro case is rotated about the input axis with an angular rate Ω_i, then a torque T, which equals $H\Omega_i$, is developed that tends to rotate the gyro through an angle, θ, about the output axis. This output angle is transformed to a voltage proportional to the input angular velocity, Ω_i, by means of a pick-off transducer. The functional diagram of the rate gyro is given in figure 103.

The unit tends to rotate so as to align its angular-momentum vector H with the input angular-velocity vector Ω_i. The torque developed is opposed by the inertia of the system about the output axis, the spring restraint K and the viscous damping F. If the moment of inertia about the input axis is denoted by J and the angular displacement by θ, the equation for the dynamic balance of the system is given by:

$$H\Omega_i = J\frac{d^2\theta}{dt^2} + F\frac{d\theta}{dt} + K\theta \qquad \text{(B-5)}$$

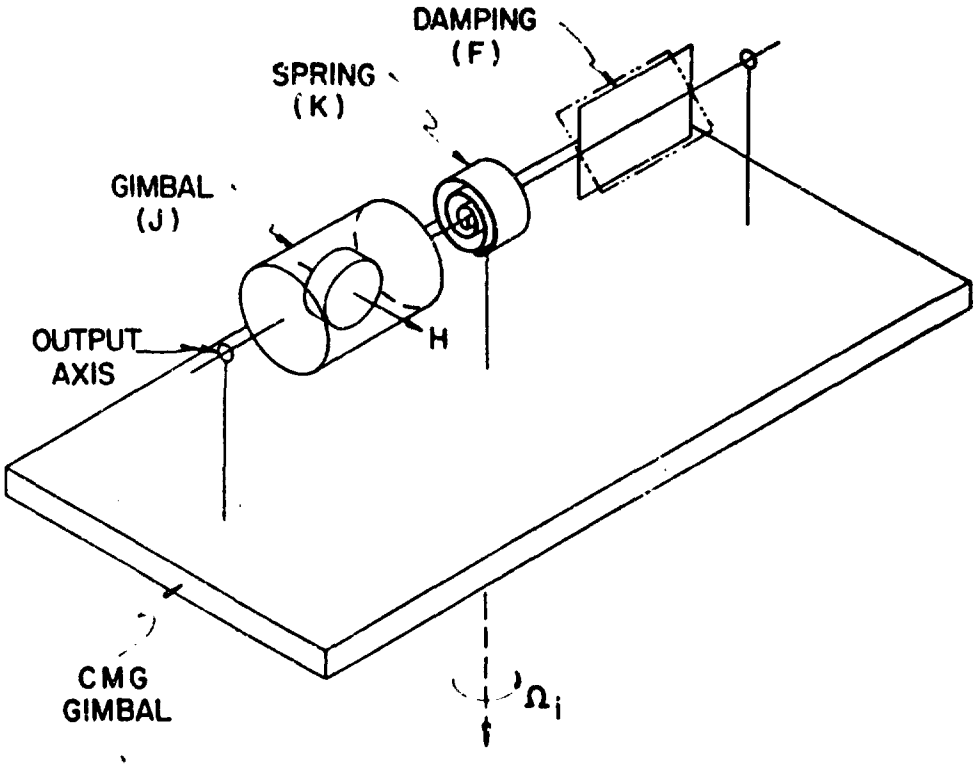

Figure 103. Function Diagram Rate Gyro

The transfer function between the output angle θ and the input angular velocity is therefore given by:

$$\frac{\theta}{\Omega_i} = \frac{H}{JS^2 + FS + K} \tag{B-6}$$

The steady-state deflection about the output axis is given by

$$\theta_{SS} = \frac{H}{K}\Omega_i \cdot \tag{B-7}$$

The deflection θ_{SS} introduces an error into the system because of misalignment of the H vector, and therefore the input, Ω_i, is no longer in line with the input axis of the gyro. In order to minimize this effect the angular rotation about the output axis must be restrained to small values. This is done by increasing the spring constant, K. As the spring constant is increased the threshold of the unit deteriorates. Also, the small angle requirement requires the pick-off transducer be sensitive, which in turn gives rise to problems of drift and noise.

The main advantage of the rate gyro for the CMG application is that it senses an inertial rate. This means that it senses the rate of the gimbal with respect to inertial space. This characteristic would provide decoupling, inherent in tachometer transducers, of the gimbals and the vehicle.

The limitations of the rate gyro are mainly threshold and life considerations. Other characteristics that must be traded-off are power, weight, size, and electronics required to amplify and transform the pick-off output, which is an AC signal, to be compatible with system input commands.

B.4.2 RATE GYRO SELECTION FOR CMG ACTUATOR SYSTEM

The rate gyros selected for comparison purposes are a fluid filled unit selected from Kearfotts C70 2021 and Bendix's non-floated magnetically damped rate gyro. The characteristics of these two instruments are tabulated in Table XXXIV. The main difference is in the resolution and threshold characteristics. The floated unit has a resolution and threshold of .005°/sec where the non-floated unit's threshold and resolution is .015°/sec.

The resolution and threshold requirements for the CMG system is listed as .01°/sec. If this requirement could be opened the non-floated unit could be used. This unit is approximately half the cost of the floated unit.

B.5 SUMMARY

For the CMG program the direct coupled DC tachometer generator was selected over the AC tachometer generator due to its wide linear operating range, temperature stability, low residual output, long life, and compatibility with the selected actuator.

The main advantages of the rate gyro is that it provides decoupling of vehicle rates with respect to the feedback transducer signals. The rate gyro has a life limitation of 1000 hours. This transducer requires warm up time, and considerable power. Also, electronics would be required to convert the AC pickoff voltage to DC to be compatible with input commands to the CMG. Implementation of a rate gyro into the CMG system where more than one CMG is used requires a more complete analysis of the overall system and is considered beyond the scope of the actuator study program.

Most of the angular position transducers mentioned in this section will meet CMG actuator feedback requirements. The main factor in selecting this component is one of system interface.

TABLE XXXIV

COMPARISON OF FLOATED VS. NON-FLOATED RATE GYRO

Rate Gyro Data	Kearfotts Fluid Filled C70 20 21 Series Rate Gyro	Bendix Magnetically Damped Rate Gyro
Performance		
Max Rate	20^{o}/sec	20^{o}/sec
Resolution and Threshold	0.005^{o}/sec	0.015^{o}/sec
Linearity	0.5% of Full-Scale to Half-Scale 2.0% of Full-Scale to Full-Scale	0.5% Full-Scale to Half-Scale 2.0% Full-Scale to Full-Scale
Sensitivity	$0.350 \frac{\text{volts}}{o/\text{sec}}$	$0.280 \frac{\text{volts}}{o/\text{sec}}$
Motor Requirements		
Excitation	26 volts, 400 cps	26 volts, 400 cps
Starting Power	3.5 watts	3.5 watts
Running Power	3.0 watts	3.0 watts
AC Pickoff		
Excitation	26 volts, 400 cps	6.3 volts, 175 ma, 400 cps or 26 volts, 175 ma, 400 cps
Input Power	0.5 watt	---
Null Voltage	20 mv	0.4% of Full Scale
General		
Weight	4.5 ounces	6 ounces
Size	1 inch Dia. x 2 inches long	1 inch Dia. x 2-11/16 inches long
Life	1000 Hours	1000 Hours

APPENDIX C

EPICYCLIC TRANSMISSION

C.1 GENERAL

A sketch of the epicyclic transmission is shown in figure 104. An efficiency of 100% is assumed for all calculations. The maximum torque load is 175 ft-lbs. The involute tooth form was assumed to have a 20° pressure angle.

C.2 LOADING FORCES (See figure 105)

$$\text{Tangent } F_T = \frac{175 \times 12}{\frac{2.843}{2}} = 1475 \text{ lbs.}$$

$$\text{Separating } F_S = 1475 \times \tan 20^\circ = 1475 \times .364 = 538 \text{ lbs.}$$

$$\text{Shaft Load } F_L = \frac{1475}{\cos 20^\circ} = \frac{1475}{.9397} = 1570 \text{ lbs.}$$

Select bearing for 150% load = 2350 lbs.

Max. Gimbal speed = 10°/sec.

$\simeq 2$ rpm

Gear Ratio (Reference paragraph 6.3) = 60

C.3 ORBIT GEAR BEARINGS (See figure 106)

Trial selection bearing (from layout sizing)

ND 1108

Catalog Rating (vacuum processed steel)

3030 lbs. load at 100 rpm 3800 hrs. avg. life

1 year. = 24 x 365 = 8750 hrs.

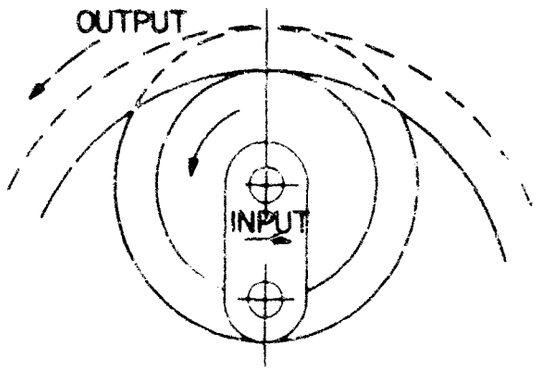

Figure 104. Epicyclic Transmission

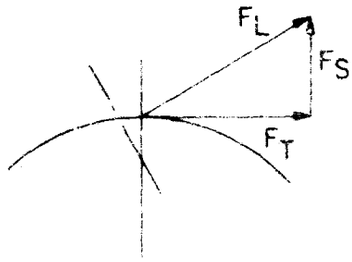

Figure 105. Loading Forces

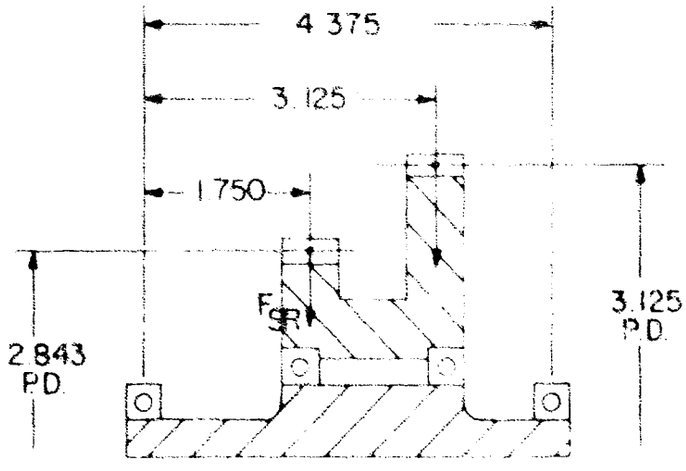

Figure 106. Orbit Gear Bearings

For B-10 life (min. life for 90% bearings) = 5 x avg. life = 5 x 8750 = 43,750 hrs. avg. life.

Load factor for 43,750 hours average life = 1.85 x load rating at 8800 hrs. avg. life.

Bearing load at 175 ft. lbs. = 1570 lbs.

1570 x 1.85 = 2910 lb. rating required.

∴ Selected bearing adequate for any duty cycle less than full load, full speed, full time.

C.4 INPUT SHAFT BEARINGS (See figure 107)

F_{SR} (separating force, reaction stage) = 538 lbs. } See Sec. C.2

F_{TR} (tangential force, reaction stage) = 1475 lbs. } See Sec. C.2

F_{SO} (separating force, output stage) = 489 lbs. } See Sec. C.5

F_{TO} (tangential force, output stage) = 1345 lbs. } See Sec. C.5

} at 100% T_{OUT} = 175 ft. lb.

Motor (input) End Bearing

$$F_S = \frac{489 \times 1.250 + 538 \times 2.625}{4.375} = \frac{611 + 1412}{4.375} = \frac{2023}{4.375} = 463 \text{ lbs.}$$

$$F_T = \frac{1475 \times 2.625 - 1345 \times 1.250}{4.375} = \frac{3870 - 1680}{4.375} = \frac{2190}{4.375} = 500 \text{ lbs.}$$

Bearing Load $\sqrt{\overline{463}^2 + \overline{500}^2} = \sqrt{(21.44 + 25)\,10^4} = 100\sqrt{46.44}$

= 681 lbs.

Gimbal (output) End Bearing

ND 3L06 (from layout sizing)
3360 lb. load at 100 rpm 3800 hr. avg. life

Bearing load = 675 lbs.
675 x 1.85 = 1250 lb. rating required

∴ Selected bearing adequate.

C.5 OUTPUT SHAFT BEARINGS (See figure 107)

Shaft load (load on bearing on line with gear face).

$$\left.\begin{aligned} \text{Tangent load } F_T &= \frac{175 \times 12}{\frac{3.125}{2}} \text{ 1345 lbs.} \\ \text{Shaft load } &= \frac{1345}{.9397} = 1430 \text{ lbs.} \end{aligned}\right\} 100\%_{\eta}$$

Trial Selection Bearing (from layout sizing)

KAYDON KA 40 CP

1290 lb. load at 100 rpm 3000 hr. avg. life

2580 lb. load at 10 rpm 3000 hr. avg. life

3600 lb. load at 2 2 rpm (max. gimbal speed) 3000 hr. avg. life

Load factor for 43750 hr. avg. life = 1.97 x load rating at 3000 hr. avg. life

Bearing load = 1430 lbs.
1430 x 1.97 = 2820 lb. rating required

∴ Selected bearing adequate for any duty cycle less than full load, full speed, full time.

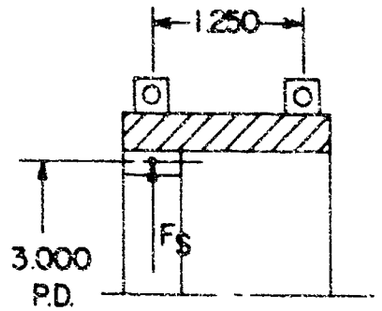

Figure 107. Output Bearings

Gimbal (output) End Bearing

$$F_S = \frac{538 \times 1.750 + 489 \times 3.125}{4.375} = \frac{942 + 1530}{4.375} = \frac{2472}{4.375} = 565 \text{ lbs.}$$

$$F_T = \frac{1345 \times 3.125 - 1475 \times 1.750}{4.375} = \frac{4200 - 2580}{4.375} = \frac{1620}{4.375} = 370 \text{ lbs.}$$

$$\text{Bearing load} = \sqrt{\overline{370}^2 + \overline{565}^2} = 100\sqrt{13.69 + 31.92} = 100\sqrt{45.61} =$$

$$= 675 \text{ lbs.}$$

Motor (inputs) End Bearing

ND LL08 (from layout sizing)

1680 lb. load at 100 rpm 3800 hr. avg. life

Load factor for 43,750 hr. avg. life = 1.85 x load rate at 3800 hrs. avg. life

Bearing load = 681 lbs.
681 x 1.85 = 1260 lb. rating required

∴ Selected bearing adequate for any duty cycle less than full load, full speed, full time.

APPENDIX D

REFERENCES

1. Final Report for a Brushless DC Torque Motor, Nasa Document No. CR-374, February 1966.

2. Electromagnetic Harmonic Drive Low Inertia Servo Actuator, Document No. ASD-TDR-63-466, Flight Control Laboratory, Aeronautical Systems Division, Wright-Patterson Air Force Base, Dayton, Ohio December 1, 1963, page 163.

3. Room Temperature Gearmotor Test Report, Model NV-B1 Gimbal Actuator, Interdepartmental Memo to M.H. Gordon from D.B. Kantz, Bendix Research Laboratories Division, Southfield, Michigan, March 9, 1966

4. Gast Rotary Vacuum Pump Catalog, Gast Manufacturing Corp, Benton Harbor, Michigan

5. Earle Buckingham, Manual of Gear Design, McGraw Hill Inc. Section 2, page 144

6. Alex Vallance and V.L. Doughtie, Design of Machine Members, McGraw Hill Inc, N.Y.C., N.Y., 1951, page 325

7. Power Gear Trains, D. Petersen, Machine Design, Volume 26, No 6, 1954, page 161

8. Kents' Mechanical Engineer's Handbook, Design and Production Volume, Twelfth Edition, pages 14-50.

9. Harmonic Drive for Industrial Applications, Harmonic Drive Division, United Shoe Machinery Corporation, Beverly, Massachusetts

10. AGMA Gear Classification Manual for Spur, Helical and Herringbone Gears, AMGA 390.01

11. Gear Train Accuracy, George W. Michalec, Machine Design, June 9, 1966, page 130

12. Gears, S.L. Cranshow, H.O Kron, and C.G. Bauter, Machine Design, Mechanical Drives Reference Issue, June 17, 1965

13. Earle Buckingham, Analytical Mechanics of Gears, McGraw Hill Inc, N.Y.C., N.Y., page 407

14. Development of Transmission and Torque Regu[illegible] Extreme Environment, W.R. Kee and J.R. Kremidas, Bendix Research Laboratories Report No 65-17, Bendix Research Laboratories, Southfield, Michigan, Table 6

15. Compound Epicyclic Gear Trains, W.A. Tuplin, Machine Design, Volume 29, No. 7, April 4, 1957, page 100

16. Harmonic Drive Mechanical Power Transmission Systems, Harmonic Drive Division, United Shoe Machinery Corporation, Beverly, Massachusetts

17. Direct Drive Servo Design Handbook, Inland Motor Corporation, Rodford, Virginia

18. Linear Stability Analysis of the CMG Control System Using Both Current and Voltage Power Amplifier Report MT-13251, R. Jenicek and R. Jann, April 25, 1966, Eclipse-Pioneer Division, Bendix Corporation, Teterboro, New Jersey

19. Reliability Stress and failure Rate Data for Electronic Equipment, MIL-HDBK 217A, U.S. Government Publication, December 1, 1965

Unclassified
Security Classification

DOCUMENT CONTROL DATA - R&D
(Security classification of title, body of abstract and indexing annotation must be entered when the overall report is classified)

1. ORIGINATING ACTIVITY (Corporate author)
The Bendix Corporation
Eclipse-Pioneer Division
Teterboro, New Jersey

2a. REPORT SECURITY CLASSIFICATION
Unclassified

2b. GROUP
N/A

3. REPORT TITLE
Control Moment Gyroscope Gimbal Actuator Study

4. DESCRIPTIVE NOTES (Type of report and inclusive dates)
Final Report

5. AUTHOR(S) (Last name, first name, initial)
Morine, L. O'Connor, T. Carnazza, J. Varner, H.
Pool, D. De Lucia, R. Ritter, M.
Kaczynski, R Vassallo, D. Modurski, J

6. REPORT DATE
August 1966

7a. TOTAL NO. OF PAGES

7b. NO. OF REFS

8a. CONTRACT OR GRANT NO. AF33(615)3465

b. PROJECT NO.

c.

d.

9a. ORIGINATOR'S REPORT NUMBER(S)
AFFDL-TR-66-158

9b. OTHER REPORT NO(S) (Any other numbers that may be assigned this report)
N/A

10. AVAILABILITY/LIMITATION NOTICES
Same as cover page

11. SUPPLEMENTARY NOTES

12. SPONSORING MILITARY ACTIVITY
Air Force Flight Dynamics Lab.
Wright-Patterson Air Force Base
Ohio

13. ABSTRACT The purpose of this study is the determination of an optimal gimbal actuator for large double gimbal control moment gyros. The optimization study is divided into three distinct phases: torquers and transmissions, which together form the actuators, and controllers. The DC torquer and an epicyclic transmission are selected as optimal, on the basis of power, weight, size, reliability and performance. Pulse width modulation of a type designated as single channel is established as the optimal controller.

To demonstrate the application of the optimal actuator configuration, a preliminary design layout was completed for mounting at one pivot of a CMG having an angular momentum of 1000 foot-pound-seconds. The design includes all necessary structure and a tachometer generator, weighs 23 pounds, consumes less than 45 watts at full torque and also fulfills all performance requirements. It has a threshold of 3% and a reliability of 0.9741 for one year and 0.9956 for two months while in operation.

DD FORM 1 JAN 64 1473

Unclassified
Security Classification

14. KEY WORDS	LINK A		LINK B		LINK C	
	ROLE	WT	ROLE	WT	ROLE	WT
Control Moment Gyros						
CMG; Actuator Study						
Gyro Gimbal Actuators						
Optimal Gimbal Actuators						

INSTRUCTIONS

1. ORIGINATING ACTIVITY: Enter the name and address of the contractor, subcontractor, grantee, Department of Defense activity or other organization *(corporate author)* issuing the report.

2a. REPORT SECURITY CLASSIFICATION: Enter the overall security classification of the report. Indicate whether "Restricted Data" is included. Marking is to be in accordance with appropriate security regulations.

2b. GROUP: Automatic downgrading is specified in DoD Directive 5200.10 and Armed Forces Industrial Manual. Enter the group number. Also, when applicable, show that optional markings have been used for Group 3 and Group 4 as authorized.

3. REPORT TITLE: Enter the complete report title in all capital letters. Titles in all cases should be unclassified. If a meaningful title cannot be selected without classification, show title classification in all capitals in parenthesis immediately following the title.

4. DESCRIPTIVE NOTES: If appropriate, enter the type of report, e.g., interim, progress, summary, annual, or final. Give the inclusive dates when a specific reporting period is covered.

5. AUTHOR(S): Enter the name(s) of author(s) as shown on or in the report. Enter last name, first name, middle initial. If military, show rank and branch of service. The name of the principal author is an absolute minimum requirement.

6. REPORT DATE: Enter the date of the report as day, month, year, or month, year. If more than one date appears on the report, use date of publication.

7a. TOTAL NUMBER OF PAGES: The total page count should follow normal pagination procedures, i.e., enter the number of pages containing information.

7b. NUMBER OF REFERENCES: Enter the total number of references cited in the report.

8a. CONTRACT OR GRANT NUMBER: If appropriate, enter the applicable number of the contract or grant under which the report was written.

8b, 8c, & 8d. PROJECT NUMBER: Enter the appropriate military department identification, such as project number, subproject number, system numbers, task number, etc.

9a. ORIGINATOR'S REPORT NUMBER(S): Enter the official report number by which the document will be identified and controlled by the originating activity. This number must be unique to this report.

9b. OTHER REPORT NUMBER(S): If the report has been assigned any other report numbers *(either by the originator or by the sponsor)*, also enter this number(s).

10. AVAILABILITY/LIMITATION NOTICES: Enter any limitations on further dissemination of the report, other than those imposed by security classification, using standard statements such as:

(1) "Qualified requesters may obtain copies of this report from DDC."

(2) "Foreign announcement and dissemination of this report by DDC is not authorized."

(3) "U. S. Government agencies may obtain copies of this report directly from DDC. Other qualified DDC users shall request through _____."

(4) "U. S. military agencies may obtain copies of this report directly from DDC. Other qualified users shall request through _____."

(5) "All distribution of this report is controlled. Qualified DDC users shall request through _____."

If the report has been furnished to the Office of Technical Services, Department of Commerce, for sale to the public, indicate this fact and enter the price, if known.

11. SUPPLEMENTARY NOTES: Use for additional explanatory notes.

12. SPONSORING MILITARY ACTIVITY: Enter the name of the departmental project office or laboratory sponsoring *(paying for)* the research and development. Include address.

13. ABSTRACT: Enter an abstract giving a brief and factual summary of the document indicative of the report, even though it may also appear elsewhere in the body of the technical report. If additional space is required, a continuation sheet shall be attached.

It is highly desirable that the abstract of classified reports be unclassified. Each paragraph of the abstract shall end with an indication of the military security classification of the information in the paragraph, represented as *(TS)*, *(S)*, *(C)*, or *(U)*.

There is no limitation on the length of the abstract. However, the suggested length is from 150 to 225 words.

14. KEY WORDS: Key words are technically meaningful terms or short phrases that characterize a report and may be used as index entries for cataloging the report. Key words must be selected so that no security classification is required. Identifiers, such as equipment model designation, trade name, military project code name, geographic location, may be used as key words but will be followed by an indication of technical context. The assignment of links, roles, and weights is optional.